5 40
#8

Selection and Investigation of Sites for the Disposal of Radioactive Wastes in Hydraulically Induced Subsurface Fractures

GEOLOGICAL SURVEY PROFESSIONAL PAPER 1215

Prepared in cooperation with the U.S. Department of Energy for the International Atomic Energy Agency

Selection and Investigation of Sites for the Disposal of Radioactive Wastes in Hydraulically Induced Subsurface Fractures

By REN JEN SUN

GEOLOGICAL SURVEY PROFESSIONAL PAPER 1215

Prepared in cooperation with the U.S. Department of Energy for the International Atomic Energy Agency

UNITED STATES GOVERNMENT PRINTING OFFICE, WASHINGTON:1982

UNITED STATES DEPARTMENT OF THE INTERIOR

JAMES G. WATT, *Secretary*

GEOLOGICAL SURVEY

Dallas L. Peck, *Director*

Library of Congress Cataloging in Publication Data

Sun, Ren Jen.
Selection and investigation of sites for the disposal of radioactive wastes in hydraulically induced subsurface fractures.

(Professional paper–U.S. Geological Survey ; 1215)
Bibliography: p.
Supt. of Docs. no.: I 19.16:1215
1. Radioactive waste disposal in the ground. 2. Waste disposal sites–Location. 3. Nuclear facilities–Waste disposal.
I. Title. II. Series: United States. Geological Survey. Professional paper ; 1215.
TD898.S873 621.48'38 80-607180
AACR1

For sale by the Superintendent of Documents, U.S. Government Printing Office
Washington, D.C. 20402

CONTENTS

ILLUSTRATIONS

TABLES

NOMENCLATURE

A	Linear regression constant; instantaneous shut-in pressure
a'	Radius of induced fracture
a	Internal radius of a thick wall cylinder; radius of stress-altered fracture region, as shown in fig. 6
B	Constant; maximum fracture separation
b	Intermolecular distance; external radius of a thick-wall cylinder
C	Constant; activity of a particular radionuclide in waste at time t; horizontal distance measured perpendicular to the average strike of shale beds
C_0	Activity of a particular radionuclide in waste at disposal time
D	Inside diameter of a pipe; denudation rate
d	Diameter of a tested sample; edge region of a fracture, as shown in fig. 6
E	Young's modulus
$F(Q,L,W)$	Friction loss in a vertical fracture
$F(Q,r,W)$	Friction loss in a horizontal fracture
fT	Average cohesive force at a fracture tip
f	$0 \leq f \leq 1$; Fanning factor
g	Acceleration due to gravity
H	Ratio of basin relief to length; horizontal displacement of a hole
h	Depth of induced fracture; length of a tested sample
K	Horizontal stress coefficient (σ_h/σ_v)
K_a	Coefficient of "active earth pressure"
K_0	Coefficient of "earth pressure at rest"
K'	Fluid consistence index (kg-force-sec$^{n'}$/m^2)
k	Constant
L	Fracture length; length of casing
MD	Depth measured along a casing axis
n	Number of half-lives of a particular radionuclide
n'	Fluid flow behavior index (dimensionless)
P	Internal pressure in a thick-wall cylinder; bottom-hole pressure in injection well; load at rock failure during tensile-strength test; pressure decay
P_i	Initiation pressure or breakdown pressure to induce a fracture
P_P	Propagation pressure to extend a fracture
ΔP	Pressure loss due to friction
P_0	Pore pressure
P_0	Pore pressure
Q	Injection rate; total injection volume
$\mathbf{R}_e$	Reynold's number
r	Radial distance
T	Tensile strength of rock
T_a	Tensile strength of rock parallel to bedding planes
T_n	Tensile strength of rock normal to bedding planes
T_{σ_y}	Tensile strength of rock parallel to stress σ_y
T_{σ_z}	Tensile strength of rock parallel to stress σ_z
$T_{1/2}$	Half-life of a particular radionuclide
t	Time
U	Horizontal movement of ground surface
V	Flow velocity
W	Fracture opening
$\bar{W}$	Surface uplift
x	x-axis; horizontal departure, distance east or west of north-south axis
y	y-axis; horizontal departure, distance north or south of east-west axis
Z	True vertical distance between two adjacent measured points
z	z-axis; vertical depth
α	a'/a; vertical deviation angle; angle with the direction of the least principal stress σ_3
β	Angle of joints with respect to a well axis; magnetic bearing
γ	Weight density of rock
θ	Polar angle from x-axis; dip angle
ν	Poisson ratio
ρ	Density
σ	Normal stress
σ_a	Stress parallel to bedding planes
σ_n	Stress normal to bedding planes
σ_h	Horizontal earth stress
σ_v	Vertical earth stress
σ_r	Radial stress
σ_t	Tangential stress
σ_x	Stress along x-axis
σ_y	Stress along y-axis
σ_z	Stress along z-axis; overburden pressure
σ_1, σ_2, σ_3	Principal stresses, the order of magnitude represented by subscript numbers, σ_3 being the least stress
τ	Shear stress
ϕ	Angle of internal friction of clastic sediments
ω	Angle of bedding planes with respect to well axis

CONVERSION TABLE

Multiply metric (SI) unit	*by*	*to obtain inch-pound unit*
Millimeter (mm)	3.9370×10^{-2}	inch (in.)
Centimeter (cm)	3.9370×10^{-1}	inch (in.)
Meters (m)	3.2808×10^{0}	foot (ft)
Kilometers (km)	6.2137×10^{-1}	miles (mi)
Square kilometers (km^2)	3.8610×10^{-1}	square miles (mi^2)
Cubic meters (m^3)	3.5315×10^{1}	cubic feet (ft^3)
Cubic meters (m^3)	2.6417×10^{2}	gallons (gal)
Millileters (mL)	2.6417×10^{-4}	gallons (gal)
Millileters (mL)	3.5315×10^{-5}	cubic feet (ft^3)
Meters per second (m/s)	3.2808×10^{0}	feet per second (ft/s)
Kilograms per second (kg/s)	2.2046×10^{0}	pounds per second (lb/s)
Cubic meters per second (m^3/s)	3.5315×10^{1}	cubic feet per second (ft^3/s)
Cubic meters per second (m^3/s)	1.5850×10^{4}	gallons per minute (gal/min)
Kilogram per cubic meters (kg/m^3)	6.2427×10^{-2}	pounds per cubic feet (lb/ft^3)
Kilogram per cubic meters (kg/m^3)	8.3454×10^{-3}	pounds per gallons (lb/gal)
Pascal (Pa)	1.4504×10^{-4}	pounds per square inch (lb/in^2)
Megapascal (MPa)	1.4504×10^{2}	pounds per square inch (lb/in^2)
Curies per liter (Ci/L)	2.8317×10^{1}	curies per cubic feet (Ci/ft^3)
Curies per liter (Ci/L)	3.7854×10^{0}	curies per gallon (Ci/gal)

SELECTION AND INVESTIGATION OF SITES FOR THE DISPOSAL OF RADIOACTIVE WASTES IN HYDRAULICALLY INDUCED SUBSURFACE FRACTURES

By Ren Jen Sun

ABSTRACT

Injection of intermediate-level radioactive wastes (specific activity of less than $6\times10^3\mu$Ci/mL, consisting mainly of radionuclides, such as strontium and cesium, having half-lives of less than 50 years) mixed with cement into a thick shale formation is a promising and feasible disposal method. Hydraulic fracturing provides openings in the shale to accommodate the wastes. Ion exchange and radionuclide-adsorption materials can be added to the grout during mixing to further increase the radionuclide-retaining capacity of the grout. After solidification of the grout, the injected wastes become an integral part of the shale formation, and therefore the wastes will remain at depth and in place as long as the injection zone is not subjected to erosion or dissolution.

Problems concerning safety of the disposal method are (1) the potential for inducing vertical fractures, (2) phase separation during and after the injections, (3) the reliability of methods for determining the orientation of induced fractures, (4) the possibility of triggering earthquakes, and (5) radionuclides being leached and transported by ground water.

In bedded shale, a difference between tensile strength normal to and that parallel to bedding planes favors the formation of fractures along bedding planes that are nearly horizontal. Even in areas where vertical stress is slightly greater than the horizontal stresses, nearly horizontal bedding-plane fractures can be hydraulically induced in shale at depths less than 1,000 meters. Test injections should be made during site evaluation to determine if horizontal bedding-plane fractures can be induced.

The orientation of induced fractures can be indirectly monitored by recording injection pressures during injection time and by measuring the decay of water injections and the uplift of ground surface after the injections; however, it can be directly determined by gamma-ray logs made in observation wells before and after each injection, if the injected fluid or wastes contain enough gamma-ray emitting radionuclides.

If waste grout is properly mixed, phase separation should be less than one percent of the total amount injected. The mobility of waste in the separated liquid is further decreased by the low permeability (less than 10^{-6} darcy) and the large ion-exchange and adsorption capacity of shale, which thus reduce the potential for contamination.

Grout injections do not cause extensive increases in pore pressure within shale, and a disposal site should be located in a geologically stable and tectonically relaxed area, that is, an area lacking local active faults. Thus a disposal in shale in such areas can avoid the two necessary and essential conditions for triggering earthquakes by fluid injections, an increase in pore pressure and rock already stressed near its breaking strength.

Waste injections are made in several stages at different levels through an injection well. After the first series of injections at the greatest depth, the well is plugged by cement at that depth. The second series of injections are made a suitable distance above the first. The repeated use of the injection well distributes the cost of constructing injection and monitoring wells over many injections, thereby making hydraulic fracturing and grout injection economically attractive as a method for the disposal of radioactive wastes.

Theoretical considerations about inducing nearly horizontal bedding-plane fractures in shale are discussed, as are field procedures for site selection, safety, and the monitoring and operation of radioactive waste disposal. Case histories are used as examples to demonstrate the application of the theory and techniques of field operations.

INTRODUCTION

Radioactive waste is the inevitable byproduct of the generation of electricity by nuclear reactors, as well as of other nuclear applications. An effective solution to the problem of disposing the long-lived and highly toxic radioactive waste is essential if the use of nuclear energy is to be expanded. Numerous methods for the disposal of radioactive waste have been proposed or studied in the last two decades. These methods include disposal on or in suitable geologic formations, in the ocean bottoms (including subduction zones), in polar ice, by shooting the wastes into space, and by transmutation (Winograd, 1974; Interagency Review Group on Nuclear Waste Management, 1979). Judged by existing technology, disposal of waste in geologic formations is probably the most feasible and practical method among the proposed alternatives.

One of the geologic disposal methods is to inject a mixture of intermediate-level radioactive wastes (specific activity of less than 6×10^3 μCi/mL, consisting mainly of radionuclides having half-lives of less than 50 years, such as strontium and cesium) and cement and additives through a deep well into fractures that have been induced in nearly impervious formations (permeability $<10^{-6}$D (darcy)) by hydraulic pressure during the injection. The injected grout is allowed to solidify under pressure to form grout sheets, which become an integral part of the rock (fig. 1); thereby the wastes are immobilized in a desired horizon of the low-permeability medium.

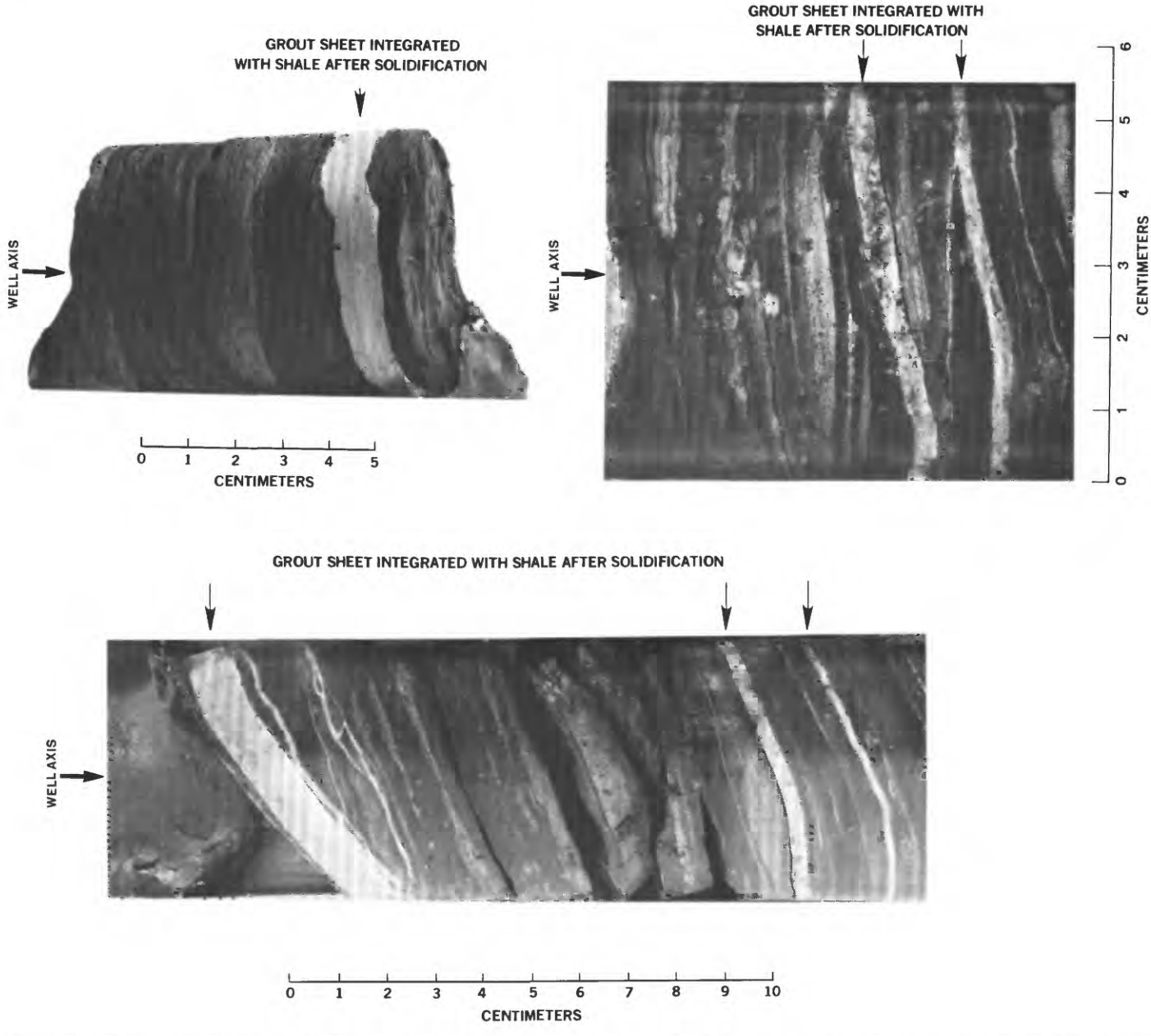

FIGURE 1.—Photographs of core samples illustrating the typical appearance of grout sheets integrated with shale after grout solidification. Arrows indicate the grout sheets. The cores shown here were obtained from different boreholes and are of sheets formed from several injections. (Courtesy of Oak Ridge National Laboratory, Tenn.)

The techniques of hydraulic fracturing have been widely used in the petroleum industry since 1947 for recovery of oil (Clark, 1949; Howard and Fast, 1970). However, disposal of wastes by grout injection using hydraulic fracturing had not been tested until 1959. In 1958, D. A. Shock of the Continental Oil Co. suggested to the U.S. Atomic Energy Commission (AEC, presently the U.S. Department of Energy) that hydraulic fracturing combined with grout injection into impermeable rocks might be used for the disposal of highly toxic radioactive waste (deLaguna and others, 1968). The AEC accepted the suggestion, and the Oak Ridge National Laboratory (ORNL), Tenn., was chosen for an experimental site.

Requirements for radioactive waste disposal by this technique include the following items: (1) The induced fractures should be horizontal or nearly horizontal, and (2) the wastes should be contained in a known and well-defined horizon for a sufficient time until the radiation emissions from the wastes decay to innocuous levels.

From 1959 through 1960, three experimental injections without wastes were made into the Conasauga Shale by hydraulic fracturing at two different locations at the ORNL. The grout was tagged with radioactive isotope ^{137}Cs. The first injection was at a shallow depth, 88 m below the land surface. After the injection, 22 core holes were drilled near the injection well. The cores provided data that showed the solidified grout sheet to be formed nearly parallel to the bedding planes (fig. 1). The second and third experiments were made at a new well that was drilled 1,830 m east of the first injection well. Similar grout was used in these two injections, which were made at depths of 285 m and 212 m, respectively. After the injections, 24 core holes were drilled near the experimental site. The core-hole data confirmed again that the grout sheets were formed parallel to bedding planes and became an integral part of the shale (fig. 1). The grout sheets are confined to an area having a maximum radius of 100 m, and the observed range in thickness of the grout sheets is from 3 to 12 mm (figs. 2, and 3). A third well having a 14-cm casing was drilled in the Conasauga Shale to a depth of 329 m, 0.8 km west of the second experimental site. From 1964 through 1965, seven experimental injections containing liquid radioactive wastes produced at the ORNL were made. The injections were at progressively shallower depths, from 288 m to 265 m. From 1966 through 1978, regular waste disposal was carried out through the well from depths of 265 m to 245 m. A total volume of 11,000 m^3 of grout containing 7,000 m^3 of radioactive wastes produced at the ORNL was injected. These wastes contained 640,000 Ci (curies) of radionuclides. Core drilling and gamma-ray logs for observation wells constructed near the injection well also indicated that the grout sheets were formed parallel to bedding planes (deLaguna and others, 1968, 1971; Weeren, 1974, 1976).

The demonstration at the ORNL shows that disposal of intermediate-level radioactive wastes in bedded shale by hydraulic fracturing is feasible. However, most experience with hydraulic fracturing in oil wells indicates that hydraulically induced fractures are generally vertical (Hubbert, 1971). Because of this experience, Earth scientists advised the AEC, through the U.S. National Academy of Sciences, not to extrapolate the results obtained at the ORNL site to other locations (Belter, 1972).

In view of this advice, the AEC sponsored an experimental program at the Western New York Nuclear Fuel Service Center near West Valley, in Cattaraugus County, N.Y., carried out jointly by the ORNL and the U.S. Geological Survey (USGS), with the permission of the State of New York, to test further the concept of disposing radioactive wastes into shale by hydraulic fracturing. The objectives of the program were (1) to demonstrate at another location the feasibility of inducing bedded-plane fractures in nearly horizontally bedded shale through hydraulic fracturing, (2) to develop an economical yet practical method for estimating and monitoring the orientation of hydraulically induced fractures, and (3) to develop site-evaluation procedures (Belter, 1972).

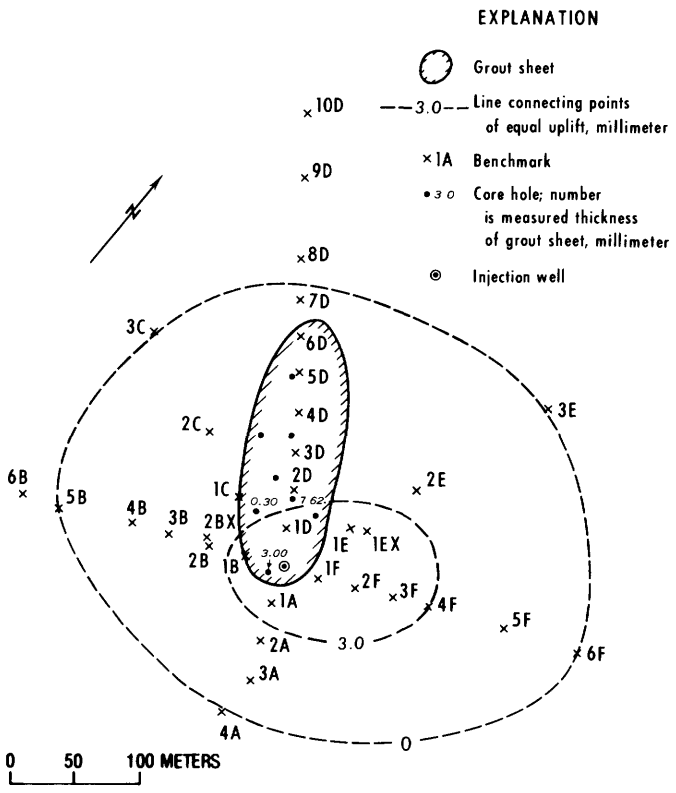

FIGURE 2.—Map of observed uplift, extent, and thickness of the grout sheet resulting from an injection, at the second experiment site, Oak Ridge National Laboratory, Tenn., on Sept. 3, 1960 (from deLaguna and others, 1968).

From 1969 through 1971, six hydraulic-fracturing injections, all of water, except the last, which was of grout, were made at the West Valley, N.Y., site. Most of the injections were tagged with radioactive tracers. The injection depths ranged from 152 to 442 m. Conclusions reached on the basis of the test results are as follows:

1. At certain shallow depths (less than 1,000 m) bedding-plane fractures can be induced hydraulically in an approximately horizontally bedded shale in which tensile strength normal to the bedding planes is much less than that parallel to the bedding planes.
2. The injected grout can be kept within a short distance vertically from the injection depth.

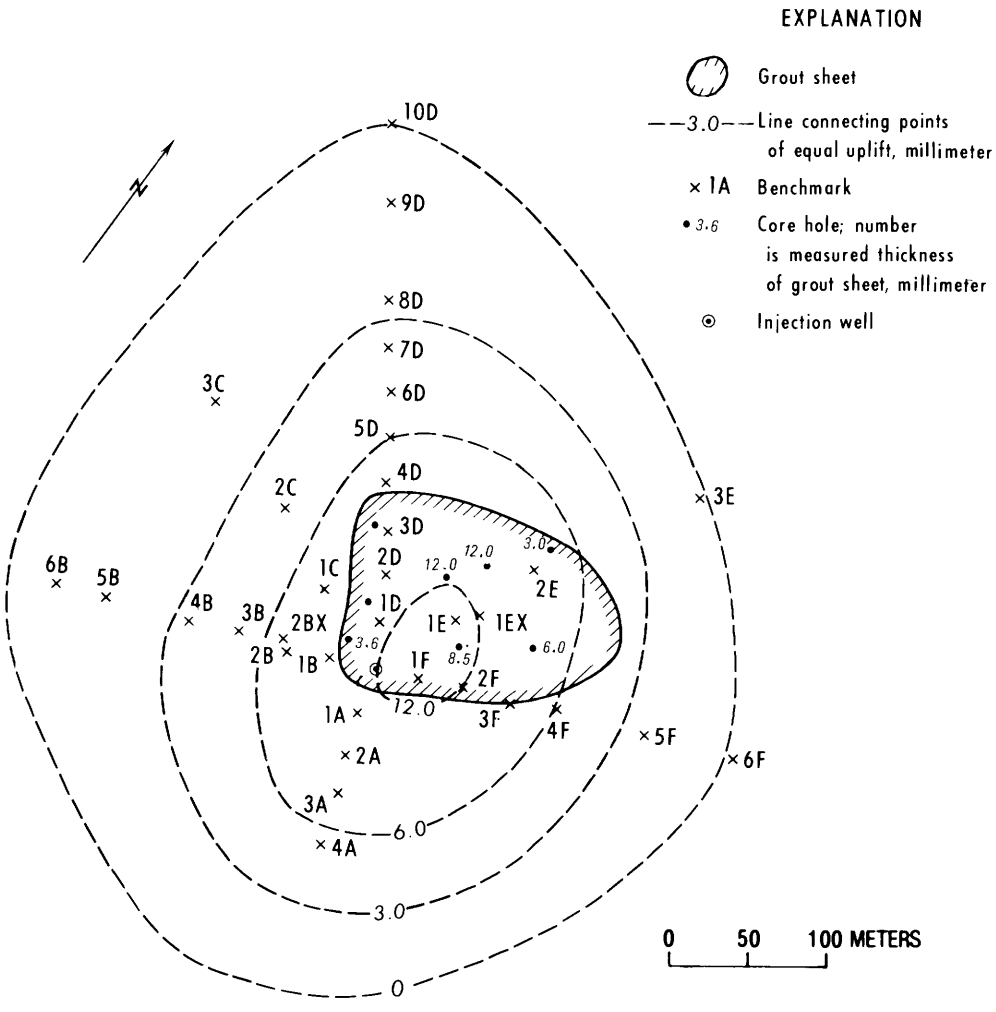

FIGURE 3.—Map of observed uplift, extent, and thickness of the grout sheet resulting from an injection, at the second experimental site, Oak Ridge National Laboratory, Tenn., on Sept. 10, 1960 (from deLaguna and others, 1968).

3. Existing joints and (or) high-angle fractures in the formation may be extended by injection pressure if they are intercepted by induced fractures; however, the extension will cease when the vertical fractures reach weak bedding planes.
4. The orientation of induced fractures can be indirectly monitored by recording injection pressures during the injection time and by measuring the pressure decay of water injections and the uplift of ground surface after injection. It can be directly determined by gamma-ray logs made in observation wells that were constructed within the area where the grout is expected to reach, if the grout contains gamma-ray-emitting radionuclides (Sun, 1973; Sun and Mongan, 1974).

The present hydraulic-fracturing disposal facility (in 1981, this facility is still being used for disposal of wastes) at the ORNL was designed for experimental injections. Because of the experiments' success, the facility was modified in 1966 to allow for the routine disposal of radioactive wastes having a specific activity of less than 530 μCi/mL. Without extensive equipment modifications, the facility can not be used for disposal either of sludge, of which 1,500 m^3 has been accumulated at the ORNL, or of wastes having a specific activity greater than 530 μCi/mL. Also, the disposal capacity of the shale underlying the present facility will be exhausted between 1985 and 1988 if the present waste-generation rate at the ORNL is maintained (U.S. Energy Research and Development Administration (ERDA), 1977).

In 1973, the ORNL proposed to establish a second hydraulic-fracturing disposal facility having the capacity to dispose sludges, as well as wastes having a specific activity as great as 6×10^3 μCi/mL. The proposed site is 245 m south of the present existing site. A site-

feasibility study was made jointly by the ORNL and the USGS in 1974, the study methods applied being those developed during the experiments conducted at the ORNL and at West Valley, N.Y.

Since enactment of the National Environmental Policy Act in 1969, all major government projects require environmental-impact statements, which should evaluate all possible environmental impacts of a proposed action, as well as the feasible alternatives to the proposed action. The environmental-impact statement for the proposed waste-disposal facility at the ORNL concluded that the hydraulic-fracturing disposal of radioactive wastes at the ORNL is the safest method and has the least cost among the alternatives, such as tank storage and fixation in glass (ERDA, 1977).

PURPOSE AND SCOPE OF THE REPORT

The feasibility of subsurface disposal by grout injection of certain types of radioactive wastes in hydraulically induced fractures in shale has been studied and well demonstrated in the United States. The purpose of this report is to provide information to authorities who are responsible for planning, approving, and executing radioactive-waste management programs to help them determine if disposal of intermediate-level radioactive wastes (specific activity of $<6\times10^3$ μCi/mL consisting mainly of radionuclides having half-lives of less than 50 years, such as strontium and cesium) by hydraulic fracturing is an acceptable alternative. The information herein is also intended to be used for the selection and evaluation of suitable sites. Safety assessment of the disposal method is also discussed. The safety assessment is important and necessary for waste-management authorities who use the information to compare the hydraulic-fracturing disposal technique with other alternatives, so that they can determine if the disposal waste can be isolated in a geologic formation, at least for the desired length of time.

The report contains sufficient theoretical discussions and case histories (in the Appendix) to allow the reader to evaluate whether the presented conclusions are justified.

ACKNOWLEDGMENTS

This report was sponsored for the International Atomic Energy Agency by the Division of Waste Management of the U.S. Department of Energy.

The author wishes to thank R. A. Robinson and H. O. Weeren, ORNL, for providing information on hydraulic-fracturing disposal at the ORNL. The author also is indebted to R. A. Farrow, USGS, for the determination from cones during a site-evaluation study at the ORNL, of the tensile strength of shale.

THEORY OF FRACTURE MECHANICS

Rock deformation can be classified into three main categories: (1) folds, (2) shear fractures, and (3) extension fractures. Ideally, folds are produced where rock under deformation responds without failure (in a macroscopic sense) to stresses. Shear fractures result where stresses produce movements parallel to the plane of the fracture. Faults are special cases of shear fracturing. Extension fractures are separations of rocks across a surface normal to the direction of the least principal stress without offset or movement parallel to the fracture surface. Extension fractures involve loss of cohesion, separation into two parts, and release of stored elastic strain energy (Badgley, 1965). Joints and hydraulically induced fractures are extension fractures.

Three well established theories that can be applied to rock fracturing are (1) the Coulomb-Navier, (2) the Mohr, and (3) the Griffith (Jaeger and Cook, 1969). The first two theories are applicable to rock failure under maximum shear stress. The last discusses rock failures under tension and can be used to explain extension fractures. Therefore, only the Griffith theory is used to discuss hydraulic-fracturing mechanics.

Two stages are involved in fracturing, namely fracture initiation and fracture propagation. Fracture initiation is defined as the failure process by which one or more preexisting fractures in rocks start to extend. Fracture propagation is a stage subsequent to initiation, in which a fracture is extending. Two kinds of propagation may be defined, stable and unstable (Bieniawski, 1967).

Stable propagation is the process of rupture by which the extension of a fracture involves definite relationship between the applied stress and the length of the fracture, and the fracture extension can accordingly be controlled. If the extension is governed by factors other than stresses – for example, the velocity of propagation – it becomes uncontrollable, and the fracture expands rapidly to complete a rupture of the material, where the applied load is constant – for example, a fracture in glass. This kind of propagation is called unstable propagation and has dynamic characteristics.

The extension of hydraulically induced fractures is dependent on the applied hydraulic pressure; a fracture will cease extending when the applied pressure falls below a critical level. Therefore, the extension of a hydraulically induced fracture is a stable propagation.

When sediments are deposited, individual grains are discrete and the sediments are without cohesion. As sediments are buried beneath younger deposits, they become compacted and cemented, resulting in the cohesion of grains, so that the rock takes on cohesive or tensile strength. The greater the cementation and compaction the greater is the cohesion.

In the propagation of extension fractures, work must be done against the stress normal to the fracture plane and against the cohesive force of the grains at the fracture tip. As the hydraulic pressure is applied, the preexisting fracture in the rock does not extend while the pressure is small. Upon reaching a certain pressure that overcomes the sum of the normal stress and the maximum cohesive force at the fracture tip, the fracture begins to extend.

The cohesive force under tensile stresses in perfect crystals is a function of the intermolecular distance b (Cottrell, 1964; Kunz, 1971), as shown in figure 4. Consider two atomic planes under tensile stresses: the molecular cohesive force is zero before the tensile stresses are applied; then it rises in proportion to the amount of separation between the separated molecules and reaches the maximum value when the separation has reached approximately one intermolecular distance from the equilibrium condition. Further separation will reduce the cohesive force, which diminishes nearly to zero when the separation between the molecules is greater than three intermolecular distances from the equilibrium condition. The maximum molecular cohesive force defines the ideal tensile strength of the material under consideration, that is, the tensile strength of a material if it were a perfect crystal. The actual tensile strength of a material is commonly several orders of magnitude less than the ideal tensile strength because of (1) defects of crystal structure, (2) variation in the mineralogy of constituent detrital grains and in the extent of cementation in a granular medium, and (3) variation in the type of cement.

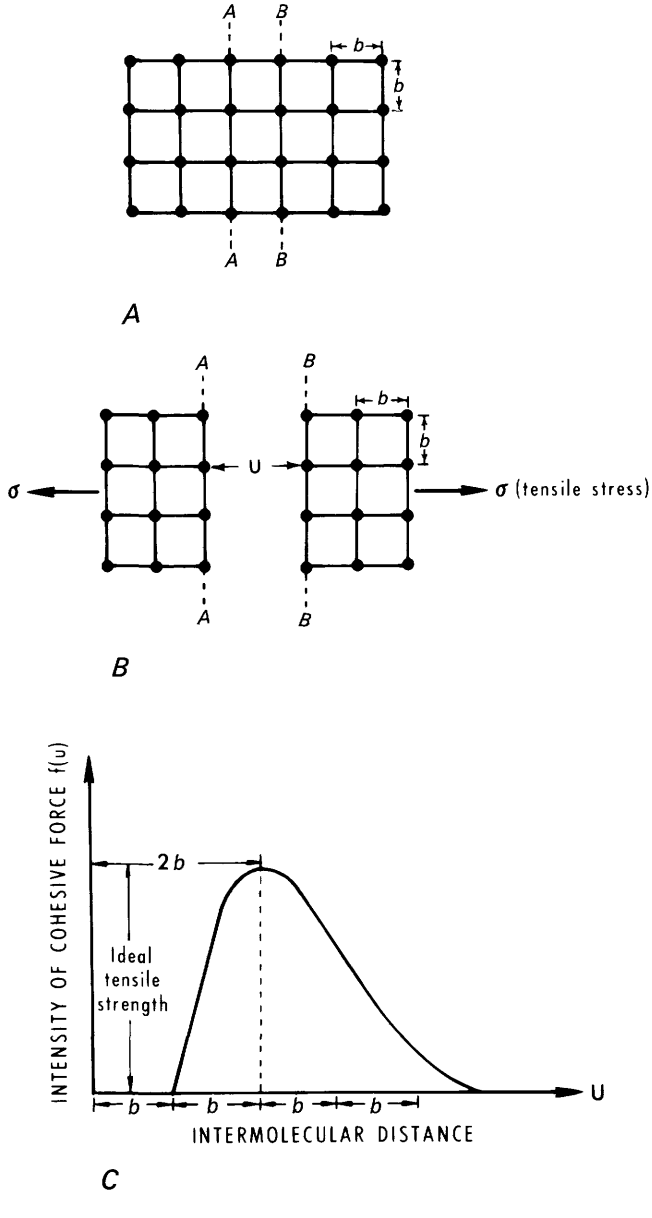

FIGURE 4.—Diagram showing the fracturing of a perfect crystal under tensile stresses (from Cottrell, 1964).

Figure 5 shows a schematic, idealized structure of molecules around a fracture tip. Consider the fracture extending from the left towards the right; the first pair of molecules at the fracture tip begin to separate as the tensile stresses increase. An increase in the applied stresses will increase the separation between the pair. The intermolecular distance increases from the equilibrium condition b to $2b$, then to $4b$; at this stage, the fracturing process is completed, the fracture extends one molecular distance b, and the applied stresses fall. The second pair of molecules now becomes the new

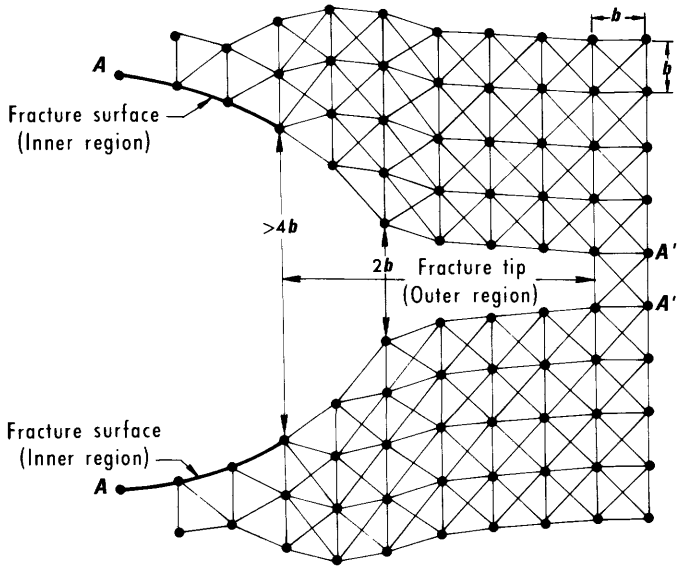

FIGURE 5.—Schematic diagram showing molecular structures around a fracture tip.

fracture tip. The applied stresses again rise and fall. The fracturing process goes on from one pair of molecules to the next.

To avoid solving complex nonlinear integral equations applied to the fracture problem, Barenblatt (1962) divided the fracture area into two regions (fig. 6). In the inner region the opposite fracture walls are relatively far apart; hence, there is no molecular cohesive force, and the fracture walls can be considered as free from such stress. The linear theory of elasticity is fully adequate to describe this region. In the edge region, the opposite fracture walls are sufficiently close to each other that the molecular cohesive force between them is strong. Plastic yielding occurs in this region. To avoid the complex nonlinear theory of elasticity and to work within the framework of the linear theory, Barenblatt made two assumptions to solve the fracture problem: (1) The size of edge region of the fracture is small compared with the size of the whole fracture, and (2) when the fracture extends, the shape of the section normal to the fracture surface in the edge region (and consequently the local distribution of the cohesive force over the fracture surface) does not depend on the pressure in the fracture and is always the same for given conditions of temperature and composition. These assumptions are here considered to be realistic.

On the basis of these assumptions, the average cohesive force at a fracture tip is defined as fT, where T is the average tensile strength of the rock and f is a constant that depends on physical properties of the rock. The value of f is $0 \leq f \leq 1$ (Barenblatt, 1962; Kenny and Campbell, 1967; Perkins and Krech, 1968; Goodier, 1968; Rice, 1965).

FACTORS CONTROLLING THE INJECTION OF RADIOACTIVE WASTES IN HYDRAULICALLY INDUCED FRACTURES

The technique of disposing radioactive wastes in a geologic formation by hydraulic fracturing is to first mix the waste with cement and additives and then to inject it through a well under pressure. The injection well penetrates the host rock and is fully cased and pressure cemented between the casing and the formation. A horizontal 360-degree slot that cuts the casing and the cement wall and penetrates the host rock is made by a hydraulic-sand jet before the injection. The applied hydraulic pressure separates the rock to form openings into which the waste is injected. The fracture at the tip of the precut slot is usually initiated by water injection. After a fracture has been initiated, waste grout is then injected. The injected grout solidifies under pressure. After solidification the injected grout becomes an integral part of the host rocks, thereby immobilizing waste and restricting it to a definite area. Two or three consecutive injections can be made through the same slot; thereafter, the well is plugged by cement up to the next injection depth, and again a horizontal slot is made. Waste injections are made in a sequence from bottom upward until the disposal capacity of the injection formation is exhausted.

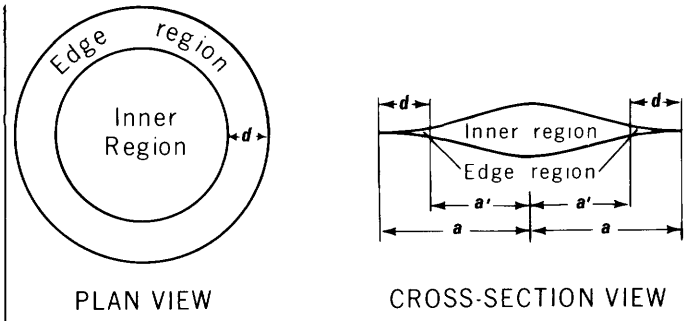

FIGURE 6.–Diagram showing two regions of a brittle fracture (from Barenblatt, 1962).

The major concern about the hydraulic fracturing waste-disposal technique is whether horizontal fractures can be induced in the host rocks, so that the injected waste can be immobilized and restricted to a desired horizon. The overwhelming experience of hydraulic fracturing in oil wells indicates that hydraulically induced fractures are generally vertical (Hubbert, 1971), an orientation that is unfavorable for the disposal of radioactive wastes. The possibility of inducing horizontal fractures by hydraulic pressure is discussed in the following sections.

The discussions are based on the assumption that the injection formation is isotropic and homogeneous. Admittedly this is not the case. Geologic formations, especially shale, are generally heterogeneous and anisotropic; however, the simplifying assumption appears to be valid in general, as the experiments made at the ORNL and West Valley, N.Y. indicate (Sun, 1969, 1973, 1976; Sun and Mongan, 1974). These experiments are presented in the appendix.

EARTH STRESSES

In the propagation of a fracture at depth, the applied pressure in the fracture must overcome the stress normal to the fracture plane and the cohesive force at the fracture tip. Therefore, during hydraulic fracturing the amount of earth stress normal to the fracture plane must be considered.

The amount of stress at a given point and at a particular depth generally results from three types of stress components. They are (1) gravitational stress, (2) tectonic stress, and (3) fluid pressure within the rock.

Gravitational stress results fundamentally from the weight of overlying rock. Two aspects of this stress need to be differentiated: (1) stress effects that result from

the present topographic conditions and (2) stress effects that result from past topographic conditions. Tectonic stresses are induced by mobility of the Earth's crust resulting from various influences as temperature and geochemical effects, and fluid pressure is caused by fluid in pores, such as oil, gas, and water.

VERTICAL EARTH STRESS

Consider a small element of rock at a depth z in a Cartesian coordinate system having its z-axis vertical (fig. 7). The equation of equilibrium in terms of vertical stress (Jaeger and Cook, 1969) is given by

$$\frac{\partial \sigma_z}{\partial z} + \frac{\partial \tau_{yz}}{\partial y} + \frac{\partial \tau_{xz}}{\partial x} - \rho g = 0, \qquad (1)$$

where σ_z is the vertical stress, τ_{yz} and τ_{xz} are shear stresses, and ρ and g are density of the rock and acceleration of gravity, respectively.

Integrating equation (1) with respect to z:

$$\sigma_z = \gamma z - \int_0^z \frac{\partial \tau_{yz}}{\partial y} dz - \int_0^z \frac{\partial \tau_{xz}}{\partial x} dz, \qquad (2)$$

where γ is the weight density (ρg) of overlying rock. Howard (1966) stated that there are only three special cases of equation 2 in which the vertical stress is equal to the weight of overlying rock per unit area, but only two of them are considered to be geologically acceptable.

Case 1.—In regions of gentle topography and simple geologic structure there are no shear components along the air-earth interface; then

$$\tau_{xz} = \tau_{yz} = 0, \qquad (3)$$

and the vertical stress is simply equal to the weight of overlying rock per unit area.

Case 2.—Through relaxation of rock by creep over long periods of time the shear stress diminishes; then

$$\int_0^z \frac{\partial \tau_{yz}}{\partial y} dz - \int_0^z \frac{\partial \tau_{xz}}{\partial x} dz = 0, \qquad (4)$$

and the vertical stress is again equal to the overburden pressure.

Case 3.—The shear stresses along the x and y axes are equal to each other but in opposite directions; thus,

$$\int_0^z \frac{\partial \tau_{yz}}{\partial y} dz = - \int_0^z \frac{\partial \tau_{xz}}{\partial x} dz. \qquad (5)$$

This case is geologically improbable, and the condition is very restrictive, especially when compounded by the choice of geographic direction for the x and y axes.

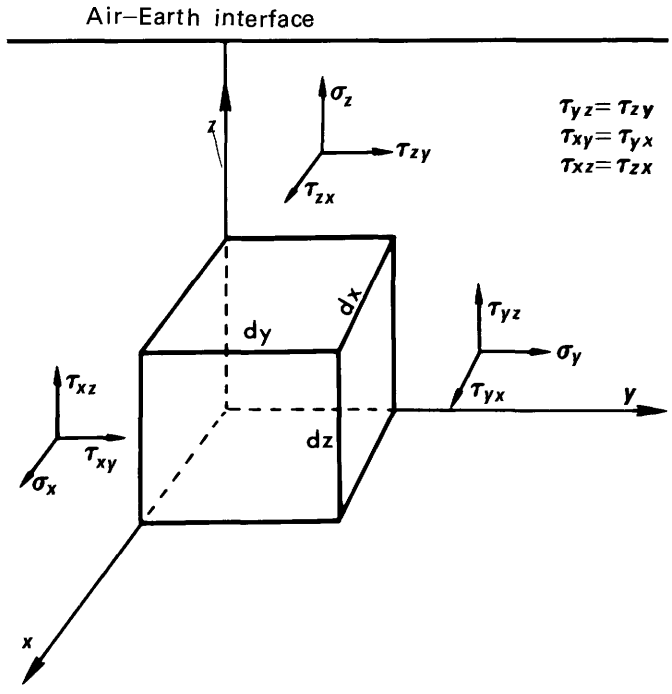

FIGURE 7.—Diagram showing stresses on a small rectangular parallelepiped element located at depth z.

Therefore, it can be concluded that in a relatively flat area having a simple geologic structure, the vertical stress can be calculated as the weight of overlying rock per unit area. However, in a topographically irregular area or in a region having a complex geologic structure, the vertical stress may or may not be the overburden pressure alone.

HORIZONTAL EARTH STRESS

No adequate analytical models are available to estimate horizontal stresses. However, experiences in soil mechanics can be used to help explain the relation between the horizontal and the vertical stresses.

Consider, for example, the simple case of an accumulation of clastic sediments subject to a principal stress solely derived from overburden pressure. The stress-strain relationship is a function of the mobilized friction coefficients between individual clastic particles, the structural arrangement of the particles, and the elastic constants of the particles. The ratio of horizontal to vertical intergranular stresses corresponding to a condition of zero lateral strain is called the coefficient of "earth pressure at rest" and is denoted by K_0 (Voight, 1966). The empirical relationship is given by

$$K_0 = 0.95 - \sin \phi, \qquad (6)$$

where ϕ is angle of internal friction of the clastic sediments (Brooker and Ireland, 1965; Voight, 1966).

It should be emphasized that very small strains have a marked effect on the value of horizontal stress. It was found that strains on the order of 10^{-3} are sufficient to fully mobilize the shear strength – that is, to reduce the ratio of horizontal to vertical stress to the coefficient of "active earth pressure," K_a (Voight, 1966), where

$$K_a = (1 - \sin \phi)/(1 + \sin \phi). \quad (7)$$

Very little is known about the precise nature of lateral restraint to be found at a geologic scale. Voight (1966) believed that horizontal strains may in fact vanish for certain types of sedimentary basins. The horizontal stress coefficient K, which is defined as σ_h/σ_v, must lie between the limiting values of the "active earth pressure" and "earth pressure at rest" and is given by

$$(1 - \sin \phi)/(1 + \sin \phi) \leq \sigma_h/\sigma_v \leq (0.95 - \sin \phi). \quad (8)$$

In general, the angle of internal friction, ϕ, is 27–30° for unjointed hard sedimentary rocks, such as sandstone and limestone, and 0–20° for soft sedimentary rocks, such as shale and clay (Fenner, 1938; Harrison and others, 1954; Perkins, 1967; Jaeger and Cook, 1969). Then, the ratio of horizontal to vertical stresses, σ_h/σ_v, can be considered to be between 0.33 and 0.55 for hard sedimentary rocks and between 0.49 and 0.95 for soft rocks. The average measured σ_h/σ_v in sedimentary basins in the United States containing sandstone and shale is 0.6 (McGarr and Gay, 1978).

Laboratory experiments show that a hysteresis effect exists during loading and unloading of rocks (Brooker and Ireland, 1965; Voight, 1966); therefore, horizontal stress is higher during unloading than loading (fig. 8). If this hysteresis effect exists in areas that have undergone significant denudation or ice-sheet unloading in the Quaternary Period, then horizontal stress probably would be higher than that calculated on the basis of the present overburden pressure.

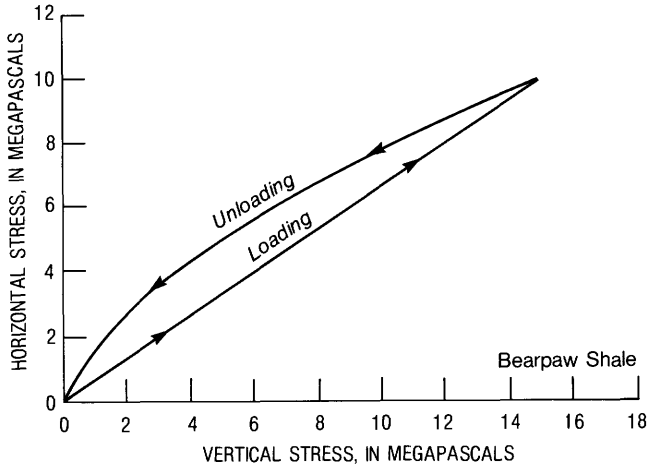

FIGURE 8.–Graph showing hysteresis during loading and unloading in uniaxial compression tests of Bearpaw Shale (from Brooker and Ireland, 1965).

TECTONIC STRESS

The earth stresses discussed in the preceding sections are only gravitational. In addition, rocks are also subjected to tectonic stress. Unfortunately, no analytical theory is available to estimate tectonic stresses. It also should be noted that regions subjected to current tectonic stresses are not only those that are seismically active. Nor are such regions necessarily characterized by tectonic structures that reflect the past stress distribution. Current stresses need not bear a geometrical relation to structures produced in prior deformational phases. There is much geologic evidence for areas subjected to multiple deformations that indicates characteristically significant changes in stress orientation over time. Moreover, significant current tectonic stresses can exist in regions regarded as geologically stable (Voight, 1966). Thus, although the observation and description of geologic deformational structures provide irrefutable evidence of past tectonic activity and the past distribution of stresses, geologic structures can be used only as guides in studying the current earth stresses; the actual stresses can only be determined in place.

MECHANICS OF HYDRAULIC FRACTURING

The mechanics of hydraulic fracturing are well documented (Hubbert and Willis, 1957; Haimson, 1968; Haimson and Fairhurst, 1969; Howard and Fast, 1970; Daneshy, 1967, 1973), and only the conditions that are needed for inducing horizontal fractures are discussed herein.

Fracture walls can be classified in two categories on the basis of the lithologic characteristics of an injection formation: (1) Both walls are relatively impermeable as are those of fractures formed in thick shale, and (2) one or both walls are permeable, as are those of fractures formed along the interface of shale and sandstone or within sandstone. One of the required conditions for the disposal of radioactive wastes is that there be a minimum possibility of grout leaching by ground water and of grout dilution during injection; therefore, it is mandatory to select low permeability formations ($< 10^{-6}$ D) as injection host rocks. Also the injection well should be cased and pressure cemented along its full length. Therefore, only the case of fractures having relatively impervious walls induced by nonpenetrating fluid is considered in the following sections.

STRESSES AROUND UNCASED BOREHOLES

During injections, hydraulically induced stresses around the well can be determined by thick-wall-cylinder stress equations (Timoshenko and Goodier, 1951). The induced radial stress σ_r, tangential stress σ_t, vertical stress σ_z, and shear stress τ of a thick-wall cylinder subject to internal pressure P, are given by

$$\sigma_r = [a^2P/(b^2-a^2)][(b^2/r^2)-1], \quad (9)$$

$$\sigma_t = -[a^2P/(b^2-a^2)][1+(b^2/r^2)], \quad (10)$$

and

$$\sigma_z = \tau_{r\theta} = \tau_{z\theta} = \tau_{rz} = 0, \quad (11)$$

where a is the internal radius of the thick-wall cylinder, b is the external radius, r is the radial distance from the center of the cylinder to a desired point, and θ is the polar angle from x-axis. The negative sign represents tension.

Because the injection well is constructed in a thick impervious formation that extends radially to a great distance, the value of b can be considered to be very large as compared with the value of well radius a. Equations 9, 10, and 11 can be rewritten as

$$\sigma_r = P(a^2/r^2), \quad (12)$$

$$\sigma_t = -P(a^2/r^2), \quad (13)$$

and

$$\sigma_z = \tau_{r\theta} = \tau_{z\theta} = \tau_{rz} = 0. \quad (14)$$

The induced radial and tangential stresses will reach maximum (the value of P) at the well face and diminish abruptly away from the well.

The effects of a well on a preexisting stress field can be calculated by analogy with an infinitely large plate subjected to uniaxial stress and containing a circular hole whose axis is perpendicular to the plate, the equation for which was solved by Kirsch in 1898 (Timoshenko and Goodier, 1951). The stresses near a well subjected to two horizontal stresses σ_x and σ_y, can be obtained by the Kirsch solution and the law of superposition (fig. 9). The results are given by

$$\sigma_r = [(\sigma_x+\sigma_y)/2](1-a^2/r^2)+[(\sigma_x-\sigma_y)/2](1+3a^4/r^4 - 4a^2/r^2)\cos 2\theta, \quad (15)$$

$$\sigma_t = [(\sigma_x+\sigma_y)/2][(1+a^2/r^2)-[(\sigma_x-\sigma_y)/2](1+3a^4/r^4)\cos 2\theta, \quad (16)$$

and

$$\sigma_{r\theta} = [(\sigma_x-\sigma_y)/2](1-3a^4/r^4+2a^2/r^2)\sin 2\theta, \quad (17)$$

where a is the radius of the well, r is the radial distance from the center of the well, and θ is the polar angle counterclockwise from the x-axis (fig. 9).

From equations 15 and 17, it can be seen that the radial and shear stresses are zero at the well face and increase abruptly toward the undisturbed earth stresses over a distance equal to a few well diameters. Equation 16 shows that at the well face ($r=a$) the tangential stress reaches a minimum value at $\theta=0°$ and $\theta=180°$, with a magnitude of $(3\sigma_y-\sigma_x)$ if $\sigma_x>\sigma_y$. This minimum stress can be either compressional or tensional depending on the ratio of σ_x/σ_y. When σ_x is greater than $3\sigma_y$ the stress is in tension. The maximum stress on the well face is at $\theta=90°$ and $\theta=270°$, with a magnitude of $(3\sigma_x-\sigma_y)$ and is always in compression. In the case where both horizontal stresses are equal ($\sigma_x=\sigma_y$), the tangential stress around the well face is the same everywhere, with a magnitude of $2\sigma_h$.

In conclusion, the effect of a well on horizontal stresses is localized to within distance equal to a few well diameters. Beyond that distance, earth stresses will be undisturbed.

The linear theory of elasticity is assumed to be approximately valid in hydraulic fracturing, and therefore stresses around the injection well can be superimposed; that is, the resultant of the induced stresses around the injection well is the algebraic sum of the induced stresses produced by the hydraulic pressure in the well and the distorted stresses due to the presence of the well.

In the initiation of a vertical fracture, the initiation pressure P_i, which is commonly called "breakdown pressure," should be equal to or greater than the sum of the minimum effective tangential earth stress at the well face and the tensile strength of the rock in the direction normal to the fracture plane. The mathematical expression for initiation of a vertical fracture can be obtained from equations 13 and 16, and when $r=a$, $\theta=0°$, and $\theta=180°$, the result is

$$P_i - P_0 \geq 3(\sigma_y - P_0) - (\sigma_x - P_0) - T_{\sigma_y}, \text{ if } \sigma_x > \sigma_y, \quad (18)$$

or

$$P_i \geq 3\sigma_y - \sigma_x - P_0 - T_{\sigma_y}, \quad (19)$$

where T_{σ_y} is the tensile strength of the rock in the direction of σ_y and is considered to be negative, and P_0 is the pore pressure at a depth where the hydraulic fracturing is being made.

Because the presence of a well distorts the existing stresses only in an area within a distance of a few well diameters from the well, the required "propagation pressure," P_P to extend the initiated vertical fracture is the sum of the minimum effective earth stress, the cohesive force at the fracture tip, and the fluid frictional loss in the fracture. The mathematical expression is given by

$$P_P - P_0 \geq \sigma_y - P_0 - f T_{\sigma_y} + F(Q,L,W), \text{ if } \sigma_x > \sigma_y, \quad (20)$$

or

$$P_P \geq \sigma_y - f T_{\sigma_y} + F(Q,L,W), \quad (21)$$

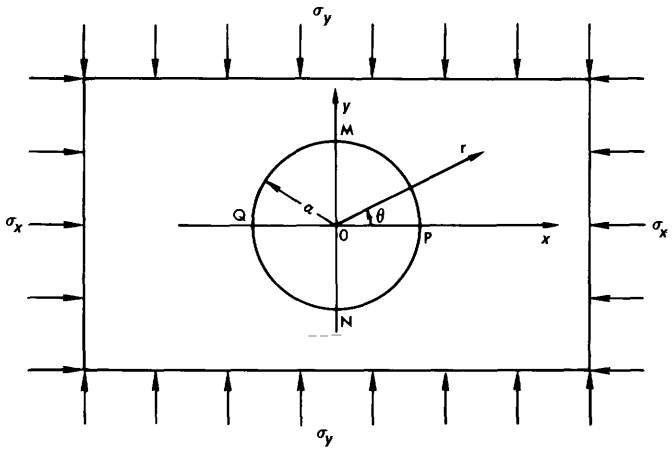

FIGURE 9.—Diagram showing stresses on an infinitely large plate containing a circular hole.

where $F(Q,L,W)$ is the fluid frictional loss in the fracture and is a function of injection rate, Q, the length, L, and the opening, W, of the fracture.

Without packers, a horizontal fracture cannot be induced at the well face, because no vertical stress can be produced in the injection well. Only if there is an artificial horizontal cut or some existing horizontal fractures at the well face is it probable that horizontal fractures can be induced.

FRACTURING IN CEMENTED AND CASED HOLES

In the case that the injection well is cased and pressure cemented over its full length, before injection, a horizontal 360° cut is made by hydraulic sand jetting. The cut, which extends about 30 cm into the host rock, serves as a plane of weakness. During an injection, the wellhead is enclosed, and the injection fluid enters the cut and creates vertical stresses.

Due to the additional tensile strength (at least several tens of megapascals) provided by casing and cement and to the precut weak horizontal plane at the well face, the induced fracture is undoubtedly in the horizontal direction, at least within moderate depths of several thousands of meters, in spite of the horizontal direction of the least principal stress. However, at greater depths, the additional tensile strength provided by the casing and cementing may be overcome by the great overburden pressure, and thus a vertical fracture could be induced at cemented and cased wells.

In areas where the least stress (sum of the earth stress and the cohesive force at the fracture tip) is in one of the horizontal directions, even if the fracture initiated at the well face is horizontal the induced fracture should become vertical as the fracture propagates away from the injection well, so that the plane of the fracture will be normal to the least stress and the required work to rupture the rock is minimum.

The breakdown pressure to form a horizontal fracture is equal to or greater than the sum of the vertical stress (σ_z) and the tensile strength of the rocks in the vertical direction. The mathematical expression is given by

$$P_i \geq \sigma_z - T_{\sigma_z}. \tag{22}$$

The propagation pressure is

$$P_P \geq \sigma_z - f T_{\sigma_z} + F(Q, r, W), \tag{23}$$

where T_{σ_z} is the tensile strength of the rock in the vertical direction and $F(Q,r,W)$ is the fluid frictional loss in the fracture and is a function of injection rate, Q, the radial distance, r, and the opening, W, of the fracture.

FRACTURING IN BEDDED ROCKS

Experimental results and geological observations show that bedded rocks have strength anistrophy or directional tensile strength. Because of low cohesion between bedding planes and because of the lineation of clay mineral and microfractures parallel to bedding planes, bedded rocks frequently have the smallest tensile strength normal to bedding planes and have the greatest tensile strength parallel to bedding planes. Laboratory data indicate that the value of the tensile strength of bedded rocks, such as shale, normal to bedding planes ranges from about 20 to 80 percent of the values parallel to bedding planes, but in most cases the value is on the order of 30 percent (Hobbs, 1964; Chenevert and Gatlin, 1965; Youash, 1965; Obert and Duvall, 1967).

Let σ_1, σ_2, and σ_3 be three principal stresses of different magnitudes. The order of magnitude is represented by the subscript numbers, respectively, σ_3 being the least stress. If the stress condition that is the most favorable for producing vertical fractures is assumed, then the maximum principal stress, σ_1, should be vertical and the least stress, σ_3, lies in one of the horizontal directions. Also if the bedding planes of the host rock make an angle of ω with the well axis (fig. 10), then the stresses along the bedding planes, σ_a, and normal to bedding planes, σ_n, can be calculated by Mohr's stress circle and are given by

$$\sigma_a = (\sigma_1 + \sigma_3)/2 + [(\sigma_1 - \sigma_3)/2]\cos 2\omega, \tag{24}$$

$$\sigma_n = (\sigma_1 + \sigma_3)/2 - [(\sigma_1 - \sigma_3)/2]\cos 2\omega, \tag{25}$$

and

$$\tau_{an} = [(\sigma_1 - \sigma_3)/2]\sin 2\omega. \tag{26}$$

Pressure required to initiate a fracture along or normal to bedding planes should be equal to or greater than

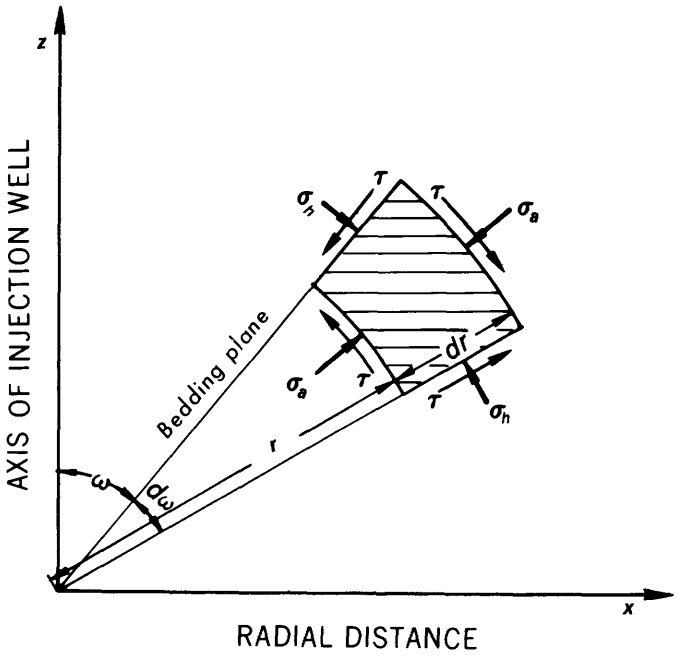

FIGURE 10.—Graph showing stresses on a bedding plane of rock with respect to the axis of an injection well.

the sum of the stress given by equations 24 or 25 and the tensile stength of the rock parallel to (T_a) or normal to the bedding planes (T_n). The mathematical expressions are given by

$$P_i \geq (\sigma_1+\sigma_3)/2+[(\sigma_1-\sigma_3)/2]\cos 2\omega - T_a \quad (27)$$

for a fracture initiated parallel to the bedding planes and

$$P_i \geq (\sigma_1+\sigma_3)/2-[(\sigma_1-\sigma_3)/2]\cos 2\omega - T_n \quad (28)$$

for a fracture initiated normal to the bedding planes.

The pressure required to propagate a fracture along or normal to bedding planes should be equal to or greater than the sum of the stress given by equations 24 or 25, the cohesive force at the fracture tip, and the fluid frictional loss in the fracture. The mathematical expressions are

$$P_P \geq (\sigma_1+\sigma_3)/2-[(\sigma_1-\sigma_3)/2]\cos 2\omega - f T_n + F(Q,r,W) \quad (29)$$

for a fracture extending normal to bedding planes and

$$P_P \geq (\sigma_1+\sigma_3)/2+[(\sigma_1-\sigma_3)/2]\cos 2\omega - f T_a + F(Q,r,W) \quad (30)$$

for a fracture extending parallel to bedding planes. The condition for extending a bedding-plane fracture is as follows:

$$(\sigma_1+\sigma_3)/2-[(\sigma_1-\sigma_3)/2]\cos 2\omega - f T_n \leq (\sigma_1+\sigma_3)/2 + [(\sigma_1-\sigma_3)/2]\cos 2\omega - f T_a \quad (31)$$

When ω is equal or less than 45°, a bedding-plane fracture is always to be extended. However, when ω is greater than 45°, then the condition for extending a bedding-plane fracture is

$$(\sigma_3-\sigma_1)\cos 2\omega \leq f(T_n - T_a). \quad (32)$$

Let $f=0.3$ (Perkins and Krech, 1968; Sun and Morgan, 1974); $\sigma_h/\sigma_v=0.7$ (see the section Horizontal earth stress); and $T_a=10$ MPa, $T_n=2$ MPa (table 27), and $\sigma_v=25$ MPa/km (Hubbert, 1957). The following table summarizes the probably depth that bedding-plane fractures would be induced hydraulically (eq 32):

Bedding-plane angle with well axis, in degrees, ω	*Depth, in meters, for extending bedding-plane fractures in areas where the least principal stress is horizontal*
0-45	All depths.
50	≤1,800
60	≤640
75	≤370
90 (horizontal bedding)	≤320

FRACTURING IN FRACTURED AND JOINTED BEDDED ROCKS

Virtually all rocks, including glacial tills, have fractures or joints. Some investigators have believed that hydraulic pressure in the injection well causes joints or existing fractures to extend (Bugbee, 1953; Heck, 1955, 1960) and, therefore, that the orientation of hydraulically induced fractures is controlled by joints or by existing natural fractures; hence, the orientation could be predicted by studying the surface joint patterns (Overby and Rough, 1968). However, laboratory studies by Lamont and Jessen (1963) showed that the orientation of hydraulically induced fractures would be determined primarily by the orientation of the least principal stress; hence hydraulic fractures can extend across preexisting joints or fractures. The location of an existing plane of weakness as joints and fractures does not alter the orientation of induced fractures appreciably. Are the latter statements true; if so, under what conditions?

Again it is assumed that (1) the dominant principal stress, σ_1, is vertical and the least principal stress, σ_3, lies in one of the horizontal directions and that (2) the existing fracture or joint plane makes an angle β and the bedding planes make an angle ω with the well axis (fig. 11). Under such conditions the pressure required to propagate an existing vertical fracture is given by

$$P_P \geq (\sigma_1+\sigma_3)/2-[(\sigma_1-\sigma_3)/2]\cos 2\beta - f T_n \cos(\omega-\beta) - f T_a \sin(\omega-\beta) + F(Q, r, W). \quad (33)$$

The pressure required to extend a bedding-plane fracture is given by

$$P_P \geq (\sigma_1+\sigma_3)/2-[(\sigma_1-\sigma_3)/2]\cos 2\omega - f T_n + F(Q, r, W). \quad (34)$$

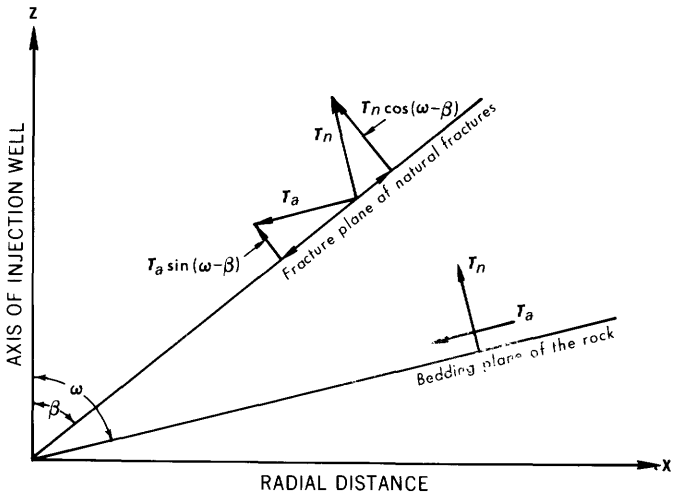

FIGURE 11.—Graph showing tensile stresses on a fracture plane of a natural fracture and bedding plane of rock with respect to the axis of an injection well.

The condition for propagating a bedding-plane fracture without extending an existing fracture is that the value of P_p calculated by equation 34 should be less than that calculated by equation 33. The result is given by

$$[(\sigma_3-\sigma_1)/2]\cos 2\omega - f T_n \le [(\sigma_3-\sigma_1)/2]\cos 2\beta - f T_n \cos(\omega-\beta) - f T_a \sin(\omega-\beta). \quad (35)$$

In the case of vertical joints, that is, $\beta=0°$, equation 35 can be written as

$$[(\sigma_3-\sigma_1)/2]\cos 2\omega - f T_n \le (\sigma_3-\sigma_1)/2 - f T_n \cos\omega - f T_a \sin\omega. \quad (36)$$

In the case of horizontal bedding planes containing vertical joints, that is $\omega=90°$ and $\beta=0°$, then equation 35 can be reduced and is given by

$$\sigma_1-\sigma_3 < f(T_n - T_a). \quad (37)$$

Based on the same values discussed in the previous section, the following table summarizes the probable depth at which vertical joints would not be extended by the bedding-plane fractures. It can be concluded that at a shallow depth (<400 m), vertical joints would not be extended in a formation having strong directional tension strength, even in an area where the maximum principal stress is vertical.

SUITABILITY OF VARIOUS ROCK TYPES FOR HYDRAULIC FRACTURING AND WASTE INJECTION

The host injection rock should be of very low intrinsic and fracture permeability (<10^{-6} D), so that groundwater movement in the injection zone is extremely slow.

Bedding-plane angle with well axis, in degrees ω	*Depth, in meters, for not extending vertical joints when bedding-plane fractures are induced in areas where the least principal stress is horizontal*
0 (vertical bedding)	Bedding plane coincides with joints; Therefore, vertical joints are extended at all depths.
15	≤1,500
30	≤750
45	≤510
60	≤400
75	≤350
90 (horizontal bedding)	≤320

The injection rock also should be characterized by appreciably lower tensile strength normal to rather than parallel to bedding planes, so that bedding-plane fractures can be induced hydraulically. The suitability of various rock types for radioactive waste disposal by hydraulic fracturing is discussed on the basis of these requirements in the following sections.

SHALE

The permeability of shale lacking closely spaced fractures or joints is low, generally ranging from 10^{-6} to 10^{-9} D (Magara, 1978; Davis, 1969; Young and others, 1964).

Layered sedimentary rocks commonly have directional tensile strengths (Hobbs, 1964); however, the difference in tensile strength between that normal to and that parallel to bedding planes is more dominant for bedded shale than for other sedimentary rocks. Field evidence indicates that joints or fractures in shale generally stop at well-bedded and poorly cemented zones.

Direct measurements of in-situ stresses in sedimentary rocks suggest that the minimum horizontal principal stress in shale is nearly equal to the overburden pressure in geologically stable areas; however, the horizontal stresses measured in other sedimentary rocks, such as sandstone, are generally much less than the overburden pressure (Simonson and others, 1978).

Shale also contains a large amount of clay minerals, which commonly have a large adsorption capacity for radionuclides. Therefore, if some radionuclides are leached out of a grout sheet, the clay minerals in shale can further retard their movement.

To summarize, shale typically provides the following properties favorable for radioactive-waste disposal by hydraulic fracturing: (1) Susceptibility to the induction of nearly horizontal bedding-plane fractures, (2) bedding planes that probably inhibit the extension of existing vertical fractures and joints, (3) extremely slow groundwater movement, and (4) further retardation by clay minerals of most radionuclides leached from the grout.

Therefore, shale is an excellent host rock for the disposal of radioactive wastes by grout injection and hydraulic fracturing.

SANDSTONE AND LIMESTONE

The permeability of sandstone and limestone generally ranges between 10^{-1} and 10^{-4} D (Davis, 1969), which is about five orders of magnitude greater than the permeability of shale. Further, the difference in tensile strength normal to and that parallel to bedding planes is small; therefore, except under particular circumstances, sandstone and limestone are not recommended as host rocks for disposal of radioactive wastes by hydraulic fracturing.

CRYSTALLINE IGNEOUS AND METAMORPHIC ROCKS

The permeability of most crystalline igneous and metamorphic rocks is probably of the same order of magnitude or even lower than that of shale; however, the differences between the directional tensile strengths, as related to bedding planes, diminish. On the other hand, most crystalline rocks are considerably fractured vertically. Nearly horizontal fractures probably can be induced hydraulically only in the areas where the least principal earth stress is vertical, that is, in areas having residual stresses evidenced by earth movements or in areas undergoing large induced isostatic rebound. Unless field evidence or in-situ stress measurements indicate that the least principal earth stress is vertical and that closely spaced vertical fractures are lacking, crystalline igneous and metamorphic rocks should not be considered as host rocks for radioactive-waste disposal by hydraulic fracturing.

SITE EVALUATION

The geohydrologic investigation during site evaluation should cover an area of at least several square kilometers beyond that of the site under consideration and should include items discussed in the following sections.

GEOLOGY

Well-bedded shale containing nearly horizontal and loosely cemented bedding planes, and lacking known faults or closely spaced joints or natural fractures appears to be the best injection formation. Shale is frequently interbedded with other sedimentary rocks, such as sandstone or limestone. If possible, densely interbedded shale should not be selected as host rock.

To insure inducing nearly horizontal bedding-plane fractures and to reduce the complexity of interpreting investigation results, areas of simple geologic structure and flat topography are preferred. Areas of great topographic relief and complex geology should be avoided if possible. The host rock should be at depth shallower than 1,000 m, thus reducing the potential for inducing vertical fractures.

The possibility of chemical and physical changes of rock characteristics by waste injection needs to be evaluated. Normally, characteristics of shale will not be changed or altered by wastes as long as radioactive decay does not raise the temperature above 100° C. However, at elevated temperatures in shale, montmorillonite-illite undergoes a phase transition involving an increase in illite and the liberation of free water. This water plus preexisting pore water is probably in the form of steam or, at least, hot water. Oxygen, carbon dioxide, hydrogen sulfide, and other gases may also be released. Interaction among preexisting minerals, volatile components, and waste is promoted by high temperatures. Experience indicates that hot moving fluids may alter existing minerals and form new ones, thus causing significant changes in permeability (Bredehoeft and others, 1978) and adsorbability. Because of limits in knowledge, it is recommended that radioactive waste whose decay results in temperatures greater than 100° C at the disposal depth should not be disposed in shale or other rocks by grout injection and hydraulic fracturing without further studies.

HYDROLOGY

The major concern about hydrology related to the disposal of radioactive wastes by hydraulic fracturing is ground-water movement. It is preferable to know the regional and local ground-water flow in the host rock. Based on this information the average travel time of ground water to points of discharge can be estimated. Ground-water investigation methods have been well documented (Hantush, 1964, Walton, 1970; Bear, 1972; Prickett and Lonnquist, 1971; Freeze and Cherry, 1979) and are not discussed in this report.

Information on total sediment load carried by streams in the area of a proposed disposal site is also valuable. This information can be used to estimate long-term erosion rates.

Surface runoff not only is one of the major forces for erosion but also can be a source or sink of local ground-water flow. Therefore, it is important to understand the interaction between streamflow and ground-water flow and the depth of the interaction. Ideally interaction is limited to approximately the upper few tens of meters below the ground surface, well above the injection rock, which should be at a depth of at least several hundred meters.

GEOLOGIC STABILITY

The chance of successfully immobilizing radioactive wastes in injected rocks depends on the disposal site being geologically stable for many thousands of years so that radionuclides can decay to a point at which their concentrations no longer constitute a health hazard. Tectonism, diapirism, volcanism, glaciation, climatic change, seismicity, and erosion are the major activities causing geologic instability. Presently no reliable methods can be used to predict these activities over millions of years. However, if injected wastes are diluted to produce lower concentrations (below the specific activity 6×10^3 μCi/mL, as done at the ORNL) and are limited to radionuclides, such as ^{90}Sr and ^{137}Cs, having half-lives of less than 50 years, then the time period for which geologic stability has to be anticipated can be reduced to about one thousand years. The reliability of predictions is increased considerably for this time period (Interagency Review Group on Nuclear Waste Management, 1979). It is still impossible to predict precisely the behavior of the grout and the ability of rocks to adsorb the radionuclides of the waste. However, the degree of uncertainty of prediction is reduced greatly.

Past geologic events such as faulting, glaciation, and seismicity have not been random; therefore, past records might be used for estimation. Regional on-site stress measurements are used not only to estimate or determine whether nearly horizontal bedding-plane fracture can be induced but also to evaluate geologic stability. Any evidence of local tectonic instability or of seismicity should be a definite cause for the area's elimination from consideration for disposal sites.

INTERFERENCE WITH RESOURCES EXPLOITATION

Resources beneath the injection zones can be developed after the disposal of wastes as long as precautions are taken during the construction of mining shafts or drill holes. Because the solidified grout sheet becomes an integral part of the host rock, penetration of radiation to mining shafts can be avoided or reduced to acceptable levels by sealing off the injection zone by use of strong casing and thick cement walls. If doubts remain on the acceptability of placing mining shafts through the injection zone, the future value of potential resources must be weighed against the benefits of disposing the radioactive wastes.

SITE INVESTIGATION

After a site is selected, the site must be investigated specifically to see whether nearly horizontal bedding-plane fractures can, in fact, be induced without the possibility of inducing vertical fractures and whether the permeability of the host rock is sufficiently low. The site investigaton should follow the procedures discussed in the following sections.

TEST DRILLING

At least one core hole is needed to obtain geophysical logs and to determine on-site subsurface geology, including lithology, frequency and condition of joints or fractures, the elastic constant, and the directional tensile strength of the host rock.

If possible, the core hole should be drilled using air. The core hole should be tested by injected water to determine formation permeability; if a significant amount of water is transmitted by interconnected joints or fractures, then the selected site should be abandoned. The core hole should be drilled to the full depth in which injection is to be made. If all evidence indicates that the selected site is suitable for waste disposal then the core hole can be constructed to be either a future injection well or one of the observation wells. An injection well is cased with fairly heavy casing and pressure cemented to its full depth. An observation well also should be cased with strong tubing or casing and pressure cemented to its full depth. The size of observation wells should be large enough to allow free movement of a logging probe along the well and free movement of drilling tools if a well is to be serviced after completion.

If the core hole is converted to an injection well, then at least four observation wells should be constructed in the same manner as the injection well at a radial distance of about 50 m from the injection well but of a smaller diameter of casing. These observation wells are to be used in locating the position of induced fractures after each fracturing, if the injection fluid is tagged with gamma-ray-emitting radionucludes.

GEOPHYSICAL LOGGING

In addition to such geophysical logs as an electric log, a caliper log, and a fracture televiewer log for lithologic identification, determination of borehole conditions, and presence and altitude of joints and fractures, gamma-ray logs and borehole-deviation logs must be run in all wells. Deviation logs are used to obtain the true position and vertical distance of the well at any desired depth. The following formulas (Gatlin 1960) are suggested to be used in calculating the true positions:

$$Z = MD\cos\alpha, \tag{38}$$

$$H = MD\sin\alpha, \tag{39}$$

$$y = H\cos\beta, \tag{40}$$

$$x = H\sin\beta, \tag{41}$$

where

Z = the true vertical distance between well survey points 1 and 2,

MD = the measured distance along the well axis between points 1 and 2,
H = the horizontal displacement of the well at any desired depth from the well center at the surface,
y = the horizontal north or south departure distance from the east-west axis at any desired depth
x = the horizontal east or west departure distance from the north-south axis at any desired depth (the origin of the east-west and the north-south axis is located at the surface of the well).
α = the vertical deviation angle determined from the deviation log, and
β = the bearing (compass direction) determined magnetically during logging.

A whole well-length gamma-ray log should be carefully run in all wells before and after each injection. The logs should be recorded on paper, rather than by visual inspection during logging. A full-length gamma-ray log not only gives opportunities for careful office studies but also serves as a public documentation of the site investigation.

The initial gamma-ray logs made during well construction are used not only to identify rock units but also to serve as baseline information on the natural gamma radiation of the rock. The baseline information is to be compared with the logs made after an injection to determine the location and depth of the induced fractures near the observation wells.

To reduce the complexity of comparing the preinjection and postinjection gamma-ray logs, logs should be run at the same speed and instrumental settings. Variation of instrumental settings during logging not only increases the complexity of data interpretation but also increases chances of missing evidence for the determination of induced fractures.

CORE ANALYSES

Cores obtained at a potential injection zone should be used for determining the tensile strengths, the elastic constants, the permeability (vertical and horizontal), and the radionuclide-adsorption capacity of the rock. These data are useful for the study of the safety of the radioactive-waste disposal at the site.

STRIKES AND DIPS OF HOST ROCKS

The average strike and dip of the selected host rock should be measured or estimated. These data are used in the prediction and confirmation of induced bedding-plane fractures near observation wells. This prediction and confirmation increases the reliability of site-investigation results and the confidence in the disposal method.

Strike and dip of rock units can be calculated from gamma-ray logs and the three-point method described by Lahee (1952, p. 711–714) and from surface-mapping data. The results discussed in the appendix (p. 74) indicate that the method was reliable when used in the ORNL site evaluation.

HYDRAULIC FRACTURING TESTS

The selected site should be tested by actual injections. At least one water injection and one grout injection, each having a total volume of about 400 m^3, should be made to determine whether bedding-plane fractures can be induced. Each of the injection tests should be made with a short-lived gamma-ray-emitting radioactive isotope. The probable altitude and orientation of induced fractures should be projected before injection by using the calculated strike and dip of the rock unit. After injection, the predicted altitudes and orientation of the induced fractures should be checked using the gamma-ray logs made in observation wells after the injection.

A water injection should be made first. The purpose of a water injection is to ascertain whether the injected shale has very low permeability and no interconnecting fractures and to determine the vertical earth stress, which may or may not be the weight of overburden at the site. (For example, Moye (1958) pointed out that the field-measured vertical earth stress is about 1.3 to 2.1 times greater than the calculated overburden pressure at Tumut Valley, Snowy Mountains, Australia.) The wellhead of the injection well should be closed under pressure upon termination of the water injection, so that pressure decay in the well can be observed thereafter. If the pressure decay is very slow (wellhead pressure is maintained for weeks or months), it indicates that the injection rock is sufficiently impermeable to groundwater movement. If nearly horizontal bedding-plane fractures have been induced, as indicated by gamma-ray logs made in observation wells after the injection, the vertical earth stress can be calculated from the pressure decay-time data (see the next section). The information on vertical earth stress at the site is useful for safety monitoring during waste injections. If the injection pressure falls below the calculated vertical earth stress during a waste injection, the injection should be terminated immediately to ascertain whether induced fractures have intercepted an extensively interconnected joint system or have become vertically orientated.

Some investigators may question the wisdom of having a water injection during a site investigation because they believe that several hundred cubic meters of water may be left in the host rock. The water could

mix with the injected grout during future waste injections and adversely affect the retention of radionuclides. However, the host rock is probably already saturated with water. The injected water eventually leaks out of the induced fractures, despite the low permeability of the rock, into the rock mass during the period of constructing the disposal equipment, if the site is selected. The volume of water injected would be small compared with the total volume of water held by the host rock in the injection zone. Therefore, the water left in the host rock by a water injection should not disturb the formation and, thus, no adverse effect would be anticipated during waste injection.

The importance of a grout injection during a site investigation is that it not only will simulate actual waste injections but also can confirm the results obtained from the water injection. Such a confirmation is important for increasing confidence in the suitability of a site for waste disposal.

INTERPRETATION OF HYDRAULIC-FRACTURING TEST DATA

Injection pressure, pressure decay, and uplift produced by injections give indirect evidence of the orientation of the induced fractures. Gamma-ray logs made in observation wells after and before each injection give the actual orientation of the induced fractures within the area between the injection well and the observation well, if the injection fluid is tagged with gamma-ray-emitting radionuclides.

INTERPRETATION OF PRESSURE DATA

Injection pressure, pressure decay, rate of injection, and volume of injection should be observed at the wellhead of an injection well. Pressure decay of a water injection is a complicated phenomena. At the present time, no analytical solution has been established. An empirical relation between pressure decay and time has been found during field experiments at West Valley, N.Y. (Sun and Mongan, 1974); the relationship is given by

$$P-P_0=Ct^{-k}, \tag{42}$$

where P is the observed pressure decay at a particular time t and P_0 is the formation fluid pressure at the injection depth. C and k are constants. Plotting $(P-P_0)$ against t on a log-log graph paper should result in a straight line if k remains unchanged. However, if the geometry of the induced fractures changes, then the value of k will change.

As the well is shut in, the fluid pressure in the induced fracture is much higher than the fluid pressure in the formation surrounding the fracture; thus, water starts to flow from the induced fracture into the formation, despite the low permeability of the host rock. Fluid pressure in the induced fractures declines, thus affecting the fluid pressure in the injection well, and the plot of the observed $(P-P_0)$ against t on a log-log graph paper will fall on a single line. As soon as the fluid pressure in the induced fracture is reduced to a value that is less than the effective earth stress normal to the fracture plane, the fracture is reduced in size. The pressure decay in the induced fracture is thus affected not only by water leaking out of the fracture but also by the reduction of the fracture volume; therefore, the slope of the line of $(P-P_0)$ plotted against t will change. The pressure at the discontinuity point of the $(P-P_0)$ and t curve can be interpreted as the effective earth stress normal to the fracture plane. If the evidence obtained from gamma-ray logs made in observation wells after the injection indicates that nearly horizontal bedding-plane fractures have been induced, then the vertical earth stress, σ_z, can be estimated as the pressure at the discontinuity point shown by the $(P-P_0)$ and t curve.

Injection pressure is composed of three elements: (1) breakdown pressure, (2) propagation pressure, and (3) instantaneous shut-in pressure. Breakdown pressure and propagation pressure have been defined previously (p. 10). Instantaneous shut-in pressure is the pressure at the instant the injection pump is stopped. At this time, no fluid is entering the injection well; therefore, the flow resistance in the induced fracture is zero, and the instantaneous shut-in pressure is equal to the sum of earth stress normal to the fracture plane and cohesive force at the fracture tip. From equation 23, it can be shown that the propagation pressure is equal to the instantaneous pressure after the injection pump has stopped.

If flow through induced fractures is assumed to be laminar and to obey Darcy's law, at least for water injection, then the injection pressure at the well should be linearly proportional to the injection rate. This assumption has been proved to be correct by using a polynomial regression on the injection data observed at the West Valley site, N.Y.; F-tests on data for the site showed that only the linear term of injection rate, Q, has significance statistically (Sun and Mongan, 1974).

During the stage of fracture initiation, the injection pressure must be built up to overcome the tensile strength of the rock. After the rock is broken, the injection pressure gradually decreases to the required propagation pressure. During this transitional stage, the injection pressures are not linearly proportional to the injection rates. Excluding these pressures, a linear regression equation can be established and is given by

$$P_P=A+BQ, \tag{43}$$

where P_P is the bottom-hole injection pressure, Q is the injection rate, and A and B are regression constants. If a

nearly horizontal bedding-plane fracture has been induced, then A is the sum of the vertical earth stress and the cohesive force, fT, at the tip of the induced fracture. The reliability of the regression constant A can also be checked by observed instantaneous shut-in pressure; that is, when Q is equal to zero,

$$P_P = A, \tag{44}$$

where A is the instantaneous shut-in pressure.

If a nearly horizontal bedding-plane fracture has been induced, the tensile strength of the rock can be estimated from equation 22 and is given by

$$T_{\sigma_z} = \sigma_z - P_i, \tag{45}$$

where T_{σ_z} is the tensile strength normal to bedding planes, σ_z the vertical earth stress, and P_i the breakdown pressure.

After the tensile strength normal to bedding plane and the vertical earth stress have been determined, the cohesive force at the tip of the nearly horizontal bedding-plane fracture can also be calculated by equations 23 and 44; it is given by

$$\sigma_z - fT_{\sigma_z} = A. \tag{46}$$

After the tensile strength normal to nearly horizontal bedding planes of the rock, the vertical earth stress at the site, the cohesive force at the fracture tip, and the pressure required to overcome flow resistance have been determined or estimated, then the breakdown and propagation pressures can be forecast. The predicted values are to be used in safety monitoring during waste injection. The foregoing discussions are illustrated by the case histories presented in the Appendix.

INTERPRETATION OF UPLIFT DATA

A large amount of foreign material is injected into a host rock, which must yield space to accommodate the injected material. Because only nearly horizontal bedding-plane fractures are expected to be induced at a waste-disposal site, the dominant force applied to the host rock during injection should be nearly vertical. No significant amount of injected fluid is expected to leak out of the induced fractures during injection, and the fractures will not be closed completely by the vertical earth stress after solidification of the grout. Uplift of ground surface is expected to result from injections. Field experiments at the ORNL and West Valley, N.Y. indicate that ground surface had been uplifted by injections (deLaguna and others, 1968; Sun, 1969; Sun and Mongan, 1974; Weeren, 1974).

Sun (1969) demonstrated an example of the rational approach to the study of the uplift problem. He first assumed the host rock to be an impervious, homogeneous, isotopic, and elastic medium. He then developed a mathematical model for calculating the amount of uplift of ground surface, the separation of horizontally induced fracture, and radius of extension of fracture. From the analysis of field data, he obtained a reasonable agreement between predicted and observed data (Sun, 1969; Sun and Mongan, 1974). Several examples of predicted and observed uplift data are shown in the case histories in the Appendix. The uplift, $\overline{W}$, and the horizontal displacement, U, of the ground surface, the maximum fracture separation, B, and the radius of the induced fracture, a', can be estimated by the following equations (Sun, 1969):

$$\overline{W} = B(\sqrt{k}\sin(\theta/2)) - [(h/a\sqrt{k})\cos(\theta/2)], \tag{47}$$

$$U = \frac{Brh}{a}\{(a + a\sqrt{k}\sin(\theta/2))/[(h + a\sqrt{k}\cos(\theta/2))^2 + (a + a\sqrt{k}\sin(\theta/2))^2] - [h\sqrt{k}\cos(\theta/2) - a\sqrt{k}\sin(\theta/2) + ak\cos\theta]/[(h\sqrt{k}\cos(\theta/2) - a\sqrt{k}\sin(\theta/2) + ak\cos\theta)^2 + (a\sqrt{k}\cos(\theta/2) + h\sqrt{k}\sin(\theta/2) + ak\sin\theta)^2]\}, \tag{48}$$

$$B = 8(1-\nu^2)(P_P - \sigma_z)\alpha^2 a/\pi E, \tag{49}$$

$$(1-\alpha^2)^{1/2} = (P_P - \sigma_z)/P_P, \tag{50}$$

and

$$a = a'/\alpha = \{3EQ/[16(1-\nu^2)\alpha^5(P_P - \sigma_z)]\}^{1/3}, \tag{51}$$

where

$k = [(r^2/a^2 + h^2/a^2 - 1)^2 + (2h/a)^2]^{1/2}$;
θ = arc cot $[(r^2 + h^2 - a^2)/2ah]$;
h = depth of the induced fractures;
r = radial distance from the injection well;
a' = radius of an induced fracture from the injection well;
a = maximum radius of stress-altered fracture region, shown in figure 6;
$\alpha = a'/a$;
ν = Poisson ratio;
E = Young's modulus;
P_P = injection pressure at the injection depth;
σ_z = vertical stress or overburden pressure; and
Q = total injection volume.

Comparison of the predicted value and core-hole data observed at the ONRL site indicated that the fracture area is sometimes elongated instead of circular (fig. 2). However, no grout sheet was observed beyond an area twice the calculated radius (Sun, 1969). Therefore, for safety monitoring purposes, some observation wells

should be constructed in a perimeter four to five times the calculated radius of the induced fractures. None of the injected grout sheets should be detected by gamma-ray logs as extending to those wells.

INTERPRETATION OF GAMMA-RAY LOGS

If bedding-plane fractures are induced, then the altitude of the induced fracture near an observation well can be estimated by the following equation:

$$\text{Fracture altitude} = \text{altitude of the injection level} \pm C \tan\theta, \quad (52)$$

where C is the horizontal distance measured perpendicular to the average strike of the shale beds between the injection altitude and the altitude of an induced fracture at the observation well; θ is the average dip angle. A plus or minus sign should be used according to the direction of dip. For observation wells located updip of the injection well, it should be a plus sign; otherwise it is a minus sign. The estimated altitude should be compared with the observed altitude of the induced fracture determined from gamma-ray logs made in the observation wells after an injection. Because of well deviations, the comparison of estimated and observed fractures should be made at the time after the true horizontal position and true depth are calculated from well-deviation records. The intensity of gamma-ray activity that indicates induced fractures reaching the observation well should be several orders of magnitude higher than the background value of the host rock. If the amplifier range of the logging unit is kept constant, the evidence of induced fractures reached the well should be clearly indicated by gamma-ray logs made in observation wells before and after an injection.

SAFETY CONSIDERATIONS

The potential for waste migration during and after waste injections and other adverse effects resulting from waste disposal, such as the triggering of earthquakes must be evaluated when the method of disposal of radioactive waste by grout injection and hydraulic fracturing is considered among other alternatives.

Ideally, after solidification of the grout, the injected wastes should become an integral part of the host rock and remain there as long as the host rock is not subjected to severe erosion and dissolution. However, a number of questions concerning the safety of the method have been raised. They are (1) whether liquid waste might separate from the grout during and after injection and migrate through existing fractures or joints, (2) whether waste can be leached out of grout sheet by ground water, (3) whether the method for determining with certainty that the orientation of the induced fractures is horizontal, or nearly so, are reliable, (4) whether grout injection and hydraulic fracturing have potential for triggering earthquakes, and (5) what is the safe isolation time required for the disposed wastes. These concerns are discussed in the following sections.

WASTE MIGRATION DUE TO SEPARATION OF LIQUID FROM GROUT

One of the major concerns about waste migration and this disposal technique is radionuclide-loss from the injected grout while it is still in the liquid phase and radionuclide-loss from the fraction remaining in the liquid phase through phase separation during solidification. These two losses can be eliminated or reduced through a correct solids to waste mixing ratio and by carefully selecting solids through laboratory experiments with simulated or actual wastes. The criteria of mixing are as follows:

1. Slurry consistency must remain stable and pumpable for several hours during injection but must permit setting soon after completion of injection (24 hours or less).
2. Free liquid separated from grout during solidification should be as low a quantity as possible and should contain no, or only very small, quantities of radionuclides.
3. The leach rate of radionuclides from solidified grout should be low and decrease rapidly with time.
4. Within a tolerable compressive strength of grout, the weight of cement added to waste should be kept low, thus reducing cost and increasing volume of waste to be disposed.

The criteria can be achieved by a proper selection of cement and additives and of correct mixing ratios, as determined in a laboratory.

Experiments at the ORNL indicate that both radiocesium and radiostrotium reacted rapidly with solids in mixing. Very little ^{90}Sr (less than 2 percent) was found in the liquid phase after contact with solids. The rapid reaction of ^{90}Sr with small particles might be explained on the basis of the composition of Portland cement. Portland cement is composed mainly of calcium silicates, which react with water to form hydrated calcium silicates. Since strontium and calcium have similar chemical behavior, ^{90}Sr rapidly entered into the reactions that are common to calcium (deLaguna and others, 1968).

Retention of radiocesium by cement solids has proved to be unsatisfactory (about 70 percent). Bentonite was used as an additive at the ORNL to provide the capacity for the retention of radiocesium in slurry and for reducing fluid loss; however, under a high molarity of salt

solutions – in excess of 5 *M* – bentonite flucuates and is ineffective as a suspending agent. Attapulgite, known to be more effective than bentonite as a suspending agent in such solutions, was therefore substituted for bentonite. To further improve radiocesium retention, illite clay was added to the ORNL wastes.

Pozzolanic material, such as fly ash, is also found to be effective and can improve radiostrontium retention and reduce required amounts of cement, thus reducing the cost of the mix.

Length of pumping time can be controlled by adding different amounts of delta gluconolactone (DGL). Phase separation was found to be highly sensitive to the composition of waste and of solids. Both DGL and attapulgite were found to affect phase separation. The greater the content of attapulgite, the lower the phase separation, but also the more viscous the slurry. Greater amounts of DGL can reduce the slurry viscosity – however, at the expense of increase phase separation. The ultimate blend of solids can only be determined through laboratory experiments. The following mixing procedure recommended by the ORNL for wastes similar to those produced in the ORNL is listed for reference (deLaguna and others, 1969; H. O. Weeren, written commun., 1980).

1. Sample and analyze the waste to be injected.
2. Prepare a solids blend containing the following materials:

	Percent by weight
Portland cement type I, gypsum retarded or equivalent	38.45
Pozzolan	38.45
Attapulgite gelling clay	15.38
Illite	7.69
Delta gluconolactone	0.03

3. Prepare a slurry using 550 cm^3 of waste in 1-L blender. Add the solids, using 15 seconds to pour into a blender and 35 seconds of additional stirring. Record the amount of solids. The blender is calibrated to rotate at 2,000 rpm at no load.
4. Pour the slurry into a 250-mL graduate to estimate the phase separation.
5. After 2–4 hours, determine the phase separation. The increase or decrease in the proportion of solids is dependent on the phase separation. If no phase separation occurs, decrease the amount of solids to obtain the minimum solids content necessary to prevent phase separation. Generally a 5–10 percent change in solids is sufficient to obtain a slurry having no phase separation.
6. Increase the addition of solids by 10 percent over the amount that yielded no phase separation, and mix as in step 3. (The increase over the minimum amount is suggested to allow a ± 10 percent in the control of the solids-to-liquid proportioning.) Determine the pumpable time (thickening time) of the slurry by measuring its viscosity.
7. Increase or decrease the delta gluconolactone (DGL) content to obtain the desired pumpable time; redetermine the phase separation if the DGL content is changed. The desired pumpable time depends on the volume of waste to be disposed of and the rate of injection.

No matter how well or carefully the slurry is mixed, phase separation is unavoidable; however, the quantity of the unbound water in the injection zone can be reduced by back bleeding after the grout solidifies. Experience at the ORNL indicates that the concentration of radionuclides in bleed-back water is low (table 16). In rocks having low permeability, such as shale, unbound water probably would be trapped in the grout sheets; this has been indicated during drilling at the ORNL site. If some of the unbound water does move away from the grout sheet, then the small quantity of radionuclides in the unbound water would probably be further reduced by adsorption or by decay and dispersion if the flow path from the disposal site to the discharge area is long. Nevertheless, the disposal site should be monitored by a series of observation wells constructed along the perimeter of the disposal site, as well as in the overlying formation above the injection zone.

LEACHING OF GROUT BY GROUND WATER

In order to reduce the leaching of radionuclides from the grout by ground water to the lowest rate possible, studies using different minerals as additives over a wide range of particle sizes and size distribution are important. The overall results of the ORNL grout mixture tested by a modified IAEA (International Atomic Energy Agency) 1971 testing method (Moore and others, 1975; Moore, 1976) indicated that the grout could give leach rates comparable with those obtained for waste incorporated in borosilicate glasses. The leach rates of the radionuclides contained in the ORNL waste are in the following order: Cs > Sr > Cm > Pu. The maximum amount of radionuclides leached from the grout sheet seems independent of the type of water, such as tap water, ground water, or sea water (Moore and others, 1975). The cumulative fraction of cesium and strontium leached from grout depended on the time and manner of curing. The amount of leached radionuclides decreased with an increase in curing time. Short-term (140 days) leach studies at the ORNL indicated that increasing the overall waste concentration had little effect on the leachability of strontium or cesium (Moore, 1976).

Core grout (cured underground for about 10 months) was also used in leaching studies at the ORNL. Because the thin grout sheets in the core did not have a uniform

geometry, the grout was ground and sieved, and only those particles passing a mesh screen having a 250-μ-diameter hole were used in the studies. Leaching was carried out in plastic bottles containing 1 g of solids per 100 mL of distilled water. The results from use of grout containing illite show that less than a few hundredths of a percent of the injected amount of radionuclides was leached out of the grout during a 504-hour test (Tamura, 1971). Conditions of these leaching studies deviate greatly from those in the ground. Cores of the grout sheets obtained at the ORNL indicate that the solidified grout sheets are strongly integrated with shale (see fig. 1); therefore, the chance for groundwater to move through the solidified grout sheets is probably less than that implied by fine particles of the ground grout in contact with distilled water. On the other hand, the laboratory studies were made over extremely short periods, and the results may be different from those of long-term leaching by ground-water flow. However, the low permeability, high ion-exchange and adsorption capacity of shale, size of the shale body (several hundreds of meters in thickness), and low concentration of radionuclides in liquid during phase separation and leaching suggest that the possibility of contamination of the biosphere by injected radioactive wastes is likely to be remote. If a very low concentration of radionuclides did reach a water source, then the concentration of radionuclides would be further diluted by that water body.

CREATION OF VERTICALLY ORIENTED FRACTURES

Careful monitoring of injection pressure during injection time will give indirect indication of the orientation of induced fractures. Any sudden drop in injection pressure, especially when the pressure is near or below the estimated vertical stress, will be a positive signal to stop the injection in order to evaluate the cause. Gamma-ray logs made in observation wells will give positive evidence of the fracture orientation, and the more observation wells used the better the determination of orientation. The possibility of inducing vertical fractures should be fully evaluated during site investigations and carefully monitored during each injection.

TRIGGERING EARTHQUAKES BY HYDRAULIC FRACTURING

In 1965, Evans (1966) showed a correlation between pressure of fluid injection, the volume of liquid wastes injected into a 3,660-m disposal well at the Rocky Mountain Arsenal, Denver, Colo., and the number of earthquakes reported in the Denver area. He concluded that the waste injection at the arsenal well had caused the Denver area earthquake. In December 1965, the U.S. Geological Survey, in cooperation with the Colorado School of Mines, Regis College, and the University of Colorado, undertook a series of studies to determine the relationship, if any, between the disposal of wastes in the arsenal well and the location and frequency of earthquakes. The results of these studies supported Evans' conclusion (Healy and others, 1966).

In February 1966 the disposal well was shut down. Despite the cessation of injection, earthquakes continued to plague the Denver area through August 1967. Two earthquakes (magnitude 5.0 of Richter scale, April 10, 1967, at a depth of 5 km), the largest in Denver area since 1882, were strongly felt throughout the Denver metropolitan area. Because these seismic events occurred 14–18 months after termination of the well injection, Major and Simon (1968) concluded that the correlation between fluid injection and earthquake occurrence upon which Evans based his view had been reduced. The overall number of earthquakes in the Denver area, however, has declined exponentially since 1967. This reduction of earthquake occurrence suggests that tremors in the Denver area were caused by release of tectonic stresses and that deep-well injection was simply the triggering force (Sun, 1977).

In 1969, the U.S. Geological Survey in cooperation with the Chevron Oil Co. studied the relationship between fluid injection for water flooding of the Rangely Oil Field, Rio Blanco County, Colo., and the number of earthquakes in the area and installed 16 seismographs around the oil field. It concluded that (1) there is an apparent relation between the number of earthquakes and the annual volume of injected fluid, (2) changes in the quantity of injection of fluid are related to changes in the number of earthquakes recorded, and (3) parts of the field lacking natural faults do not produce earthquakes, even when the pore pressures in the rock are quite high (Gibbs and others, 1972). In November 1970, four injection wells straddling a fault zone were backflowed to reduce the pore pressure in the hypocentral region. The wells were backflowed and pumped for a period of 6 months. Within a very short time following the initiation of backflowing, earthquake occurrence within an area of about a 900-m radius of the backflowing wells decreased markedly in frequency and ultimately almost ceased (Raleigh, 1972).

From the foregoing discussion it can be concluded that injection of fluid does have the potential to trigger earthquakes under certain conditions. It is important to know if disposal of radioactive wastes through grout injection and hydraulic fracturing also has the potential to trigger earthquakes. The following discussion evaluates this potential.

HISTORICAL MANMADE EARTHQUAKES

Manmade earthquakes associated with dam construction have long been acknowledged and well documented. Carter (1945, 1970) associated earthquakes near Hoover Dam, Boulder City, Nev., with the filling of Lake Mead. He suggested that the earthquakes around Lake Mead were directly or indirectly a result of fluctuation in surficial crustal loading. Anderson and Laney (1975), however, offered a different explanation. They suggested that a hydraulic connection between the lake water and the deep aquifer system, which includes buried faults, is needed to cause the release of seismic energy in the Lake Mead area. Where hydraulic connection between the lake and the aquifer is prevented by strata of very low permeability (evaporites), as in the eastern basin, seismicity does not occur despite the large volume of impounded water in the area.

The Palisades Reservoir, in southeast Idaho, also triggers earthquakes. Epicenters are concentrated near the reservoir, and the number of earthquakes is related to water fluctuations in the reservoir. Schleicher (1975) suggested that the area around the Palisades Reservoir would almost certainly be subject to earthquakes even if the reservoir were not there. The effect of construction of the reservoir was to trigger faulting when tectonic stresses were on the verge of causing it anyway.

Earthquakes attributed to the fluctuation of water levels and the filling of reservoirs are also reported and documented in other parts of the world. For example, Marathon and Kremasta Lakes in Greece, Vajont Dam in Italy, Lake Eucumbene in the Snowy Mountains in Australia, Kariba Dam in Rhodesia, and Koyna Dam in India were all in areas in which small to moderate earthquakes began a few months after river closure (Carter, 1970). All these reservoirs are located in areas that were generally considered aseismic; however, potentially active or active faults are found in all these reservoir sites (Carter, 1970).

Even river flooding has been related to the occurrence of earthquakes. McGinnis (1963) observed that an abnormally large number of earthquake epicenters have been detected within 320 km of New Madrid, Mo. The area is composed of extensive alluvial valleys, is extensively fractured, and shows evidence of major and minor faults. McGinnis concluded that the correlation of the mean monthly river stage and the earthquake frequency in the alluvial valleys indicates that an increase in the rate of change of water-load variation tends to increase earthquake activity.

MECHANISM FOR TRIGGERING EARTHQUAKES

The mechanism by which earthquakes are triggered by man's activity is not clearly known. However most investigators (Healy and others, 1966; Carter, 1970; Gibbs and others, 1972; Schleicher, 1975) generally agree that the following conditions are associated with manmade earthquakes:

1. Rock at the site must be under high stress and near its breaking strength or on the brink of sliding on a preexisting fault plane or planes.
2. The rock is possibly associated with a potentially active fault or faults.
3. Change of pore pressure in the rock is probably the triggering force.

If rock pores are saturated with water, then the rock is also subject to a hydraulic pressure, P_0, throughout the interconnected pores. The three principal earth stresses, σ_1, σ_2, σ_3 will be reduced to $\sigma_1 - P_0$, $\sigma_2 - P_0$, and $\sigma_3 - P_0$, and the normal and shear stresses acting across a plane perpendicular to σ_1, σ_3 plane and making an arbitrary angle α with the direction of the least principal stress, σ_3, are given by (Hubbert and Rubey, 1959) as

$$\sigma = \frac{\sigma_1 + \sigma_3}{2} + \frac{\sigma_1 - \sigma_3}{2} \cos 2\alpha - P_0 \tag{53}$$

and

$$\tau = \frac{\sigma_1 - \sigma_3}{2} \sin 2\alpha. \tag{54}$$

The relation of pore pressure to rock failure is shown in figure 12. At first, the rock is assumed to be dry and under three principal stresses of differing magnitude and is not subject to fracture. Now, without changing the magnitude of the principal stresses, let the rock be saturated with water and the pore pressure in the rock increase from 0 to P_0. From equation 53, it is seen that the diameter of the Mohr circle remains constant but that the center of the Mohr circle is moved towards the left along the normal stress axis by a distance equal to the pore pressure, P_0, as shown in figure 12. If the pore pressure is continuously increased from P_0 to $P_0 + \triangle P_0$, the diameter of the Mohr circle still remains constant, but the center of the circle is translated farther left by a distance equal to the increment of the pore pressure $\triangle P_0$. Obviously, if the pore pressure in the rock increases sufficiently, the Mohr circle will be continuously moved to the left until it touches the Mohr envelope (line of fracture), and then the rock starts to fracture (Hubbert and Ruby, 1960; Jaeger, 1962).

Injection of fluid and seepage from reservoirs certainly will increase pore pressure in the rock. If rock in the area of a potentially active fault or faults has already been stressed to the verge of breaking, then the increasing pore pressure would positively contribute to the fracturing or slippage of the rock. Fracturing and (or) slippage of rock would release elastic energy that had already been stored in the rock, thus triggering earth-

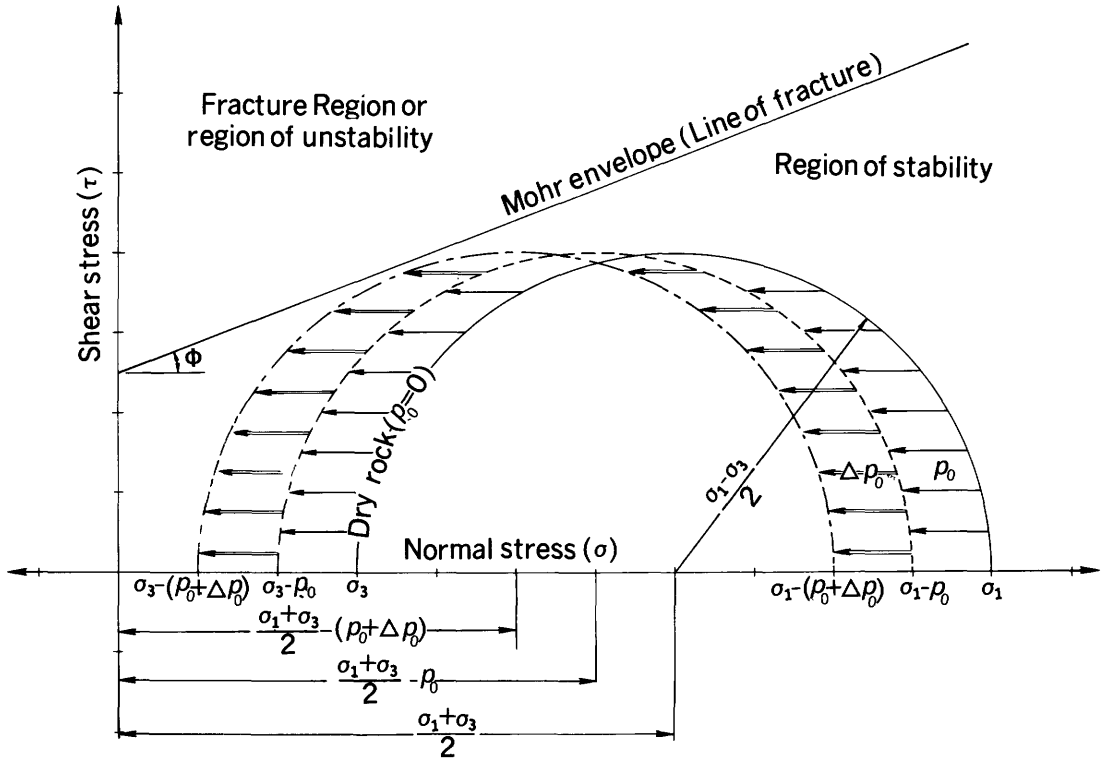

FIGURE 12. – Diagram of Coulomb-Navier fracture criteria showing how rock failure can be affected by an increase in pore pressure (principal stresses are kept constant).

quakes. Therefore, fluid injection and reservoir seepage would simply modify earthquake timing, intensity, and location when the rock is already stressed to the verge of breaking by tectonic stresses or has the potential to slide on a preexisting fault plane or planes.

THE POSSIBILITY OF TRIGGERING EARTHQUAKES BY HYDRAULIC FRACTURING AND GROUT INJECTION

The mechanism of disposing radioactive waste by grout injection and hydraulic fracturing is different from that of disposing by the injection of fluid. The injected grout becomes an integral part of the host rock after solidification which occurs within one or two days. Owing to the very low permeability (10^{-6} D) of the selected host rock and the quick solidification of the grout, pore pressure in the host rock is unlikely to be increased by injections except locally and for short times. Even during the injection stage, when the waste grout is in its liquid state, the injected waste grout is confined in the induced bedding-plane fractures because of the low permeability of the host rock and the high viscosity of the grout. In addition, the disposal sites are to be located in areas free of potentially active faults and lacking very closely spaced fractures and joints. Because the two required and necessary conditions for triggering earthquakes – potentially active faults and an increase of pore pressures – are not associated with the waste-grout-injection technique, the possibility of triggering earthquakes by grout injection and hydraulic fracturing does not occur.

In an attempt to obtain seismic signals during grout injection and hydraulic fracturing at the ORNL, at the first two of the four injections in 1972, an array of six-microseismometers was installed in an area approximately 450 m in diameter with the injection well in the center. During the last two injections, the diameter of the seismometer array was increased to 600 m, and a downhole seismometer was installed during the fourth injection to reduce surface noise and to improve sensitivity. All the four injections were made at a depth of 254 m. No meaningful seismic signals were obtained from any of the four injections (Weeren, 1974). This indicates that seismic signals generated by grout injection and hydraulic fracturing, if any, are so small that they can not be differentiated from ambient ground noise. The inconclusive seismic result is expected because the energy required to induce fractures along weakly bedded shale to overcome the tiny cohesive force along the shale bedding planes is small (Sun and Mongan, 1974).

In conclusion, no earthquake should be triggered by hydraulic fracturing and grout injection, either during or after injection.

ISOLATION TIME REQUIRED FOR INJECTED WASTES

The length of isolation time required for injected waste is primarily dependent on the decay periods of radionuclides contained in the disposed waste and can be estimated by the following equation (U.S. Bureau of Radiological Health, 1970):

$$C = C_0 e^{-0.693n}, \quad (55)$$

where C_0 is the activity of a particular radionuclide contained in the waste at the disposal time; C is the activity remaining after a time interval, t; n is the number of half-lives, $n = t/T_{1/2}$; $T_{1/2}$, is the half-life of the radionuclide.

If the safe activity of radionuclides is assumed to be one millionth (10^{-6}) of its initial activity, then the required containment time can be calculated as 20 half-lives of a particular radionuclide (eq 55). For example, for waste containing 99 percent of ^{90}Sr and ^{137}Cs, only 600 years of isolation is required. For the radionuclides having half-lives of only 28 and 30 years, respectively, the projection of geologic and hydrologic factors controlling such processes as erosion and leaching for the isolation period can probably be estimated with confidence on the basis of geologic and hydrologic knowledge and conceptual models. However, if ^{129}I is the major concern among the radionuclides, then even its one half-life (17×10^6 years) is too long for any reliable prediction of the isolation time.

CONCLUSION

In a shale formation characterized by directional tensile strength, the pressure needed to induce a vertical fracture across horizontally orientated bedding planes is much greater than the pressure needed to form bedding-plane fractures. Existing joints and (or) high-angle natural fractures may be extended by pressure if they are intercepted by induced bedding-plane fractures; however, vertical extension will cease where these natural fractures or joints intercept weak bedding planes. It is therefore concluded that horizontal bedding-plane fractures can be induced hydraulically in a nearly horizontally bedded shale at depths shallower than 1,000 m; deeper, the advantage of directional tensile strength may be overcome by the large overburden pressure. The injection experience at Oak Ridge, Tenn., and West Valley, N.Y., supports the conclusion that induced fractures may migrate up and down as much as 20 m from the injected altitude over a distance several hundreds of meters from an injection well (see the Appendix).

The orientation of the induced fractures can be indirectly monitored by observing injection pressures during injection time and by measuring the pressure decay of water injections and the uplift of the ground surface after injections. The orientation, also can be confirmed by gamma-ray logs made in observation wells before and after each injection if the injected fluid or grout contains gamma-ray-emitting radionuclides.

At least one water-injection test and one grout-injection test should be made during a site evaluation. Pressure-decay data obtained from a water injection can be used, not only to evaluate the orientation of induced fractures and the permeability of the injection shale but also to determine the effective stress normal to the fracture plane. The vertical stress may or may not be equal to the calculated overburden pressure. At Oak Ridge, Tenn., the vertical earth stress is about twice that of the calculated overburden pressure, as indicated by the pressure-decay data for water injections (see the case histories for Oak Ridge in the Appendix). A grout injection not only confirms the conclusions made after a water injection but also simulates conditions encountered during waste injections.

Intermediate-level radioactive wastes (specific activity $< 6 \times 10^3$ μCi/mL, consisting mainly of radionuclides having half-lives of less than 50 years, such as strontium and cesium) mixed with cement and ion-exchange and adsorption materials can be injected into shale by hydraulic-fracturing and grout injections. After the solidification of the grout, the wastes are immobilized and become an integral part of the shale and will remain at depth as long as the shale is not subjected to severe erosion and dissolution. The injected wastes will thus be kept within a known horizon. It can be concluded that grout disposal of radioactive wastes by hydraulic fracturing in shale is safe and feasible if the shale formation is carefully selected, tested, and evaluated and if the grout is properly mixed and the injection is cautiously conducted. However, risk analyses comparing with other alternatives should be carefully evaluated before the grout injection method is selected.

At least four observation wells made with strong tubing and pressure cemented should be constructed at a radial distance of 50 m in four directions from the injection well for determining the orientation of induced fractures after injections. Four or more additional observation wells should be constructed at radial distances far enough away from the injection well so that they are at a distance greater than that expected to be reached by any grout sheet. The distance beyond which the grout is not expected to extend can be estimated by equation 51. If the injected wastes contain gamma-ray-emitting ra-

dionuclides, these observation wells can be used for monitoring safety. More observation wells will increase confidence that the injected wastes are isolated in a known horizon.

Because a waste-disposal site must be in a geologically stable area lacking potentially active faults and because there is no general and extensive increase in pore pressure of the rock mass due to grout injections, there is no danger that grout injection would trigger earthquakes during or after the injections.

Waste disposal is conducted by injections in several stages through different levels. The first series of injections starts at the greatest depth, then the injection zone is plugged off by cement. The next series of injections are started at a suitable distance above the first injection zone. The repeated use of the injection well distributes the costs of constructing injection and monitoring wells over many injections, thereby making hydraulic fracturing and grout injection economically attractive as a method for disposing intermediate-level radioactive wastes.

REFERENCES CITED

Anderson, R. E., and Laney, R. L., 1975, The influence of late Cenozoic stratigraphy on distribution of impoundment-related seismicity at Lake Mead, Nevada-Arizona: U.S. Geological Survey Journal of Research, v. 3, no. 3, p. 337–343.

Badgley, P. C., 1965, Structural and tectonic principles: New York, Harper & Row, 521 p.

Barenblatt, G. I., 1962, The mathematical theory of equilibrium cracks in brittle fracture, *in* Dryden, H. L., and Von Karman, T., eds., Advances in applied mechanics: New York, Academic Press, p. 55–129.

Bear, Jacob, 1972, Dynamics of fluid in porous media: New York, American Elsevier, 764 p.

Belter, W. G., 1972, Deep disposal systems for radioactive wastes, *in* Cook, T. D., ed., Underground waste management and environmental implications: American Association of Petroleum Geologists Memoir 18, p. 341–354.

Bieniawski, Z. T., 1967, Mechanism of brittle fracture of rock: International Journal of Rock Mechanics and Mining Sciences, v. 4, p. 395–406.

Bredehoeft, J. D., England, A. W., Stewart, D. B., Trask, N. J., and Winograd, I. J., 1978, Geologic disposal of high-level radioactive wastes–Earth science perspectives: U.S. Geological Survey Circular 779, 15 p.

Brooker, E. W., and Ireland, H. O., 1965, Earth pressure at rest related to stress history: Canadian Geotechnical Journal, v. 2, no. 1, p. 1–15.

Bugbee, J. M., 1953, Discussion of rock rupture as affected by fluid properties by Scott, P. P., Jr., Bearden, W. G., and Howard, G. E.: American Institute of Mining, Metallurgical, and Petroleum Engineers Transactions, v. 198, p. 111–124.

Carter, D. S., 1945, Seismic investigation in the Boulder Dam area, 1940–1944, and the influence of reservoir loading on local earthquake activity: Seismological Society of America Bulletin, v. 35, p. 175–192.

——— 1970, Reservoir loading and local earthquakes: Geological Society of America Engineering Geology Case Histories, no. 8, p. 51–61.

Chenevert, M. E., and Gatlin, Carl, 1965, Mechanical anistropies of laminated sedimentary rocks: Journal of Petroleum Engineers, v. 5, no. 1, p. 67–77.

Clark, J. B., 1949, A hydraulic process for increasing the productivity of wells: American Institute of Mining, Metallurgical, and Petroleum Engineers Transactions, 186, p. 1–8.

Cottrell, A. H., 1964, The mechanical properties of matter: New York, John Wiley, 430 p.

Daneshy, A. A., 1967, Initiation and extension of hydraulic fractures in rocks: Journal of Petroleum Engineers, September, p. 310–318.

——— 1973, A study of inclined hydraulic fractures: Journal of Petroleum Engineers, April, p. 61–69.

Davis, C. V., and Sorensen, K. E., 1969, Handbook of applied hydraulics: New York, McGraw-Hill, p. 2–6.

Davis, S. N., 1969, Porosity and permeability of natural materials, *in* DeWiest, R. J. M., ed., Flow through porous media: New York, Academic Press, p. 53–89.

deLaguna, Wallace, 1972, Hydraulic fracturing test at West Valley, New York: Oak Ridge National Laboratory, ORNL–4827, 64 p.

deLaguna, Wallace, Tamura, Tsuneo, Weeren, H. O., Struxness, E. G., McClain, W. C., and Sexton, R. C., 1968, Engineering development of hydraulic fracturing as a method for permanent disposal of radioactive wastes: Oak Ridge National Laboratory, ORNL–4259, 261 p.

deLaguna, Wallace, Weeren, H. O., Binford, F. T., Witkowski, E. J., and Struxness, E. G., 1971, Safety analysis of waste disposal by hydraulic fracturing at Oak Ridge: Oak Ridge National Laboratory, ORNL–4665, 41 p.

Eardley, A. J., 1951, Structural geology of North America: New York, Harper & Brothers, 623 p.

Evans, D. M., 1966, The Denver area earthquakes and the Rocky Mountain Arsenal disposal well: Mountain Geologist, v. 3, no. 1, p. 23–26.

Fenner, R., 1938, Investigation on analysis of rock pressure [in German]: Gluckauf, v. 74, no. 32, p. 681–695.

Freeze, R. A., and Cherry, J. A., 1979, Groundwater: New Jersey, Prentice-Hall, 604 p.

Gatlin, Carl, 1960, Petroleum engineering–drilling and well completions: New Jersey, Prentice-Hall, 341 p.

Gibbs, J. F., Healy, J. H., Raleigh, B. C., and Coakley, John, 1972, Earthquakes in the oil field at Rangely, Colorado: U.S. Geological Survey open-file report, 27 p.

Goodier, J. N., 1968, Mathematical theory of equilibrium cracks, *in* Liebowitz, Harold, ed., Fracture: New York, Academic Press, v. 2, p. 1–66.

Haimson, Bezallel, 1968, Hydraulic fracturing in porous and nonporous rock and its potential for determining in-situ stresses: Minneapolis, University of Minnesota, unpublished Ph.D. dissertation, 234 p.

Haimson, Bezallel, and Fairhurst, Charles, 1969, Hydraulic fracturing in porous-permeable materials: Journal of Petroleum Technology, July, p. 812–817.

Hantush, M. S., 1964, Hydraulics of wells, *in* Chow, V. T., ed., Advances in hydrosciences, v. 1: New York, Academic Press, p. 281–432.

Harrison, Eugene, Kieschnick, W. F., Jr., and McGuire, W. J., 1954, The mechanics of fracture induction and extension: American Institute of Mining, Metallurgical, and Petroleum Engineers Transactions, v. 201, p. 252–263.

Healy, J. H., Jackson, W. H., and Van Schaack, J. R., 1966, Microseismicity studies at the site of the Denver earthquakes in geophysical and geological investigations relating to earthquakes in Denver area, Colorado: U.S. Geological Survey open-file report, pt. 5, 19 p.

Heck, E. T., 1955, Fractures and joints: Producers Monthly, February, p. 20–23.

——— 1960, Hydraulic fracturing in light of geologic conditions: Producers Monthly, September, p. 12–13, 16–19.

Hobbs, D. W., 1964, The tensile strength of rocks: International Journal of Rock Mechanics and Mining Sciences, v. 1, p. 385–396.

Howard, G. C., and Fast, C. R., 1970, Hydraulic fracturing: American Institute of Mining, Metallurgical, and Petroleum Engineers Monograph, v. 2, 203 p.

Howard, J. H., 1966, Vertical normal stress in the Earth and the weight of overburden: Geological Society of America Bulletin, v. 77, p. 657–660.

Hubbert, M. K., 1957, Reply to Reynolds, J. J., and Coffer, H. F., Discussion on mechanics of hydraulic fracturing by Hubbert, M. K., and Willis, D. G., 1957: American Institute of Mining, Metallurgical, and Petroleum Engineers Transactions, v. 210, p. 153–166, 167–168.

——— 1971, Natural and induced fracture orientation: American Association of Petroleum Geologists Memoir, 18, p. 235–238.

Hubbert, M. K., and Rubey, W. W., 1959, Role of fluid pressure in mechanics of overthrust faulting, part 1: Geological Society of America Bulletin, v. 70, no. 2, p. 155–166.

——— 1960, Role of fluid pressure in mechanics of overthrust faulting – A reply: Geological Society of America Bulletin, v. 71, no. 5, p. 617–628.

Hubbert, M. K., and Willis, D. G., 1957, Mechanics of hydraulic fracturing: American Institute of Mining, Metallurgical, and Petroleum Engineers Transactions v. 210, p. 153–166.

Interagency Review Group on Nuclear Waste Management, 1979, Report to the President by the Interagency Review Group on Nuclear Waste Management: U.S. Department of Energy, TID–29442, 149 p.

International Atomic Energy Agency, 1971, Leach testing of immobilized radioactive waste solids, a proposal for a standard method, Hespe, E. D., ed.: Atomic Energy Review, v. 9, no. 1, p. 195–207.

Jaeger, J. C., 1962, Elasticity, fracture and flow with engineering and geological applications: New York, John Wiley, 208 p.

Jaeger, J. C., and Cook, N. G. W., 1969, Fundamentals of rock mechanics: London, Methuen & Co., 513 p.

Kenny, Peter, and Campbell, J. D., 1967, Fracture toughness: Progress in Material Science, v. 13, 181 p.

Kunz, V. J., 1971, The fundamentals of crack mechanics – a critical review: Technica, v. 17, p. 1535–1557.

Lahee, F. H., 1952, Field geology: New York, McGraw-Hill, 883 p.

Lamont, Norman, and Jessen, F. W., 1963, The effects of existing fractures in rocks on the extension of hydraulic fracturing: American Institute of Mining, Metallurgical, and Petroleum Engineers Transactions, v. 228, p. 203–209.

McClain, W. C., and Meyers, H. O., 1970, Seismic history and seismicity of the southeastern region of the United States: Oak Ridge National Laboratory, ORNL–4582, 46 p.

McGarr, Arthur, and Gay, N. C., 1978, State of stress in the Earth's crust: Annual Review of Earth and Planetary Science, v. 6, p. 405–436.

McGinnis, L. D., 1963, Earthquakes and crustal movement as related to water load in the Mississippi Valley region: Illinois State Geological Survey Circular 334, 20 p.

McMaster, W. M., 1963, Geologic map of the Oak Ridge Reservation, Tennessee: Oak Ridge National Laboratory, ORNL–TM–713, 23 p.

——— 1967, Hydrological data for the Oak Ridge area, Tennessee: U.S. Geological Survey Water-Supply Paper 1839–N, 60 p.

McMaster, W. M., and Waller, H. D., 1965, Geology and soils of Whiteoak Creek basin, Tennessee: Oak Ridge National Laboratory, ORNL–TM–1108, 37 p.

Magara, Kinji, 1978, Compaction and fluid migration – practical petroleum geology: New York, Elsevier Scientific Publishing Co., 319 p.

Major, M. W., and Simon, R. B., 1968, A seismic study of the Denver (Derby) earthquakes: Colorado School Mines Quarterly, v. 63, no. 1, p. 9–55.

Melton, L. L., and Saunders, C. D., 1957, Rheological measurements of non-Newtonian fluids: American Institute of Mining, Metallurgical, and Petroleum Engineers Transactions, v. 210, p. 196–201.

Moore, J. G., 1976, Continuation of cesium and strontium leach studies, pt. 2 *of* Development of cementitious grouts for the incorporation of radioactive wastes: Oak Ridge National Laboratory, ORNL–5142, 144 p.

Moore, J. G., Godbee, H. W., Kibbey, A. H., and Joy, D. S., 1975, Leach Studies, pt. 1 *of* Development of cementitious grouts for the incorporation of radioactive waste: Oak Ridge National Laboratory, ORNL–4962, 111 p.

Moye, D. G., 1958, Rock mechanics in the investigation and construction of T.1 underground power station, Snowy Mountains, Australia: Geological Society of America Engineering Geology Case Histories, no. 3, p. 13–44.

Obert, Leonard, and Duvall, W. I., 1967, Rock mechanics and the design of structures in rock: New York, John Wiley, 650 p.

Ostle, Bernard, 1954, Statistics in research; basic concepts and techniques for research workers: Iowa State College Press, 487 p.

Overbey, W. K., Jr., and Rough, R. L., 1968, Surface studies predict orientation of induced formation fractures: Producers Monthly, June, p. 16–19.

Perkins, T. K., 1967, Application of rock mechanics in hydraulic fracturing theories: 7th World Petroleum Congress, Mexico, Proceedings, v. 3, p. 75–84.

Perkins, T. K., and Krech, W. W., 1968, The energy balance concept of hydraulic fracturing: Journal of the Society of Petroleum Engineers, March, p. 1–12.

Prickett, T. A., and Lonnquist, C. G., 1971, Selected digital computer techniques for ground-water resource evaluation: Illinois State Geological Survey Bulletin, no. 55, 62 p.

Raleigh, B. C., 1972, Earthquakes and fluid injection: American Association of Petroleum Geologist Memoir 18, p. 273–279.

Reichmuth, D. R., 1968, Point load testing of brittle materials to determine tensile strength and relative brittleness: American Institute of Mining, Metallurgical, and Petroleum Engineers 9th Symposium on Rock Mechanics, April 17–19, 1967, Golden, Colo., Proceedings, p. 134–160.

Rice, J. R., 1965, Plastic yielding at a crack tip: 1st International Conference on Fracture, Japan, Proceedings, v. 1, p. 283–308.

Schleicher, David, 1975, A model for earthquakes near Palisades Reservoir, Southeast Idaho: U.S. Geological Survey Journal of Research, v. 3, no. 4, p. 393–400.

Schumm, S. A., 1963, The disparity between present rates of denudation and orogeny: U.S. Geological Survey Professional Paper 454–H, 13 p.

Simonson, E. R., Abou-Sayed, A. S., and Clifton, R. J., 1978, Containment of massive hydraulic fractures: Society of Petroleum Engineers Journal, February, p. 27–32.

Slagle, K. A., 1962, Rheological design of cementing operations: Journal of Petroleum Technology, March, p. 323–328.

Sun, R. J., 1969, Theoretical size of hydraulically induced horizontal fractures and corresponding surface uplift in an idealized medium: Journal of Geophysical Research, v. 74, no. 25, p. 5995–6011.

——— 1973, Hydraulic fracturing as a tool for disposal of wastes in shale: American Association of Petroleum Geologists Symposium

on Underground Waste Management and Artificial Recharge, September 26–30, 1973, New Orleans, La., v. 1, p. 219–270.

——— 1976, Geohydrologic evaluation of a site for disposal of radioactive wastes by grout injection and hydraulic fracturing at Holifield National Laboratory (formerly Oak Ridge National Laboratory), Oak Ridge, Tennessee: U.S. Geological Survey Open-File Report 75–671, 77 p.

——— 1977, Possibility of triggering earthquakes by injection of radioactive wastes in shale at Oak Ridge National Laboratory, Tennessee: U.S. Geological Survey Journal of Research, v. 5, no. 2, p. 253–262.

Sun, R. J., and Mongan, C. E., 1974, Hydraulic fracturing in shale at West Valley, New York–A study of bedding-plane fractures induced in shale for waste disposal: U.S. Geological Survey Open-File Report 74–365, 152 p.

Tamura, Tsuneo, 1971, Sorption phenomena significant in radioactive waste disposal, *in* Cook, T. D., ed., Underground waste management and environmental implications: American Association of Petroleum Geologists Memoir 18, p. 318–330.

Timoshenko, Stephen, and Goodier, J. N., 1951, Theory of elasticity: New York, McGraw-Hill, 506 p.

U.S. Bureau of Radiological Health, 1970, Radiological health handbook: U.S. Public Health Service, 458 p.

U.S. Energy Research and Development Administration (presently U.S. Department of Energy), 1977, Management of intermediate level radioactive waste, Oak Ridge National Laboratory, Oak Ridge, Tennessee–Final environmental impact statement: U.S. Energy Research and Development Administration, ERDA–1553, 3,113 p.

U.S. National Oceanic and Atmospheric Administration and U.S. Geological Survey, 1975, United States earthquakes, 1973: U.S. Department of Commerce and U.S. Department of Interior, 112 p.

Voight, Barry, 1966, Interpretation of in situ stress measurement: International Society on Rock Mechanics, 1st Congress, Lisbon, Proceedings, v. 3, p. 332–348.

Walton, W. C., 1970, Ground-water resource evaluation: New York, McGraw-Hill, 664 p.

Weeren, H. O., 1974, Shale fracturing injections at Oak Ridge National Laboratory–1972 series: Oak Ridge National Laboratory, ORNL–TM–4467, 97 p.

——— 1976, Shale fracturing injections at Oak Ridge National Laboratory–1975 series: Oak Ridge National Laboratory, ORNL–TM–5545, 69 p.

Weeren, H. O., Brunton, G. D., deLaguna, Wallace, and Moore, J. G., 1974, Hydrofracture site proof study at Oak Ridge National Laboratory: Oak Ridge National Laboratory, ORNL–TM–4713, 43 p.

Winograd, I. J., 1974, Radioactive waste storage in the arid zone: American Geophysical Union Transactions, v. 55, no. 10, p. 884–894.

Youash, Y. Y., 1965, Experimental deformation of layered rocks: University of Texas, Austin, unpublished Ph.D. dissertation, 195 p.

Young, Allen, Low, P. F., and McLatchie, A. S., 1964, Permeability studies of argillaceous rocks: Journal of Geophysical Research, v. 69, no. 20, p. 4237–4245.

APPENDIXES: CASE HISTORIES

The technique of hydraulic fracturing has been widely applied since 1947 in the water flooding of oil fields (Howard and Fast, 1970); it was first proposed as a means to dispose of radioactive waste in shale by grout injection and has been used in experimental studies at the Oak Ridge National Laboratory from 1959 through 1965. A total of 10 experimental injections were made at three different injection wells. Since 1966 the hydraulic-fracturing and grout-injection disposal techniques have become operational, 17 injections had been made up to 1978. A total volume of 6,400 m^3 of radioactive waste containing 641,300 Ci of radionuclides has been injected for disposal.

To further study the feasibility of this disposal method at another location and to devise economic and reliable methods for determining the orientation of the hydraulically induced fractures to insure that the disposed wastes are isolated in a desired horizon, experimental studies were made jointly by the Oak Ridge National Laboratory and the U.S. Geological Survey from 1969 through 1971 at West Valley, N.Y. Five water injections and one grout injection that was tagged with gamma-emitting radioisotopes as tracers were made into another shale formation. No actual waste was disposed during these experimental studies.

Because the methods developed during the West Valley studies can be applied to the ORNL disposal site, the West Valley case history, which has been fully discussed by Sun and Mongan (1974), is presented first.

HYDRAULIC FRACTURING AT WEST VALLEY, N.Y.

West Valley is located approximately 56 km south-southeast of Buffalo, N.Y., and is in the north portion of Cattaraugus County with an altitude of about 457 m. The hydraulic fracturing study site is located on the property of Western New York Nuclear Service Center near the town of West Valley (fig. 13). The area is drained by Buttermilk Creek, which flows northward and enters Cattaraugus Creek, which enters Lake Erie.

The injection depths ranged from 153 m through 442 m. Injections were made in the injection well in sequence from the bottom upward. For a given test the well was plugged by cement to the desired injection depth and a horizontal 360° slot was made near the bottom of the unplugged part of the wall (as described in detail on p. 59).

SITE GEOLOGY

Because the purpose of the study was to evaluate the feasibility of the disposal method and not to select a site, the regional geology and hydrology were not investigated for the study. Only the site geology that might affect the orientation of the hydraulically induced fractures was briefly examined.

The test site is underlain by sedimentary rocks of Cambrian through Devonian age and is within the Appalachian Plateaus province. The area has been only slightly affected by tectonic events. No faults or folds

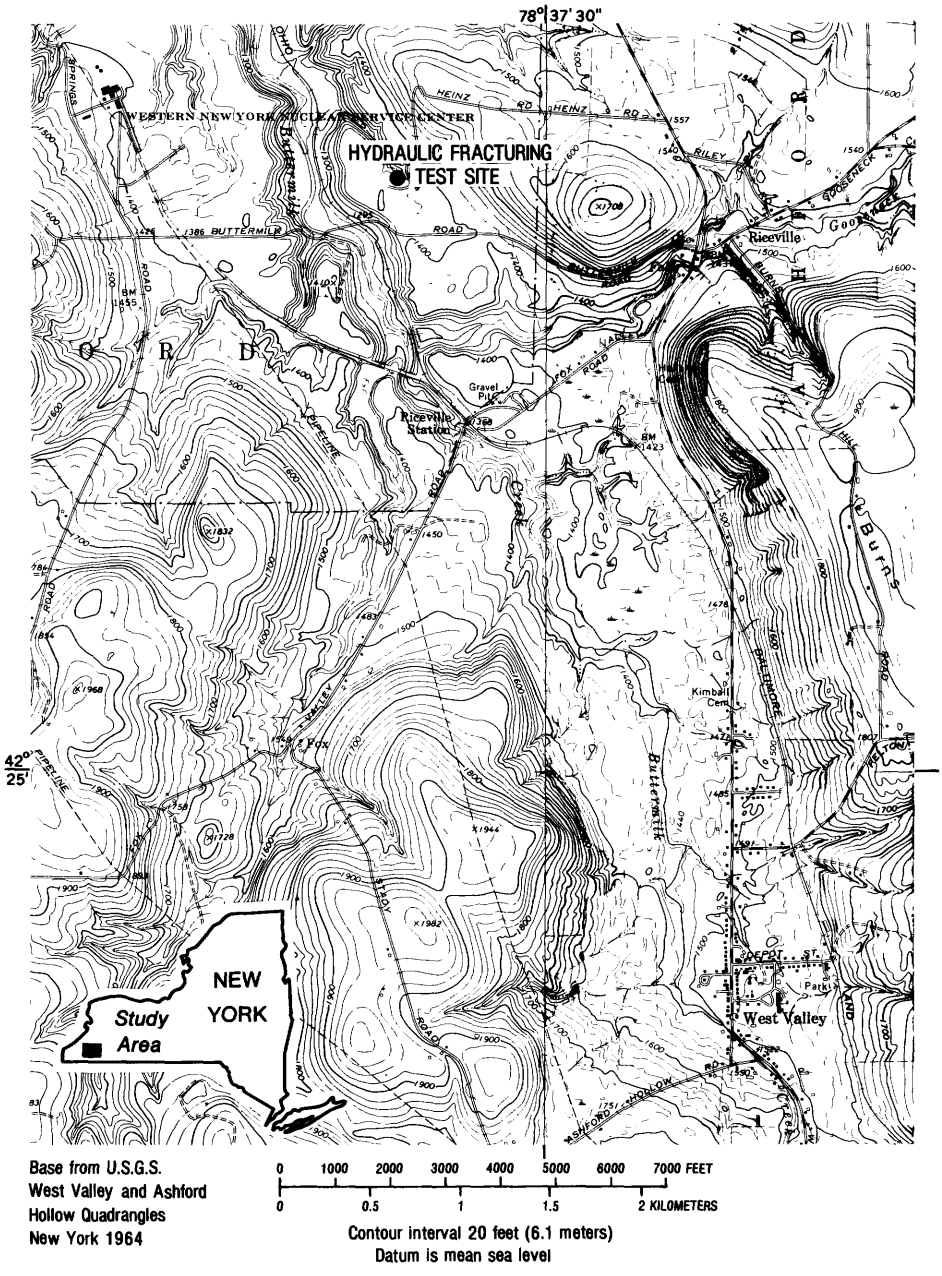

FIGURE 13. – Location of the hydraulic-fracturing test site, West Valley, N.Y.

have been mapped at the site. The nearest mapped fault is the Clarendon-Linden Fault, approximately 45 km east of the site.

The rocks involved in the tests are mostly Devonian shales and some interbedded siltstone. The area is covered by glacial deposits as much as 60 m thick. The rocks involved in the fracturing injections probably belong to Devonian shale in the Canadaway Group (New York State usage). The shale involved in the first two injections (at 442 m depth) may belong to the older Rhinestreet Shale Member of the West Falls Formation (Sun and Mongan, 1974). A layer of siltstone 30 m thick was found in a core hole at a depth of 290–320 m. The siltstone contains thin layers of silty shale. The bedding planes of the shale were nearly horizontal, probably dipping southward at the regional dip of 1–2°.

Three sets of principal joints have been identified by G. H. Chase, of the U.S. Geological Survey, at the outcrop area near the test site. The trends are N. 68° E., N. 45° W., and N. 13° W. in descending order in frequency of occurrence (fig. 14). All joints are vertical or nearly so. The average joint spacing is about 60 cm, and the

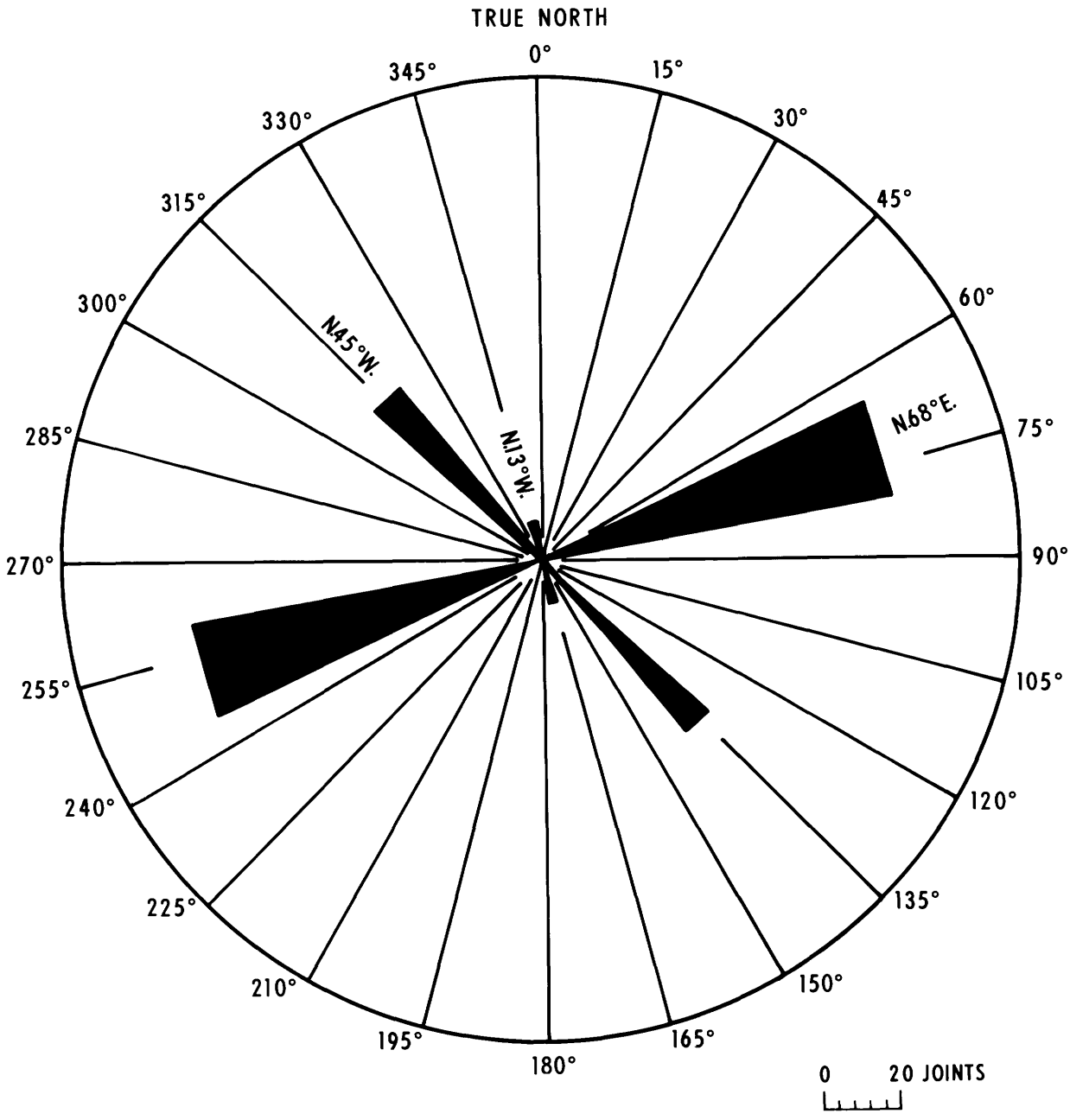

FIGURE 14.—Diagram showing the observed trend of three principal joint sets, West Valley, N.Y. (written commun., G. H. Chase, 1969).

average wall separation is 3 mm wide and filled with sediments. The vertical length of the joints ranges from <30 cm to 2 m. Most of them are 30 cm or less. From surface studies and cores and geophysical logs it was estimated by Chase that probably 20 percent of the joints are open (Sun and Mongan, 1974).

WELL CONSTRUCTION

A core hole was drilled to a depth of 463 m in order to obtain lithologic and petrophysical information. The core hole was then cased with rather weak steel tubing and was pressure cemented in place. This well was used as one of the four observation wells during the study and was named the East-observation well. Before converting the core hole to an observation well, gamma-ray, electric, and 3-dimensional sonic, density, and caliper logs were made in the hole to obtain information on subsurface geology.

The injection well, which was constructed of good quality steel casing and was pressure cemented to a full

depth of 463 m, was located 46 m from the core hole (figs. 15, and 16). Density, caliper, gamma-ray, and hole-deviation surveys were made in the injection well before the well was cased and was pressure cemented.

Three more observation wells were constructed to the south, the west, and the north, each 46 m from the injection well (fig. 16). These observation wells were also cased with strong tubing and were pressure cemented to a full depth of 463 m. Gamma-ray logs were made in all these observation wells before and after each injection to determine the orientation of induced fractures.

INJECTIONS

Only three water injections and one grout injection are discussed here as examples of the study. Two water injections were made through the same slot at a depth of 442 m; one injection was made without tracer, and the other, with radioactive tracers. The grout injection was the last injection during the study and was made with a radioactive tracer and at a depth of 152 m. Before the grout injection a water injection without tracer was made at the same depth through the same slot. All injection results indicate that the theory and methods discussed in the text are approximately valid and that the orientation of induced fractures can be determined by direct surveys through observation wells or by evidence deduced from injection data. Results of injections made at the same depth and through the same slot are nearly duplicated.

WATER INJECTION

The first water injection was made on October 9, 1969. About 433 m^3 of water without tracer was injected through a precut slot at a depth of 442 m. The rock at this depth is a well-bedded petroliferous shale. A zone of vertical joints at a depth of 439-442 m had been determined by G. H. Chase, from a geophysical log.

Pressures discussed that apply to the theory are pressures at injection depth, commonly called "bottom-hole pressures"; however, pressures observed during test injections were surface pressures measured at the wellhead of an injection well (fig. 15). Bottom-hole pressures used in the interpretation of water injections were computed from observed pressures by adding the calculated static pressure in the well casing and by subtracting the pressure loss due to friction in injection pipe. For water injections, the frictional pressure loss in the injection pipe was calculated by the Darcy-Weisbach equation (Davis and Sorensen, 1969), which is given as

$$\Delta P = 500 f L V^2/D, \quad (56)$$

where

ΔP = pressure loss due to friction, in pascals;
f = Fanning frictional factor of casing, dimensionless;
L = length of pipe, in meters;
D = inside diameter of pipe, in meters; and
V = flow velocity, in meters per second.

The injection was started at a very low rate that could not be detected on a flow meter near the wellhead. At this low rate the injection pressure increased rapidly. Twenty-two minutes after the injection started, the pressure near the wellhead reached 9.65 MPa (megapascals) (table 1), and a trace of flow was detected on the flow meter. The injection rate was progressively increased in two steps, from 0.001 m^3/s to 0.002 m^3/s and then to 0.003 m^3/s. Each injection step lasted about 10 minutes. After the increase to 0.003 m^3/s, an injection pattern consisting of flow rates of 0.006 m^3/s, 0.013 m^3/s, and 0.025 m^3/s, each occuring for an interval of one-half hour, was established. This pattern was repeated over and over until the end of the injection (fig. 17).

Six hours from the start, after a total of 223 m^3 of water had been injected, the injection was stopped to allow for instrument adjustment. The injection was resumed 45 minutes later using the regular injection pattern, but this time starting at the rate of 0.025 m^3/s. The observed pressures, injection rates, and calculated bottom-hole pressures are listed in table 1.

If flow through an induced fracture is assumed to be laminar and to obey Darcy's law, then the injection pressure at the well should be linearly proportional to the injection rate. This assumption has been proved to be at least approximately correct by using a polynomial regression of the injected data, which showed by F-tests that only the linear term of Q (injection rate) has significance (Ostle, 1954).

During the stage of fracture initiation, injection pressure must be built up to overcome the tensile strength of the rock. After the rock is broken, injection pressure gradually decreases to the required propagation pressure. During this transitional stage, injection pressures are not linearly proportional to the injection rates. Excluding these pressures, a linear regression equation fit to data collected before the injection pause and having a correlation coefficient of 0.88 has been found (fig. 18); the result is

$$P = 11.96 + 24.05\,Q, \quad (57)$$

where P is bottom-hole pressure, in megapascals, and Q is the injection rate, in cubic meters per second.

Because the regression coefficient of Q was determined from a small sample size of P and Q taken from the true population, it is possible that the values of P and Q may be independent in the true population and the regression equation has no meaning statistically. Therefore, it is essential to test whether the regression

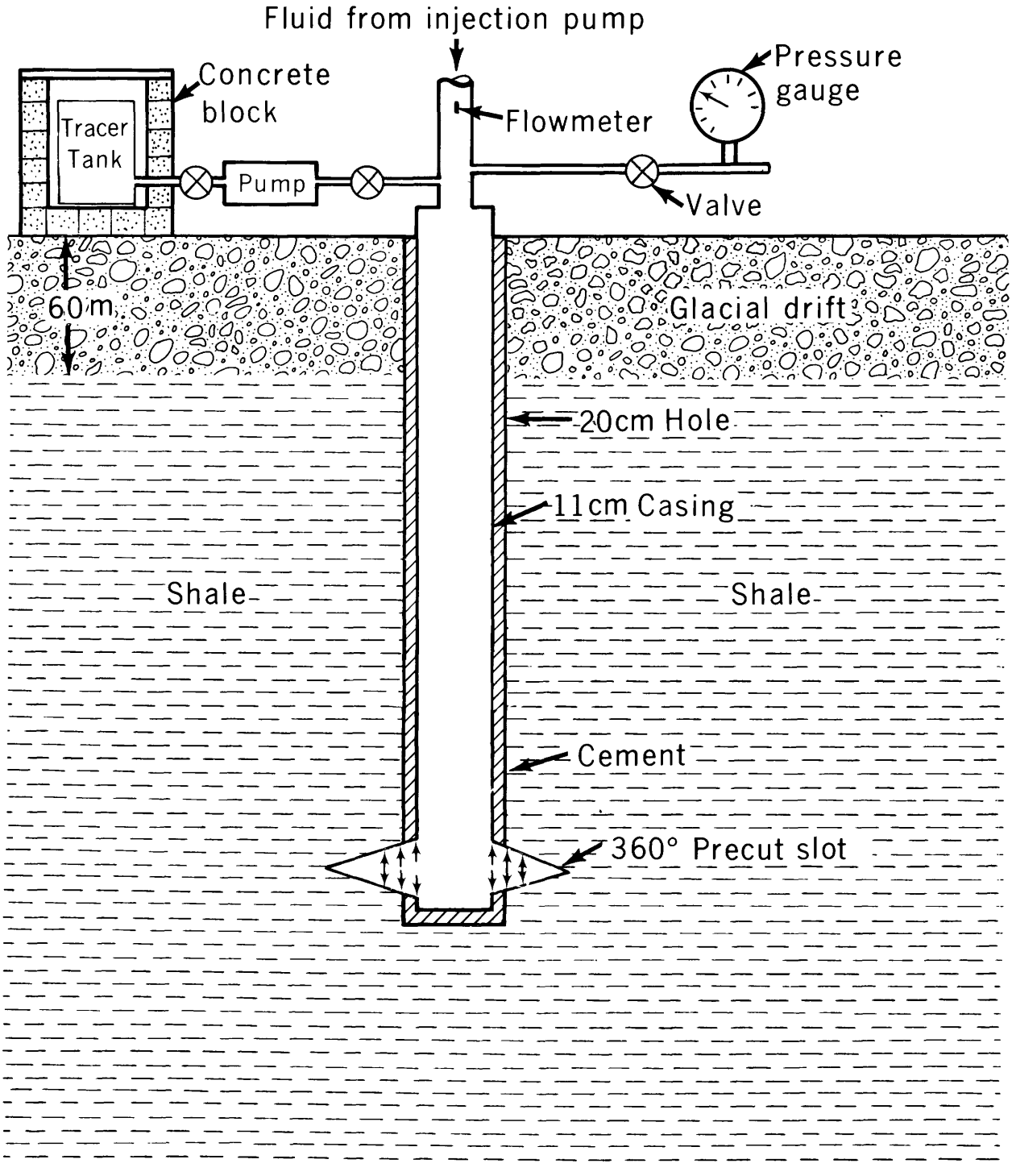

FIGURE 15.–Schematic diagram of the injection well, West Valley, N.Y.

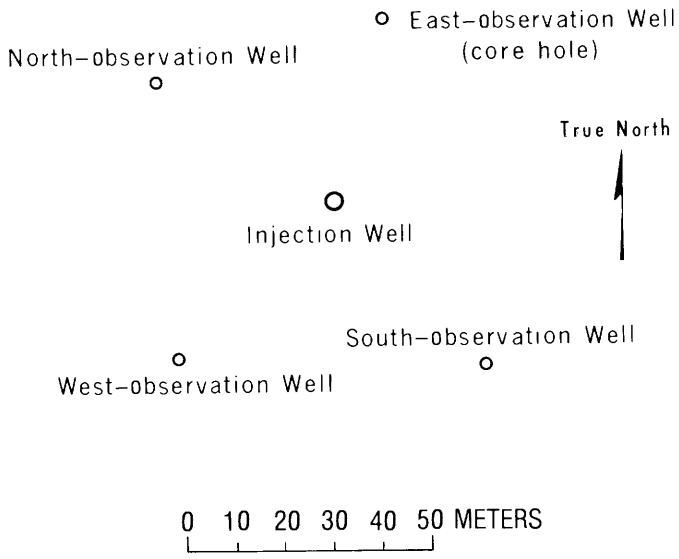

FIGURE 16.–Well locations, West Valley, N.Y.

TABLE 1.–*Injection pressure of a water injection at 442 m, Oct. 9, 1969, West Valley, N.Y.*

[tr., trace]

Time (min)	Observed wellhead pressure (MPa)	Calculated bottom-hole pressure (MPa)	Rate of injection ($m^3/s \times 10^{-3}$)	Accumulated injection volume (m^3)
2	0.97	5.3	0	0
20	6.48	10.81	0	0
22	9.65	13.98	tr.	tr.
23	7.65	11.91	tr.	tr.
25	7.17	11.50	tr.	tr.
26	7.58	11.91	tr.	tr.
28	7.58	11.91	1.04	
31	7.58	11.91	1.04	
35	7.52	11.91	1.04	0.4
39	7.72	12.05	1.89	
41	7.65	11.98	1.89	
48	7.69	12.02	1.89	
49	7.65	11.98	1.89	
53	7.58	11.91	1.89	
54	8.45	12.78	1.89	
55	8.96	13.29	1.89	2.7
56	9.10	13.42	3.15	
57	9.65	13.98	3.15	
58	9.51	13.84	3.15	
59	10.00	14.32	3.15	
60	9.52	13.84	3.15	
62	9.65	13.98	3.15	
64	10.00	14.32	3.15	4.6
68	10.89	15.19	6.31	
69	9.38	13.67	6.31	
70	8.55	12.84	6.31	
71	8.45	12.74	6.31	5.9
72	8.34	12.64	6.31	
73	8.21	12.50	6.31	
75	8.17	12.43	6.31	7.5
76	8.14	12.43	6.31	
78	8.00	12.29	6.31	9.1
80	7.93	12.22	6.31	
82	7.86	12.16	6.31	
83	7.83	12.12	6.31	11.1
86	7.79	12.09	6.31	
87	7.79	12.09	6.31	
89	7.79	12.09	6.31	
93	7.86	12.16	6.31	
98	7.86	12.16	6.31	
99	8.41	12.61	12.62	
101	8.41	12.61	12.62	
103	8.27	12.47	12.62	20.2
108	8.14	12.33	12.62	24.0
113	8.07	12.27	12.62	27.8
118	8.07	12.27	12.62	31.8
123	8.03	12.23	12.62	35.5
128	8.07	12.27	12.62	39.4
133	8.48	12.33	25.23	
138	8.41	12.27	25.23	
143	7.93	12.22	6.31	
148	7.79	12.09	6.31	55.6
150	7.79	12.09	6.31	56.3
153	7.76	12.05	6.31	57.5
158	7.76	12.05	6.31	59.9
163	7.79	12.09	6.31	62.0
164	7.79	12.09	6.31	62.2
168	7.79	12.09	6.31	63.9
170	8.00	12.20	12.62	
173	8.07	12.27	12.62	
181	8.07	12.27	12.62	69.9
183	8.07	12.27	12.62	72.2
185	8.07	12.27	12.62	73.9
188	8.07	12.27	12.62	75.8
193	8.07	12.27	12.62	79.6
198	8.07	12.27	12.62	83.5
203	8.00	12.20	12.62	87.3
206	8.03	12.23	12.62	
208	8.03	12.23	12.62	90.6
211	8.34	12.20	25.23	
213	8.41	12.27	25.23	95.5
218	8.62	12.47	25.23	107.0
223	8.69	12.54	25.23	110.0
228	8.69	12.54	25.23	
233	8.65	12.51	25.23	125.4
238	8.62	12.47	25.23	
241	7.79	12.09	6.31	
243	7.76	12.05	6.31	139.1
248	7.76	12.05	6.31	140.7
253	7.76	12.05	6.31	
258	7.76	12.05	6.31	144.3
263	7.76	12.05	6.31	
268	7.76	12.05	6.31	148.6
271	8.07	12.27	12.62	
273	8.07	12.27	12.62	151.8
278	8.10	12.30	12.62	
283	8.07	12.27	12.62	160.1
288	8.07	12.27	12.62	
293	8.10	12.30	12.62	167.9
298	8.10	12.30	12.62	171.7
303	8.83	12.68	25.23	
305	8.96	12.82	25.23	
308	8.89	12.75	25.23	185.8
313	8.79	12.64	25.23	
318	8.76	12.61	25.23	202.4
323	8.79	12.64	25.23	
328	8.79	12.64	25.23	219.1

TABLE 1.—*Injection pressure of a water injection at 442 m, Oct. 9, 1969, West Valley, N.Y.*—Continued

Time (min)	Observed wellhead pressure (MPa)	Calculated bottom-hole pressure (MPa)	Rate of injection ($m^3/s \times 10^{-3}$)	Accumulated injection volume (m^3)
331[1]	8.76	12.61	25.23	223.7
332	8.72	12.05	0	
333	7.65	11.98	0	
334	7.58	11.91	0	
335	7.55	11.88	0	
336	7.52	11.85	0	
337	7.48	11.81	0	
338	7.46	11.79	0	
339	7.45	11.78	0	
340	7.41	11.74	0	
341	7.38	11.71	0	
342	7.38	11.71	0	
343	7.35	11.68	0	
348	7.27	11.60	0	
353	7.21	11.53	0	
358	7.16	11.49	0	
363	7.10	11.43	0	
368	7.07	11.40	0	
373	7.02	11.35	0	
376	7.00	11.33	0	
379[2]	11.51	15.37	25.23	
380	10.69	14.54	25.23	226.2
381	10.20	14.06	25.23	227.8
383	9.72	13.58	25.23	230.8
388	9.45	13.30	25.23	238.6
393	9.31	13.16	25.23	246.4
398	9.31	13.16	25.23	254.4
403	9.21	13.06	25.23	262.6
406	9.21	13.06	25.23	
408	9.17	13.02	25.23	270.6
411	7.96	12.26	6.31	
413	7.89	12.19	6.31	274.7
418	7.86	12.16	6.31	
423	7.86	12.16	6.31	278.8
428	7.86	12.16	6.31	280.9
433	7.86	12.16	6.31	
438	7.86	12.16	6.31	284.6
441	8.62	12.82	12.62	
443	8.69	12.89	12.62	
448	8.69	12.89	12.62	
453	8.69	12.89	12.62	295.2
458	8.69	12.89	12.62	
463	8.69	12.89	12.62	303.2
468	8.72	12.92	12.62	
471	10.00	13.85	25.23	
473	9.79	13.64	25.23	311.4
476	9.65	13.51	25.23	
478	9.51	13.37	25.23	319.2
483	9.45	13.30	25.23	
488	9.38	13.23	25.23	334.9
493	9.38	13.23	25.23	343.2
498	9.38	13.23	25.23	351.3
501	7.93	12.22	6.31	
503	7.93	12.22	6.31	
508	7.93	12.22	6.31	358.8
513	7.86	12.16	6.31	
518	7.86	12.16	6.31	362.6
523	7.93	12.22	6.31	364.4
528	7.93	12.22	6.31	366.3
531	8.83	13.02	12.62	
533	8.83	13.02	12.62	368.7
538	8.79	12.99	12.62	
543	8.79	12.99	12.62	376.6
548	8.83	12.99	12.62	380.7
553	8.83	12.99	12.62	
558	8.89	12.99	12.62	388.5
561	10.14	13.99	25.23	
563	10.07	13.92	25.23	394.1
568	9.72	13.58	25.23	
573	9.72	13.58	25.23	409.5
578	9.65	13.51	25.23	415.7
583	9.58	13.44	25.23	432.7
586	9.52	13.37	25.23	428.4
588[3]	----	----	----	432.6

Notes:
Calculated bottom-hole pressure (for injection)
= observed wellhead pressure + static pressure in casing − frictional loss in injection pipe.

Calculated bottom-hole pressure (for pressure decay)
= observed wellhead presssure + static pressure in casing.

[1] Injection stopped; 45-minute pause.
[2] Injection restarted.
[3] End injection.

coefficient determined from the sample size is significant in a statistical sense. The significance of the regression coefficient of 24.05 of Q in the regression equation has been tested statistically by assuming a probability of Type I error equal to 5 percent (95-percent level of confidence). The conclusion is that the values of P are dependent on the values of Q statistically (Sun and Mongan, 1964).

Because of the simple geologic structure and the relatively flat topography at the test site (fig. 13), it is reasonable to consider that the vertical earth stress is equal to the overburden pressure. The average specific gravity of shale and glacial drift at the test site are 2.6 and 2.0 respectively (deLaguna, 1972). Therefore, the overburden pressure at the injection depth can be estimated as

$$\sigma_z = 9.8\times10^{-3}\,(2.0\times60+2.6\,(442-60)),$$
$$= 10.9 \text{ MPa}.$$

When Q was nearly zero, the observed injection pressure rose to 14 MPa (fig. 17), which was the breakdown pressure. As discussed previously, a horizontal fracture was probably initiated at the well face, owing to the high tensile strength provided by the casing and the horizontal slot cut through the casing and into the shale. The tensile strength of the shale in the vertical direction, T_{σ_z}, can be estimated by equation 45, and the result is

$$T_{\sigma_z} = 10.9 - 14,$$
$$= -3.1 \text{ MPa}.$$

After 3 m^3 of water had been injected, the injection pressures increased rapidly beyond the propagation pressures predicted by the regression equation (eq 57). These high pressures may suggest the formation of additional fractures.

From equation 57, the normal propagation pressure at the rate of 0.006 m^3/s is 12.1 MPa; however, the observed highest presure at 0.006 m^3/s was 15.2 MPa (fig. 17). This pressure could be the breakdown pressure at the stage of formation of additional fractures. The ten-

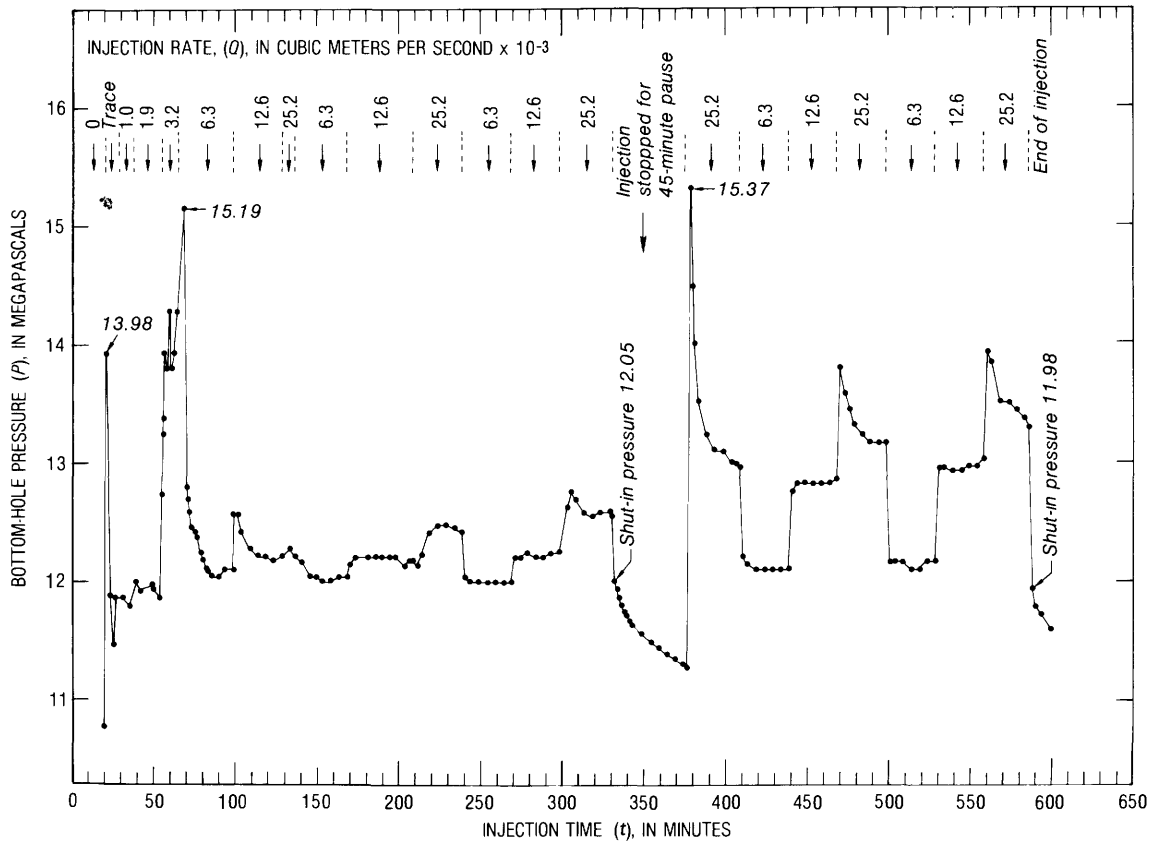

FIGURE 17.–Pressure plotted against time, the water injection at 442 m, Oct. 9, 1969, West Valley, N.Y.

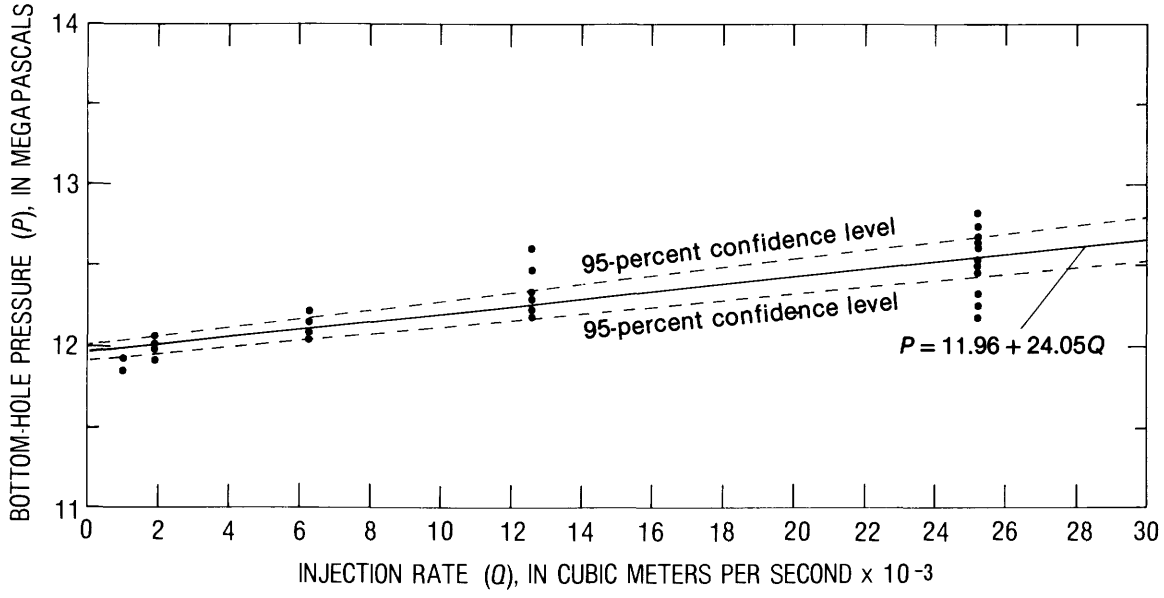

FIGURE 18.–Pressure plotted against injection rate, before a 45-minute pause, the water injection at 442 m, Oct. 9, 1969, West Valley, N.Y.

sile strength of the shale calculated on the basis of this breakdown pressure is 4.2 MPa, which is about 1.1 MPa higher than the estimated value based on the first breakdown pressure.

When the injection is stopped, Q will be zero. The instantaneous shut-in pressure can be calculated from equation 57, resulting in 12 MPa. The observed instantaneous shut-in pressure during the 45-minute pause was 12.1 MPa (fig. 17), virtually the same as the value calculated by equation 57.

The average cohesive force at the fracture tip can be estimated by equation 46 if Q is equal to zero, and the result is

$$f T_{\sigma_z} = 10.9 - 12,$$
$$= -1.1 \text{ MPa},$$

and

$$f = 0.35.$$

After the 45-minute pause, the injection was resumed at a rate of 0.025 m^3/s. The calculated propagation pressure for this rate should be 12.6 MPa (eq. 57); however, the observed pressure was 15.4 MPa, which was probably the breakdown pressure at the reinjection stage. The tensile strength of the shale estimated on the basis of this breakdown pressure is 3.9 MPa, which is 0.8 MPa higher than the first calculated value (3.1 MPa) but is close to the value calculated on the basis of breakdown pressure observed at 0.006 m^3/s.

After the fracture was reinitiated, the injection pressure diminished to the normal propagation pressure. The regression equation (fig. 19), which has a correlation coefficient of 0.89, for the injection period after the pause is

$$P = 11.96 + 60.01\, Q. \quad (58)$$

Again the regression coefficient has been found to be significant at the 95-percent confidence level.

After completion of the injection, the well was shut in at the wellhead. The observed instantaneous shut-in pressure was 12 MPa, which closely matches the estimated shut-in pressure obtained by equations 57 and 58. Pressure decay was observed for about 8 days; the results are shown in table 2 and figure 20.

The observed injection pressure at the end of the first part of the injection, before 45-minute pause, at an injection rate of 0.025 m^3/s was 12.6 MPa, and the observed shut-in pressure was 12.05 MPa (table 1); the difference between the two pressures was 0.55 MPa. Therefore, the pressure needed to overcome friction loss of one unit of injection rate was 22 MPa/(m^3/s), which is close to the regression coefficient of Q determined statistically – that is, 24 MPa/(m^3/s) (eq 57). The observed injection pressure at the end of the injection at an injection rate of 0.025 m^3/s was 13.4 MPa, and the observed shut-in pressure was 12 MPa (table 1); the difference

TABLE 2.–*Pressure decay of a water injection at 442 m, Oct. 9, 1969, West Valley, N.Y.*

Time since end of injection (min)	Observed wellhead pressure (MPa)	Calculated bottom-hole pressure, P (MPa)	$P-P_0$ (MPa)
0	7.65	11.98	7.89
1	7.58	11.91	7.82
2	7.52	11.85	7.76
3	7.48	11.81	7.72
4	7.46	11.79	7.70
5	7.46	11.79	7.70
10	7.32	11.65	7.56
15	7.25	11.58	7.49
20	7.21	11.53	7.44
25	7.17	11.50	7.41
30	7.15	11.48	7.39
45	7.07	11.40	7.31
60	6.99	11.32	7.23
75	6.94	11.27	7.18
90	6.89	11.22	7.13
105	6.85	11.18	7.09
120	6.82	11.15	7.06
135	6.78	11.11	7.02
165	6.72	11.05	6.96
195	6.67	11.00	6.91
225	6.63	10.96	6.87
255	6.61	10.93	6.84
285	6.59	10.92	6.83
315	6.56	10.89	6.80
345	6.54	10.87	6.78
375	6.49	10.82	6.73
405	6.46	10.79	6.70
435	6.42	10.75	6.66
465	6.39	10.72	6.63
495	6.34	10.67	6.58
525	6.30	10.63	6.54
555	6.27	10.60	6.51
585	6.23	10.56	6.47
615	6.19	10.52	6.43
645	6.16	10.49	6.40
705	6.09	10.42	6.33
735	6.05	10.38	6.29
765	6.01	10.34	6.25
795	5.97	10.30	6.21
825	5.94	10.27	6.18
885	5.87	10.20	6.11
915	5.83	10.16	6.07
945	5.79	10.12	6.03
1,005	5.73	10.06	5.97
1,185	5.56	9.89	5.80
1,305	5.45	9.78	5.69
1,575	5.29	9.62	5.53
2,205	5.03	9.36	5.27
2,415	4.98	9.31	5.22
2,625	4.93	9.26	5.17
2,985	4.83	9.16	5.07
3,705	4.67	9.00	4.91
3,930	4.62	8.95	4.86
4,295	4.53	8.86	4.77
5,065	4.41	8.74	4.65
5,775	4.27	8.60	4.51
6,585	4.15	8.48	4.39
7,185	4.07	8.40	4.31
7,995	3.96	8.29	4.20
8,745	3.88	8.21	4.12
9,465	3.79	8.12	4.03
10,065	3.73	8.06	3.97
10,905	3.66	7.99	3.88
11,265	3.63	7.96	3.87

Note: Static ground-water pressure at injection level, $P_0 = 4.09$ MPa.

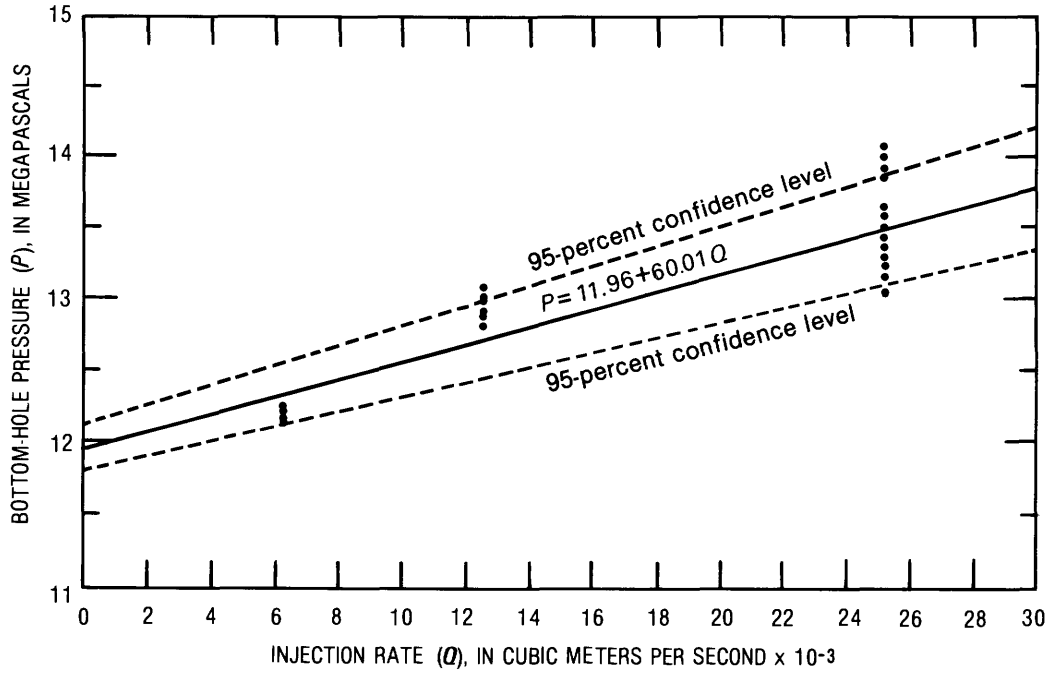

FIGURE 19.—Pressure plotted against injection rate, after a 45-minute pause, the water injection at 442 m, Oct. 9, 1969, West Valley, N.Y.

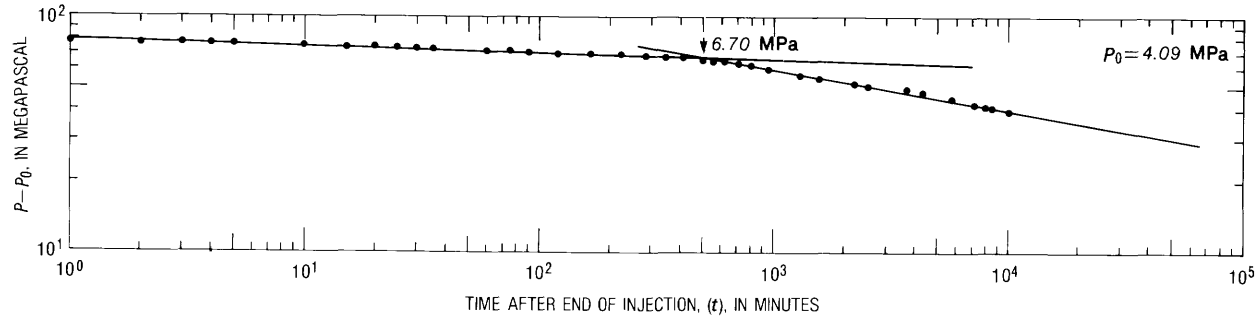

FIGURE 20.—Pressure decay plotted against time, the water injection at 442 m, Oct. 9, 1969, West Valley, N.Y.

between the two pressures is 1.4 MPa. The pressure required to overcome frictional loss of one unit of injection rate was 56 MPa/(m³/s), which is close to the regression coefficient of 60 MPa/(m³/s) (eq 58). From these correlations, it probably can be concluded that the determined regression equations (eqs 57, and 58) are meaningful.

Water level in the core hole was measured by G. H. Chase (written commun., 1970) on May 22, 1969, and was found to be 18 m below the land surface. Adjusted by the difference in altitude between the core hole and the injection well, the depth to water was 24 m in the injection well. The hydraulic pressure P_0 in the formation at the injection depth of 442 m was therefore calculated as 4.1 MPa (a meter of water produces 9,800 Pa pressure).

The log-log plot of $(P-P_0)$ against observation time t (fig. 20) appears to fall on two straight lines that intersect at $t=500$ minutes and $(P-P_0)=6.7$ MPa. Therefore, the earth stress normal to the fracture plane is estimated to be 10.79 MPa (4.09+6.7=10.79 MPa), which closely correlates to the calculated overburden pressure which is 10.9 MPa. It can be concluded that the earth stress normal to the fracture planes is equal to simply the weight of overburden, and therefore the induced fracture is probably nearly horizontal.

The injection water was not tagged with gamma-ray-emitting radioactive isotopes; therefore, no field evidence is available to indicate the orientation of the induced fractures.

The second water injection was made on June 26, 1970, at the same depth and through the same slot where the first water injection was made. A total of 425 m³ of water tagged with radioactive isotope of $^{95}Zr/^{95}Nb$ was injected. The injection was started at a

very low rate, and injection pressure built up steadily. The rock was apparently ruptured at a bottom-hole pressure of 16.1 MPa (fig. 21; table 3). After the breakdown, the injection rate was increased to 0.002 m^3/s. This rate was maintained for 70 minutes. When the injection rate was increased again, the pressure rose quickly until it reached a peak of 24.2 MPa; at this time, the injection rate was 0.01 m^3/s. This second peak may indicate the formation of additional fractures. Thereafter, the pressure dropped to a normal propagation pressure (fig. 21). The regression equation of P and Q, having a correlation coefficient of 0.73, is (fig. 22)

$$P = 13.95 + 224.06Q. \quad (59)$$

Instantaneous shut-in pressure determined from the regression equation is 14 MPa; however, the observed value was 13.3 MPa (fig. 21). The pressure drop within 1 minute was 1.2MPa; thereafter the pressure decay was very slow (table 4). Therefore, the correct instantaneous shut-in presssure is probably around 12 MPa, which is the same as that obtained from the first injection test (table 2).

The injection well was shut in under pressure on Oct. 9, 1969, after the first injection was stopped. Two weeks before the second injection, the injection well was bled and was shut in again on June 25, 1970, one day before the injection. A residual pressure of 1.1 MPa was noted at the well head (G. H. Chase, written commu., 1970). Therefore, there was at least 5.4 MPa ($1.1 \times 10^6 + 442 \times 9800 = 5.4$ MPa) pressure remaining in the fractures, though it probably was higher than this value. The high regression coefficient of Q likely is the result of this residual pressure in the fractures.

If the shale is assumed to be ruptured at 16.1 MPa (fig. 21; table 3), then the tensile strength of the shale in the direction normal to bedding planes at the injection depth can be estimated by equation 45. The result is given by

$$T_{\sigma_z} = (10.9 - 4.1) - (16.1 - 5.4),$$
$$= -3.9 \text{ MPa},$$

which is close to the tensile strengths calculated from the first water injection on Oct. 9, 1969, at the same injection depth; the tensile strengths fall in the range of 3.1 to 4.2 MPa.

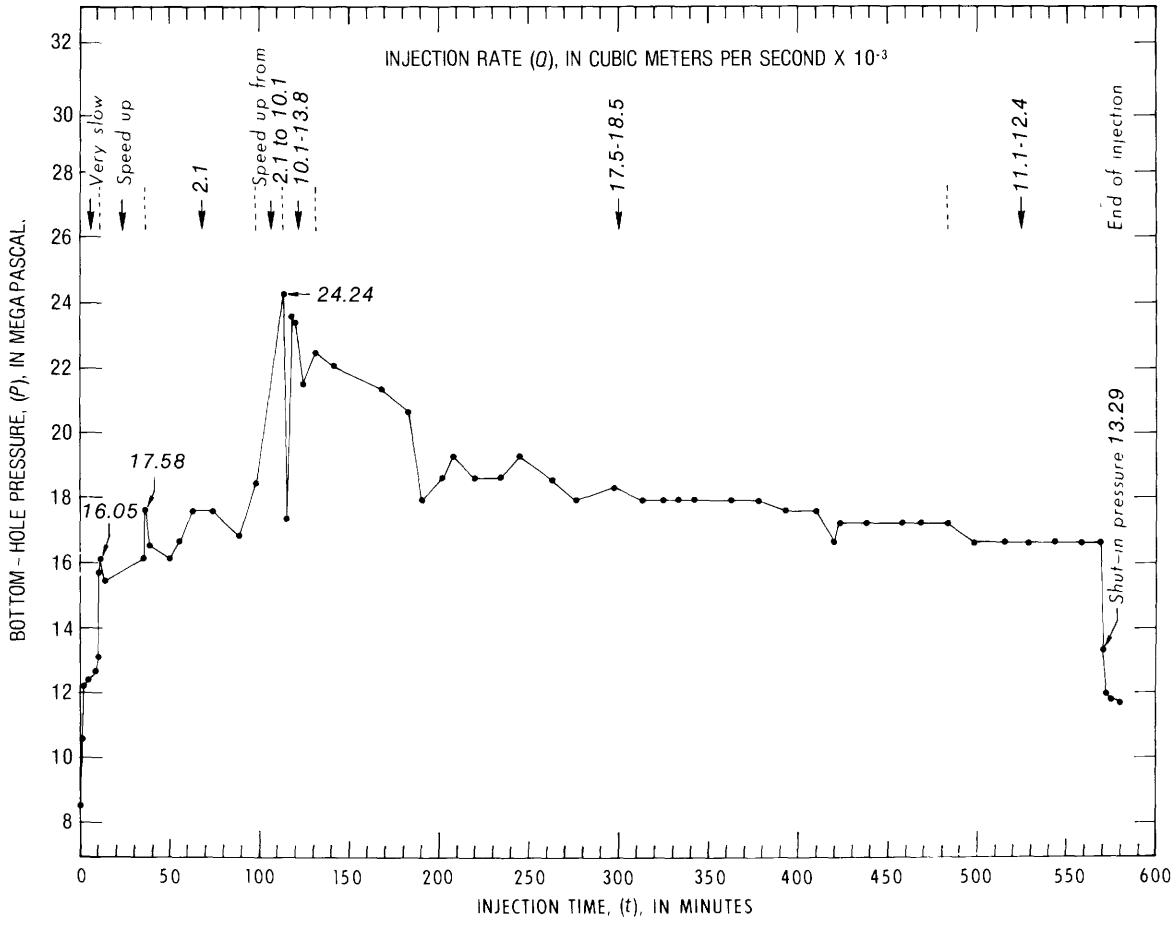

FIGURE 21.–Pressure plotted against time, the water injection at 442 m, June 26, 1970, West Valley, N.Y.

TABLE 3.—*Injection pressure of a water injection at 442 m, June 26, 1970, West Valley, N.Y.*

[tr., trace]

Time (min)	Observed wellhead pressure (MPa)	Calculated bottom-hole pressure (MPa)	Rate of injection ($m^3/s \times 10^{-3}$)	Accumulated injection volume (m^3)
1	6.21	10.54	(1)	
2	7.86	12.19	(1)	
3	7.93	12.26	(1)	
4	8.07	12.40	(1)	0.4
8	8.27	12.60	(1)	
10	8.76	13.09	(2)	
11	11.38	15.71	(2)	
13[3]	11.72	16.05	(2)	
36	11.03	15.36	(2)	
37	11.72	16.05	(2)	
38	13.24	17.58	2.14	2.8
43[4]	12.13	16.46	2.14	
50	11.72	16.04	2.14	3.7
55	12.27	16.60	2.14	4.5
62	13.24	17.56	2.14	5.5
73	13.24	17.56	2.14	7.1
88	12.41	16.73	2.14	9.4
98	14.13	18.46	2.14	10.8
110	15.86		(2)	
113	19.99	24.24	10.09	14.2
115	13.10	17.35	10.60	15.4
118	19.31	23.53	11.92	17.1
120	19.17	23.37	13.25	18.1
124	17.24	21.43	13.75	22.2
132	18.27	22.48	13.25	26.9
142	17.93	22.03	18.04	32.6
153	12.41	16.74	0	42.9
156	7.75	12.09	0	42.9
168	17.24	21.34	18.04	53.0
183	16.55	20.65	18.04	70.5
191	13.79	17.89	18.04	78.5
202	14.48	18.58	18.04	89.7
208	15.17	19.27	18.04	96.1
220	14.48	18.58	18.04	109.0
234	14.48	18.58	18.04	122.8
246	15.17	19.27	18.04	135.8
263	14.48	18.57	18.55	154.2
276	13.79	17.89	18.04	158.0
298	14.13	18.24	18.04	179.5
313	13.79	17.89	18.04	194.8
325	13.79	17.89	18.04	208.2
333	13.79	17.89	18.04	
343	13.79	17.89	18.04	226.7
363	13.79	17.91	17.47	246.8
378	13.79	17.91	17.47	261.9
393	13.44	17.56	17.47	277.4
411	13.44	17.56	17.47	294.9
421	12.41	16.60	13.75	303.2
423	13.10	17.20	18.04	305.1
438	13.10	17.20	18.04	320.6
458	13.10	17.20	18.04	337.6
468	13.10	17.20	18.04	346.7
483	13.10	17.20	18.55	363.0
498	12.41	16.63	12.43	375.9
515	12.41	16.63	12.43	388.3
528[5]	12.41	16.64	11.92	397.6
543	12.41	16.64	11.67	408.4
558	12.41	16.64	11.67	416.7
569[6]	12.41	16.65	11.10	424.9

[1] Very slow.
[2] Rate increased.
[3] To fix leaks of piping.
[4] Start isotope injection.
[5] End isotope injection.
[6] End injection.

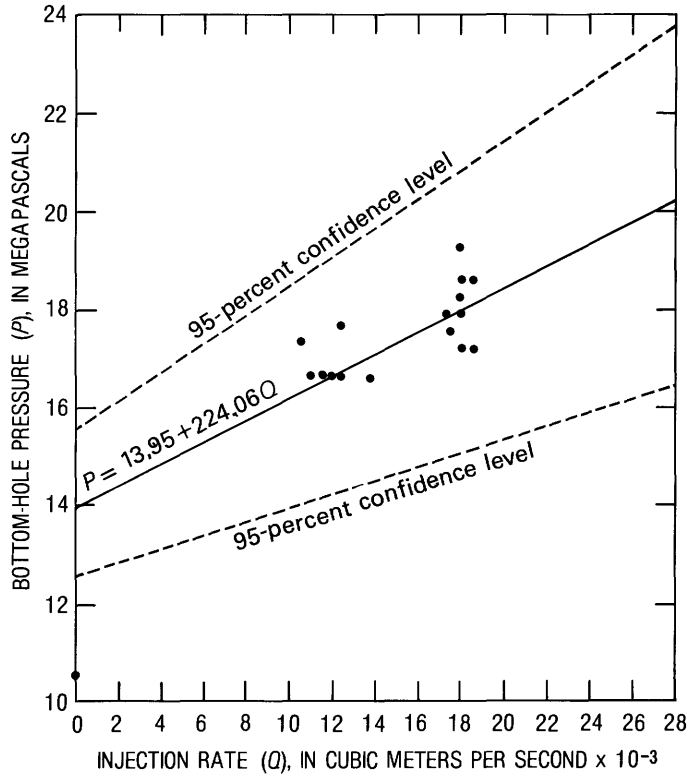

FIGURE 22.—Pressure plotted against the injection rate, the water injection at 442 m, June 26, 1970, West Valley, N.Y.

Average cohesive force at the fracture tip and the value of f can be estimated by equation 46; the results are

$$f T_{\sigma_z} = (10.9 - 4.1) - (14 - 5.4),$$
$$= -1.8 \text{ MPa},$$

and

$$f = 0.46.$$

The value of f is 35 percent greater than the value obtained from the first water injection. However, if the observed shut-in pressure were used (that is, 12 MPa), the f value would be 0.28, which is close to the value determined from the first water-injection data. The difference between the regression constant at $Q = 0$ and the observed instantaneous shut-in pressure is probably due to the observed residual pressure caused by the first water injection.

No attempt was made to use the peak pressure at 0.01 m^3/s to estimate the tensile strength because the injection rate at this time was increased from 0.002 m^3/s to 0.01 m^3/s in 5 minutes (table 3). Actual frictional loss would be much higher than the expected frictional loss calculated from equation 59 during this short time interval.

After the well was shut in, pressure decay was observed for nearly 13 days. The decay data are shown in table 4. The log-log plot of $(P - P_0)$ against time t is shown in figure 23. All data apparently fall on two

TABLE 4.—*Pressure decay of a water injection at 442 m, June 26, 1970, West Valley, N.Y.*

Time since end of injection (min)	Observed wellhead pressure (MPa)	Calculated bottom-hole pressure, P (MPa)	$P-P_0$ (MPa)
1	8.96	13.29	9.20
2	7.79	12.12	8.03
3	7.65	11.98	7.89
4	7.58	11.91	7.82
5	7.52	11.85	7.76
6	7.45	11.78	7.69
7	7.45	11.78	7.69
8	7.38	11.71	7.62
9	7.38	11.71	7.62
10	7.34	11.67	7.58
12	7.31	11.64	7.55
13	7.31	11.64	7.55
14	7.27	11.60	7.51
15	7.24	11.57	7.48
18	7.17	11.50	7.41
20	7.17	11.50	7.41
24	7.12	11.45	7.36
29	7.10	11.43	7.34
34	7.03	11.36	7.27
39	7.00	11.33	7.24
44	7.00	11.33	7.24
49	6.95	11.28	7.19
54	6.93	11.26	7.17
64	6.89	11.22	7.13
79	6.86	11.19	7.10
94	6.83	11.16	7.07
109	6.79	11.12	7.03
124	6.76	11.09	7.00
139	6.72	11.05	6.96
169	6.69	11.02	6.93
199	6.62	10.95	6.86
229	6.58	10.91	6.82
259	6.55	10.88	6.79
299	6.48	10.81	6.72
319	6.48	10.81	6.72
349	6.45	10.78	6.69
379	6.41	10.74	6.65
439	6.38	10.71	6.62
469	6.34	10.67	6.58
499	6.31	10.64	6.55
529	6.27	10.60	6.51
559	6.24	10.57	6.48
589	6.21	10.54	6.45
619	6.21	10.54	6.45
649	6.17	10.50	6.41
679	6.17	10.50	6.41
709	6.17	10.50	6.41
739	6.17	10.50	6.41
799	6.14	10.47	6.38
859	6.10	10.43	6.34
987	6.03	10.36	6.27
1,024	6.00	10.33	6.24
1,039	6.00	10.33	6.24
1,219	5.93	10.26	6.17
1,399	5.86	10.19	6.10
1,639	5.72	10.05	5.96
2,269	5.47	9.80	5.71
2,359	5.45	9.78	5.68
2,419	5.43	9.76	5.67
2,479	5.40	9.73	5.64
2,584	5.38	9.71	5.62
2,629	5.38	9.71	5.62
2,689	5.34	9.67	5.58
2,749	5.32	9.65	5.56
2,809	5.31	9.64	5.55
2,839	5.31	9.64	5.55
3,079	5.24	9.57	5.48
3,509	5.09	9.42	5.33
3,769	5.03	9.36	5.27
3,979	4.98	9.31	5.22
4,234	4.92	9.25	5.16
4,489	4.87	9.20	5.11
5,164	4.76	9.09	5.00
5,389	4.74	9.07	4.98
5,899	4.70	9.03	4.94
6,619	4.60	8.93	4.84
6,799	4.60	8.93	4.84
7,339	4.54	8.87	4.78
7,999	4.48	8.81	4.72
8,359	4.45	8.78	4.69
8,839	4.40	8.73	4.64
9,469	4.35	8.68	4.59
10,219	4.30	8.63	4.54
10,969	4.27	8.60	4.51
11,134	4.23	8.56	4.47
11,629	4.19	8.52	4.43
12,439	4.14	8.47	4.38
13,039	4.10	8.43	4.34
13,729	4.03	8.36	4.27
14,269	4.03	8.36	4.27
14,509	4.02	8.35	4.26
15,589	3.99	8.32	4.23
16,819	3.90	8.23	4.23
18,274	3.82	8.15	4.06

Note: Static ground-water pressure at injection level, $P_0 = 4.09$ MPa.

straight lines. $(P-P_0)$ at the point of intersection of the two lines is 6.4 MPa; therefore, the estimated earth stress normal to the fracture plane is 10.5 MPa (6.4 + 4.09 = 10.49 MPa), which is close to the estimated overburden pressure, 10.9 MPa. Therefore, it can be concluded that the induced fractures are probably nearly horizontal.

Ten days after the end of the water injection, July 6, 1970, gamma-ray logs were made in all four observation wells. The East-observation well was found to be plugged at 424 m by cement, and the South-observation well was also blocked at 442 m. No significant radioactivity above the background level was recorded in either of the two wells. Strong gamma-ray activity however, was recorded in the North-observation well (fig. 24). The radioactivity was observed over a vertical distance of 6 m (436–442 m), indicating that at least three layers of bedding-plane fractures were induced. Strong gamma-ray activity was also recorded in the West-observation well (fig. 24) and observed over a vertical distance of 2 m (442–444 m), showing that only one layer of bedding-plane fracture was induced.

On Aug. 24, 1970, two months after the water injection and after the South-observation well had been cleaned out by a rig, gamma-ray logs were run again in the three observation wells. No efforts were made to

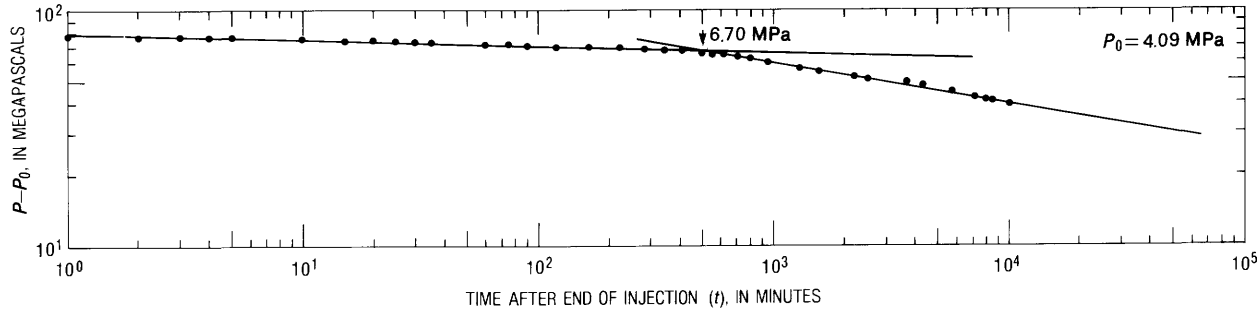

FIGURE 23.—Pressure decay plotted against time, the water injection at 442 m, June 26, 1970, West Valley, N.Y.

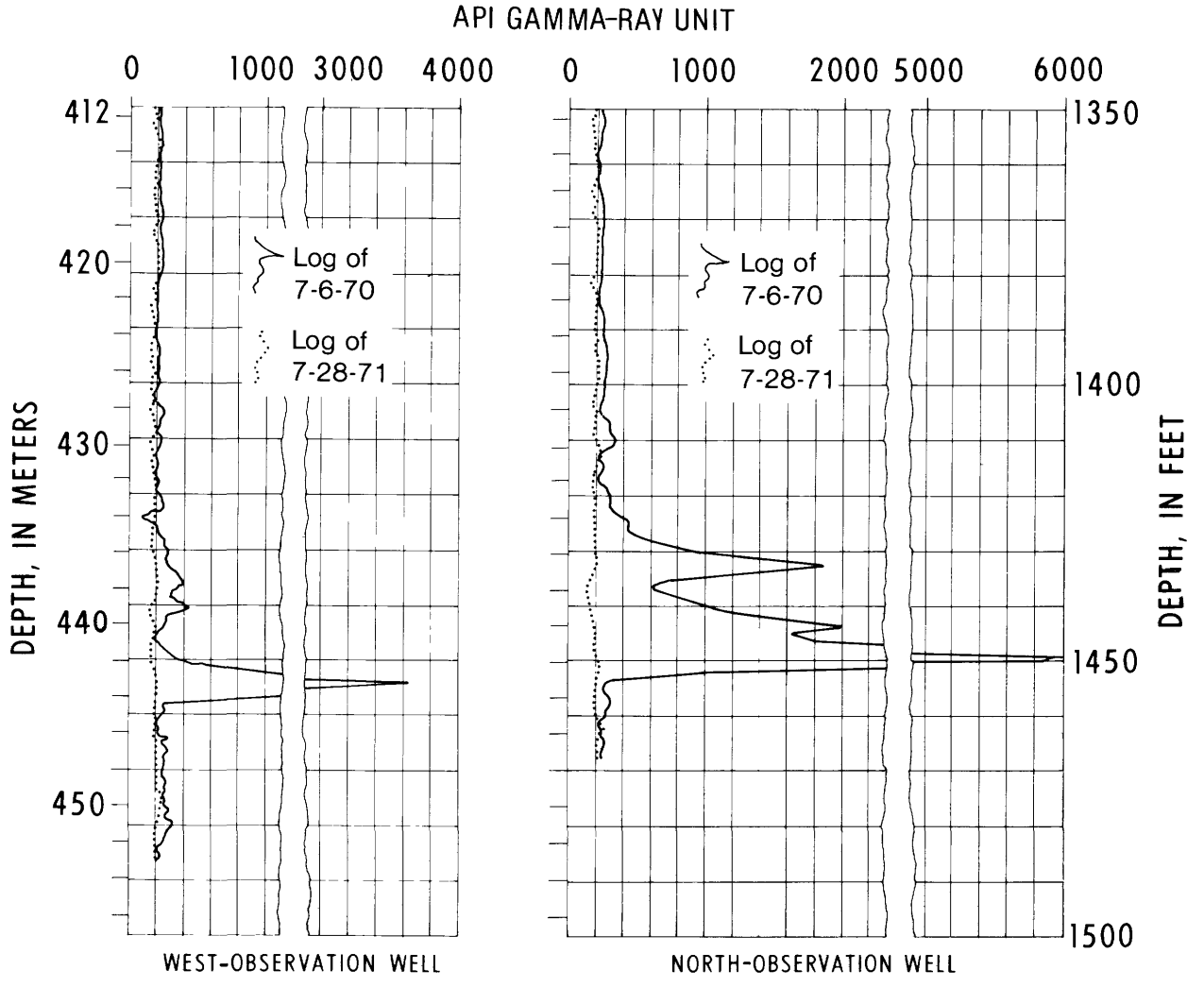

FIGURE 24.—Gamma-ray activities observed in observation wells along the casing axis, July 6, 1970, after the water injection at 442 m; depths to gamma-ray activity have been adjusted to the measuring point at the injection well, in accord with the altitude difference between the wells, West Valley, N.Y.

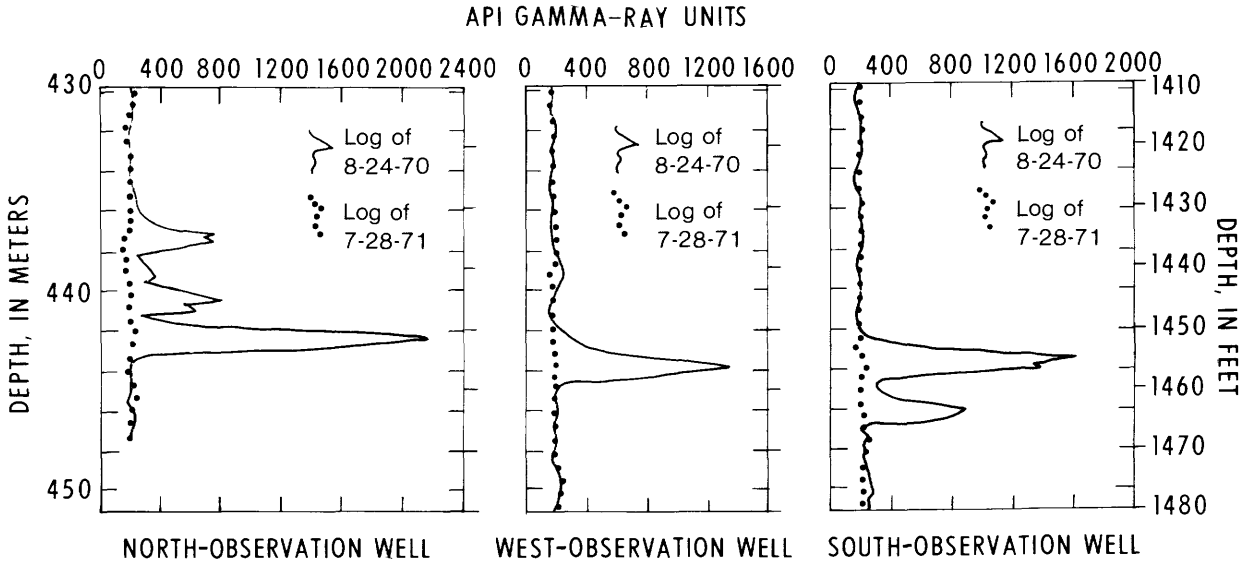

FIGURE 25.—Gamma-ray activities observed in observation wells along the casing axis, Aug. 24, 1970, after water injection at 442 m; depths to gamma-ray activity have been adjusted to the measuring point at the injection well in accord with altitude difference between the wells, West Valley, N.Y.

clean out the cement in the East-observation well because of the small-diameter well tubing. Strong gamma-ray activity was recorded in the South-observation well at this time, and a vertical spread of less than 4 m (443–447 m) was observed (fig. 25), and two layers of bedding-plane fractures were induced. The gamma-ray activity observed at the other two observation wells, North- and West-observation wells, was approximately at the same depth as recorded before; however, the intensity was reduced to less than half of the values recorded on July 6, 1970, because of radioactive decay (figs. 24, and 25).

GROUT INJECTION

Only one grout injection was made at a depth of 152 m at the West Valley site during the study. Before the grout injection, a total of 195 m^3 of water without a radioactive tracer was injected. The observed injection pressures associated with injection rates are shown in table 5 and figure 26. The regression equation of P and Q having a correlation coefficient of 0.91, was found (fig. 27) and is given by

$$P = 3.88 + 10.93Q. \quad (60)$$

Observed shut-in pressure was 3.8 MPa (table 6), which is close to the value indicated by the regression equation. Pumping rate was kept at 0.002 m^3/s during the first hour of the injection. It was then increased to 0.028 m^3/s over a 1½ hour interval. The rock was ruptured at 4.3 MPa (fig. 26.)

The overburden pressure estimated from the density of rock at a depth of 152 m is 3.5 MPa. The difference between the overburden pressure and the rupture pressure is the value of the tensile strength of shale normal to the fracture plane. If nearly horizontal bedding-plane fractures are assumed to be induced, then the tensile strength of shale normal to bedding planes at the injection depth was 0.8 MPa, which is one-fourth of the value determined from the data for water injections made at 442 m. By inspecting cores, the shale at 152 m depth was found to have been more easily ruptured along bedding planes than was the shale at 442 m depth.

Average cohesive force at fracture tip is calculated as

$$fT_{\sigma_z} = 3.5 - 3.9,$$
$$= -0.4 \text{ MPa},$$

and

$$f = 0.50.$$

The pore pressure at 152 m depth was found to be 1.3 MPa. The differences between the observed pressure decay P and pore pressure P_0 over time t are plotted on a log-log graph paper in figure 28. All data appear to fall on two straight lines. The two lines intersect at $t = 37$ minutes and $P - P_0 = 2.1$ MPa. Therefore, the earth stress normal to the fracture plane is 3.4 MPa (2.1 + 1.25 = 3.35 MPa), which is nearly equal to the calculated overburden pressure. Therefore, it can be concluded that the induced fractures are probably horizontal. No radioactive isotopes were added to the injection water; therefore, no field evidence is available to support this conclusion.

TABLE 5.—*Injection pressure of a water injection at 152 m, May 29, 1971, West Valley, N.Y.*

Time (min)	Observed wellhead pressure (MPa)	Calculated bottom-hole pressure (MPa)	Rate of injection ($m^3/s \times 10^{-3}$)	Accumulated injection volume (m^3)
0	2.76	4.25	0	0
3	2.69	4.19	.69	.4
5	2.62	4.12	3.09	.8
10	2.52	4.01	1.96	1.4
15	2.45	3.94	1.96	2.0
20	2.41	3.91	1.96	2.6
25	2.38	3.88	2.02	3.2
30	2.38	3.88	2.02	3.8
35	2.38	3.88	2.02	4.4
40	2.38	3.88	2.02	5.0
45	2.38	3.88	2.02	5.6
50	2.38	3.88	2.02	6.2
55	2.38	3.88	2.02	6.8
60	2.38	3.88	2.08	7.4
65	2.45	3.94	3.09	8.4
70	2.45	3.94	3.47	9.4
75	2.48	3.96	3.85	10.6
80	2.48	3.96	4.79	12.0
85	2.48	3.96	5.17	13.6
90	2.48	3.96	6.18	15.4
95	2.48	3.96	7.44	17.6
100	2.48	3.96	7.26	19.8
105	2.52	3.99	8.71	22.4
110	2.52	3.99	9.34	25.2
115	2.52	3.99	10.41	28.4
121	2.55	4.01	11.23	32.4
125	2.55	4.01	11.99	35.3
130	2.59	4.04	13.12	39.2
135	2.92	4.34	17.54	44.5
140	2.92	4.24	25.74	52.2
145	2.92	4.25	26.37	60.1
150	2.92	4.25	26.50	68.1
155	2.92	4.25	26.87	76.1
160	2.92	4.25	27.00	84.2
165	2.90	4.22	27.63	92.5
170	2.85	4.17	27.63	100.8
175	2.83	4.14	27.88	109.2
185	2.83	4.14	28.32	126.2
190	2.85	4.16	28.14	134.6
195	2.85	4.16	28.51	143.2
200	2.85	4.16	28.51	151.7
205	2.85	4.16	28.64	160.3
210	2.85	4.16	28.39	168.8
215	2.85	4.16	28.89	177.5
220	2.84	4.15	28.51	186.0
225[1]	2.84	4.15	28.51	195.0

[1]End of injection.

TABLE 6.—*Pressure decay of a water injection at 152 m, May. 29, 1971, West Valley, N.Y.*

Time since end of injection (min)	Observed wellhead pressure (MPa)	Calculated bottom-hole pressure, P (MPa)	$P-P_0$ (MPa)
0	2.30	3.80	2.55
1	2.25	3.74	2.49
2	2.21	3.71	2.46
3	2.19	3.68	2.43
4	2.17	3.66	2.41
5	2.15	3.65	2.40
6	2.14	3.63	2.38
7	2.12	3.62	2.37
8	2.11	3.61	2.36
9	2.10	3.59	2.34
10	2.09	3.58	2.33
15	2.03	3.53	2.28
20	1.98	3.47	2.22
25	1.93	3.42	2.17
30	1.89	3.38	2.13
35	1.84	3.34	2.09
40	1.81	3.31	2.06
45	1.77	3.26	2.01
50	1.73	3.23	1.98
55	1.70	3.20	1.95
60	1.67	3.16	1.91
65	1.63	3.13	1.88
70	1.60	3.09	1.84
75	1.57	3.06	1.81
80	1.54	3.04	1.79
85	1.51	3.01	1.76
90	1.49	2.99	1.74
100	1.45	2.94	1.69
110	1.40	2.90	1.65
120	1.37	2.86	1.61
130	1.33	2.83	1.58
140	1.31	2.80	1.55
155	1.26	2.76	1.51
170	1.23	2.73	1.48
185	1.20	2.70	1.45
200	1.17	2.67	1.42
215	1.15	2.65	1.40
230	1.13	2.63	1.38
245	1.11	2.60	1.35
260	1.09	2.59	1.34
275	1.07	2.56	1.31
290	1.05	2.55	1.30
320	1.03	2.52	1.27
350	1.01	2.50	1.25
380	.99	2.48	1.23
410	.97	2.46	1.21
440	.94	2.44	1.19
470	.93	2.43	1.18
500	.91	2.41	1.16
530	.90	2.39	1.14
560	.88	2.38	1.13
590	.88	2.37	1.12
620	.87	2.36	1.11
650	.86	2.36	1.11
680	.85	2.34	1.09
710	.84	2.34	1.09
740	.83	2.33	1.08
770	.83	2.32	1.07
800	.82	2.31	1.06
830	.81	2.31	1.06
860	.80	2.30	1.05
890	.80	2.30	1.05
920	.79	2.29	1.04
950	.79	2.28	1.03
980	.78	2.28	1.03
1,010	.77	2.27	1.02
1,040	.77	2.26	1.01

Note: Static ground-water pressure at injection level, $P_0 = 1.25$ MPa.

On July 23, 1971, a total of 155 m^3 of water and grout tagged with gamma-ray-emitting isotope of $^{95}Zr/^{95}Nb$ was injected at the same depth, 152 m, through the same slot where the water injection was made on May 29, 1971.

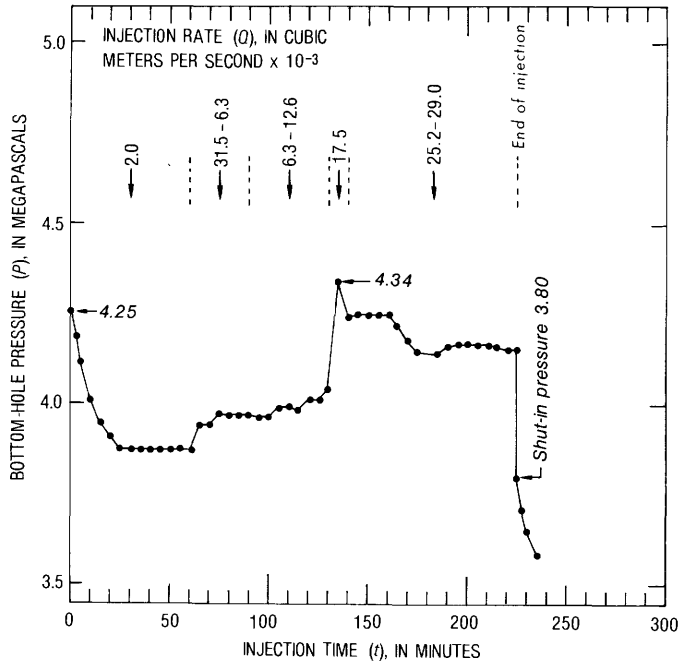

FIGURE 26.—Pressure plotted against time, the water injection at 152 m, May 29, 1971, West Valley, N.Y.

The injection was started with 9 m³ of water, after which cement and bentonite were added. The volume of injected grout was 146 m³ (table 7).

Because grout has high viscosity, the friction loss in casing was calculated by using a non-Newtonian flow equation (Slagle, 1962; Melton and Saunders, 1957), which is expressed as

$$\mathbf{R}_e = (0.816 V^{2-n'} \rho)/[K'(800/D)^{n'}], \quad (61)$$

$$\Delta P = 2.0 \times 10^{-4} \frac{L \rho V^2 f}{D}, \quad (62)$$

where

$f = 16/\mathbf{R}_e$, for laminar flow when $\mathbf{R}_e \leq 2{,}100$;

$f = 0.0045 + 0.645(\mathbf{R}_e)^{-0.7}$ for turbulent flow;

and

$\mathbf{R}_e$ = Reynold's number, dimensionless;

ΔP = fractional loss (or pressure drop), in megapascals;

ρ = fluid density, in kilograms per cubic meters;

V = average or bulk velocity of fluid, in meters per second;

D = inside diameter of tubing or casing, in centimeters;

f = Fanning friction factor, dimensionless;

K' = fluid consistency index (or characteristic of fluid), in N sec$^{n'}$/m²;

n' = fluid flow behavior index, dimensionless.

The values of K' and n' of the injected grout (July 23, 1971) were 32.52 and 0.09, respectively (K. A. Slagle, written commun., 1971). The calculated bottom-hole pressure and the observed wellhead pressure, and the injection rates and times are shown in table 7 and figure 29.

TABLE 7.—*Injection pressure of a grout injection at 152 m, July 23, 1971, West Valley, N.Y.*

[tr., trace]

Time (min)	Observed wellhead pressure (MPa)	Calculated bottom-hole pressure (MPa)	Rate of injection ($m^3/s \times 10^{-3}$)	Accumulated injection volume (m^3)
0[1]	0.28	1.77	0.32	
3	2.07	3.56	.32	
4	2.38	3.87	.32	
5	2.45	3.94	.63	
10	2.21	3.70	.32	
15	2.52	4.01	.95	
22	2.59	4.08	.95	0.1
25	2.55	4.05	1.14	.3
30[2]	2.52	4.01	1.14	.6
45	2.48	3.97	2.93	3.3
50	2.55	4.04	2.12	3.9
55	2.55	4.04	2.73	4.7
60	2.55	4.04	2.78	5.5
65	2.55	4.04	2.78	6.4
70	2.55	4.04	2.84	7.2
75	2.55	4.04	3.41	8.3
80[3]	2.55	4.04	3.41	8.9
85[4]	2.17	4.05	2.90	9.8
90	2.17	4.05	2.52	10.5
95	2.38	4.25	2.84	11.4
100	2.28	4.16	2.46	12.1
105	2.21	4.07	4.54	13.5
110	2.21	4.07	3.66	14.6
115	2.31	4.17	5.36	16.2
120	2.14	4.00	4.98	17.7
125	2.21	4.07	6.43	19.6
130	2.28	4.14	5.80	21.3
135	2.55	4.41	8.20	23.8
140	2.55	4.41	8.96	26.5
145	2.62	4.47	9.08	29.2
150	2.55	4.41	8.77	31.9
155	2.41	4.27	9.59	34.7
160	2.21	4.05	9.78	37.7
165	2.34	4.19	10.72	40.9
170	2.28	4.12	11.54	44.3
175	2.28	4.12	13.69	48.4
180	2.28	4.12	12.36	52.2
185	2.38	4.21	14.64	56.5
190	2.41	4.25	14.89	61.0
195	2.41	4.25	15.90	65.8
201	2.34	4.18	14.95	71.2
205	2.34	4.18	17.22	75.3
210	2.34	4.18	15.90	80.1
215	2.28	4.11	16.02	84.9
220	2.14	3.98	15.01	89.4
225	2.21	4.04	15.65	94.1
230	2.21	4.04	15.52	98.7
235	2.14	3.97	15.65	103.4
245	2.10	3.94	15.96	113.0
260	2.14	3.97	15.65	127.0
265	2.14	3.97	15.52	131.7
275[5]	2.07	3.90	16.60	141.3
280	2.07	3.90	15.90	146.0
290[6]	2.07	3.90	15.27	155.2

[1] Water injection.
[2] Start isotope injection.
[3] Start cement and bentonite.
[4] Grout density (average) = 1.44 g/cm³.
[5] End isotope injection.
[6] End injection.

The regression equation of P and Q, having a correlation of 0.65 was found (fig. 30) and is expressed as

$$P = 4.0 + 13.12Q. \quad (63)$$

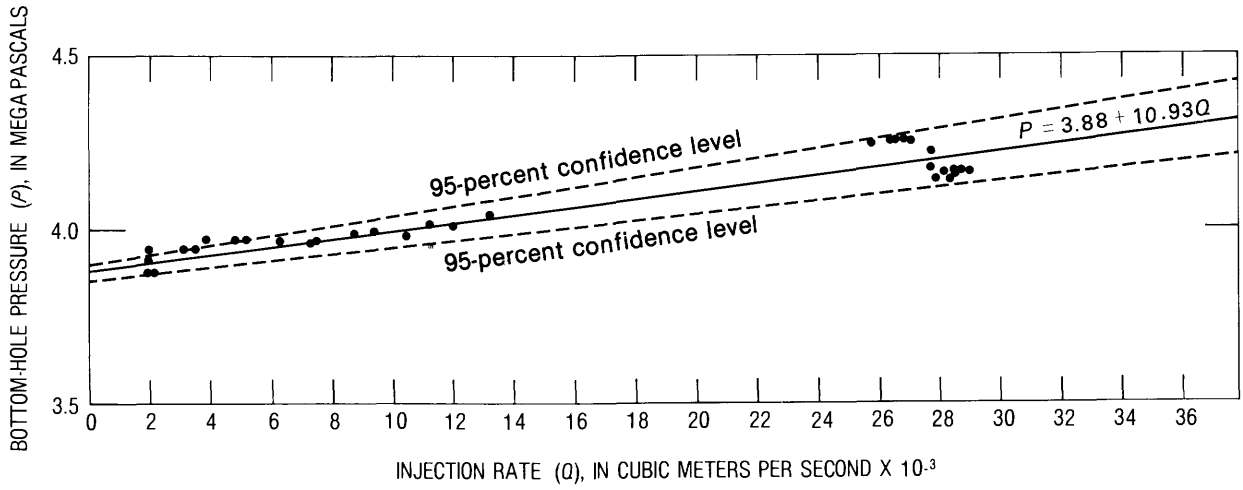

FIGURE 27.–Pressures plotted against injection rate, the water injection at 152 m, May 29, 1971, West Valley, N.Y.

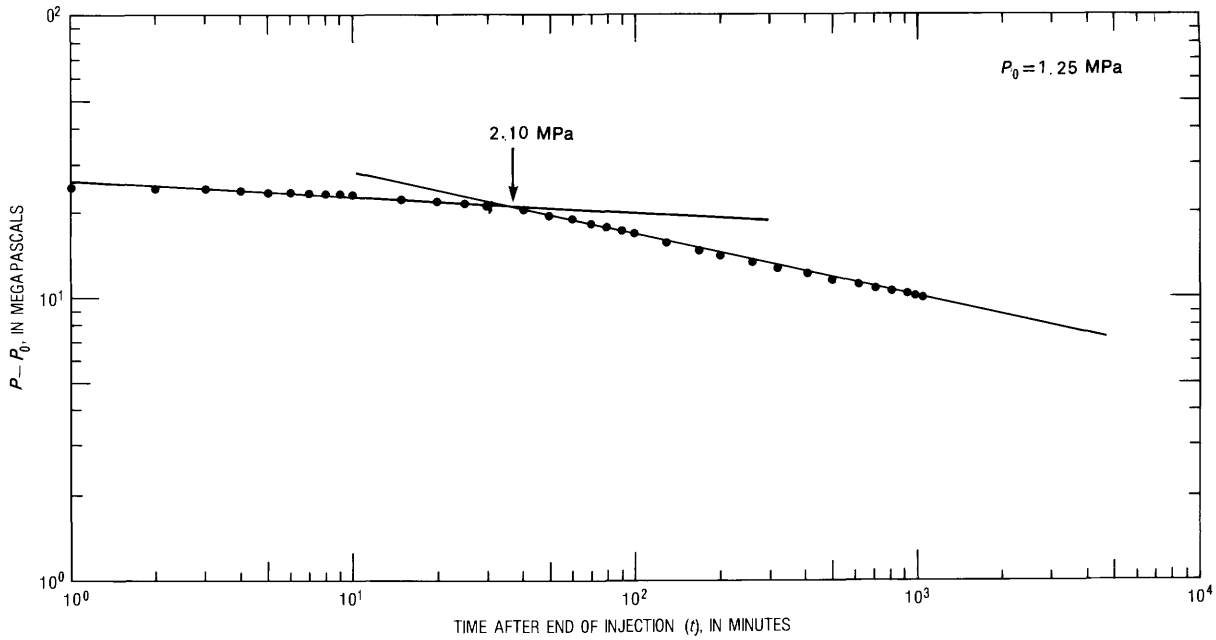

FIGURE 28.–Pressure decay plotted against time, the water injection at 152 m, May 29, 1971, West Valley, N.Y.

No breakdown pressure was observed. However, several high pressures indicating the formation of new fractures were noted during the injection. The tensile strength of the rock at the injection depth probably could be estimated from these high pressures. The injection pressure at 0.003 m^3/s was 4.3 MPa, from which the tensile strength of the shale normal to the fracture plane at the injection depth of 152 m was estimated as

$$T_{\sigma_z} = 3.5 + 13.12 \times 0.0003 - 4.3,$$
$$= -0.8 \text{ MPa}.$$

The tensile strength of the shale estimated from other high pressures is also near 0.8 MPa. The value of the tensile strength estimated from this grout injection is similar to that estimated from the previous water injection at the same depth.

Gamma-ray logs were made on July 28, 1971, five days after the injection, in three observation wells. The results are shown in figure 31. No gamma-ray survey was made in the East-observation well because its casing was ruptured during the injection. The well was plugged by grout at a depth of 151 m.

Gamma-ray logs obtained from the other three observation wells together with the evidence of plugging of the East-observation well strongly suggest that bedding-plane fractures were induced, at least within a distance of 46 m from the injection well.

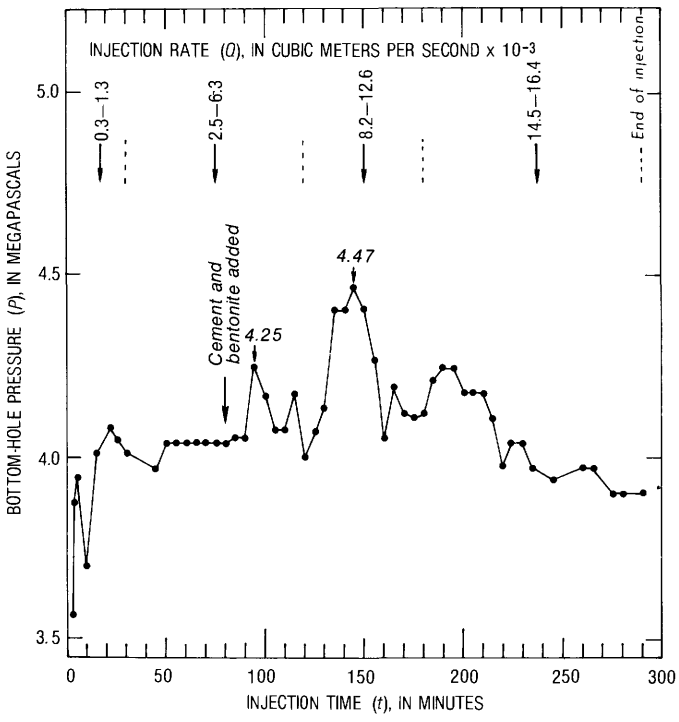

FIGURE 29. – Pressure plotted against time, the grout injection at 152 m, July 23, 1971, West Valley, N.Y.

Precise levels were surveyed by the U.S. Geological Survey before and after the grout injection. To insure that the level rods would be held on the highest point at all times, all bench-mark tablets were straightened and leveled by a hand level before the precise levelings were made. The leveling results are shown in table 8 and figure 32.

The correlation between the observed uplift and the uplift calculated by equation 47 is shown in figure 33. The calculated radius of the induced fracture is 110 m, and the calculated maximum separation of the fracture during injection time is 6.5 mm.

SUMMARY

Table 9 summarizes the results of all six injections made at West Valley, N.Y. (Sun and Mongan, 1974). Results from injections made at the same depth at different times are consistent. No actual data on tensile strength of the shale are available; therefore, there is no way to check whether the calculated tensile strengths are approximately right.

Bedding-plane fractures had been induced, as indicated by gamma-ray logs, within 10 m of the injection depth. Orientation of the induced fractures can be determined indirectly by monitoring injection pressure during injection time and by measuring the pressure decay of water injections and the uplift of ground surface. Constructing observation wells with strong tubing and good cement helps prevent damage to the well by induced fractures, and the size of observation well needs to be large enough to accommodate drilling tools if the well needs to be serviced after completion. The unsuitability of the East-observation well during the study indicates the importance of proper well construction.

RADIOACTIVE WASTE DISPOSAL AT THE OAK RIDGE NATIONAL LABORATORY, TENN.

The Oak Ridge National Laboratory waste disposal site is located in Melton Valley, Oak Ridge, Tenn. (fig. 34), within the reservation of the U.S. Department of Energy (DOE). The reservation is in the Tennessee section of the Appalachian Valley and Ridge province and occupies parts of Anderson and Roane Counties. The reservation is bounded on the northeast, southeast, and southwest by the Clinch River. The area is approximately 22 km long, 10 km wide, and comprises about 220 km^2.

The first grout injection was made in 1959 at a shallow depth of 90 m. A total volume of 102 m^3 of grout composed of water, cement, and bentonite tagged with ^{137}Cs was injected. Twenty-two core holes were drilled, data from which indicated that bedding-plane fractures had been induced. In 1960, a second experimental well was constructed roughly 1.83 km east of the first injection site. Two injections were made through this well at depths of 212 m and 285 m, respectively. A total volume of 345 m^3 of grout containing ^{137}Cs was injected at a depth of 285 m. After this injection, the injection well was plugged with cement to a depth of 213 m. A new horizontal slot was cut through the casing and cement wall at a depth of 212 m. A total volume of 502 m^3 grout also tagged with ^{137}Cs was injected again into this well. Twenty-four core holes were drilled to determine the positions of the two grout sheets. Both grout sheets were found to be conformable to bedding planes. A third well was drilled to a depth of 329 m, 0.8 km west of the second experimental site (fig. 34), thereafter named as the present fracturing site. (In 1981 this well is still being used for waste injections.) From 1964 through 1965, eight experimental injections of actual radioactive wastes produced at the ORNL were injected through this well. The results strongly indicated that the disposal of wastes in shale by grout injection is safe and economical. Operational injections then began in 1966. The disposal site will reach full capacity between 1985 and 1988. A new disposal site was selected at a distance of 245 m south of the present injection well (fig. 34), and a site evaluation study was conducted. The results indicate that the proposed site is acceptable. The following discussions summarize the experimental and operational injections and the site evaluation.

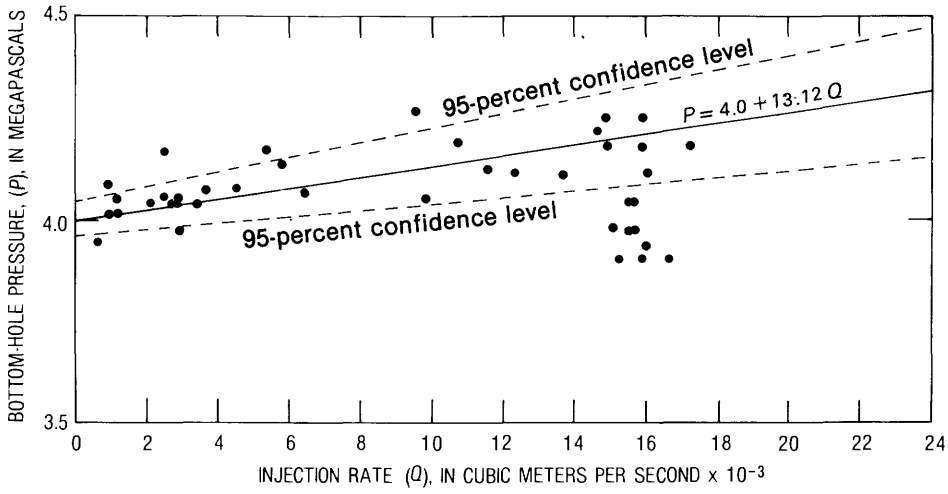

FIGURE 30. – Pressure plotted against injection rate, the grout injection at 152 m, July 23, 1971, West Valley, N.Y.

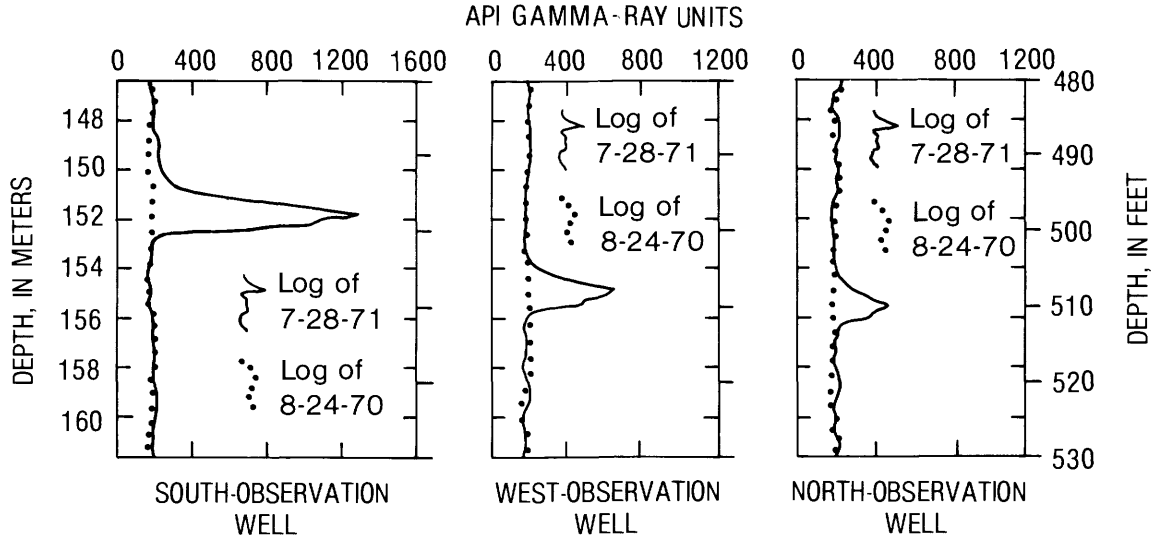

FIGURE 31. – Gamma-ray activities observed in observation wells along the casing axis, July 28, 1971, after the grout injection at 152 m; depths to gamma-ray activity have been adjusted to the measuring point at the injection well in accord with altitude difference between wells, West Valley, N.Y.

GEOLOGY AND HYDROLOGY

The Appalachian Valley and Ridge province in the Oak Ridge area is about 80 km wide and is marked by a series of major subparallel thrust faults that trend northeast and dip southeast. In each of the faults, layers of rock units roughly 3 km thick have moved as much as several tens of kilometers to the northwest. Older formations have been thrust over younger formations. Deformation of the rock strata of the Oak Ridge area resulted from compressional forces orginating during the Appalachian revolution at the end of Paleozoic time. The strata reacted to the pressure by faulting and folding (Eardley, 1951; McMaster, 1963; deLaguna and others, 1968). At least 3,000 m of rock has been eroded since the thrust faults were formed (deLaguna and others, 1968).

The thrust fault of immediate interest to the waste disposal at the ORNL is the Cooper Creek Fault, which affects four formations at the site (fig. 35). They are the Rome Formation (interbedded sandstone, siltstone, shale, and locally, dolomite) of Early Cambrian age, the Conasauga Group (calcareous shale interbedded with limestone and siltstone) of Middle and Late Cambrian age, the Knox Group (dolomite) of Late Cambrian and Early Ordovician age, and the Chickamauga Limestone of Middle and Late Ordovician age. Two thin-bedded red calcareous shales, each 60 m thick, were found in the

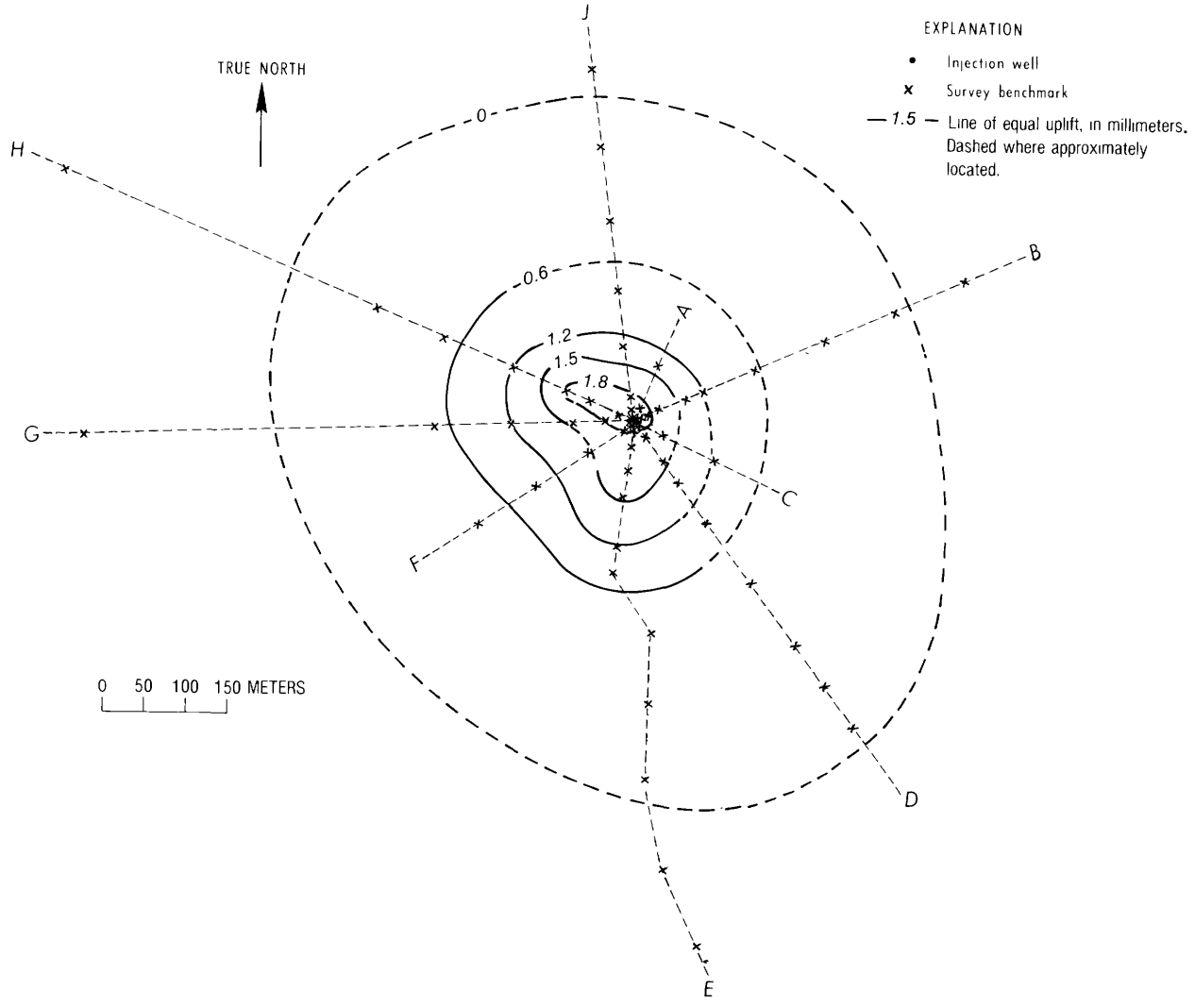

FIGURE 32.—Uplift produced by the grout injection at 152 m, West Valley, N.Y.

Chickamauga Limestone at the ORNL during the drilling of a test well (fig. 35).

The formation exposed at the ORNL waste-injection site is the Conasauga Group; all formations above the group have been eroded. The thickness of the Conasauga Group is 400 m at the injection site. The injection rock is the bottom 90 m of the Conasauga, the Pumpkin Valley, which is a dense argillaceous shale that is very thin bedded and dominantly red. The Pumpkin Valley is overlain by the Rutledge, 300 m thick, composed of gray calcareous shale interbedded with generally thin beds or lenses of limestone. The contact between the Pumpkin Valley and the Rutledge is marked by three layers of limestone.

The formations all dip to the southeast. Near the outcrop area, the Rome formation dips 45°; however, away from the outcrop, dips flatten out to 10°–20°. The beds within the fault sheets are, in general, relatively little deformed. The Pumpkin Valley is generally undeformed, but locally it is marked by drag folds varying in amplitude from a few centimeters to as large as a couple of meters. The measured geothermal gradient is 1.34° C per 100 m; the average air temperature is 14.5° C, as shown in figures 36 and 37 (deLaguna and others, 1968;

TABLE 8. – *Ground elevation affected by a grout injection at 152 m, July 23, 1971, West Valley, N.Y.*

Bench mark	Distance from injection well (m)	Altitude of benchmark, in meters		Uplift (mm)
		Before injection	After injection	
A1	16.89	423.95586	423.95763	1.77
A2	51.08	416.85725	416.85871	1.46
B1	7.59	423.56822	423.57007	1.86
B2	15.30	423.65289	423.65469	1.80
B3	30.36	422.64138	422.64266	1.28
B4	68.34	419.50151	419.50276	1.25
B5	92.08	424.90601	424.90702	1.01
B6	159.11	428.23041	428.23114	.73
B7	250.12	434.91805	434.91878	.73
B8	340.58	449.27322	449.27383	.61
B9	430.19	468.33834	468.33940	1.06
C1	37.73	424.60810	424.60978	1.68
D1	7.65	423.81577	423.81751	1.74
D2	22.95	423.89557	423.89719	1.62
D3	60.84	423.05368	423.05515	1.47
D4	92.84	423.80447	423.80514	.67
D5	153.71	422.60438	422.60514	.76
D6	245.39	423.14275	423.14311	.36
D7	336.74	424.93817	424.93863	.46
D8	428.21	427.21890	427.21926	.36
D9	488.41	428.61936	428.61994	.58
E1	7.62	423.57760	423.57919	1.59
E2	30.51	423.90603	423.90773	1.70
E3	60.93	423.88317	423.88490	1.73
E4	91.41	423.79273	423.79441	1.68
E5	152.40	424.59713	424.59835	1.22
E6	243.81	425.00410	425.00468	.58
E8	315.16	426.36396	426.36396	0
E9	399.29	426.36811	426.36799	−.12
E10	490.73	427.64775	427.64729	−.46
E11	593.14	425.99863	425.99814	−.49
E12	688.85	429.60950	429.60914	−.36
F1	7.59	423.41191	423.41374	1.83
F2	15.24	423.38692	423.38884	1.92
F3	68.55	424.10131	424.10277	1.46
F4	144.72	425.59922	425.60029	1.07
F5	227.62	424.28053	424.28157	1.04
G1	7.68	423.30758	423.30947	1.89
G2	38.04	423.77731	423.77914	1.83
G3	76.23	423.50271	423.50424	1.53
G4	152.46	424.83265	424.83384	1.19
G5	243.84	423.47092	423.47175	.83
G6	676.66	421.84518	421.84564	.46
H1	7.65	423.39116	423.39314	1.98
H2	23.07	422.82359	422.82554	1.95
H3	60.81	423.14147	423.14342	1.95
H4	91.17	423.28265	423.28448	1.83
H5	160.57	422.48252	422.48371	1.19
H6	253.99	422.82039	422.82121	.82
H7	341.86	423.10218	423.10285	.67
H8	746.76	421.03304	421.03292	−.12
J1	7.62	423.40996	423.41182	1.86
J2	15.24	423.22903	423.23092	1.89
J3	33.50	420.21697	420.21874	1.77
J4	90.28	423.95431	423.95549	1.18
J5	157.67	423.00427	423.00540	1.13
J6	242.19	424.31345	424.31458	1.13
J7	333.18	427.78747	427.78875	1.28
J8	424.83	429.44055	429.44165	1.10

U.S. Energy Research and Development Administration, 1977).

The permeability of the Conasauga Group determined from core samples in the laboratory ranges from 10^{-7} to 10^{-8} D; even with fractures present in the core, the permeability determined is 10^{-5} D. Mineralogical examination of the Pumpkin Valley core indicates that clay minerals, kaolinite, illite, and chlorite make up the bulk of the samples. Quartz is present in moderate quantities, but calcite is conspicuous by its absence. The abundance of clay minerals indicates that the shale selected for injection has sufficient ion-exchange and adsorption capacity (deLaguna and others, 1968).

Records of 11 stations in and around the ORNL indicate that the annual precipitation is 130 cm for the water years 1936 through 1960. Maximum monthly runoff is likely to be in December through March, when rainfall is normally high and soil moisture and groundwater storage are at a maximum. Minimum runoff occurs in September through November, when rainfall is low and soil moisture and ground-water storage are at a minimum (McMaster, 1967).

The waste-injection site is located in Melton Valley, a part of the Whiteoak Creek drainage basin (fig. 34). Chestnut Ridge forms the northwestern drainage divide, and Cooper Ridge, the southeastern divide of the drainage basin. Most of Bethel Valley (the laboratory area) is drained by Whiteoak Creek; however, Melton Valley is drained by Melton Branch, a tributary to Whiteoak Creek. Whiteoak Creek flows southwestward through Bethel Valley to a water gap in Haw Ridge and enters Melton Valley, where it is joined by Melton Branch; it then flows southwestward through a small impoundment known as Whiteoak Lake before entering the Clinch River (fig. 34).

The dolomite of the Knox Group of Chestnut Ridge is the principal aquifer in the Whiteoak Creek drainage basin. Bethel Valley is underlain by the Chickamauga Limestone. A substantial quantity of water is probably stored in many small openings in the weathered zone of the limestone within 30 m of the land surface. Low-flow measurements (the flow equaled or exceeded 90 percent of time is 0.085 m^3/s) show that 90 percent of the Whiteoak Creek low flow originates as ground-water discharge from the dolomite of the Knox Group of Chestnut Ridge and the Chickamauga Limestone of Bethel Valley, and as ORNL plant effluents (McMaster, 1967).

The Rome Formation of Haw Ridge forms the northwestern water divide of Melton Branch. This formation has very little capacity for receiving, storing and transmitting water. In the weathered rock, the occurrence of ground water is largely limited to small openings that occur along joints and bedding planes. Melton

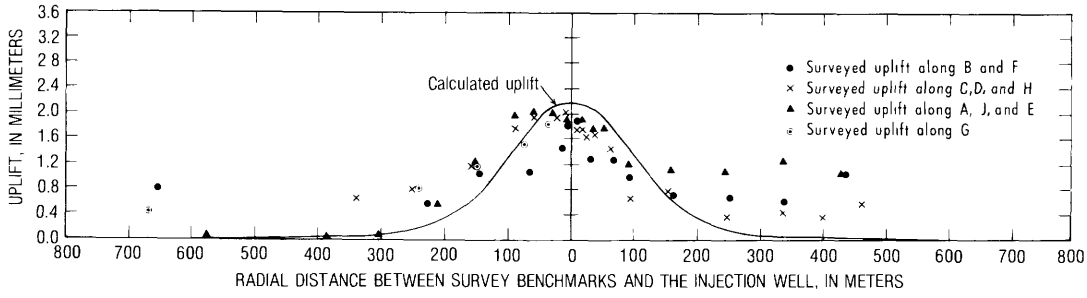

FIGURE 33.—Calculated and surveyed uplift produced by a grout injection at 152 m, West Valley, N.Y.

TABLE 9.—*Instantaneous shut-in pressure, calculated overburden pressure, tensile strength of shale, average cohesive force at fracture tip, and value of f, West Valley, N.Y.*

No.	Date	Injection Depth (m)	Injection fluid	Total injection volume (m^3)	Calculated overburden pressure		Instantaneous shut-in pressure		Calculated tensile strength (MPa)	Calculated average cohesive force at fracture tip, fT[1] (MPa)	Value of f	Remarks
					By specific gravity (MPa)	By pressure-decay data (MPa)	Observed (MPa)	Predicted (MPa)				
1	Oct. 9, 1969.	442	Water _____	433	10.90	10.84	12.05	11.96	3.09	1.06	0.34	Before 45-minute pause.
	Oct. 9, 1969.	442	Water _____	433	10.90	10.84	11.98	11.96	3.92	1.06	.27	After 45-minute pause.
2	June 26, 1970.	442	Water _____	425	10.40	10.43	13.29	15.20	3.87	1.78	0.45	
3	Aug. 27, 1970.	374	Water _____	343	9.16	9.49	9.87	9.89	4.15	0.73	0.18	
4	May 10, 1971.	308	Water _____	374	7.48	7.36	8.06	Regression equation has not been established.	3.12	0.58	0.19	
5	May 29, 1971.	152	Water _____	195	3.52	3.10	3.80	3.88	0.73	0.36	0.49	
6	July 23, 1971.	152	Water and grout.	9 (water); 142 (grout).	3.52	_____	Did not observe.	4.00	0.76–0.83	0.48	0.58–0.63	

[1]Average cohesive forces at the fracture tip, fT, are calculated on the basis of the regression equations of P and Q. The value of fT calculated on the basis of the observed instantaneous shut-in pressures are essentially the same as those based on the regression equations.

Valley is underlain by the Conasauga Group. Ground water in the Conasauga occurs principally in the weathered zone, where openings along joints and bedding planes have been slightly enlarged by weathering and circulating water. Because these enlarged openings occur only at shallow depths, 0–10 m below land surface, the total capacity of shale of the Conasauga Group for receiving, storing, and transmitting water is small (McMaster and Waller, 1965). In the late fall, periods of no flow have frequently occurred in Melton Branch (McMaster, 1963).

There is no known movement of ground water below a depth of 100 m. The isolation of the Pumpkin Valley member of the Conasauga Group is further demonstrated by the fact that the Pumpkin Valley contains small amounts of disseminated sodium chloride and methane gas (U.S. Energy Research and Development Administration, 1977). Cores taken from 30 m below the land surface showed no signs of iron stains, weathering, and solution cavity. A geothermal measurement (fig. 36) also indicates that there is no significant movement of ground water deeper than 200 m.

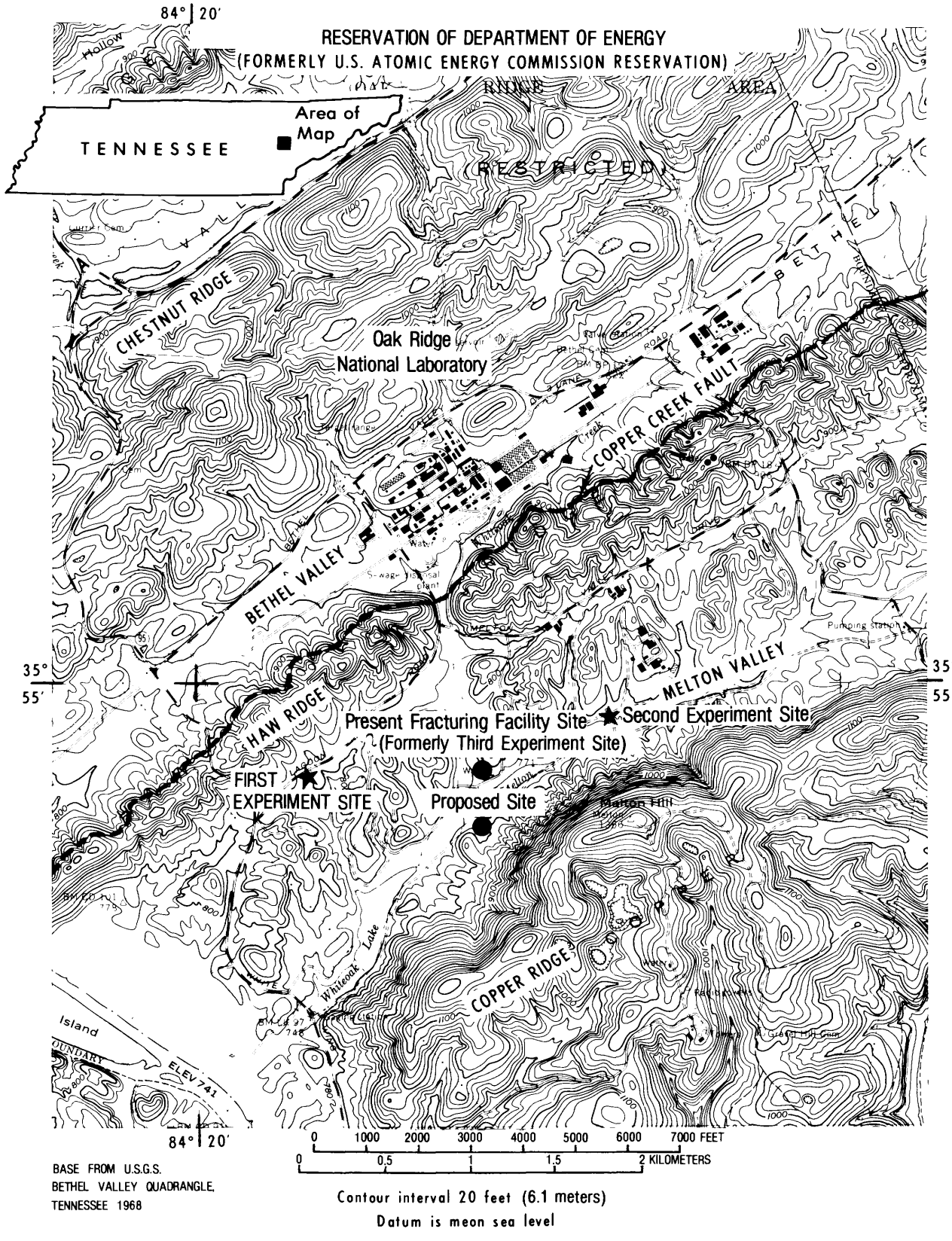

FIGURE 34.—Location of hydraulic-fracturing-experiment sites, present fracturing site, and proposed site, Oak Ridge National Laboratory, Tenn.

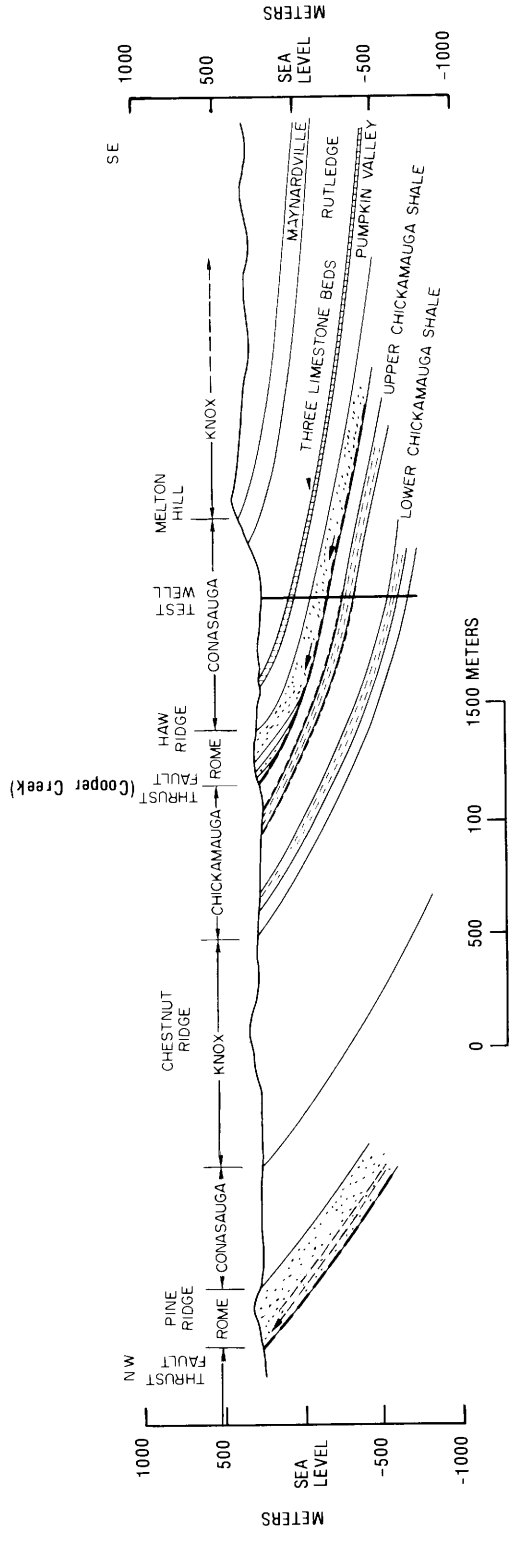

FIGURE 35.–Section showing subsurface geology near the hydraulic-fracturing sites, Oak Ridge National Laboratory, Tenn. (from deLaguna and others, 1968).

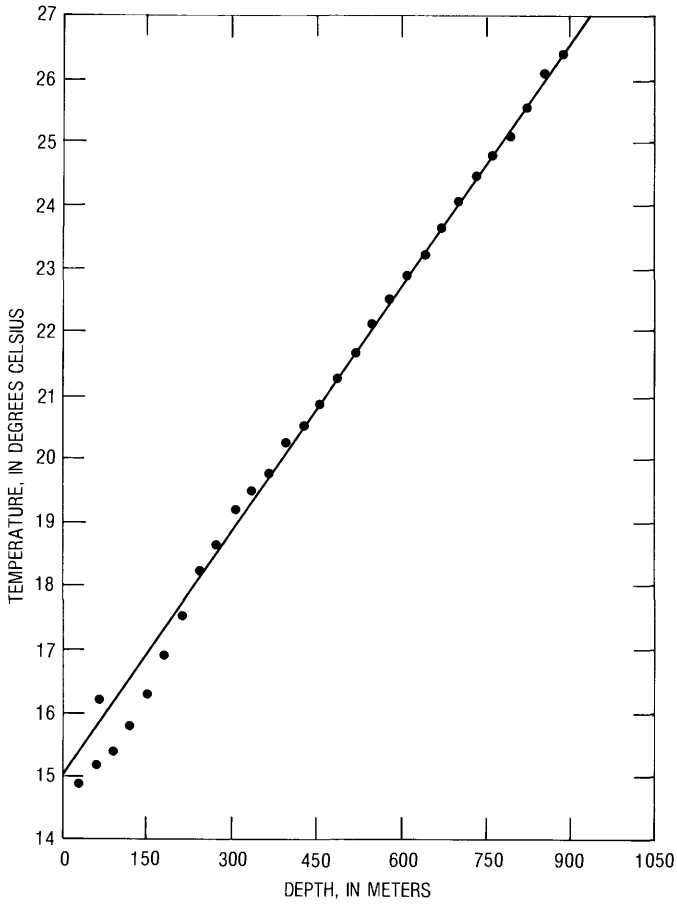

FIGURE 36.—Graph of temperature plotted against depth at the present fracturing site, Oak Ridge National Laboratory, Tenn. (from deLaguna and others, 1968).

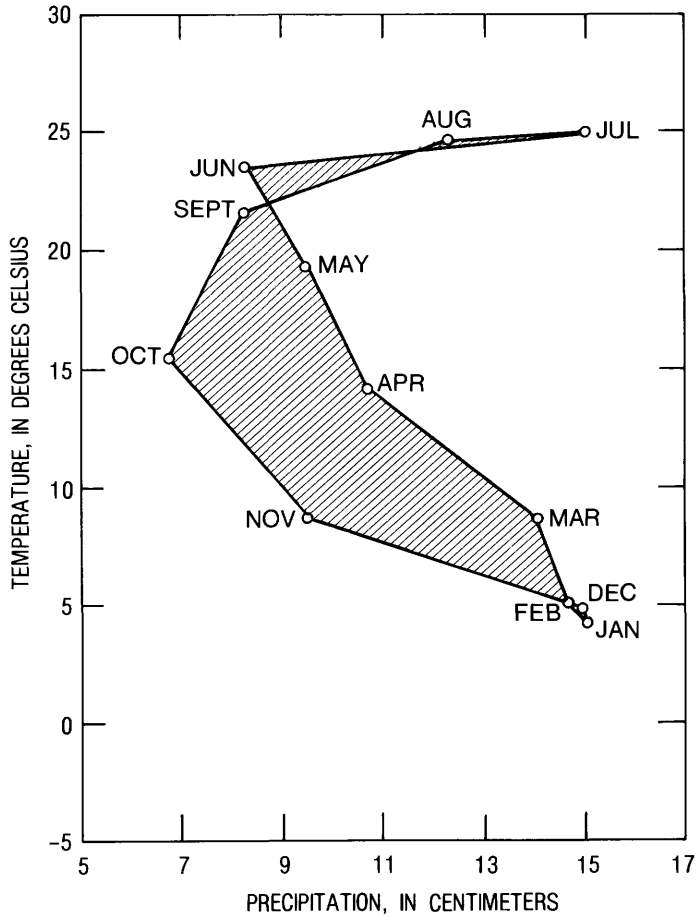

FIGURE 37.—Graph of average monthly temperatures and precipitation, Oak Ridge, Tenn. (from U.S. Energy Research and Development Administration, 1977).

SEISMICITY

Available information for the period 1699 through 1973 indicates that no earthquakes have been reported within 16 km of Oak Ridge; however, earthquakes have been reported in the area predominantly to the south and east (fig. 38). The largest earthquake (intensity Modified Mercali VII) was recorded near Luttrell, Tenn., March 28, 1913 (McClain and Meyers, 1970; U.S. National Oceanic and Atmospheric Administration and U.S. Geological Survey, 1975). However, no field evidence or literature on active or potentially active faults in the vicinity of the ORNL site have been found.

NATURE OF RADIOACTIVE WASTES PRODUCED AT THE OAK RIDGE NATIONAL LABORATORY

Radioactive wastes disposed of by grout injection and hydraulic fracturing at the ORNL site are produced by a number of different research, development, and production programs conducted at the ORNL, including basic radiochemistry studies; development of reactor-fuel reprocessing methods; production of radioisotopes for medical, industrial, and research uses; production of transuranium isotopes for research; and operation of research reactors. The wastes are neutralized with sodium hydroxide to reduce corrosiveness and are stored in underground stainless steel tanks, which are periodically pumped to underground concrete collection tanks. The addition of sodium hydroxide causes some of the dissolved materials to precipitate from the waste solution. The precipitates settle as sludge at the bottom of the storage tanks. The liquid above the sludge is fed to an evaporator, which concentrates the liquid waste by a factor of 20 to 30. The concentrated waste is stored in the underground concrete collection tanks for temporary storage; it is then periodically disposed in shale by grout injection. Roughly 300 m^3 of concentrated liquid waste is produced at the ORNL each year (U.S. Energy Research and Development Administration, 1977). The approximate chemical composition and radionuclide content of the ORNL waste are shown in table 10 (deLaguna and others, 1971; Weeren, 1976;

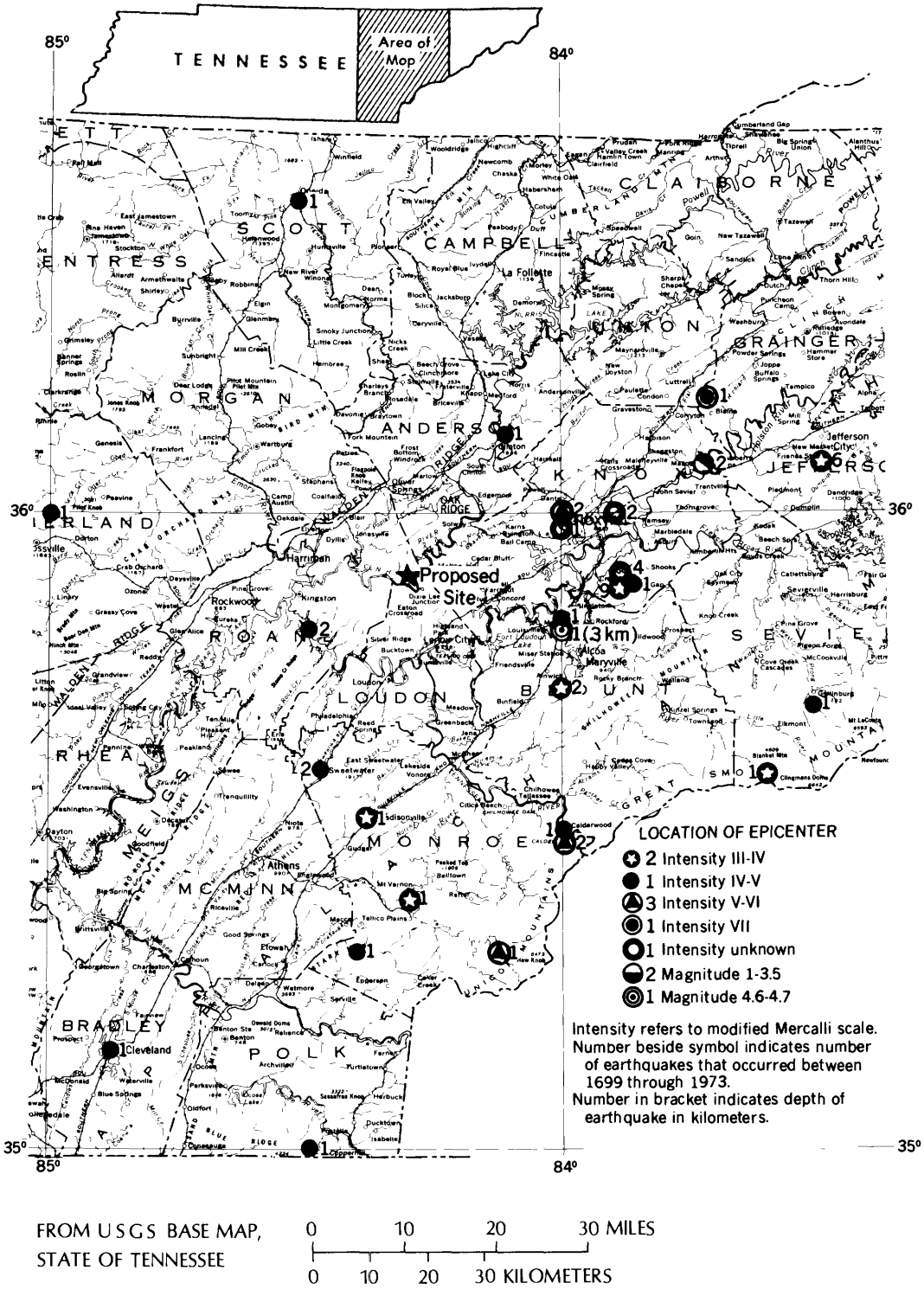

FIGURE 38.—Location of epicenters near Oak Ridge, Tenn., determined on the basis of available information (McClain and Meyers, 1970; U.S. National Oceanic and Atmospheric Administration and U.S. Geological Survey, 1975) for the period 1966 through 1973.

TABLE 10.—*Approximate waste composition produced at the Oak Ridge National Laboratory, Tenn.*

[From deLaguna and others, 1971; Weeren, 1976; ERDA, 1977. M, moles per liter]

Compound or element	Composition
NaOH	0.05–0.7 M
$Al(NO_3)_3 \cdot 9H_2O$	.005–0.04 M
NH_4NO_3	.003–0.06 M
$NaNO_3$	.1–1.0 M
Na_2SO_4	.09–0.2 M
NaCl	.04–0.2 M
Na_2CO_3	.01–0.2 M
$Al_2(SO_4)_3$	.005–0.2 M
$(NH_4)_2SO_4$	.01–0.2 M
^{137}Cs	.3 Ci/L
^{90}Sr	.03 Ci/L
^{244}Cm	.3 mCi/L
Long lived radionuclides (half life > 30 yrs)	< 10 nCi/g

U.S. Energy Research and Development Administration, 1977).

SUMMARY OF DISPOSED RADIOACTIVE WASTES

During 1964 and 1965, seven experimental injections had been made through the present disposal well. The first two experimental injections were made with synthetic wastes and the last five injections were made with actual wastes. Experimental results have indicated that grout injection by hydraulic fracturing is suitable and economical for disposal of the radioactive wastes at the ORNL; therefore since 1966 operational injections have been made periodically. At the end of 1978, a total of 17 operational injections were made.

From 1964 through 1978, a total volume of 6,400 m^3 (excluding synthetic waste) of intermediate-level

TABLE 11.—*Radioactive-waste injected in Pumpkin Valley shale, Oak Ridge National Laboratory, Tenn., 1964–1978*

[NA, not analyzed]

Name of injection	Injection date	Injection depth (m)	Injection altitude (m)[1]	Waste injected (m^3)	Grout volume (m^3)	Solids/liquids (kg/m^3)	Radionuclides (in Ci, except ^{239}Pu and ^{244}Cm, which are in grams)							
							^{90}Sr	^{137}Cs	^{106}Ru	^{60}Co	^{144}Ce	^{198}Au	^{239}Pu	^{244}Cm
Test injection														
1[2]	Feb. 13, 1964	288.0	−46.7	141.2	152.8	75.2								
2[2]	Feb. 20–21, 1964	281.6	−40.3	107.1	143.0	813.0						30		
3	Apr. 8, 1964	278.0	−36.6	126.8	247.2	1,565.5	4.9	74	0.4	0.1				
4	Apr. 17, 1964	274.3	−33.0	135.9	217.5	1,329.8	.9	50	1.2	.1				
5	May 28, 1964	271.3	−29.9	558.7	799.7	842.0	608.0	193	35.0	4.0	4,099			
6A[3]	May 19, 1965	268.2	−26.9	16.7	21.5	454.8								
6B	May 22, 1965	265.8	−24.4	242.2	351.2	719.0	330.0	1,562	2.0	1.0				
7	Aug. 16, 1965	265.8	−24.4	263.3	467.1	828.7	492.0	3,358	2.0	14.0				
Operational injection														
ILW-1A	Dec. 12, 1966	265.8	−24.4	141.7	208.2	744.7	41.0	11,500	1.0	16.0	20	NA	NA	
ILW-1B	Dec. 13, 1966	265.8	−24.4	98.4	152.1	742.4	38.0	7,600	8.0	3.0	13	NA	NA	
ILW-2A	Apr. 20, 1967	262.7	−21.4	308.1	461.0	718.5	564.0	31,329	99.0	236.0		NA	NA	
ILW-2B	Apr. 24, 1967	262.7	−21.4	243.5	411.0	773.4	474.0	26,350	83.0	199.0		NA	NA	
ILW-3A[3]	Nov. 28, 1967	262.7	−21.4	117.3										
ILW-3B	Nov. 29, 1967	262.7	−21.4	196.8	555.5	659.1	9,000.0	17,000	400.0	200.0				
Water test	Dec. 13, 1967	259.7	−18.3		169.2									
ILW-4A[3]	Apr. 3, 1968	259.7	−18.3	90.9										
ILW-4B	Apr. 4, 1968	259.7	−18.3	235.4	494.6	611.2	4,300.0	51,900	200.0				17.8	NA
ILW-5	Oct. 30, 1968	256.6	−15.3	309.6	435.9	671.1	500.0	69,400	300.0	100.0			18.5	NA
ILW-6	June 11, 1969	256.6	−15.3	300.3	478.2	647.1	8,900.0	89,000	100.0	200.0			3.9	NA
ILW-7	Sep. 23, 1970	256.6	−15.3	314.2	551.4	659.1	2,747.0	44,833	236.0	72.0			28.60	0.230
ILW-8	Sep. 29, 1972	253.6	−12.3	275.2	411.1	874.8	45.0	27,917	2,523.0				2.13	.002
ILW-9	Oct. 17, 1972	253.6	−12.3	258.5	431.5	934.7	231.0	23,359	376.0				None	.068
ILW-10	Nov. 8, 1972	253.6	−12.3	320.8	503.3	850.9	1,331.0	18,817	593.0				None	.346
ILW-11	Dec. 5, 1972	253.6	−12.3	286.8	495.0	862.8	1,099.0	23,486	379.0				None	1.791
ILW-12	Jan. 24, 1975	250.5	−9.2	97.3	159.3	791.0	1,324.0	12,752					None	.012
ILW-13	Apr. 29, 1975	250.5	−9.2	306.6	477.3	755.0	3,368.0	35,750					.49	.214
ILW-14	June 20, 1975	250.5	−9.2	314.0	525.0	802.9	2,874.0	30,592					None	.043
ILW-15	June 30, 1975	250.5	−9.2	344.4	549.0	503.3	138.3	26,390					10.75	None
ILW-16	Nov. 17, 1977	247.5	−6.2	208.9	300.9	862.8	1,618.0	14,964					None	None
ILW-17	Sep. 1, 1978	244.4	−3.1	311.5	520.4	838.9	90.0	22,270					1.19	.027
Total				6,672.1	10,689.9		40,118.1	590,446	5,338.6	1,045.2	4,132	30	83.36	2.733

Total radioactivity 641,342.7 Ci.

NOTE.—Data sources: Injections 1–7, ILW-1A through ILW-2B, deLaguna and others, 1968, 1971; ILW-3A through ILW-7, deLaguna and others, 1971; ILW-8 through ILW-11, Weeren, 1974; ILW-12 through ILW-14, Weeren, 1976; ILW-15 through ILW-17, Weeren, written commun., 1979.

[1]Mean sea level.
[2]Synthetic waste.
[3]Stopped owing to difficulties. Activity merged with B.

radioactive waste (5.6×10^{-3} μCi/mL ≤ specific activity ≤ 5.3×10^{2} μCi/mL containing mainly of ^{90}Sr and ^{137}Cs) was disposed of through the present injection well at depths ranging from 244 to 288 m (table 11). The waste contained a total activity of 641,300 Ci among which were 590,400 Ci of ^{137}Cs, 40,000 Ci of ^{90}Sr, 80 g of ^{239}Pu, 3 g of ^{244}Cm, and 10,500 Ci of other radionuclides, including ^{60}Co, ^{106}Ru, and ^{144}Ce.

INJECTION PROCESSES AND THE DISPOSAL PLANT

The injection processes and disposal plant at the ORNL have been discussed by many investigators (deLaguna and others, 1968, 1971; Weeren, 1974, 1976). The following paragraphs are a summation of these reports.

The major equipment used in injection consists of a waste pump, a jet mixer, a surge tank, and an injection pump (fig. 39). An artist's sketch of the disposal plant is shown in figure 40. The injection capacity of the waste-injection pump is 40 MPa at 3 m^3/s and 7 MPa at 20 m^3/s. A standby injection pump (fig. 39) having a similar injection capacity is equipped to flush the injection well with water to free it of grout in the unlikely event of a failure of the injection pump. Five underground waste storage tanks (figs. 39, 40) having a total capacity of 340 m^3 were constructed at the disposal site to receive wastes delivered from storage tanks at the laboratory site before injection.

Solids that consist of cement, fly ash, attapulgite clay, illite or its equivalent, and a retarder, such as delta gluconolactone, are preblended before injection in accord with the desired proportion designed by laboratory tests. The solids are mixed by blowing them back and forth between two pressure tanks; they are then stored in four bulk storage bins for injection use (fig. 41). During each injection the preblended solids are aerated and allowed to flow through a metering hopper into a mixer. A mass flowmeter was installed below the metering hopper to continuously weigh the solids. Concentrated liquid waste is pumped into the mixer under pressure (0.7 MPa). Preblended solids are then dropped into the mixer by gravity through a chute and are mixed thoroughly with the waste by a jet stream (figs. 42, 43,) thus forming the grout, which is continuously discharged to a surge tank, from where it is injected into shale by injection pump (fig. 42). The control of the proportion of waste with the preblended solids is critical. The variation should be within 5 percent of the designed proportion but not exceed 10 percent. The mix ratio is controlled manually by referring to mass-flow-meter and waste-flow-meter readings.

A considerable volume of water is required for casing slotting and equipment washing. The water is contamin-

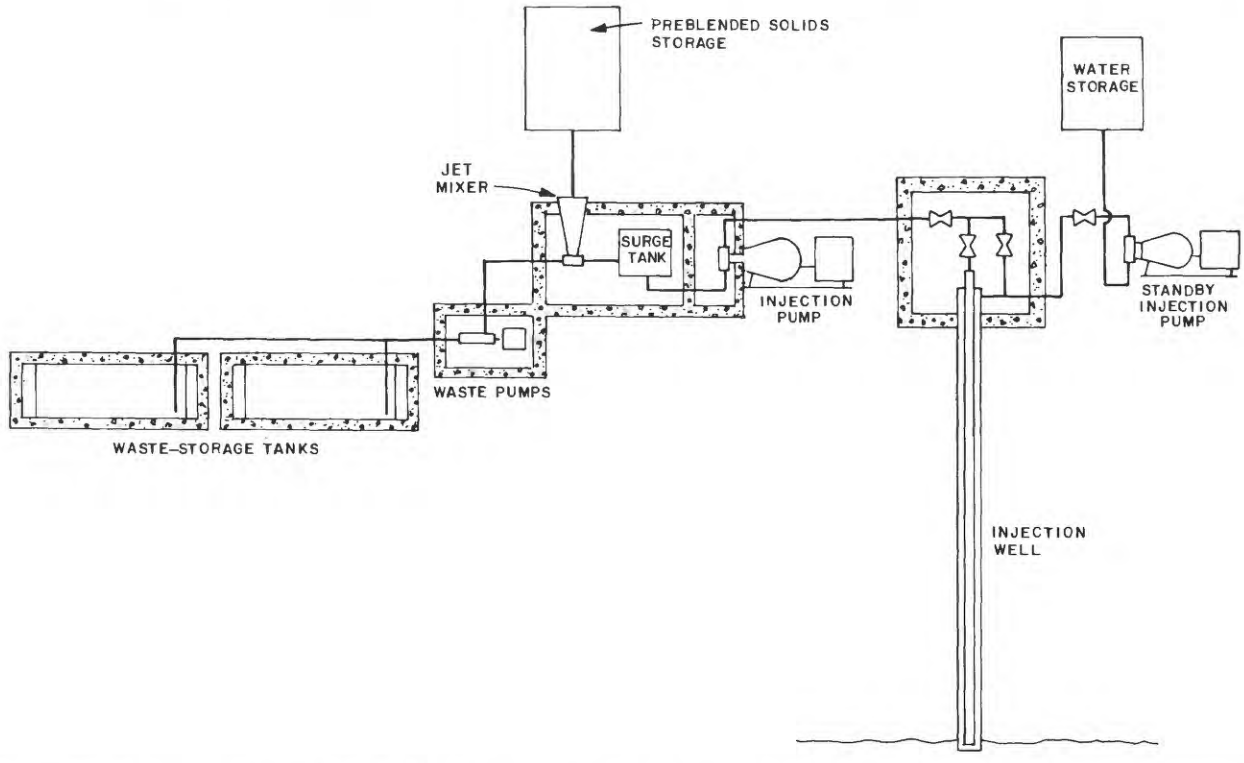

FIGURE 39.—Schematic diagram of the hydraulic-fracturing and waste-grout-injection facility, Oak Ridge National Laboratory, Tenn. (Courtesy of Oak Ridge National Laboratory.)

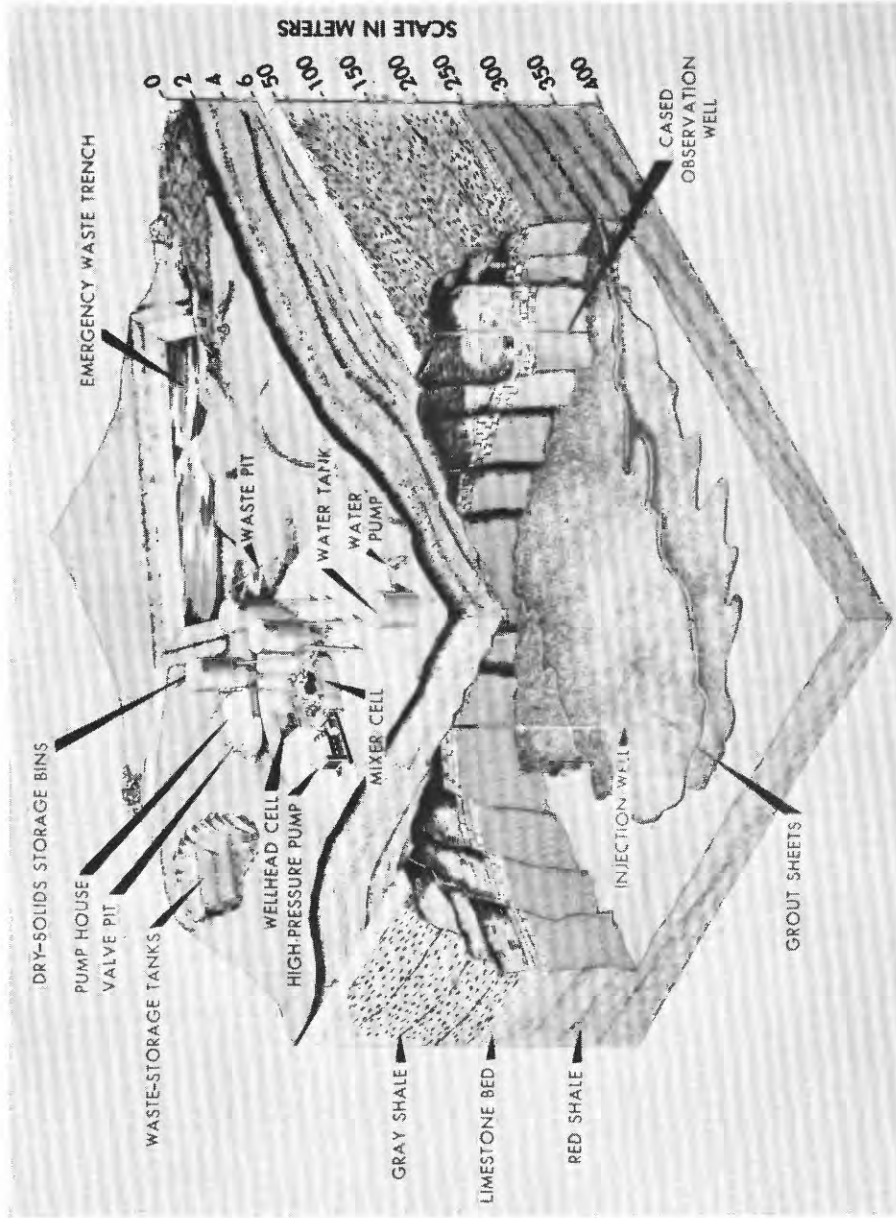

FIGURE 40.—Artist's sketch of the hydraulic-fracturing and waste-grout injection, Oak Ridge National Laboratory, Tenn. (Courtesy of Oak Ridge National Laboratory.)

FIGURE 41.–Photograph showing equipment for proportioning and blending dry solids for waste-grout injection, Oak Ridge National Laboratory, Tenn. (Courtesy of Oak Ridge National Laboratory.)

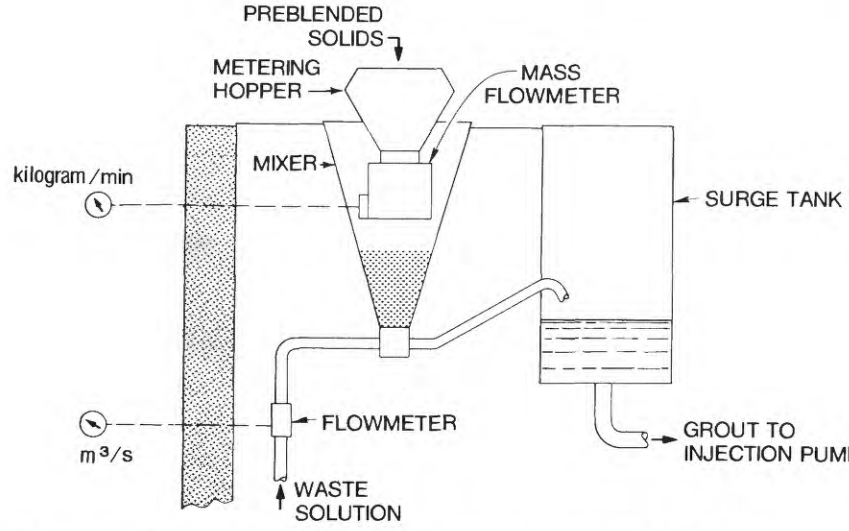

FIGURE 42.—Diagram showing the arrangement of the mass flowmeter in a mixer cell for waste-grout injection, Oak Ridge National Laboratory, Tenn. (from deLaguna and others, 1968).

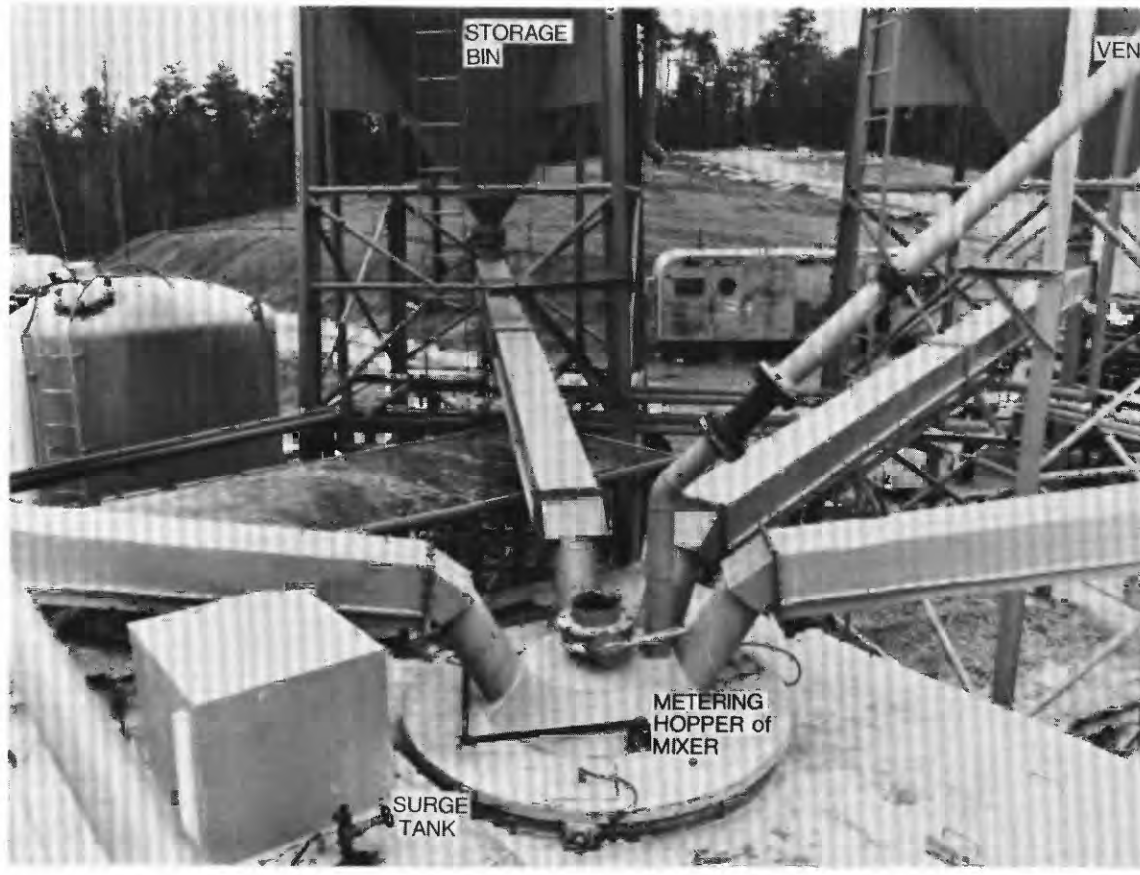

FIGURE 43.—Photograph showing conveyors for moving preblended solids from storage bins to a mixer for waste-grout injection, Oak Ridge National Laboratory, Tenn. (Courtesy of Oak Ridge National Laboratory.)

FIGURE 44.—Photograph showing cell enclosing the wellhead of the waste-injection well, Oak Ridge National Laboratory, Tenn. (Courtesy of Oak Ridge National Laboratory.)

ated and must be injected with waste. To achieve a maximum disposal efficiency, the contaminated water must be reused, and for this purpose a concrete-lined waste pit was constructed to temporarily store the contaminated water (fig. 40).

An emergency waste trench was also dug as a precaution against the possibility of a wellhead rupture (fig. 40). During such an incident the pressurized grout would flow back from the injection well and discharge to the trench; the trench would then be covered with earth fill.

The mixer, surge tank, injection pump, waste pump, and injection wellhead are all enclosed in concrete cells constructed with 30-cm thick walls and roofed with sheet metal to avoid radiation exposure of operators and to limit areas that could be contaminated if the piping or equipment ruptures or leaks (figs. 44, 45). A safety-glass window was installed in a wall of the cell to allow inspection during injection.

The injection well consists of a surface casing 46 m in length and 25 cm in diameter. The surface casing was cemented by pressure over the entire length. A small casing, 14 cm in diameter and 320 m in length, was placed inside the surface casing and was also pressure cemented for the entire length, as shown in figure 46.

Two different types of wellheads are used during injections. One is used for slotting, and the other, for injection. During slotting, a packoff flange is bolted to the 14-cm tubing head (fig. 47). A string of tubing 64 mm in diameter with a swivel attached is placed at a desired injection depth and is supported by a crane. A stream of slurry consisting of sand and water is pumped down through the tubing under pressure and discharges out of a jet nozzle. The tubing string is slowly rotated by a hydraulic power swivel; therefore, the abrasive under high pressure can cut the casing, cement wall, and shale in a complete circle. The slurry, after most of its energy has been spent, returns to surface throught the annulus. The schematic diagram of the slotting operation is shown in figure 48. The contaminated water used in slotting is stored in a waste pit and can be used for fracture initiation or injected along with waste.

During waste injection the packoff flange is replaced by an adapter flange and shut-off valve (figs. 49, 50). The adapter flange supports the 64 mm tubing string,

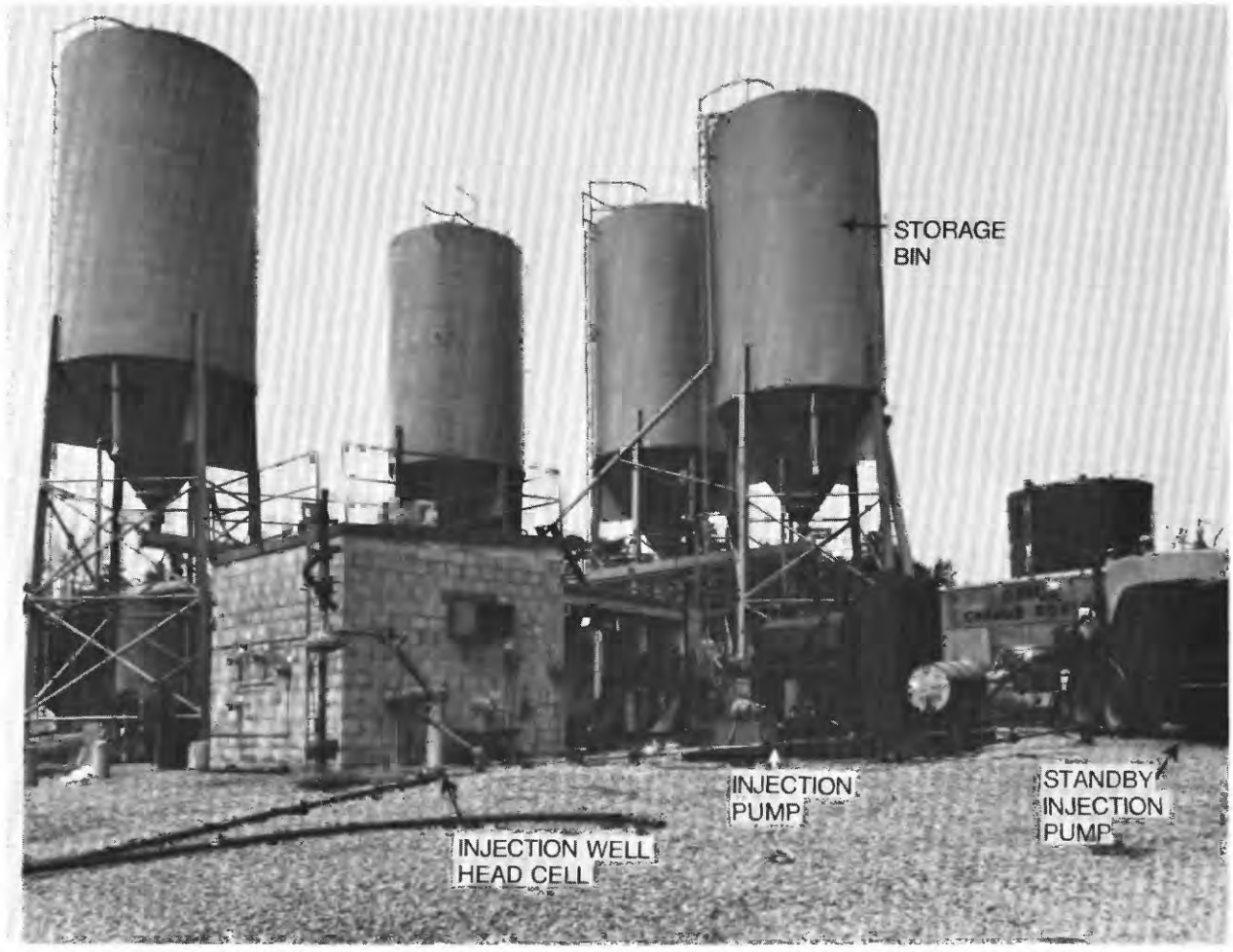

FIGURE 45.—Photograph showing bins, waste-injection wellhead cell, injection pump, and standby injection pump, Oak Ridge National Laboratory, Tenn. (Courtesy of Oak Ridge National Laboratory.)

which is placed at a depth several meters above the desired injection depth. The annulus between the tubing string and the 14-cm casing is filled with water. Since the tubing string is open to the annulus near the bottom of the well, the pressure in the annulus is equal to injection pressure, excluding friction loss in the tubing. After a fracture is initiated by water, the grout injection follows. When the last of the waste solution has been injected, a small volume of fresh water is pumped down the well to "overflush" the grout out of the injection well for use in the next injection. The injection well is then shut in under pressure until the grout sets. Several injections can be made through the same slot (table 11); the old slot is then plugged with cement, and a new slot is made a few meters above the old slot.

INJECTIONS

By the end of 1978, 25 injections had been made through the present injection well. Seven were experimental injections, one was a water injection, and the others were operational grout injections. Trouble with cement flow occurred during injection 6, an experimental injection. The injection was made in two stages, which were named 6A and 6B. Four operational injections were also named A and B (table 11) because the injection was interrupted either owing to the lack of storage capacity at the disposal site, such as during injections ILW–1A and ILW–1B, or because of difficulties of achieving desirable mixing ratio of solids and wastes, such as during injections ILW–2A and ILW–2B. After the fourth operational injection, the injection number was not subdivided again, even if the injection was interrupted.

Most of the injections have been discussed by many investigators (deLaguna and others, 1968, 1971; Sun 1969; Weeren, 1974, 1976). The examples of injections discussed in the following sections are chosen to show the correlation between the grout size estimated on the basis of the uplift model (see p. 18) and that observed in the field and to show the results of operational grout

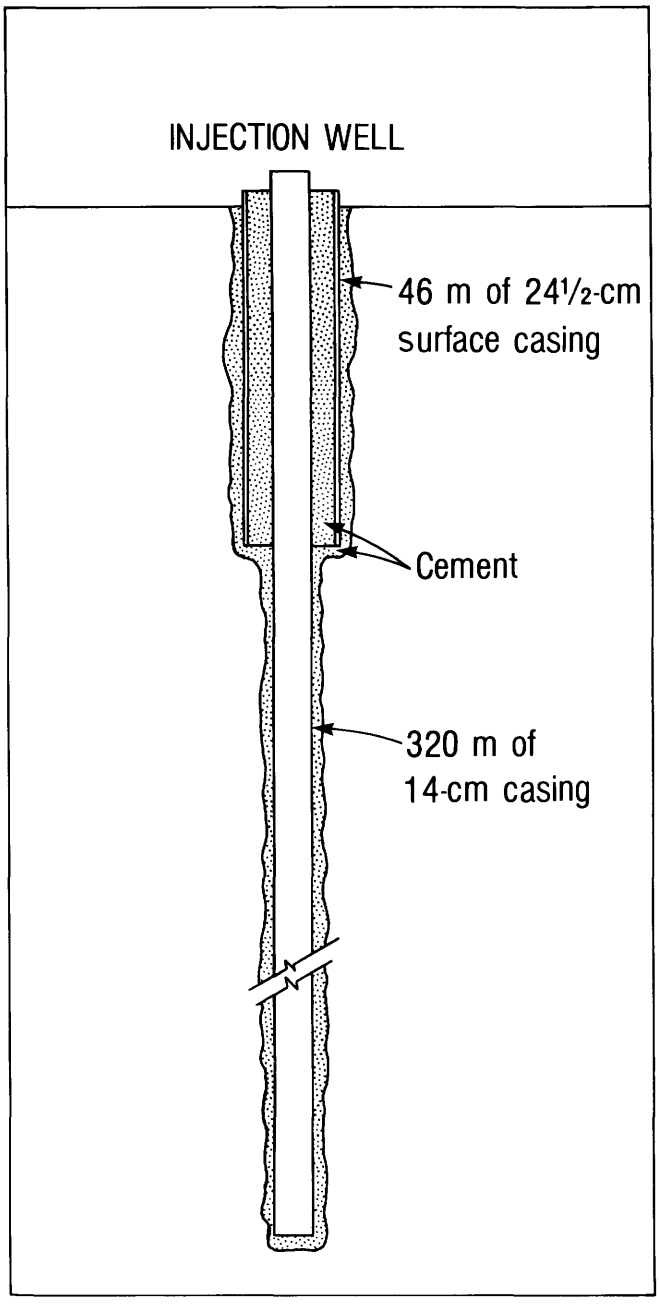

FIGURE 46. – Schematic diagram showing construction of the waste-injection well, Oak Ridge National Laboratory, Tenn. (from deLaguna and others, 1971).

mixing, as well as the procedures for determining the attitudes of grout-sheets by gamma-ray logs.

EXPERIMENTAL INJECTIONS

Two experimental injections were made in September 1960 through the second experimental well. Twenty-four core holes were drilled to determine the extent and thickness of the grout sheets. Precise leveling was run after each injection. The injection data are summarized in table 12, and the thickness of grout sheets measured in core holes and the uplift of the ground surface are shown in figures 2 and 3. The calculated maximum grout thickness and radius of grout sheet are shown in table 12, and a comparison of calculated with observed values for uplift are shown in figures 51 and 52. Generally speaking, the calculated uplift is in good agreement with the observed uplift.

The core-hole data indicates that the induced fractures were probably formed in the weakest bedding planes and grout did not flow radially from the injection well. The maximum thickness of grout sheet did not occur near the injection well (figs. 2, 3). This was probably owing to water injection at the end of each injection to clean grout out of the injection well. The thickness of grout sheet as measured in cores is less than the calculated fracture separation (table 12). This is not surprising in view of the fact that the induced fractures must have enough separation for slurry to flow during injection and because the calculated fracture separation is the condition that existed during the injection time. After the injection the separation of the induced fractures was reduced owing to compaction under overburden pressure. The grout in the cores appeared to be nearly as hard as the shale into which the slurry was injected (fig. 1).

The uplift model was further tested by a comparison of the uplift calculated with that observed during the experimental injections 1 through 7 at the present disposal site, 0.8 km west of the second experimental site. The comparison is shown in figure 53 and apparently indicates a good agreement. The locations of survey benchmarks are shown in figure 54. The uplifts were also surveyed after operational injections ILW-7 and ILW-11. However, the author has no detailed injection data for these injections; therefore, there are no calculations of uplifts for comparison.

TABLE 12. – *Physical properties of grout, injection pressure, calculated grout radius, and maximum fracture separation, September 1960, Oak Ridge National Laboratory, Tenn.*

Parameters	Injection date	
	September 3	September 10
Injection depth ---------- meters ----	285	212
Inside diameter of injection casing - millimeters ----	104	104
Injection rate ---------- cubic meters per second ----	.009	.016
Injection volume ---------- cubic meters ----	346	503
Wellhead breakdown pressure --- megapascals ----	15.89	15.20
Wellhead injection pressure ---------- do ----	12.75	14.91
Bottom-hole injection pressure ---------- do ----	16.28	17.56
Calculated overburden pressure ---------- do ----	13.58	10.10
Assumed Young's modulus ---------- do ----	1.8×10^4	1.8×10^4
Assumed Poison ratio ----------	.1	.1
Density of fluid ----- kilograms per cubic meter ----	1.38×10^3	1.44×10^3
n' ----------	.109	.065
K' ---------- newtons-sec$^{n'}$ per square meter ----	16.04	29.69
Calculated grout radius ---------- meters ----	77	65
Calculated maximum fracture separation ---------- millimeters ----	29	62
Observed grout thickness ---------- do ----	8	12

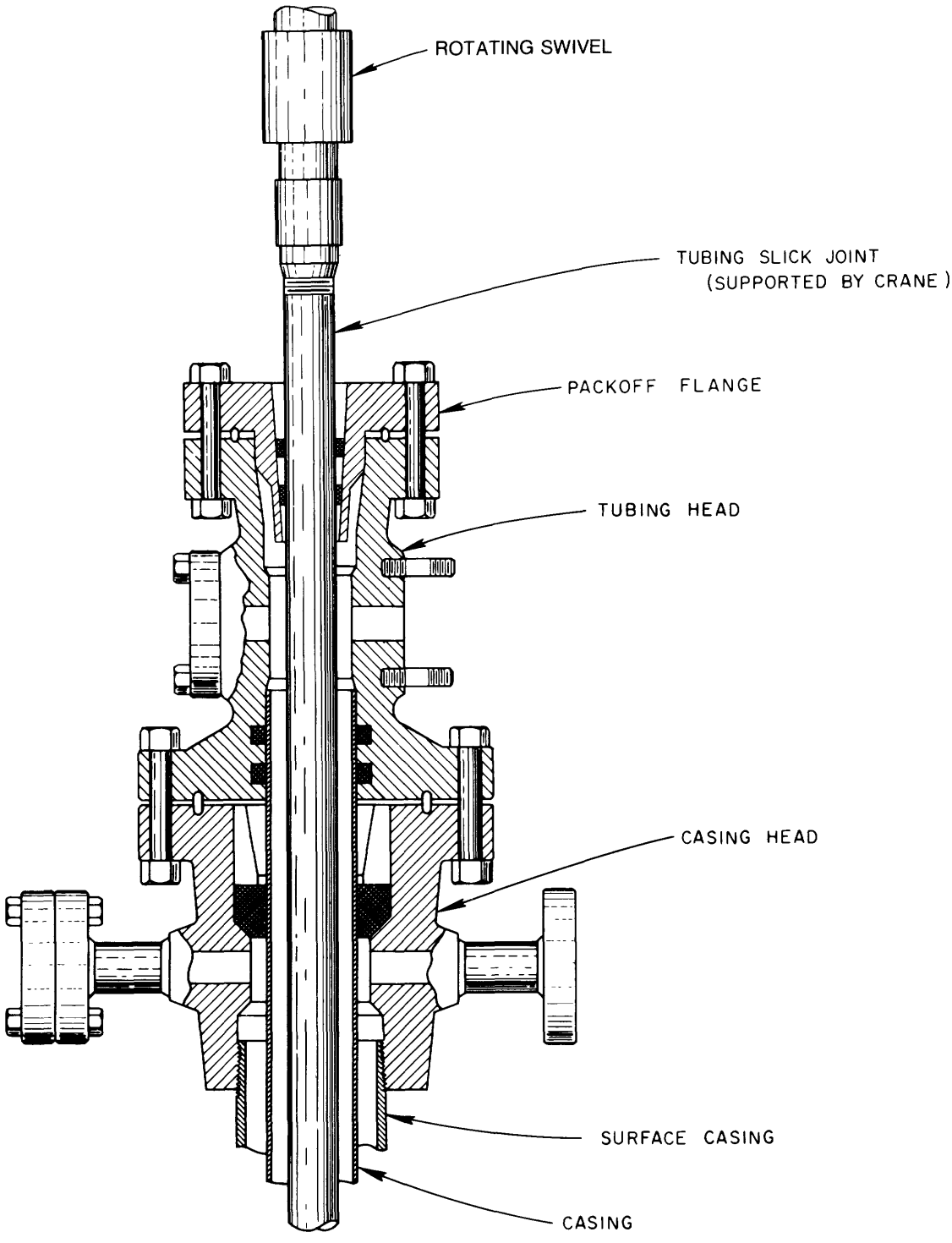

FIGURE 47.—Schematic diagram showing wellhead arrangement for slotting by hydraulic jet, Oak Ridge National Laboratory, Tenn. (Courtesy of Oak Ridge National Laboratory.)

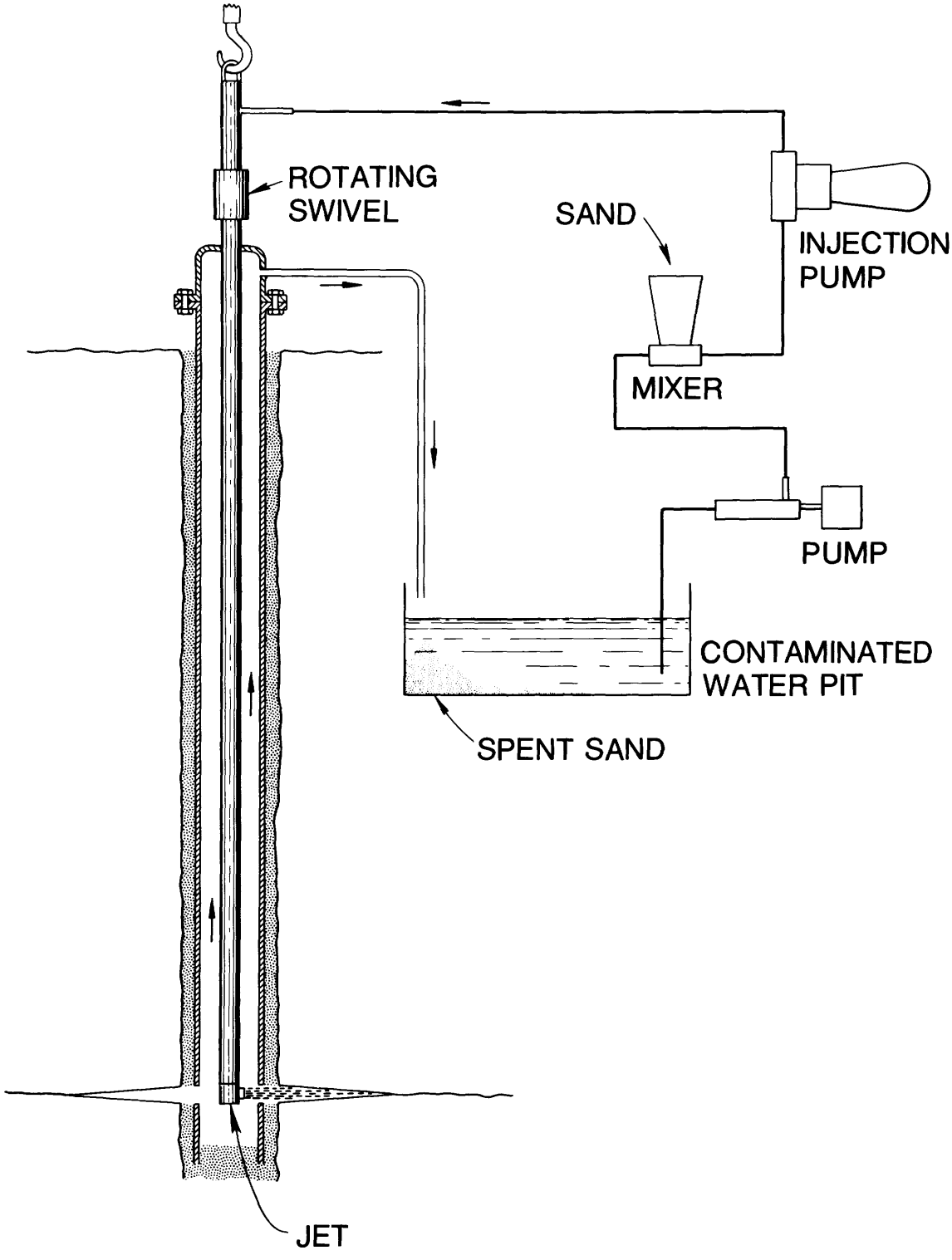

FIGURE 48.–Schematic diagram showing slotting operation for hydraulic-fracturing and waste-grout injection, Oak Ridge National Laboratory, Tenn. (Courtesy of Oak Ridge National Laboratory.)

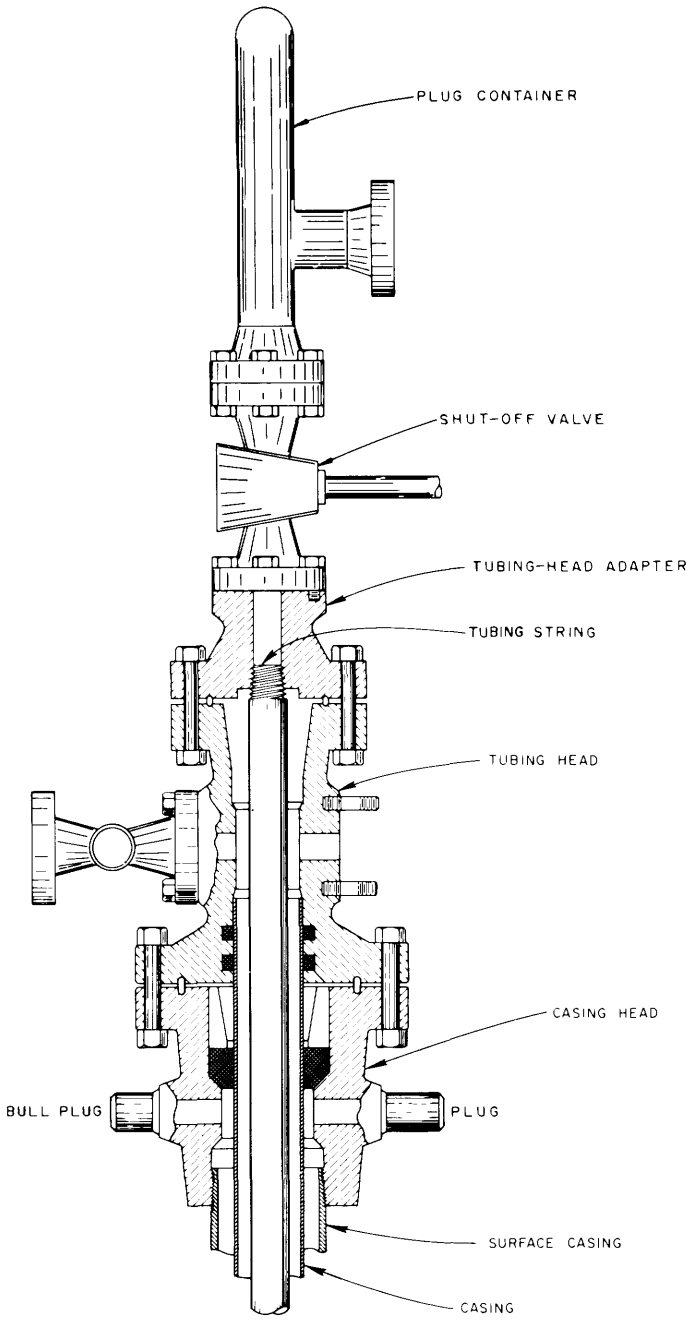

FIGURE 49.—Schematic diagram showing wellhead arrangement for waste-grout injection, Oak Ridge National Laboratory, Tenn. (Courtesy of Oak Ridge National Laboratory.)

OPERATIONAL INJECTIONS

At the end of 1978, there had been 17 operational injections. A total volume of 5,000 m³ of radioactive liquid waste contained in 8,100 m³ of grout had been injected at depths between 244 m and 266 m (table 11). Half of the injections have been discussed by Weeren (1974; 1976) and deLaguna and others (1968). The following discussions were summarized from these reports.

During September through December 1972, injections ILW-8 through ILW-11 were made at a depth of 254 m. Four tanks of waste were injected. The chemical composition of waste is shown in table 13. Waste contained in tank 1 and part of the wastes in tank 2 were injected during injection ILW-8. Only waste in tank 2 was injected during injection ILW-9. Injection ILW-10 included 38 m³ of waste remaining in tank 2 and of the wastes in tanks 3 and 4. The remaining wastes in tanks 3 and 4 were injected during injection ILW-11. The composition of solids used in all four injections was approximately as follows:

Materials	*Percent by weight*
Portland cement	38.45
Fly ash	38.45
Attapulgite 150	15.38
Grundite	7.69
Retarder	.03

The average solids and waste mixing ratio is indicated in table 11. The concentrations of radionuclides in the injected waste are shown in table 14. It was learned during the injections that bleed back after injection is an important factor, as is discussed in the following section.

BLEED BACK THROUGH THE INJECTION WELL

No matter how well the slurry is mixed there always is liquid separation. The unbound water eventually leaks through fracture walls into shale pores under pressure. To reduce as much as possible the amount of separated unbound water leaking from grout into a shale formation, it is necessary to bleed back the unbound water to the ground surface through the injection well after the grout has been solidified.

A summary of the bleed-back data is shown in table 15. It is not surprising that both wellhead pressure and initial rate of bleed back decrease with increase in shut-in time because the unbound water leaks through fracture walls under pressure during such time, despite the low permeability of the shale. The concentrations of ra-

TABLE 13.—*Chemical composition, in moles per liter, of waste disposed of by injections, September–December, 1972, Oak Ridge National Laboratory, Tenn.*

[From Weeren, 1974]

Constituent	Tank			
	1	2	3	4
Na^+	1.66	1.24	0.57	0.59
Al^{3+}	.007	.037	.002	.0011
NH_4^+	.003	.03	.044	.05
OH^-	.18	.28	.15	.16
NO_3^-	.84	1.03	.30	.30
Cl^-	.093	.217	.049	.044
SO_4^{2-}	.094	.183	.111	.125
CO_3^{2-}	.193	.288	.093	.10

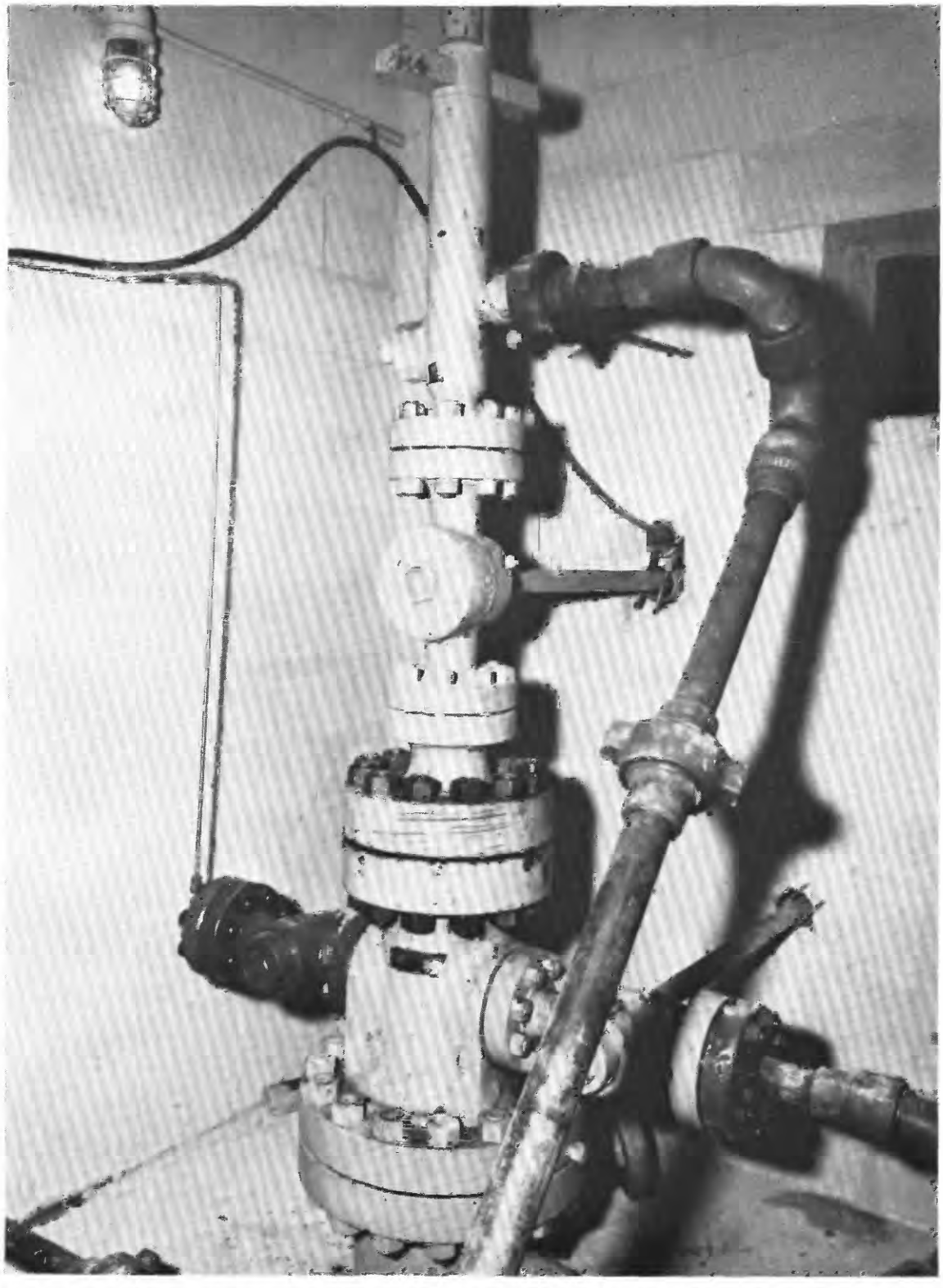

FIGURE 50.–Photograph showing well-head of injection well, Oak Ridge National Laboratory, Tenn. (Courtesy of Oak Ridge National Laboratory.)

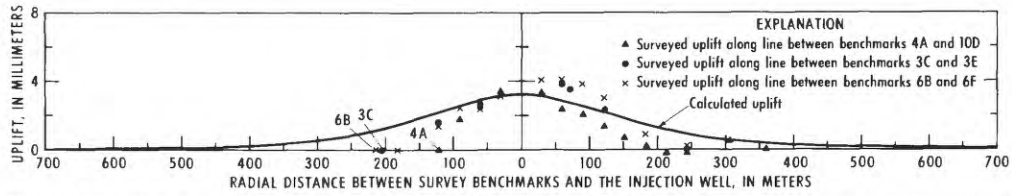

FIGURE 51.—Calculated and surveyed surface uplift produced by the grout injection, Sept. 3, 1960, second experiment site, Oak Ridge National Laboratory, Tenn. (Locations of benchmarks are shown in figs. 2 and 3.)

TABLE 14.—*Specific activity, in curies per liter, of major radionuclides contained in wastes disposed of by injections, September–December 1972, Oak Ridge National Laboratory, Tenn.*

[From Weeren, 1974]

Radionuclides	Injection number			
	ILW-8	ILW-9	ILW-10	ILW-11
^{90}Sr	1.65×10^{-4}	8.93×10^{-4}	4.15×10^{-3}	3.83×10^{-3}
^{137}Cs	1.01×10^{-1}	9.04×10^{-2}	5.87×10^{-2}	8.19×10^{-2}
^{106}Ru	9.17×10^{-3}	1.45×10^{-3}	1.85×10^{-3}	1.32×10^{-3}
^{244}Cm	6.74×10^{-7}	2.18×10^{-5}	8.98×10^{-5}	5.20×10^{-4}
^{239}Pu	4.76×10^{-7}	None	None	None

dionuclides in the bleed-back water are shown in table 16. Although the bleed back is only 4 percent of the total injected volume and the radionuclides contained in the bleed back are only several tenths of one percent of the total injected radionuclides, the concentration of radionuclides in the bleed back is still high, and the bleed back was therefore stored for use during the next injection. Because of the low permeability of the shale, some of the separated liquid that could not be bled back through the injection well would probably be trapped in induced fractures or in the shale. During the drilling of observation well S–100, when the grout sheet of experimental injection 3 was intersected at a depth of 276 m, water flowed slowly from the grout seam. A sample of the flowing water was anaylzed, indicating the following results: Cl^-, 36,500 ppm (parts per million); Na^+, 31,100 ppm; NO_3^-, 28,600 ppm; Ca^{2+}, 2,930 ppm; OH^-, 2,000 ppm; SO_4^{2-}, 1,620 ppm; Mg^{2+}, 380 ppm; H^3, 7.3×10^{-7} Ci/L; ^{90}Sr, 6.8×10^{-8} Ci/L; and ^{137}Cs, 3.7×10^{-7} Ci/L, (deLaguna and others, 1968). This finding raises the concern that free radionuclides may be left in the shale, whether as a result of phase separation or of other causes. The bleed-back data and the water found in the grout seam indicate that the amount of free radionuclides in the shale is low. If the ground-water flow paths from the injection area to a nearby groundwater body as long and the shale's permeability is low and its adsorption capacity high, then the possibility that radionuclides in the unbound water could migrate into the nearby biosphere is further reduced by radioactive decay, as well as hydrodynamic dispersion. However, a series of observation wells constructed along the perimeter of the injection area and in formations lying above the injection zone are required to monitor the possible migration.

TABLE 15.—*Bleed back from injections, September–December 1972, Oak Ridge National Laboratory, Tenn.*

[From Weeren 1974]

Injection	Injection date	Date wellhead valve opened	Days after injection	Well-head pressure at time valve opened (MPa)	Initial flow rate (m^3/s)	Final flow rate (m^3/s)	Recovered volume (m^3)
ILW-8	Sep. 29, 1972	Oct. 9, 1972	10	1.69	1.16×10^{-5}	6.52×10^{-6}	4.40
ILW-9	Oct. 17, 1972	Oct. 27, 1972	10	2.14	1.26×10^{-4}	7.57×10^{-5}	12.80
ILW-10	Nov. 8, 1977	[1]Nov. 20, 1972	12	1.41	4.99×10^{-4}	4.10×10^{-4}	2.50
		Nov. 30, 1972	22	1.03	2.71×10^{-4}	2.33×10^{-4}	2.20
ILW-11	Dec. 5, 1972	[1]Dec. 14, 1972	9	1.69	3.22×10^{-4}	-----	2.16
		[1]Dec. 29, 1973	24	1.17	1.70×10^{-4}	-----	1.60
		[1]Jan. 19, 1973	45	0.97	1.01×10^{-4}	-----	1.10
		Apr. 4, 1973	120	0.57	4.73×10^{-5}	5.99×10^{-7}	[2]43.90

[1]Valve closed again.
[2]Measured on Apr. 22, 1973.

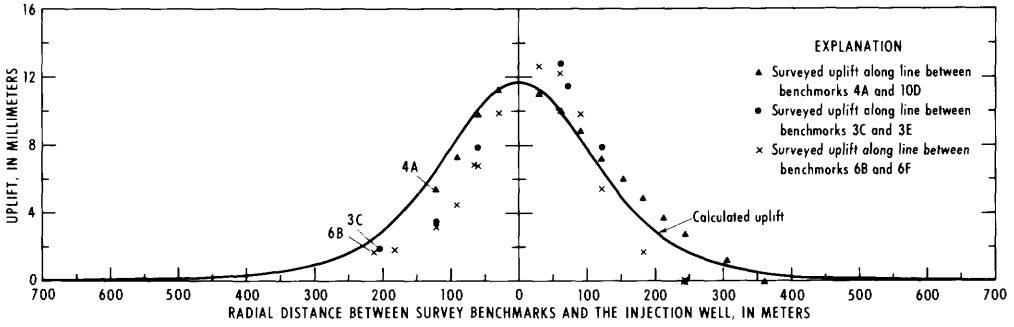

FIGURE 52.—Calculated and surveyed surface uplift produced by the grout injection, Sept. 10, 1960, second experiment site, Oak Ridge National Laboratory, Tenn. (Locations of benchmarks are shown in figs. 2 and 3.)

TABLE 16.—*Specific activity, in curies per liter, of radionuclides in bleed-back solution, September–December 1972, Oak Ridge National Laboratory, Tenn.*

[From Weeren, 1974. NA, not analyzed]

	Injection			
	ILW-8	ILW-9	ILW-10	ILW-11
Radionuclides				
Gross α	$<4.5\times10^{-9}$	4.0×10^{-8}	NA	1.5×10^{-8}
^{90}Sr	9.8×10^{-5}	4.8×10^{-5}	1.4×10^{-4}	1.5×10^{-4}
^{137}Cs	----------	5.5×10^{-4}	----------	6.6×10^{-4}
^{106}Ru	NA	6.9×10^{-4}	NA	NA
^{134}Cs	NA	8.5×10^{-6}	NA	NA
^{60}Co	NA	6.6×10^{-6}	NA	NA
Other				
Na^+	24 mg/mL	-----	22 mg/mL	35.3 mg/mL
ph	12.3	12.6	11.4	10.0

POSITION OF GROUT SHEET

The extent and altitude of the grout sheet can be determined by coring after the grout is solidified; however, this process is costly and time consuming. If a series of observation wells has been constructed and if the injected wastes contain gamma-ray-emitting radionuclides, then one alternative would be to obtain gamma-ray logs in the observation wells before and after injection. Intensified gamma-ray peaks that are above those of background gamma-ray activity of shale would indicate that the induced fractures have intercepted the wells at the depth indicated. In logs made after two or three injections, it is difficult to associate the observed gamma-ray peaks with the appropriate injections.

Only logs made after each injection are available for injections ILW-8 through ILW-11 (Weeren, 1974). Figure 55 indicates the location of the observation wells in which the gamma-ray logs were run. Figure 56 shows the grout sheets found in the observation wells projected on a line passing through the injection well in the direction along the formation dip. The actual observed grout sheets intercept the observation wells at altitudes and locations listed in table 17. From figures 55, 56, and table 17, it seems that the grout sheets have formed

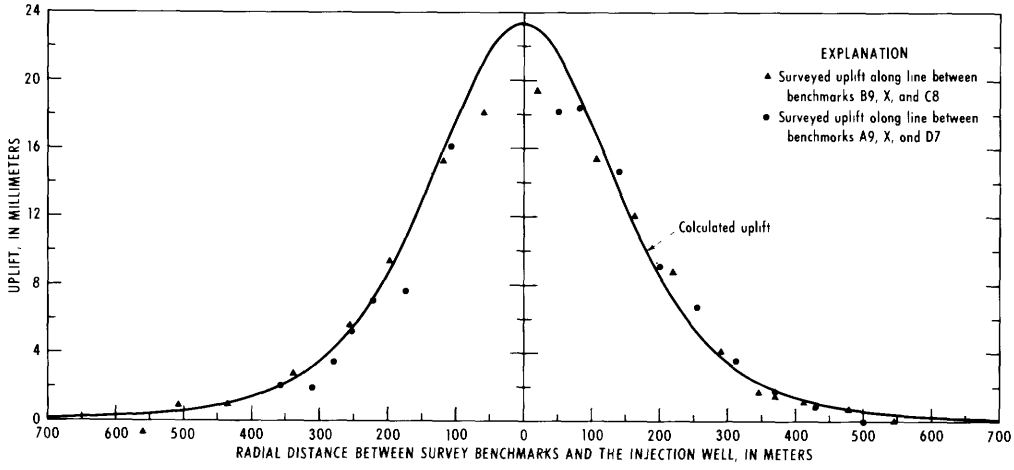

FIGURE 53.—Calculated and observed surface uplift produced by the experimental injections 1 through 7, present fracturing site, Oak Ridge National Laboratory, Tenn. (Locations of benchmarks are shown in fig. 54.)

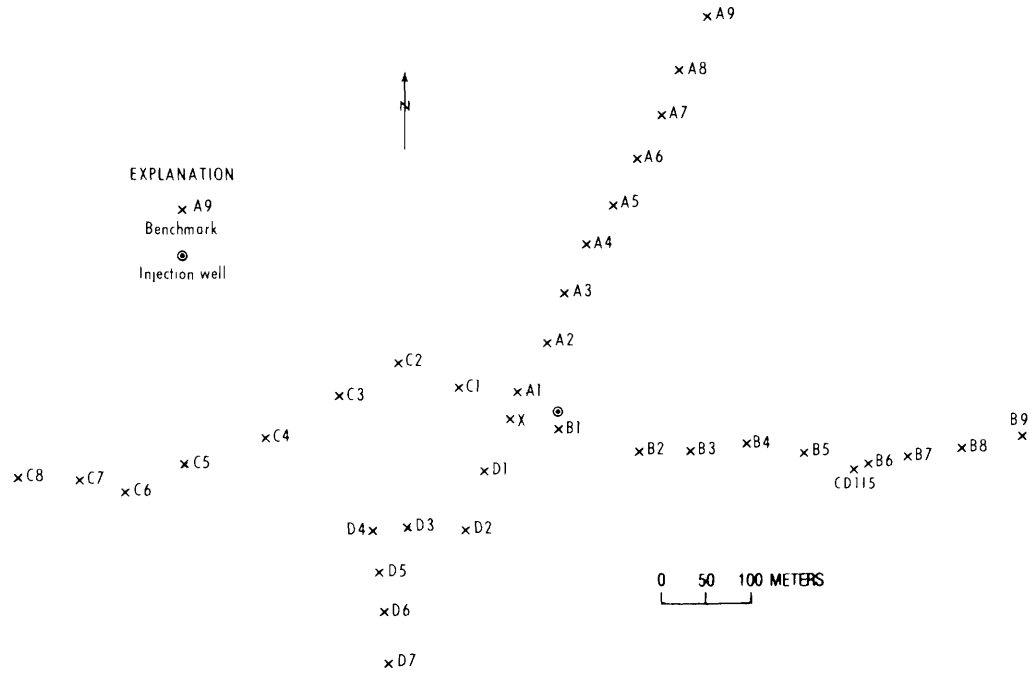

FIGURE 54. – Locations of benchmarks, the present fracturing site, Oak Ridge National Laboratory, Tenn.

TABLE 17. – *Altitude, in meters referred to mean sea level, of grout sheet determined from gamma-ray logs made in observation wells, September–December 1972, Oak Ridge National Laboratory, Tenn.*

[From Weeren, 1974. NF, not found]

Observation well	Injection			
	ILW-8	ILW-9	ILW-10	ILW-11
Injection altitude	−12	−12	−12	−12
W 300	NF	−12 to −14	−3 to −6	NF
NW 100	−5	NF	14	9
N 100	NF	NF	12	7 to 12
N 150	NF	−10	5 to 7	3 to 5
NE 125	NF	NF	4 to 10	−2 to 4
E 320	NF	NF	NF	NF
S 100	−14 to −16	−16	NF	−7
S 220	NF	NF	NF	NF

along bedding planes and lie in an interval 20 m above or below the injection altitude; however, these data might not indicate the true altitude of the grout sheets because no data are available regarding well deviations. The experience obtained during a later site investigation indicated that measurements for unadjusted altitudes of grout sheets were commonly 7–8 m higher than those adjusted for well deviation, and that determinations of the location of the grout sheets also were shifted several tens of meters away from those of the surface location of the observation wells (see fig. 62). Therefore, these unadjusted results may be in error.

MONITORING SYSTEM

In addition to observation wells for gamma-ray logging, the ORNL also constructed a series of so-called rock-cover monitoring wells. The well location is indicated in figure 55. These wells are cased and pressure cemented to a depth of 152 m and have 30 m of open hole below the cased and cemented section (fig. 57). The purpose of these rock-cover wells is to determine the integrity of the shale formation lying above the waste-disposal zone to insure that no vertical fractures were formed owing to the injections and that surface water could not migrate to the waste-disposal zone by way of such fractures. The integrity test is done by pumping water into rock-cover wells at a standard wellhead pressure of 0.5 MPa to observe the change of rate of acceptance before and after injection. The tests are repeated after about every fourth injection.

Three types of response to the tests have been observed. First, wells may take no measurable amount of water; second, may take a small amount of water in the first hour and then a decreasing amount thereafter. In the third type of the response, the well may take the same small amount of water during the first and second hour of the test (deLaguna and others, 1971; Weeren, 1974). During the experimental injections, pressure variations were observed in the rock-cover wells filled with water and equipped with pressure gages. In the

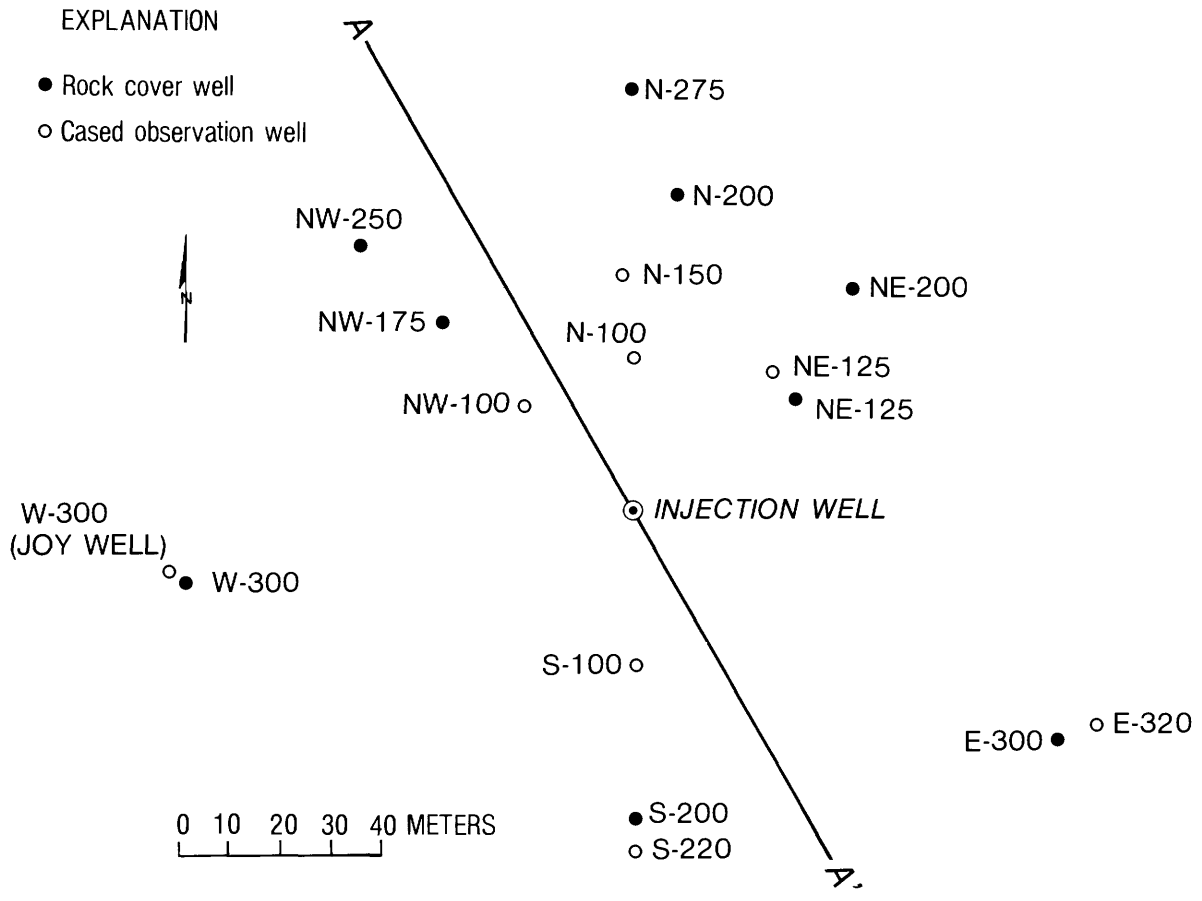

FIGURE 55.—Locations of observation wells, at the present fracturing site, Oak Ridge National Laboratory, Tenn. (Courtesy of Oak National Laboratory.)

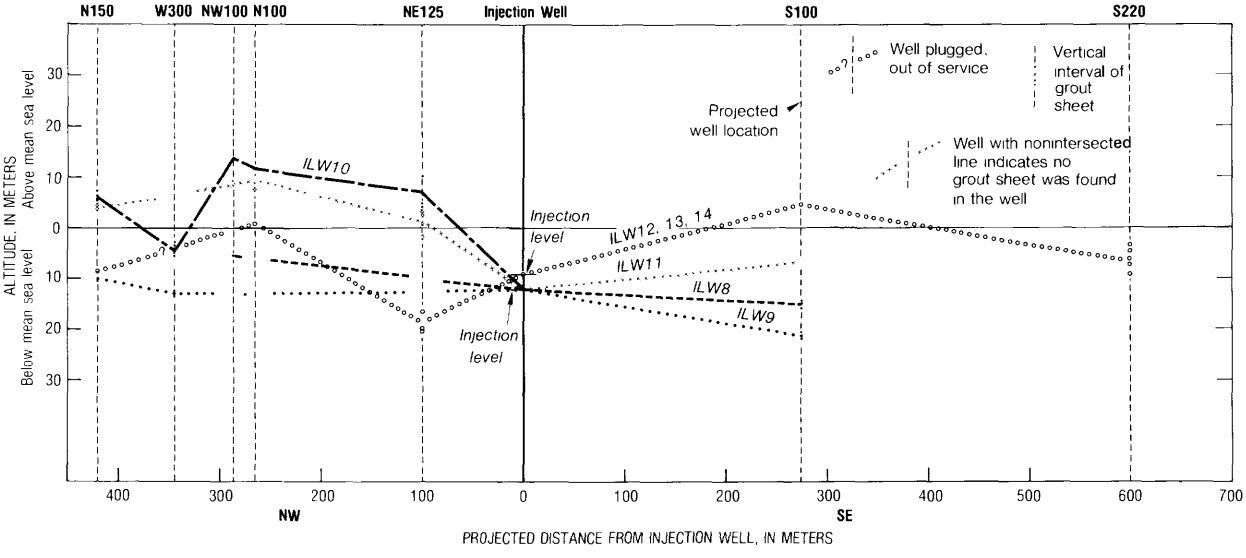

FIGURE 56.—Cross-section showing the grout sheets formed by waste injections ILW-8 through ILW-14, Oak Ridge National Laboratory, Tenn., as interpreted from gamma-ray logs made in observation wells after injections and projected on a line (*AA'*, fig. 55), in the direction along dip and passing through the center of the injection well.

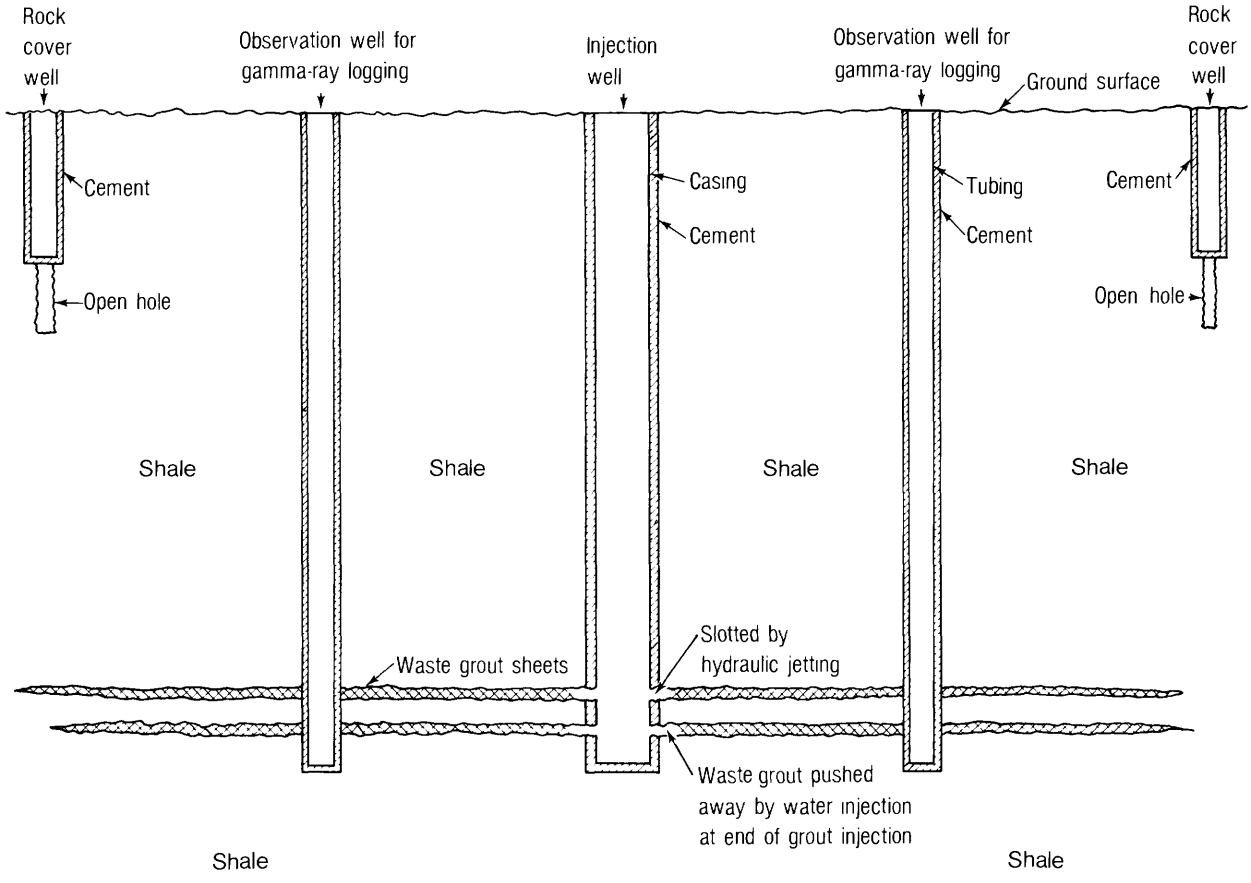

FIGURE 57.–Schematic diagram showing the injection well, observation wells, and waste grout sheet in shale, Oak Ridge National Laboratory, Tenn.

area where the grout sheets were detected by gamma-ray logs, the pressure in the rock-cover wells rose, while in the area where the gamma-ray logs indicated no grout sheets, the pressure in the rock-cover wells dropped slightly (deLaguna and others, 1971). This evidence probably can be explained by changes in strain around the open-hole section of the rock-cover wells. In the grout-sheet area the shale is probably compressed by uplift due to the accommodation of the injected grout thus increasing pressure in the rock-cover wells. The uplift does not stop at the edge of the grout sheet and must extend away from the edge without shearing the rock. Therefore, the volume of rock beyond the edge of the grout sheet should expand, thus increasing the rock porosity slightly, which causes the pressure in the rock-cover wells to drop slightly. The pressure changes measured in rock-cover wells and the grout sheets indicated by gamma-ray logs for the injections ILW-8 through ILW-11 are shown in table 18.

TABLE 18.–*Rock-cover wells having positive or negative difference in pressures measured before and during an injection and results of gamma-ray-logs, September-December 1972, Oak Ridge National Laboratory, Tenn.*

[From Weeren, 1974]

Injection	Results of gamma-ray log		Pressure difference in rock cover well		
	Positive	Negative	Positive	Negative	Ambiguous[1]
ILW-8	NW 100 S 100	W 300 N 100 N 150 NE 125 E 320 S 220	NW 175 NW 250 NE 125	N 275 N 200 NE 200	W 300 S 200 E 300
ILW-9	W 300 N 150 S 100	NW 100 N 100 NE 125 E 320 S 220	NE 125 NE 200 S 200	E 300 N 200 N 275 NW 250	W 300 NW 175
ILW-10	W 300 NW 100 N 150 N 100 NE 125	E 320 S 100 S 220	NW 175 N 275 N 200 NE 125 NE 200	W 300 S 200 E 300	NW 250
ILW-11	NW 100 N 150 N 100 NE 125 S 100	W 300 E 320 S 220	NW 175 N 200 NE 125 NE 200	NW 250 W 300 S 200 N 275 E 300	----------

[1]No clear sign of positive or negative pressure.

SITE EVALUATION

Because the present disposal site approaches its full injection capacity and the disposal facility can not handle the injection of accumulated sludge, a new fracturing site was proposed, which is 245 m south of the present facility (fig. 34). The new site was evaluated jointly by the ORNL and the USGS in 1974 (Sun, 1976; Weeren and others, 1974). The following sections are a summation of the evaluation.

TEST DRILLING

Although the proposed site is only 245 m from the present disposal site, where numerous test holes and injections had been made in past years, one test hole with core was drilled at the proposed site to insure that the subsurface geology and hydrology would not deviate greatly from that at the present site. Cores were taken from depths of 212 to 362 m. In the interval from 212 to 250 m the rock is gray shale interbedded with thin limestone layers. From 250 to 302 m the shale is purple and silty and lacks limestone layers. From 302 m to the top of the Rome Formation (357 m) the shale is gray or purple and increasingly sandy. From 357 to 362 m the rock is hard, white sandstone interbedded with shale and is part of the Rome Formation. Bedding planes are very evident and dip 10°–20° SE. The subsurface geology indicated by cores is similar to that at the present site. The purple and gray shale between 250 and 357 m comprises the Pumpkin Valley Shale of the Conasauga Group, into which radioactive waste is scheduled to be injected.

The test hole was converted into an observation well, known as the South-observation well. Gamma-ray logs were made in this well before and after the well was cased and cemented. Three more observation wells, the East-, West-, and North-observation wells, were constructed at a radial distance of 60 m from the injection well and also were cased and pressure cemented. The injection well was constructed with a 14-cm casing and was pressure cemented in a way similar to that of the present injection well. The locations of all wells are shown in figure 58 and are listed in table 19. Gamma-ray logs were also made in all wells before they were cased and pressure cemented. Thereafter, gamma-ray logs were made again in only some of the wells. These gamma-ray logs were used to determine not only the background level of gamma-ray activity of the injection shale but also the contacts between rock units.

Laboratory determinations of rock tensile strength had never been made for shales at the New York and Oak Ridge sites. Therefore, the author took advantage of this site evaluation to determine, in the laboratory, the tensile strength of the shale scheduled for injection to make a comparison with tensile strength calculated from test injections.

Well deviation, determination of dip and strike, and tensile strength of the injection shale are discussed in the following sections.

WELL DEVIATION

All wells drift from the vertical axis, as indicated by deviation logs. All measured depths were corrected for the angle of deviation to obtain true vertical depths and true horizontal locations at the particular depths of interest. The corrections were made by using equations 38 through 41. The calculated true vertical depths and true horizontal positions at 30 m intervals in all wells are listed in table 20.

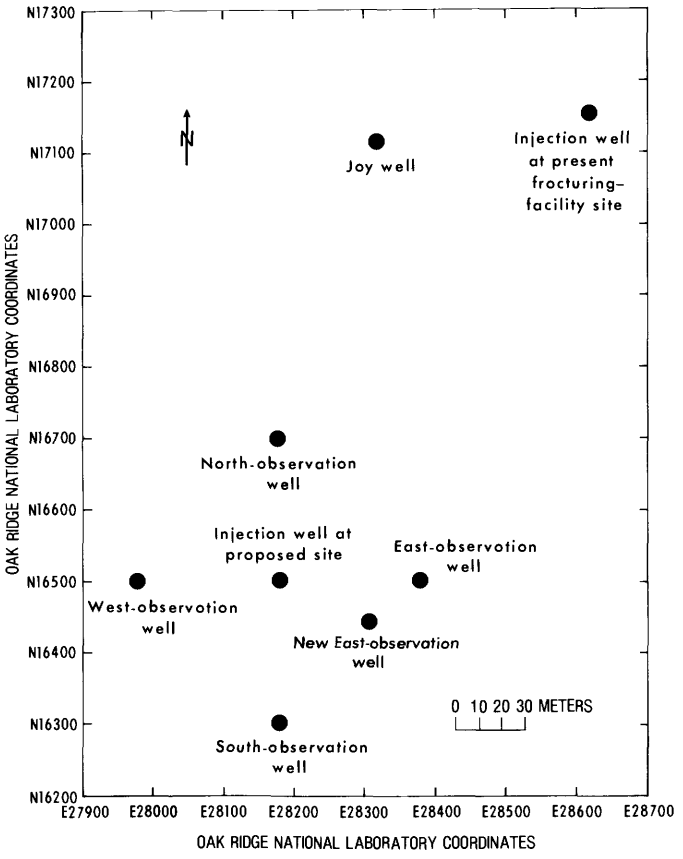

FIGURE 58.—Locations of wells, at the proposed disposal site, Oak Ridge National Laboratory, Tenn.

TABLE 19.—*ORNL coordinates and altitude, in meters above mean sea level, of wells at the proposed disposal site, Oak Ridge National Laboratory, Tenn.*

Well	Coordinates		Altitude
Injection well at present site	N 17155	E 28617	241.3
Injection well at the proposed site	16503	28178	240.3
Old East-observation well	16503	28378	240.2
New East-observation well	16445	28307	241.3
South-observation well	16304	28179	243.6
West-observation well	16502	27978	238.5
North-observation well	16702	28172	235.1

STRATIGRAPHY OF THE INJECTION SHALE

Three rock units present in the Conasauga Group have been identified in the gamma-ray logs and cores. From top to bottom, they are gray limestone interbedded with

TABLE 20.—*Data on observations and calculations for a deviation survey made at the proposed disposal site, Oak Ridge National Laboratory, Tenn.*

[N, north; S, south; E, east; W, west]

Measured depth (m)	Course length *MD* (m)	Vertical deviation angle, α	Calculated vertical depth (m)		Calculated horizontal displacement, *H* (m)	Magnetic bearing, β	Displacement from surface well center, in meters							
							y		*x*		Total			
											y		*x*	
			Z	Total			N	S	E	W	N	S	E	W
Injection well														
[Total depth after cementing and casing, 338 m]														
30.48	30.48	1°45′	30.47	30.47	0.93	N. 30° W.	0.81			0.47	0.81			0.47
60.96	30.48	4°	30.41	60.88	2.13	N. 40° W.	1.63			1.37	2.44			1.84
91.44	30.48	8°	30.18	91.06	4.24	N. 55° W.	2.43			3.47	4.87			5.31
121.92	30.48	9°12′	30.09	121.15	4.87	N. 73° W.	1.42			4.66	6.29			9.97
152.40	30.48	12°	29.81	150.96	6.34	N. 72° W.	1.96			6.03	8.25			16.00
182.88	30.48	9°48′	30.04	181.00	5.19	S. 85° W.		0.45		5.17	7.80			21.17
213.36	30.48	10°36′	29.96	210.96	5.61	N. 72° W.	1.73			5.33	9.53			26.50
243.84	30.48	21°30′	28.36	239.32	11.17	N. 58° W.	5.92			9.47	15.45			35.97
274.32	30.48	16°	29.30	268.62	8.40	N. 52° W.	5.17			6.62	20.62			42.59
304.80	30.48	16°36′	29.21	297.83	8.71	N. 35° W.	7.13			4.99	27.75			47.58
343.51	38.71	17°18′	36.96	334.79	11.51	N. 33° W.	9.65			6.27	37.40			53.85
Old East-observation well														
[Total depth after cementing and casing, 334 m]														
30.48	30.48	0	30.48	30.48	0	----	0		0		0		0	
60.96	30.48	2°30′	30.45	60.93	1.33	N. 35° E.	1.09		.76		1.09		.76	
91.44	30.48	4°24′	30.39	91.32	2.34	N. 85° E.	.20		2.33		1.29		3.09	
121.92	30.48	5°36′	30.33	121.65	2.97	S. 55° E.		1.71	2.44			0.42	5.53	
152.40	30.48	2°30′	30.45	152.10	1.33	S. 30° E.		1.15	.66			1.57	6.19	
182.88	30.48	4°	30.41	182.51	2.13	S. 80° W.		.37		2.09		1.94	4.10	
213.36	30.48	12°	29.81	212.32	6.34	N. 60° W.	3.17			5.49	1.23			1.39
243.84	30.48	16°42′	29.19	241.51	8.76	N. 55° W.	5.02			7.17	6.25			8.56
274.32	30.48	18°18′	28.94	270.45	9.57	N. 58° W.	5.07			8.12	11.32			16.68
304.80	30.48	15°24′	29.39	299.84	8.09	N. 73° W.	2.37			7.74	13.69			24.42
345.95	41.15	16°30′	39.46	339.30	11.69	N. 63° W.	5.31			10.41	19.00			34.83
New East-observation well														
[Total depth after cementing and casing, 347 m]														
45.72	45.72	1°	45.71	45.71	0.80	N. 60° E.	0.40		0.69		0.40		0.69	
76.20	30.48	4°	30.41	76.12	2.13	N. 60° E.	1.07		1.84		1.47		2.53	
106.68	30.48	4°	30.41	106.52	2.13	N. 80° E.	.37		2.10		1.84		4.63	
137.16	30.48	3°	30.44	136.96	1.60	N. 70° E.	.55		1.50		2.39		6.13	
167.64	30.48	2°	30.46	167.42	1.06	N. 48° W.	.71			0.79	3.10		5.34	
198.12	30.48	4°30′	30.39	197.81	2.39	S. 85° W.		0.21		2.38	2.89		2.96	
228.60	30.48	14°	29.57	227.38	7.37	N. 80° W.	1.28			7.26	4.17			4.30
259.08	30.48	16°	29.30	256.68	8.40	N. 80° W.	1.46			8.27	5.63			12.57
289.56	30.48	16°30′	29.22	285.91	8.66	N. 64° W.	3.79			7.78	9.42			20.35
320.04	30.48	20°	28.64	314.55	10.42	N. 56° W.	5.83			8.64	15.25			28.99
350.52	30.48	14°	29.57	344.12	7.37	N. 28° W.	6.51			3.46	21.76			32.45

TABLE 20.—*Data on observations and calculations for a deviation survey made at the proposed disposal site, Oak Ridge National Laboratory, Tenn.*—Continued

[N, north; S, south; E, east; W, west]

Measured depth (m)	Course length *MD* (m)	Vertical deviation angle, α	Calculated vertical depth (m)		Calculated horizontal displacement, *H* (m)	Magnetic bearing, β	Displacement from surface well center, in meters							
							y		*x*		Total			
											y		*x*	
			Z	Total			N	S	E	W	N	S	E	W
South-observation well														
[Total depth after cementing and casing, 338 m]														
30.48	30.48	3°30′	30.42	30.42	1.86	N. 88° W.	0.06			1.86	0.06			1.86
60.96	30.48	5°48′	30.32	60.75	3.08	N. 60° W.	1.54			2.67	1.60			4.53
91.44	30.48	4°30′	30.39	91.14	2.39	N. 65° W.	1.01			2.17	2.61			6.70
121.92	30.48	8°36′	30.14	121.28	4.56	N. 65° W.	1.93			4.13	4.54			10.83
152.40	30.48	11°12′	29.90	151.18	5.92	N. 58° W.	3.14			5.02	7.68			15.85
182.88	30.48	12°30′	29.76	180.94	6.60	N. 58° W.	3.50			5.60	11.18			21.45
204.22	21.34	13°	20.79	201.73	4.80	N. 62° W.	2.25			4.24	13.43			25.69
207.26	3.05	13°36′	2.96	204.69	.72	N. 62° W.	.34			.63	13.77			26.32
213.36	6.10	14°24′	5.91	210.60	1.52	N. 63° W.	.69			1.35	14.46			27.67
243.84	30.48	14°36′	29.50	240.10	7.68	N. 65° W.	3.25			6.96	17.71			34.63
274.32	30.48	16°	29.30	269.40	8.40	N. 65° W.	3.55			7.61	21.26			42.24
304.80	30.48	17°30′	29.07	298.47	9.17	N. 62° W.	4.31			8.10	25.57			50.34
335.28	30.48	17°	29.15	327.62	8.91	N. 62° W.	4.18			7.87	29.75			58.21
364.24	28.96	15°30′	27.91	355.53	7.74	N. 62° W.	3.63			6.83	33.38			65.04
West-observation well														
[Total depth after cementing and casing, 342 m]														
30.48	30.48	1°	30.48	30.48	0.53	N. 90° W.	0			0.53	0			0.53
60.96	30.48	3°	30.44	60.91	1.60	S. 80° W.		0.28		1.57		0.28		2.10
91.44	30.48	5°	30.36	91.28	2.66	N. 80° W.	.46			2.62	.18			4.72
121.92	30.48	7°15′	30.48	121.76	3.85	N. 85° W.	.34			3.83	.52			8.55
152.40	30.48	11°30′	29.87	151.63	6.08	N. 83° W.	.74			6.03	1.26			14.58
182.88	30.48	12°30′	29.76	181.38	6.60	N. 82° W.	.92			6.53	2.18			21.11
213.36	30.48	15°	29.44	210.83	7.89	N. 72° W.	2.44			7.50	4.62			28.61
243.84	30.48	18°45′	28.86	239.69	9.80	N. 58° W.	5.19			8.31	9.81			36.92
274.32	30.48	19°30′	28.73	268.42	10.17	N. 58° W.	5.39			8.63	15.20			45.55
304.80	30.48	15°	29.44	297.86	7.89	N. 55° W.	4.52			6.46	19.72			52.01
335.28	30.48	11°30′	29.87	327.73	6.08	N. 38° W.	4.79			3.74	24.51			55.75
351.13	15.85	11°30′	15.53	343.26	3.16	N. 45° W.	2.23			2.23	26.74			57.98
North-observation well														
[Total depth after cementing and casing, 330 m]														
30.48	30.48	3°30′	30.42	30.42	1.86	S. 70° E.		0.64	1.75			0.64	1.75	
60.96	30.48	5°18′	30.35	60.77	2.82	S. 55° E.		1.61	2.31			2.25	4.06	
91.44	30.48	2°42′	30.45	91.22	1.44	S. 85° E.		.13	1.43			2.38	5.49	
121.92	30.48	2°36′	30.45	121.67	1.38	N. 35° E.	1.13		.79			1.25	6.28	
152.40	30.48	5°36′	30.33	152.00	2.97	N. 28° W.	2.63			1.40	1.38		4.88	
182.88	30.48	15°30′	29.37	181.37	8.15	N. 35° W.	6.68			4.67	8.06		.21	
213.36	30.48	23°	28.06	209.43	11.91	N. 37° W.	9.51			7.17	17.56			6.96
243.84	30.48	25°30′	27.51	236.94	13.12	N. 43° W.	9.60			8.95	27.16			15.91
274.32	30.48	22°30′	28.16	265.10	11.66	N. 48° W.	7.80			8.67	34.96			24.58
304.80	30.48	17°24′	27.06	292.16	14.03	N. 52° W.	8.64			11.06	43.60			35.64
341.38	36.58	25°12′	33.10	325.26	15.58	N. 50° W.	10.01			11.93	53.61			47.57

TABLE 21.—*Observed contact between rock units and calculated dip and strike at the proposed disposal site, Oak Ridge National Laboratory, Tenn.*

[Depth of rock contact was observed from gamma-ray logs and adjusted by well deviation logs. N, north; S, south; E, east; W, west]

Contact between rock units	Measured depth (m)	True vertical depth (m)	Horizontal position from surface well center, in meters				Altitude, mean sea level (m)
			N	S	W	E	
Injection well							
Rutledge Limestone–Gray shale	167	165	8.0		18.5		75
Gray shale–Rutledge Limestone	198	196	8.7		23.8		45
Rutledge Limestone–Pumpkin Valley Shale	234	230	13.6		32.9		10
Pumpkin Valley Shale–Rome Sandstone	338	330	34.0		51.6		−89
Old East-observation well							
Rutledge Limestone–Gray shale	176	175		1.9		4.6	65
Gray shale–Rutledge Limestone	205	205	0.2			0	36
Rutledge Limestone–Pumpkin Valley Shale	242	240	5.9		8.1		0
Pumpkin Valley Shale–Rome Sandstone	346	339	19.0		34.8		−99
South-observation well							
Rutledge Limestone–Gray shale	177	175	10.5		20.3		78
Gray shale–Rutledge Limestone	209	206	14.0		26.7		37
Rutledge Limestone–Pumpkin Valley Shale	251	247	18.5		36.3		−3
Pumpkin Valley Shale–Rome Sandstone	357	348	32.4		63.2		−105
West-observation well							
Rutledge Limestone–Gray shale	158	157	1.4		15.8		82
Gray shale–Rutledge Limestone	190	188	2.8		22.9		50
Rutledge Limestone–Pumpkin Valley Shale	227	223	6.9		32.3		15
Pumpkin Valley Shale–Rome Sandstone	334	326	24.3		55.6		−88
North-observation well							
Rutledge Limestone–Gray shale	152	151	1.8			4.9	84
Gray shale–Rutledge Limestone	187	185	9.4		0.8		50
Rutledge Limestone–Pumpkin Valley Shale	218	213	18.9		8.2		22
Pumpkin Valley Shale–Rome Sandstone	330	318	50.6		44.0		−83

Calculated dip and strike

Contact between rock units	Dip	Strike
Rutledge Limestone–Gray shale	10°30′	N. 51° E.
Gray shale–Rutledge Limestone	9°24′	N. 53° E.
Rutledge Limestone–Pumpkin Valley Shale	14°36′	N. 70° E.
Pumpkin Valley Shale–Rome Sandstone	13°00′	N. 71° E.

calcareous shale, 195 m thick; gray calcareous shale interbedded with less limestone, 34 m thick; and purple or gray argillaceous shale (Pumpkin Valley Shale), 100 m thick. Underlying the Conasauga Group is the Rome Formation.

The strike and dip of the rock units were determined from gamma-ray logs and by the three-point method described by Lahee (1952, p. 711–714). The calculated strikes and dips of all rock units are shown in table 21. The calculated average dip of the proposed injection shale (Pumpkin Valley Shale) at the proposed site is 13° SE. at a strike of N. 70° E.

TENSILE STRENGTH OF THE INJECTION SHALE

Rock samples were selected from cores taken from depths ranging from 214 to 360 m and shipped to the U.S. Geological Survey's rock mechanics laboratory in Denver, Colo., for a determination of the tensile strengths of the Pumpkin Valley Shale and the sandstone of the Rome Formation. One hundred and thirty-seven samples were selected, and 87 were used in the tensile-strength tests, which were supervised by R. A. Farrow of the U.S. Geological Survey.

Three methods were used in the tests: line load, point load, and direct pull. Both the line and point loads were applied by using a device described by Reichmuth (1968). Direct-pull tests were made both parallel to and normal to bedding planes. Samples were cemented by epoxy to flat plates designed for the tests and then stressed to failure. Test loads, in all tests, were applied with a Baldwin Lima Hamilton Universal machine, Model FTG[1], at a rate of 0.69 MPa/s for the direct-pull test and of 440 N/s for other tests.

Tensile strengths determined by line load were calculated by the following equation:

$$T = 6.37 \times 10^{-3} P/dh, \tag{64}$$

where

T = tensile strength, in megapascals,

P = load at rock failure, in newtons,

d = diameter of tested sample, in centimeters,

and

h = length of tested sample, in centimeters.

The tensile strength determined by the line-load test is the tensile strength parallel to bedding planes.

Direct-pull tests were made both parallel to and normal to bedding planes. The tensile strength parallel to bedding planes was determined by using an apparatus specially designed for this test. The apparatus consists of a thick-wall tubing 57 mm in inside diameter and 56 mm long. The tubing was split axially and fitted with pulling flanges. Samples were oriented in such a way that the direction of pull would be along bedding planes, then cemented in place with epoxy. Masking tape, placed at the joint where the two halves of the tubing joined, prevented epoxy from cementing the tubing. Most of the test resulted in epoxy bond failure at

[1]Any use of trade names and trademarks in this publication is for descriptive purposes only and does not constitute endorsement by the U.S. Geological Survey.

stresses ranging from 3 to 6 MPa, instead of rock failure. Direct-pull tests made along the axis of the core is not necessarily truly orthogonal to bedding planes because of the dip and deviation of the core hole. The samples were pulled in a direction 80° to the bedding planes. Therefore, the tensile strength normal to bedding planes is probably a few percent less than that determined in the laboratory.

The results of point-load tests were disappointing; only 9 of 29 samples produced results.

In summary, 83 samples of Pumpkin Valley Shale and 4 samples of Rome Sandstone were tested. The average tensile strength parallel to bedding planes is 12.4 MPa for Rome Sandstone and 6.2 MPa for Pumpkin Valley Shale. The tensile strength normal to bedding planes ranges from 0 to 3.4 MPa for Pumpkin Valley Shale. The maximum, minimum, and standard deviation values of all tests are shown in table 22.

It is necessary to note that all rock samples used in the tests were weakened by expansion resulting from removal of confining stresses. The actual in-situ tensile strengths in all directions are probably greater than the values determined in the laboratory.

TEST INJECTIONS

The test injections were not carried out in the order suggested by the U.S. Geological Survey, which is that a water injection should be made before a grout injection. The ORNL was concerned that a certain amount of water would probably be left in the shale after a water injection and that water could adversely affect the retention of radionuclides during waste injections. The ORNL also considered that since the proposed site is only 245 m from the present site, where a water injection was made in 1967, it would not have been necessary to conduct multiple injections, as suggested by the USGS, for site evaluations. The USGS objected to the ORNL's view for the following reasons:

1. The natural joint system can differ considerably within a distance of a few hundred meters.
2. All formations are already saturated with water to some degree, so that a small amount of water left by a water injection probably will not seriously affect the system.
3. A water injection not only indicates the degree of permeability of the injection zone but also can confirm the test results through a comparison of both water- and grout-injection results.
4. Local vertical earth stress can be determined from pressure decay of a water injection.

Nevertheless, ORNL decided to make only one grout injection.

After the grout injection, gamma-ray logs indicated that only two of the four observation wells, the South- and West-observation wells, had been intercepted by the induced fractures. The observed locations of the induced fractures correlated well with the calculated orientations. However, no gamma-ray peaks were noted in the East-observation well, presumably because the well was 5 m shallower than the altitude where the induced fractures was calculated to intercept the observation well. The North-observation well is near the present fracturing site. A gamma-ray log made before the test grout injection indicates that some induced fractures formed by past waste injections at the present site had already intercepted the well. Therefore, unless some new gamma-ray peaks were formed outside of the depth range where the induced fractures formed during past waste injec-

TABLE 22.—*Tensile strength of rocks at proposed site, Oak Ridge National Laboratory, Tenn., determined in the U.S. Geological Survey Denver Rock Mechanics Laboratory, Colo.*

Testing method	Tensile strength, in megapascals						
	Arithmetic mean	Maximum value	Minimum value	Standard deviation	Standard error of mean	98-percent confidence limit	
						Lower	Upper
Rome Sandstone							
Line load[1]	12.6	15.2	10.5	2.3	1.2	10.3	14.9
Pumpkin Valley Shale							
Line load[2]	7.3	12.5	3.6	2.3	0.4	6.5	8.0
Direct pull[3]	1.6	3.4	.3	1.1	.4	.9	2.4
Direct pull[4]	---	---	---	---	---	---	---
Point load[5]	---	---	---	---	---	---	---
Pumpkin Valley Shale, parallel to bedding planes[6]							
	6.0	12.5	1.9	3.0	0.4	5.1	6.8

[1]Four samples were tested, of tensile strength parallel to bedding planes.
[2]Thirty-five samples were tested, of tensile strength parallel to bedding planes.
[3]Eight samples were tested, of tensile strength normal to bedding planes.
[4]Tensile strength parallel to bedding planes. Eleven samples were tested: 7 samples resulted in bond failure at stresses ranging from 3.0 to 6.3 MPa; 4 samples failed at 2.4, 2.9, 3.4, and 4.0 MPa, respectively.
[5]Twenty-nine samples were tested; only 9 samples had poor results. Average tensile strength parallel to bedding planes is 1.9 MPa.
[6]Tensile strength. Average results determined by different methods.

tions had intercepted the well, there is no way to distinguish the previously induced fractures from the newly formed fractures. The gamma-ray logs made in the North-observation well after the test grout injection nearly repeated the one made before the injection. Therefore, it cannot be concluded from the gamma-ray logs whether or not the injected grout had reached the vicinity of the North-observation well during the test grout injection.

It is not necessary that all four observation wells should be intercepted by the induced fractures; however, it is desirable and indeed necessary to have more than two of four observation wells yielding a positive sign that the induced fracture had reached the observation wells, because if only two observation wells were intercepted by the grout, it may be interpreted that the interception is accidental. Therefore, it was concluded that the test grout injection was not sufficient to make an affirmative conclusion, and the USGS suggested two more injections – a water and a new grout injection – be made after deepening the East-observation well (Sun, 1976). Since then, both the ORNL and the USGS have agreed that a water injection was needed.

Because the test grout injection was made before the water injection, the test grout injection is discussed first in the following paragraphs.

TEST GROUT INJECTION

A test grout injection was made on June 14, 1974. In April 1974, the author, using measurements of the pressure decay of a water injection made in 1967 at the present fracturing site and the shale tensile strength estimated on the basis of injections made at West Valley, N.Y. (Sun and Mongan, 1974), made calculations to predict wellhead breakdown and shut-in pressure for the test injection. On the basis of the pressure decay of the water injection of 1967, the vertical earth stress at the proposed site is estimated to be 1.8 times the value of the calculated overburden pressure. For purposes of the prediction, the injection depth was assumed to be 335 m, and the density of shale, 2.7 (deLaguna and others, 1968); the vertical stress was then estimated as

$$(2)\,(2.7)\,(335)\,(9.8\times10^{-3})=17.7 \text{ MPa}.$$

On the basis of experience obtained in West Valley, N.Y., the tensile strength of shale normal to bedding planes and the cohesive stress at fracture tip were assumed to be 4 MPa and 2.5 MPa (for $f=0.6$) or 1.2 MPa (for $f=0.3$), respectively. The estimated wellhead breakdown pressure was calculated as

wellhead breakdown pressure
= bottom-hole breakdown pressure – static head in the casing,
$=(17.7+4)-((9.8\times10^{-3})\times335)$,
= 18.4 MPa.

The wellhead shut-in pressure was estimated as the sum of overburden pressure and cohesive stress at fracture tip less the static pressure in the casing and was equal to 16 MPa (16.8 MPa for $f=0.6$ and 15.6 MPa for $f=0.3$).

These predicted values were given to the Oak Ridge Operations Office, DOE (then U.S. Atomic Energy Commission), by the U.S. Geological Survey, April 29, 1974 (letter by G. D. DeBuchananne addressed to J. J. Schreiber).

The shale was fractured at a 18.3 MPa wellhead pressure during slotting on June 12, 1974 (Weeren and others, 1974), virtually confirming the predicted value. The wellhead shut-in pressure of the grout injection was 14.5 MPa (table 23), also closely approximately the calculated value. As this was the only prediction made so far, it may have coincided accidentally and therefore the accuracy of the prediction needs further testing.

TABLE 23.—*Injection pressure of the test grout injection at 332 m., June 14, 1974, at the proposed disposal site, Oak Ridge National Laboratory, Tenn.*

Time (min)	Observed wellhead pressure (MPa)	Calculated Bottom-hole pressure (MPa)	Rate of injection ($m^3/s\times10^{-3}$)
30	5.72	8.89	
45[1]	13.79	16.96	
46	17.93	21.10	
47	21.37	24.55	
48	22.48	25.65	
50	20.68	23.86	
55	18.62	21.79	
60	16.72	19.89	
62	21.65	24.82	
65	18.89	22.06	
68	22.48	25.65	
70	18.62	21.79	
75	19.31	22.48	
80	16.55	19.72	
85	16.55	19.72	
90	15.31	18.48	
95[2]	13.65	16.82	
100	13.79	16.96	
105[3]	12.55	15.72	
110	12.41	15.58	
115	13.44	16.62	
120	13.38	16.55	
125	12.34	15.51	
130	12.41	15.58	
135[4]	15.17	18.34	
140	15.86	19.03	
145	16.41	19.58	
150	16.55	19.72	
155	16.89	20.06	
160	16.55	19.72	
165	16.27	19.44	
170	16.20	19.37	
175	16.27	19.44	
180	16.27	19.44	
185	16.27	19.44	
190	16.13	19.31	
195	16.13	19.31	

TABLE 23.—*Injection pressure of the test grout injection at 332 m., June 14, 1974, at the proposed disposal site, Oak Ridge National Laboratory, Tenn.*—Continued

Time (min)	Observed wellhead pressure (MPa)	Calculated Bottom-hole pressure (MPa)	Rate of injection ($m^3/s \times 10^{-3}$)
200	16.13	19.31	
205	16.20	19.37	
210[5]	16.96	20.13	
215	17.93	21.10	
220	18.62	21.79	15.27
225	16.69	19.86	
230	14.89	18.06	16.72
235	14.34	17.51	
240	14.07	17.24	16.40
245	14.20	17.37	
250	14.48	17.65	16.91
255	14.13	17.31	
260	14.62	17.79	16.72
265	14.89	18.06	
270	15.31	18.48	17.22
275	16.96	20.13	
280	16.55	19.72	15.77
285	15.72	18.89	
290[6]	13.24	16.41	
295	13.44	16.62	
300[7]	17.58	20.75	
305	16.82	19.99	
310	16.69	19.86	17.03
315	16.82	19.99	
320	16.82	19.99	16.72
325	16.69	19.86	
330	16.69	19.86	16.40
335	16.96	20.13	
340	16.96	20.13	16.40
345	16.82	19.99	
350	16.41	19.58	17.03
355	16.55	19.72	
360	16.69	19.86	16.59
365	15.86	19.03	
370	18.06	21.24	15.96
375	17.65	20.82	
380	17.79	20.96	16.40
385	17.51	20.68	
390	17.37	20.55	16.40
395	17.24	20.41	
400	17.51	20.68	16.72
405	17.79	20.96	
410	17.51	20.68	16.40
415	17.51	20.68	
420	17.37	20.55	16.59
425	17.58	20.75	
430	17.93	21.10	16.28
435	18.06	21.24	
440	17.93	21.10	15.46
445	17.65	20.82	
450	17.65	20.82	16.40
455	17.65	20.82	
460	17.79	20.96	16.40
465	17.10	20.27	
470	17.65	20.82	16.59
475	18.06	21.24	
480	17.93	21.10	16.40
485	18.20	21.37	
490	18.27	21.44	16.59
495	18.96	22.13	
500	19.31	22.48	15.77
505	19.99	23.17	
510	23.10	26.27	12.93
515	24.41	27.58	
520	20.13	23.30	14.51
525	19.65	22.82	
530	18.27	21.44	15.01
535	19.31	22.51	
540	20.55	23.72	13.56
545	19.31	22.48	
550	18.20	21.37	16.40
555	17.93	21.10	
560	17.93	21.10	16.09
565	17.93	21.10	
570	17.65	20.82	16.72
575	17.93	21.10	
580	17.93	21.10	16.40
585	17.65	20.82	
590	17.10	20.27	16.09
595	16.20	19.37	
600	16.89	20.06	
	14.48	[7]17.65	

[1]Start injection.
[2]Stop injection.
[3]Injection was on and off irregularly.
[4]Start injection, most of the time with water.
[5]Normal injection started at hour 1310. Before this hour, the injection was run irregularly.
[6]Stop injection for cleaning surge tank window.
[7]Instantaneous shut-in pressure.

Interpretation of Injection Data

The injection well was slotted by a hydraulic jet at a depth of 332 m measured along the casing (the true injection depth after adjustment for well deviation was 324 m). The grout injection was started at 0940 hours (eastern daylight time) on June 14, 1974, and immediately ran into difficulties. The mixture of the grout could not be controlled, and the mixer was jammed with solids. The injection was interrupted at irregular intervals. When the injection pump was off, the instantaneous shut-in pressures were 14 MPa wellhead pressure or 17 MPa bottom-hole pressure. The normal injection was actually started at 1310 hours. The injection was then stopped again for a brief period from 1430 hours to 1440 hours for cleaning the window of the surge tank (hereafter, this stop is referred to as a brief pause). A total volume of 370 m^3 of grout tagged with radioactive tracer ^{198}Au (half-life is 2.7 days) was injected into the Pumpkin Valley Shale. The injection was completed at 1940 hours.

The grout was injected through a string of tubing that was placed 3 m above the injection level. The annulus between the casing and tubing was filled with water. Injection pressures were monitored in the annulus at the

wellhead of the injection well. The bottom-hole pressure could be calculated by adding static pressure in the well to the observed wellhead pressure. The calculated bottom-hole pressure, therefore, excludes the friction losses of the grout in the tubing.

Except for the 40-minute period from 1805 hours to 1845 hours, the injection rate was kept constant at 0.015 m^3/s for the entire injection period. During this 40-minute period, the injection rate dropped suddenly from 0.015 m^3/s to 0.010 m^3/s; thereafter the injection rate increased to 0.015 m^3/s. The observed injection pressures and injection rates are listed in table 23 and graphed in figure 59.

Outside of the 40-minute period, the variation of injection rates was only 0.0006 m^3/s, so that the statistical random variation of the injection rate cannot be separated from the observation error. In essence, the injection rate is equivalent to a single rate, consequently, the linear-regression method cannot be used to find the relation between the injection pressure and the injection rate. However it has been demonstrated that the coefficient of the injection rate in a linear equation can be found by using the difference between the injection pressure and the instantaneous shut-in pressure (Sun and Mongan, 1974).

The average injection rate was 0.015 m^3/s at an average injection pressure of 20.7 MPa. The instantaneous shut-in pressure was 17.7 MPa. The coefficient of the injection rate, therefore, is calculated to be 196 MPa/(m^3/s). The linear equation is then established as

$$P = 17.7 + 196\,Q. \qquad (65)$$

As determined from the 1967 water-injection pressure decay data (deLaguna and others, 1968), the vertical stress at the actual injection depth was estimated to be 15.4 MPa ($1.8 \times 2.7 \times 9.8 \times 10^{-3} \times 324 = 15.4$ MPa). The bottom-hole breakdown pressure was 21.5 MPa (18.3 MPa $+ 9.8 \times 10^{-3} \times 324 = 21.5$ MPa). Tensile strength normal to bedding planes is estimated from the difference between the bottom-hole breakdown pressure and the estimated vertical stress, that is, 6.1 MPa (21.5 − 15.4 = 6.1 MPa). Because

$f T$ = instantaneous shut-in pressure − vertical stress,
= 17.7 − 15.4,
= 2.3 MPa,

therefore

$$f = 0.38, \quad \text{for } T = 6.1 \text{ MPa}.$$

The tensile strength of shale normal to bedding planes as determined by hydraulic fracturing is three times

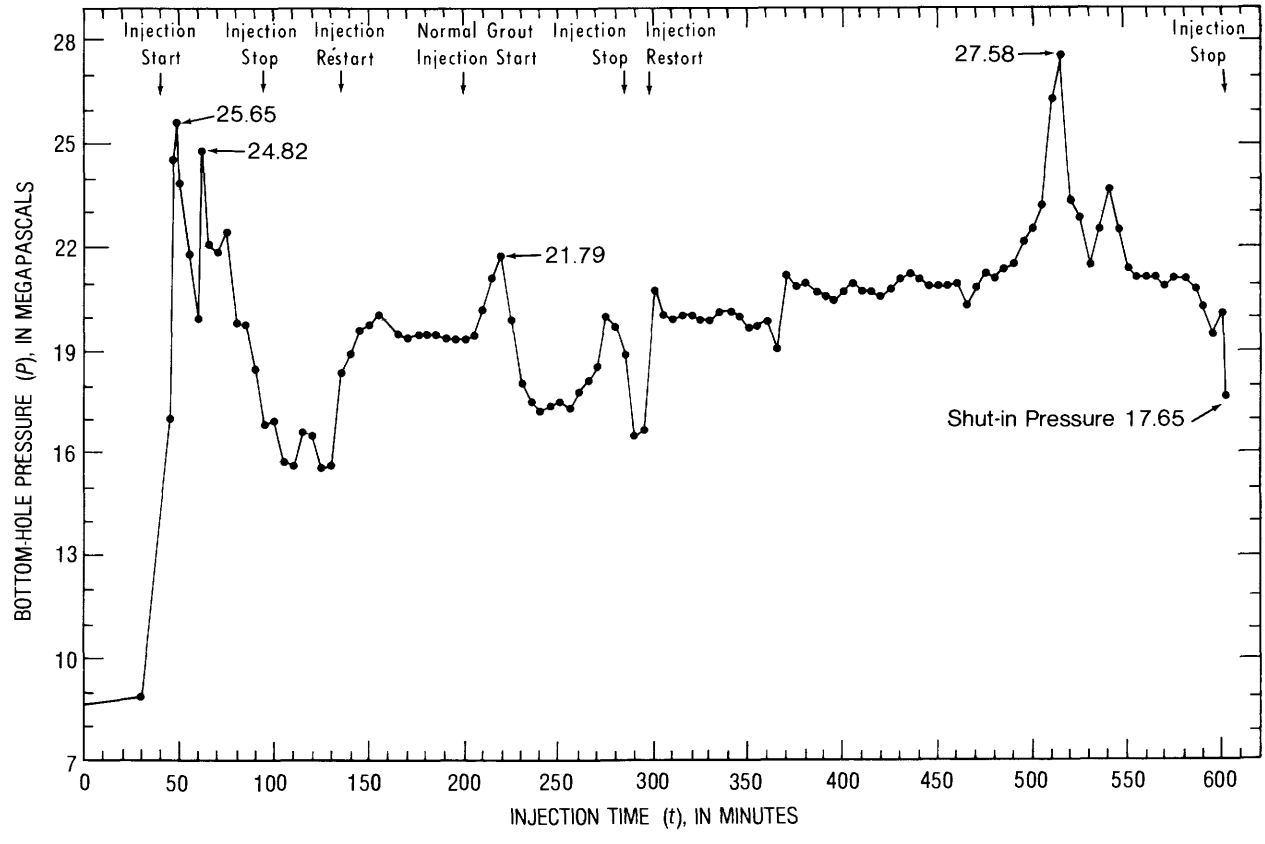

FIGURE 59.—Pressure plotted against time, the grout injection at 332m, June 14, 1974, at the proposed disposal site, Oak Ridge National Laboratory, Tenn.

greater than the average value found in laboratory (table 27); as discussed before, this is probably due to stress relaxation when confining stress is removed from the core.

Altitude of Induced Fractures

The altitudes of induced fractures were determined by gamma-ray logs made in observation wells before and after the test grout injection. Repeated logs were made to confirm that the logs were reproducible. The logger amplifier has 7 sensitivity ranges; namely 0.001, 0.002, 0.005, 0.01, 0.02, 0.05, and 0.1 milliroentgen per hour (mR/hr). The sensitivity to gamma-ray activity decreases as the number of sensitivity range increases. For example, at a sensitivity range of 0.001 mR/hr the logger is 100 times more sensitive to gamma-ray energy than it is at a sensitivity range of 0.1 mR/hr. The amplitude of a deflection of a gamma-ray log made with a sensitivity range of 0.001 mR/hr is, therefore, 100 times greater than that indicated on a log of the same source made at a sensitivity range of 0.1 mR/hr. Therefore, it is necessary to keep the sensitivity range in mind when gamma-ray logs are compared.

Past waste grout sheet intercepted by North-observation well—The location of the North-observation well is about 190 m, S. 45° W. from the present injection well. Four peaks of gamma-ray activity greater than the background activity level for shale were noted from the gamma-ray logs made in the North-observation well before the test grout injection. The peaks were at depths of 242, 246, 271, and 324 m, respectively (fig. 60, table 24). These peaks indicate that the well has intercepted waste grout sheets made during past injections at the present injection well north of the observation well.

The strongest gamma-activity among the four peaks was at a depth of 271 m measured along the casing (fig. 60). Adjusted for well deviation, the altitude of this peak is at −27 m (27 m below mean sea level (msl)) (table 24), and if the calculated dip and strike (13° SE., and N. 70° E.) of the Pumpkin Valley Shale at the proposed site were used, then the bedding-plane fractures indicated by this peak would intercept the present injection well at an altitude of −16 m msl. Most of the wastes were injected at altitudes ranging from −12 to −18 m msl (table 11). Therefore, it can be concluded that this gamma-ray peak results from past waste injections made at the present injection well.

The second strongest gamma-activity peak was observed at an altitude of −4 m msl. On the basis of the same dip and strike the altitude at which the fracture indicated by this second peak may be projected to intercept the present injection well at 9 m msl. The altitudes of −0.5 and −74 m msl observed for the other two gamma-ray-activity peaks when projected to the present injection well are either 24 m above or 21 m below the past waste injection altitude. Table 11 indicates that all wastes were injected between −12 to −47 m msl; therefore, it may be concluded that some waste grout has probably migrated 20 m above or below the injection level during past injections over a distance at least 200 m from the injection site.

TABLE 24.—*Waste grout sheet intercepted by the North-observation well from past waste injections made at the present fracturing site, Oak Ridge National Laboratory, Tenn.*

[Interpreted from gamma-ray logs made in the North-observation well at the proposed disposal site before the test grout injection, June 14, 1974. N, north; S, south; W, west; E, east]

Depth measured along casing (m)	Vertical depth[1] (m)	Altitude mean sea level (m)	Horizontal position from surface well center, in meters			
			N	S	W	E
242.3 ------	235.5	−0.5	26.7		15.5	
246.0[2] -----	238.9	−3.9	27.7		16.5	
271.0[3] -----	262.0	−27.0	34.1		23.6	
323.7 ------	309.3	−74.2	48.8		41.8	

[1]Measured depth adjusted by deviation survey.
[2]Second strongest gamma-ray activity peak.
[3]Strongest gamma-ray activity peak.

Grout sheets produced by test grout injection.—A comparison of gamma-ray logs made in the North-observation well before and after the test grout injection shows no significant change in gamma-ray activity at any depth. Two of the logs obtained after the test grout injection were made by using sensitivity ranges of 0.002 mR/hr and 0.01 mR/hr, respectively. If the gamma-ray activity shown by the log made using a sensitivity range of 0.002 mR/hr is reduced by a factor of 5, then the shape and the relative quantity of the gamma-ray activity indicated by the log would be similar to that recorded on the log made using a sensitivity range of 0.01 mR/hr. This indicates the reproducibility of the logs. If the log made using a sensitivity range of 0.002 mR/hr is reduced by a factor of 2.5, the activity recorded on the log would be very close to that recorded on the log made in the North-observation well before the test grout injection at a sensitivity of 0.005 mR/hr. Comparison of the logs indicates that no additional grout sheets have intercepted the North-observation well since the test grout injection. The probable altitude at which the North-observation well would have been intercepted by the bedding-plane fractures induced by the test grout injection at the proposed disposal site was calculated to be −67 m msl. A gamma-ray activity peak produced by past waste injections is at −74 m msl, or about 7 m below the calculated altitude at which the induced fractures would be expected to have intercepted the well. Therefore, it cannot be determined whether the injected grout did not reach the vicinity of the North-observation well or whether the injected grout did reach the observation well

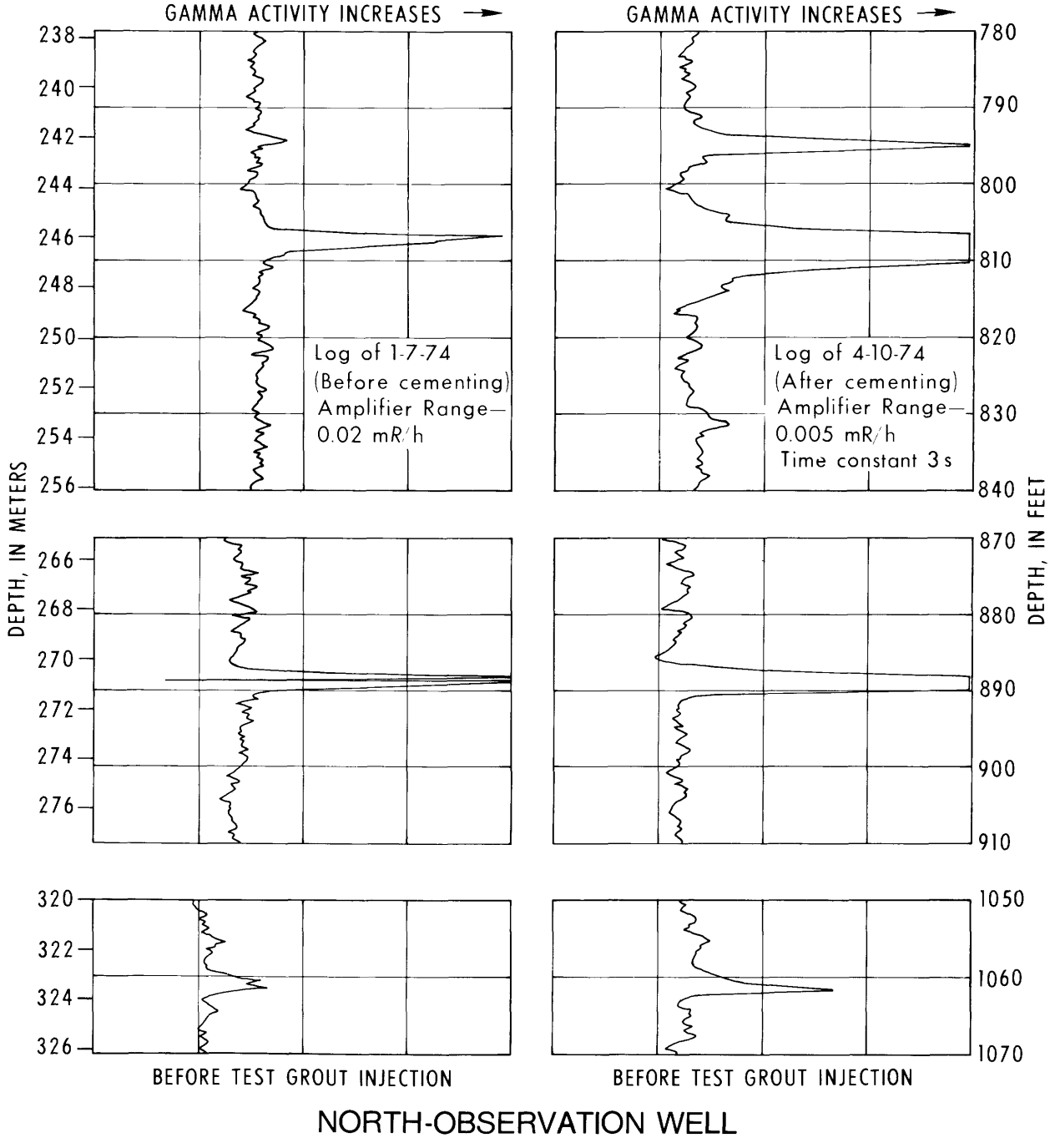

FIGURE 60.—Gamma-ray activities observed in the North-observation well along the casing axis before the test grout injection, June 14, 1974, at the proposed disposal site, Oak Ridge National Laboratory, Tenn.

but followed weak planes between the older waste grout sheets and shale at −74 m msl; in the latter case, the gamma-ray activity produced by the tracer in the test grout injection could not be differentiated from that produced by older waste injections.

Six gamma-ray activity peaks were noted after the test grout injection on a gamma-ray log made in the West-observation well at depths ranging from 328 to 332 m measured along the casing (table 25, and fig. 61). Grout sheets were formed within a 5-m zone. The projected horizontal position of the six gamma-ray activity peaks and the altitudes of the grout sheets were calculated and are shown in table 25. The horizontal distance between the injection depth and the observed gamma-ray activity peaks was determined along a line perpendicular to the calculated strike of the Pumpkin Valley Shale and was estimated to be 12 m (fig. 62). The injection depth was −84 m msl. If bedding-plane frac-

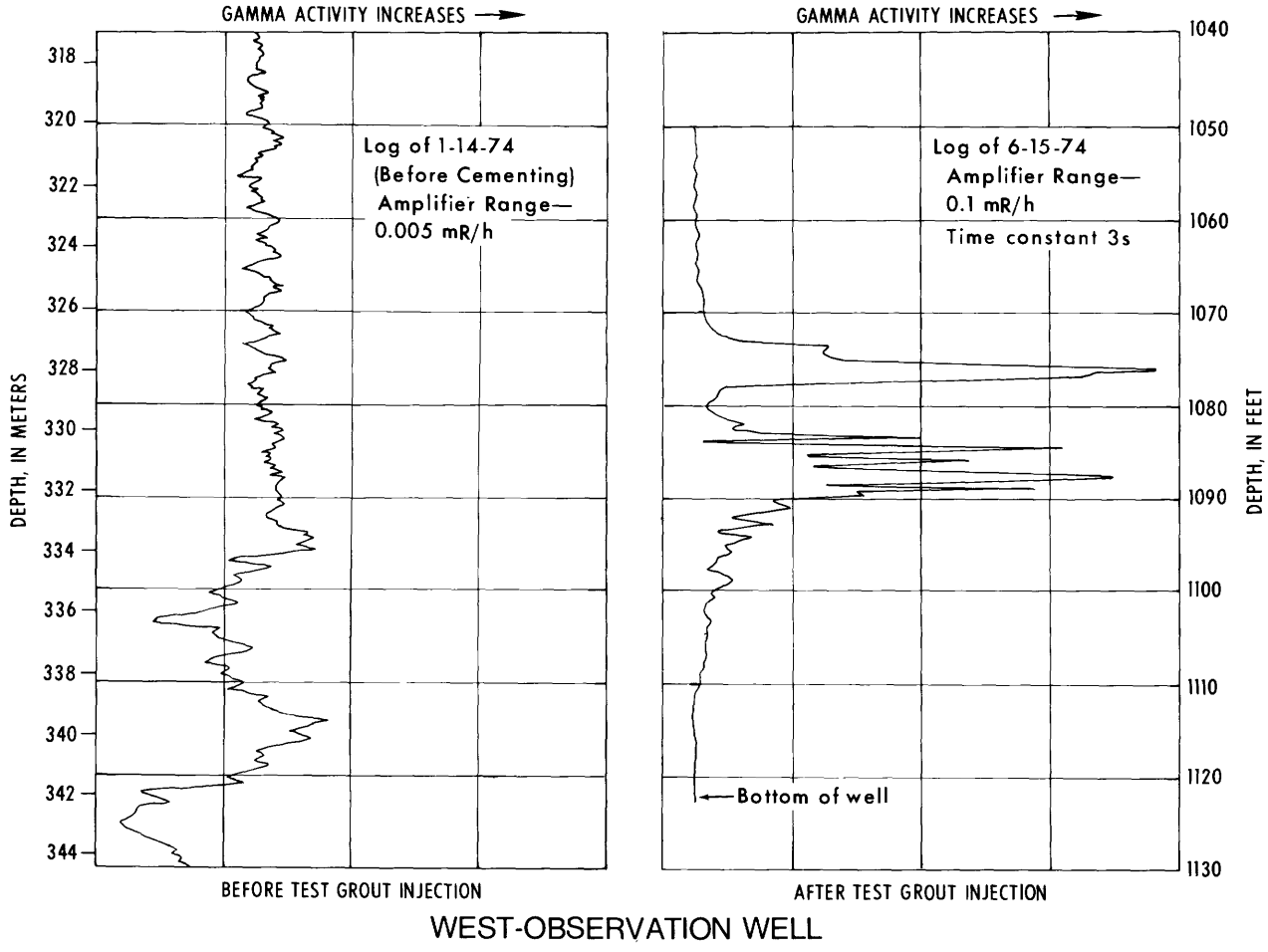

FIGURE 61.—Gamma-ray activities observed in the West-observation well along the casing axis, before and after the test grout injection, June 14, 1974, at the proposed disposal site, Oak Ridge National Laboratory, Tenn.

TABLE 25.—*Grout sheet from the test grout injection at 332 m, June 14, 1974, intercepting observation wells at the proposed disposal site, Oak Ridge National Laboratory, Tenn.*

[The injection altitude was −83.7 m msl. N, north; S, south; W, west; E, east]

Depth measured along casing (m)	Vertical depth[1] (m)	Altitude mean sea level (m)	Horizontal position from surface well center, in meters			
			N	S	W	E
New East-observation well						
341.1 --------	335.0	−93.8	19.7		31.4	
South-observation well						
349.0 --------	340.8	−97.3	31.5		61.4	
349.6 --------	341.4	−97.8	31.5		61.6	
349.9 --------	341.7	−98.1	31.1		61.7	
West-observation well						
328.0 --------	320.3	−81.8	23.3		54.9	
330.1 --------	322.4	−83.9	23.7		55.1	
330.4 --------	322.7	−84.2	23.7		55.2	
331.0 --------	323.3	−84.8	23.8		55.2	
331.3 --------	323.6	−85.1	23.9		55.3	
331.9 --------	324.1	−85.7	24.0		55.4	

[1]Measured depth adjusted by deviation survey.

tures were induced near the West-observation well, then the altitude at which they would intercept the well can be estimated by using the calculated dip and strike of the shale. The calculation is

$$\text{fracture altitude} = -84 + 12 \tan 13°,$$
$$= -81 \text{ m msl.}$$

This calculated altitude is close to the observed altitude of the gamma-ray activity peaks, which are from −82 to −86 m msl (table 25).

Three gamma-ray activity peaks were noted on a gamma-ray log made in the South-observation well at depths between 349 m and 350 m measured along the casing (table 25, fig. 63). The altitudes of the peaks, after adjustment for well deviation, are shown in table 25. The horizontal distance between the injection altitude and the altitudes of the gamma-ray activity peaks in the direction of the dip was estimated to be 56 m (fig. 62). Therefore, the altitudes at which the South-

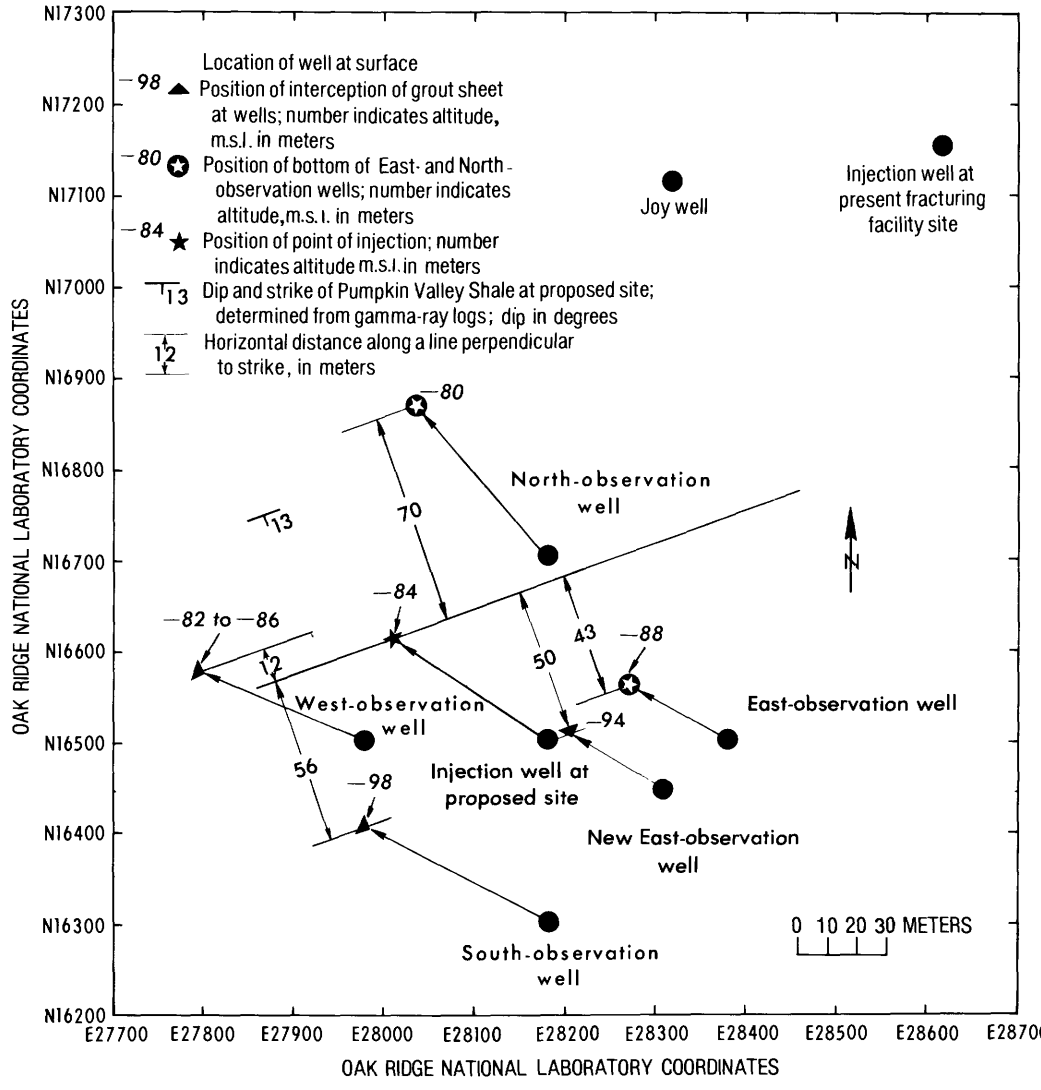

FIGURE 62.—Location of point of injection and altitudes of gamma-ray peaks observed in observation wells after the test grout injection, June 14, 1974, at the proposed disposal site, Oak Ridge National Laboratory, Tenn.

observation well would be intercepted by the induced bedding-plane fractures is calculated as

$$\text{fracture altitude} = -84 - 56 \tan 13°,$$
$$= -97 \text{ m msl},$$

which is close to the observed peak altitudes, that is, −97 m and −98 m msl, respectively.

No significant change in gamma-ray activity was registered on logs made in the East-observation well before and after the grout injection. The projected horizontal distance along the dip between bottom of the East-observation well and the injection altitude was estimated to be 43 m (fig. 62). The altitude at which the East-observation well would be intercepted by the induced bedding-plane fractures is calculated as

$$\text{fracture altitude} = -84 - 43 \tan 13°,$$
$$= -94 \text{ m msl}.$$

The depth corresponding to this altitude measured along the casing adjustesd by well deviation was 340 m. The total drilling depth was 344 m; however, after casing and cementing the well depth was reduced to 334 m, which is 6 m shallower than the calculated altitude where the East-observation well would be intercepted by the induced fractures. The gamma-ray log indicates two possibilities: (1) induced fractures intercept the well

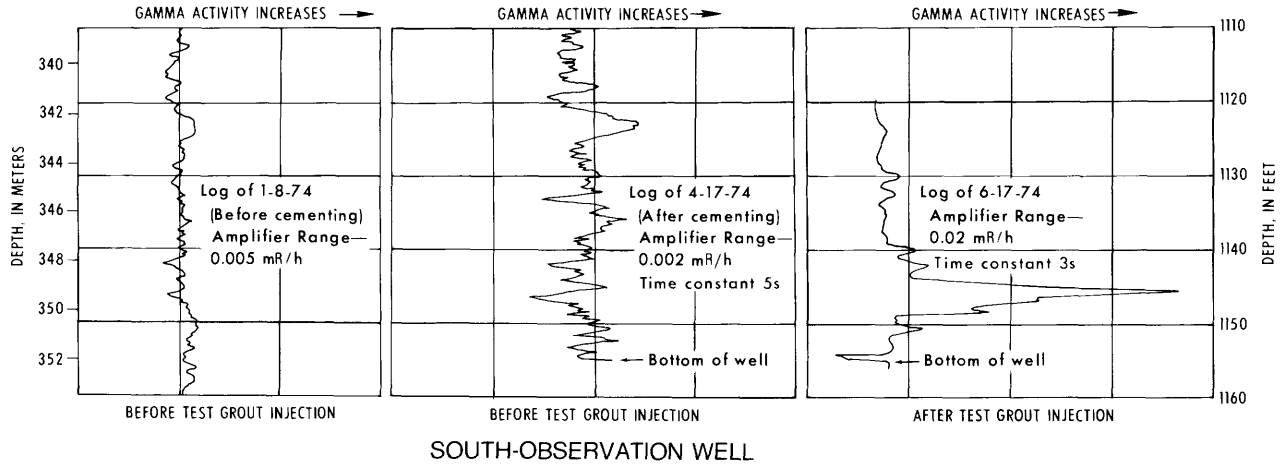

FIGURE 63.—Gamma-ray activities observed in the South-observation well along the casing axis, before and after the test grout injection, June 14, 1974, at the proposed disposal site, Oak Ridge National Laboratory, Tenn.

beneath the well bottom or (2) no grout sheets reached the well.

Before the water injection made on October 30, 1975, gamma-ray logs were made again in all four observation wells in September 1975, 87 days after the test grout injection. All logs reproduced the pattern of the logs made immediately after the test grout injection. Gamma-ray activity peaks were still observed distinctly at the zones discussed, but these peaks could not have been due to the tracer, ^{198}Au, which has a half life of 2.7 days. After 32 half lives (87 days after the injection) the tracer should have decayed to below the detection limits. As explained by the ORNL personnel several hundred gallons of contaminated waste pit water containing ^{137}Cs and ^{90}Sr were injected during the test grout injection (J. A. Lenhard, written commun., Nov. 16, 1976), and thus the gamma-ray peaks observed on logs resulted from ^{137}Cs not from tracer ^{198}Au.

In 1976, a new East-observation well was drilled by the ORNL 30 m south-west of the old East-observation well. A single gamma-ray activity peak was noted on a gamma-ray log made in the new East-observation well at a depth of 341 m measured along the casing (fig. 64). Adjusted for well deviation, the altitude at which the observation well was intercepted by the induced fracture was calculated to be −94 m msl. The horizontal distance along the dip between the injection altitude and the altitude for the gamma-ray peak was estimated to be 65 m (fig. 62). The projected altitude at which the new East-observation well could be intercepted by the test injection grout sheet is calculated as

$$\text{fracture altitude} = -84 - 50 \tan 13°,$$
$$= -96 \text{ m msl},$$

which is close to the observed altitude of −94 m msl.

Thus, three of the four observation wells have been intercepted by the grout sheets produced by the test grout injection near the calculated altitudes, and it is concluded that bedding-plane fractures have been induced by the test grout injection.

TEST WATER INJECTION

A test water injection was made on October 30, 1975, through the same slot as the test grout injection made on June 14, 1974. The scheduled injection volume was 378 m^3 of water tagged with 25 Ci of ^{198}Au and 25 Ci of ^{199}Au. The injection rates were scheduled to start at 0.003 m^3/s, increase to 0.006 m^3/s, then 0.013 m^3/s, and finally increase to the full capacity of the injection pump (0.017 m^3/s). The first three steps would last two hours for each step. Unfortunately one of the two injection pumps broke down after about one hour of injection at the pump's highest capacity, and the injection was stopped shortly thereafter. The final injection volume was 209 m^3 tagged with half the prepared tracers. Pressure decay was observed for about 18 days after the injection. The injection and pressure-decay data are shown in tables 26 and 27, respectively. The linear regression equation of P and Q established from the injection data is given by

$$P = 20 + 197\,Q. \qquad (66)$$

If $Q = 0$; then $P = 20$ MPa, which closely correlates with the observed shut-in bottom-hole pressure, 19.9 MPa (table 27).

The earth stress normal to the bedding-plane fractures determined from pressure decay is 16 MPa (fig. 65), corroborating the previously estimated vertical stress of 15.4 MPa, determined from the 1967 water

TABLE 26.—*Injection pressure of the test water injection at 332 m, Oct. 30, 1975, at the proposed disposal site, Oak Ridge National Laboratory, Tenn.*

Time (min)	Observed wellhead pressure (MPa)	Calculated bottom-hole pressure (MPa)	Rate of injection ($m^3/s \times 10^{-3}$)
1	13.17	16.34	
3	13.44	16.62	
5	13.72	16.89	
6	12.93	16.10	
7	11.93	15.10	
9[1]	11.10	14.27	0
10	10.69	13.86	
139[2]	11.76	14.93	0
140	13.20	16.38	
142	14.62	17.79	1.89
143	14.82	18.00	
146	15.00	18.17	
147	15.10	18.27	
148	15.24	18.41	
150[3]	15.27	18.44	
155	15.51	18.68	
160	15.79	18.96	
165	15.96	19.13	
170	16.10	19.27	
175	16.20	19.37	
180	16.31	19.48	
185	16.48	19.65	
190	16.51	19.68	1.89
195	16.58	19.75	2.40
200	16.69	19.86	
205	16.79	19.96	
210	16.86	20.08	
215	16.93	20.10	2.40
220	17.00	20.17	2.65
225	17.06	20.24	
230	17.10	20.27	2.65
235	17.10	20.27	2.84
240	17.10	20.27	
245	17.10	20.27	2.84
250	17.00	20.17	2.65
255	18.13	21.30	5.65
256	18.44	21.62	
257	18.62	21.79	
258	19.13	22.30	
259	19.31	22.48	
260	19.44	22.61	5.65
265	19.86	23.03	8.45
270	20.03	23.20	
275	20.24	23.41	
280	20.37	23.55	
285	20.42	23.59	
290	20.42	23.59	
295	20.34	23.51	
298	20.27	23.44	
299	20.24	23.41	
300	20.24	23.41	
301	20.24	23.41	8.45
302	19.44	22.61	5.43
303	19.20	22.37	
304	19.00	22.17	
305	18.79	21.96	
306	18.62	21.79	
307	18.48	21.65	
308	18.31	21.48	
309	18.17	21.34	
310	18.03	21.20	
311	17.93	21.10	
312	17.83	21.00	
313	17.72	20.89	

TABLE 26.—*Injection pressure of the test water injection at 332 m, Oct. 30, 1975, at the proposed disposal site, Oak Ridge National Laboratory, Tenn.*—Continued

Time (min)	Observed wellhead pressure (MPa)	Calculated bottom-hole pressure (MPa)	Rate of injection ($m^3/s \times 10^{-3}$)
315	17.48	20.65	5.43
318	18.27	21.44	6.62
319	18.55	21.72	
320	18.86	22.03	
325	19.41	22.58	6.62
330	19.62	22.79	7.95
335	19.79	22.96	
340	19.89	23.06	
345	19.89	23.06	
350	19.87	23.04	
355	19.82	22.99	7.95
360	19.79	22.96	7.59
365	19.75	22.93	
370	19.68	22.86	7.59
372	19.79	22.96	9.90
373	19.82	22.99	
374	19.86	23.03	
375	19.89	23.06	
376	19.93	23.10	
377	19.99	23.17	
378	20.03	23.20	
379	20.06	23.24	
380	20.11	23.28	
385	20.13	23.30	9.90
390	20.10	23.27	13.25
395	20.06	23.24	
400	19.96	23.13	13.25
405	19.86	23.03	12.74
410	19.75	22.93	12.74
415	19.65	22.82	13.25
420	19.59	22.77	
425	19.51	22.68	
430	19.41	22.58	
435	19.20	22.37	13.25
450	19.06	22.24	16.78
455	19.03	22.20	16.78
460	18.96	22.13	16.40
463	19.13	22.30	
464	19.15	22.32	
465	19.17	22.34	
470	19.21	22.38	
475	19.20	22.37	
480	19.17	22.34	
485	19.03	22.20	
490	18.96	22.13	
495	18.87	22.04	
500[4]	18.80	21.97	16.40
503	18.20	21.37	9.21
504	18.10	21.27	
505	18.13	21.30	
506	18.10	21.27	
510	18.00	21.17	
515	17.87	21.04	
520	17.77	20.95	
525	17.66	20.84	
530[5]	17.58	20.75	
535	17.49	20.66	
540	17.44	20.62	
545	17.37	20.55	
550[6]	17.34	20.51	

[1]Shut down for repairing leaks.
[2]Pressure gage was out of order.
[3]Start injection of tracers.
[4]One pump was out of order.
[5]Stop injection of tracers.
[6]End injection.

TABLE 27.—*Pressure decay of the test water injection at 332 m, Oct. 30, 1975, at the proposed disposal site, Oak Ridge National Laboratory, Tenn.*

Time since end of injection (min)	Observed well-head pressure (MPa)	Calculated bottom-hole pressure (MPa)	$(P-P_0)$ (MPa)
2	16.72	19.89	16.77
5	16.44	19.62	16.50
10	15.93	19.10	15.98
15	15.62	18.79	15.67
20	15.31	18.48	15.36
25	15.07	18.24	15.12
30	14.86	18.03	14.91
35	14.65	17.82	14.70
40	14.48	17.65	14.53
45	14.31	17.48	14.36
50	14.17	17.34	14.22
55	14.03	17.20	14.08
60	13.89	17.06	13.94
65	13.79	16.96	13.84
70	13.69	16.86	13.74
80	13.48	16.65	13.53
90	13.27	16.44	13.32
100	13.12	16.29	13.17
110	13.17	16.11	12.99
120	12.81	15.98	12.86
130	12.67	15.84	12.72
140	12.63	15.80	12.68
150	12.45	15.62	12.50
160	12.34	15.51	12.39
170	12.22	15.39	12.27
180	12.12	15.29	12.17
190	12.03	15.20	12.08
200	11.93	15.10	11.98
210	11.86	15.03	11.91
225	11.72	14.89	11.77
240	11.62	14.79	11.67
255	11.51	14.69	11.57
270	11.41	14.58	11.46
285	11.31	14.48	11.36
300	11.20	14.38	11.26
315	11.14	14.31	11.19
330	11.03	14.20	11.08
860	9.29	12.46	9.34
890	9.23	12.40	9.28
920	9.19	12.36	9.24
970	9.11	12.28	9.16
1,035	9.01	12.18	9.06
1,140	8.81	11.98	8.86
1,200	8.70	11.87	8.74
1,260	8.61	11.78	8.66
1,430	8.38	11.55	8.43
1,675	8.07	11.24	8.12
1,930	7.81	10.98	7.86
2,160	7.58	10.76	7.64
2,400	7.47	10.65	7.53
2,640	7.28	10.45	7.33
2,880	7.15	10.32	7.20
3,120	7.01	10.18	7.06
3,360	6.87	10.05	6.93
3,600	6.72	9.89	6.77
3,850	6.67	9.85	6.73
4,105	6.55	9.72	6.60
4,315	6.50	9.67	6.55
4,560	6.38	9.55	6.43
4,800	6.31	9.48	6.36
5,040	6.22	9.39	6.27
5,335	6.17	9.34	6.22
5,490	6.12	9.29	6.17
5,760	6.05	9.22	6.10

TABLE 27.—*Pressure decay of the test water injection at 332 m, Oct. 30, 1975, at the proposed disposal site, Oak Ridge National Laboratory, Tenn.*—Continued

Time since end of injection (min)	Observed well-head pressure (MPa)	Calculated bottom-hole pressure (MPa)	$(P-P_0)$ (MPa)
6,000	6.00	9.17	6.05
6,240	5.90	9.07	5.95
6,480	5.83	9.01	5.89
6,720	5.83	9.01	5.89
6,960	5.76	8.94	5.82
7,200	5.72	8.89	5.77
7,440	5.67	8.84	5.72
7,650	5.62	8.79	5.67
7,920	5.59	8.76	5.64
8,400	5.48	8.65	5.53
8,700	5.45	8.62	5.50
9,180	5.37	8.54	5.42
9,625	5.32	8.49	5.37
10,140	5.24	8.41	5.29
10,620	5.17	8.34	5.22
11,320	5.09	8.26	5.14
11,580	5.03	8.20	5.09
12,080	5.00	8.17	5.05
12,540	4.96	8.14	5.02
13,020	4.90	8.07	4.95
13,500	4.84	8.01	4.89
14,460	4,76	7.93	4.81
15,360	4.69	7.86	4.74
15,655	4.67	7.84	4.72
16,795	4.60	7.77	4.65
17,080	4.56	7.74	4.62
18,225	4.48	7.65	4.53
18,555	4.47	7.64	4.52
19,680	4.38	7.55	4.43
19,972	4.37	7.54	4.42
21,100	4.30	7.47	4.35
21,420	4.28	7.45	4.33
22,600	4.21	7.38	4.26
24,030	4.14	7.31	4.19
25,448	4.08	7.25	4.13
25,692	4.05	7.22	4.10

Note: Static ground-water pressure at injection level, $P_0 = 3.12$ MPa.

injection at the present disposal site. The permeability of the injected shale, indicated by the pressure decay data, is low, as expected. If the tensile strength of the shale is assumed to be 6.1 MPa, then $f = 0.66$.

A comparison of gamma-ray logs made before and after the water injection shows no indication that any of the four observation wells are intercepted by the induced fractures at any depth. The water injection was made at the same depth and through the same slot through which the test grout injection was made. It was anticipated that the injected water would probably flow along weak planes induced by the test grout injection between the shale and the previously formed grout sheets or that, in other words, a series of thin fractures would be induced in the grout sheet zone. Because the grout sheets are contaminated by ^{137}Cs, which produces higher gamma-ray energy than that produced by the tracers in the injection water, it is not surprising that none of the gamma-ray logs made in the observation wells after the water injection show evidence that frac-

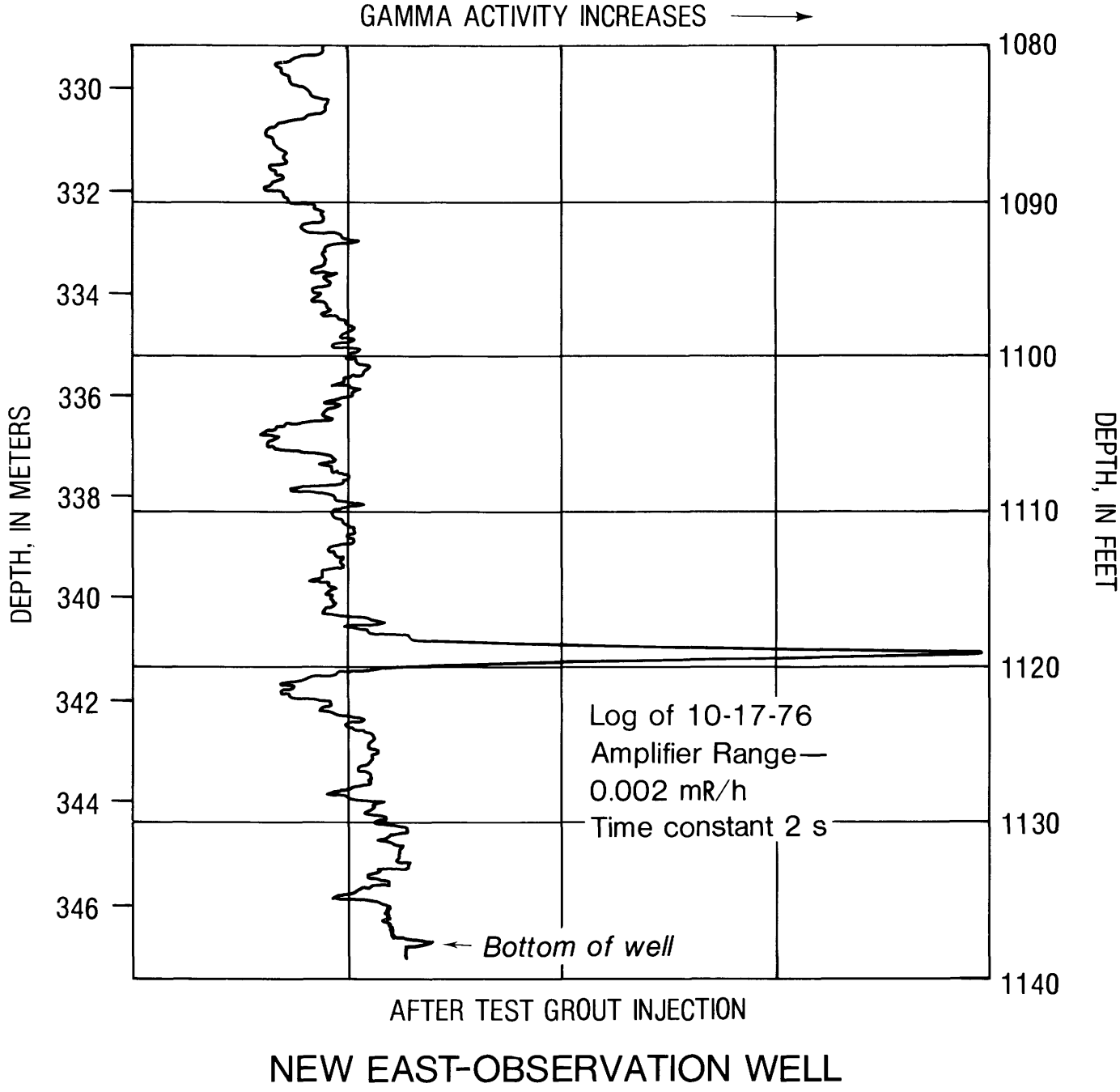

FIGURE 64.—Gamma-ray activities observed in the new East-observation well along the casing axis, 85 days after the test grout injection, June 14, 1974, at the proposed disposal site, Oak Ridge National Laboratory, Tenn.

tures induced by the water injection intercepted the wells.

However, the water-injection pressure data confirm the conclusions reached from data gathered during the test grout injection.

POTENTIAL FOR THE EXHUMATION OF WASTES

The injected wastes become an integral part of the shale after the solidification of the grout and so remain as long as the shale is not subject to erosion. Therefore, consideration should be given to the factors involved in eroding and possibly exposing the injected wastes.

Over 99 percent of radionuclides contained in the wastes generated at the ORNL are ^{90}Sr and ^{137}Cs (table 11), which have half-lives of 28 and 30 years, respectively. Within 1,000 years, these radionuclides will decay to where the radiation-emission levels are innocuous.

On the basis of the dissolved and suspended sediment

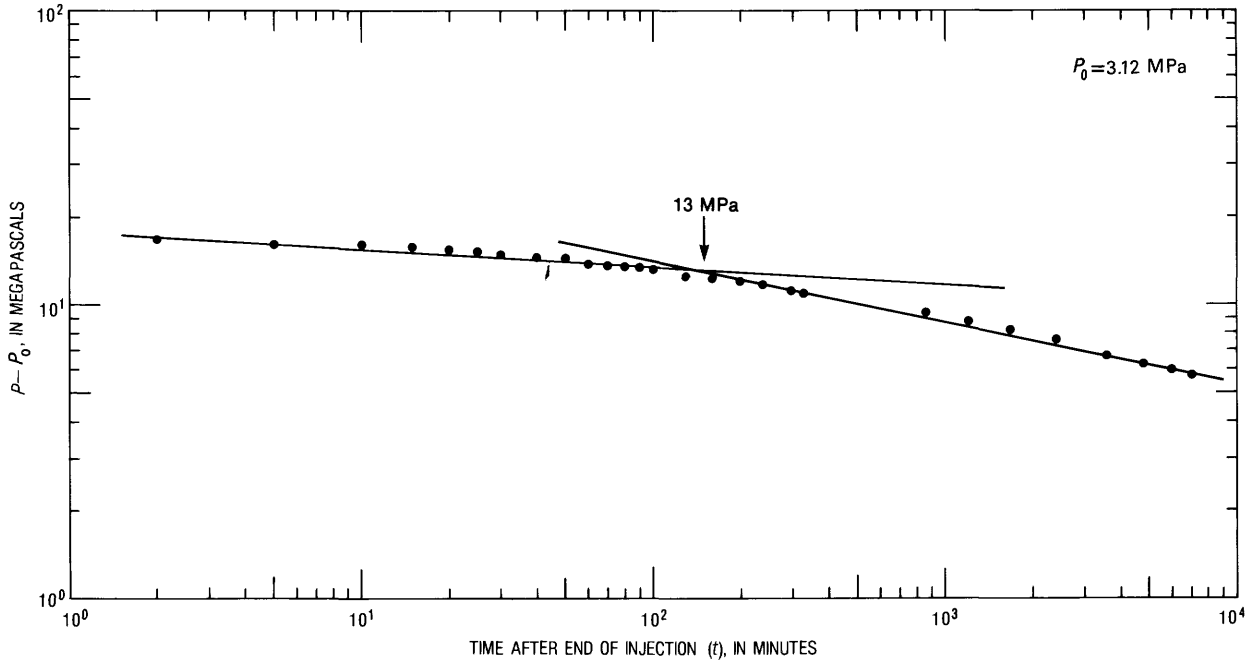

FIGURE 65.—Pressure decay plotted against time, the water injection at 332 m, Oct. 30, 1975, at the proposed disposal site, Oak Ridge National Laboratory, Tenn.

loads of streams, the climate, topographic, and geologic type, and the size of the drainage areas, Schumm (1963) concluded that denudation rates are an exponential function of the drainage-basin relief and length ratio. The mathematical form of this relationship is

$$\log D = 26.966\, H - 2.2398, \qquad (67)$$

where

D = denudation, in meters per 1,000 years, and
H = ratio of basin relief to length.

The relief-to-length ratio of Melton Branch basin (the injection site) is taken as 0.031 ((365.8 − 231.6)/4328 = 0.031); the denudation rate of the basin is then estimated to be 0.04 m per 1,000 years. Wastes are to be injected into Pumpkin Valley Shale, which is about 213 m below the surface. Using the estimated denudation rate, it would take 5.4×10^6 years to expose the wastes injected in the uppermost part of the Pumpkin Valley Shale by erosion. Even if the unlikely erosion rate of 1 m per 1,000 years is assumed, which is the average maximum erosion rate for young mountain ranges of high relief, such as the Alps (Schumm, 1963), it would still take 2×10^5 years to expose the grout sheets. This time interval would be sufficient for radionuclides contained in the wastes to decay to harmless radiation-emission levels, and thus the possibility of their contaminating the biosphere by erosion processes is negligible.

SUMMARY

On the basis of injection data, gamma-ray logs, and estimation of erosion rate, it is concluded that the hydraulic-fracturing disposal sites at the ORNL are safe for the purpose of disposing radioactive wastes generated at the ORNL by grout injections in shale. However, as a precaution, more monitoring observation wells need to be constructed in areas not expected to be reached by waste-grout sheet and in the formation lying above the injection zone, in order to increase confidence that the injected wastes are isolated and restricted to a known horizon.